Sialylated Glycans as Regulators of Cell Activation and Cell Death

---

Dissertation

zur

Erlangung der naturwissenschaftlichen Doktorwürde
(Dr. sc. nat.)

vorgelegt der

Mathematisch-naturwissenschaftlichen Fakultät

der

Universität Zürich

von

Marek William James Whitehead

aus dem

Vereinigten Königreich Grossbritannien und Nordirland

Promotionskommission

Prof. Dr. Thierry Hennet (Vorsitz)

Prof. Dr. Dr. Gerhard Rogler

Prof. Dr. Christophe Lacroix

Prof. Dr. Lubor Borsig

Zürich, 2018

“Ever since receiving the invitation to write this prefatory chapter, I have been wondering "Why me?" After reviewing the list of previous authors of this chapter, I was even more puzzled until I realized that this may have been a move to show that it is not necessary to be a genius to contribute to science.”

“This was quite a gamble on the part of the university. I had never had a real course in pharmacology, nor had I done any research that was even marginally pharmacological. Moreover, my two predecessors, Carl Cori and Herbert Gasser, were both Nobel Laureates, and there was no sign that I would get to Sweden except as a tourist”.

Oliver Howe Lowry

(1910-1996)

I chose these citations as it is my uttermost belief that the most fulfilling and exciting way to do science is with the mind of a humble person.

Table of contents

Summary

Glycans are structurally the most complex type of biological macromolecule. The diversity of structures by far exceeds what has been observed for other molecules such as proteins. They are also functionally extremely diverse and contribute to biological processes such as protein folding, intracellular trafficking, immune cell polarization and much more. The synthesis of most mammalian glycans takes place in the endoplasmic reticulum and in the Golgi apparatus. The latter is responsible for synthesizing the diversity that is observed in glycans. It contains a plethora of glycosyltransferases which synthesize the glycans that are secreted as free oligosaccharides such as human milk oligosaccharides or occur on proteins and lipids. The process is therefore not a template-driven process and instead compares more to a melting-pot where various reactions take place simultaneously and where enzymes compete for substrates. As a consequence, the created epitopes are diverse and it is challenging to associate functions to the specific glycan epitopes due to the absence of a linear synthesizing process such as for proteins. Therefore I used chemically synthesized oligosaccharides to discover unknown functions of glycans.

Previously the unconjugated human milk oligosaccharide 3-sialyllactose was shown to stimulate the maturation of mesenteric lymph node derived dendritic cells. Additionally, the human milk oligosaccharides lacto-N-fucopentaose III and lacto-N-neotetraose induce the proliferation of peritoneal macrophage populations. Therefore I speculated that other human milk oligosaccharides should also be able to influence antigen presenting cells like dendritic cells, monocytes or macrophages. Monocytic THP-1 cells and mesenteric lymph node derived dendritic cells were used as a model system to determine the stimulatory influence of human milk oligosaccharides on the activation of antigen presenting cells. 3-fucosyl-3-sialyllactose and sialyllacto-N-tetraose c induced a cell-density dependent, increased production of lactate by both cell-types which caused acidification of the surrounding media. Interestingly, lactate is known to stimulate M2 polarization of macrophages which is associated with the increased production of the immune dampening cytokines IL-10 and TGF-β. The results of this study are presented in manuscript 1 of this doctoral thesis.

I next decided to focus my efforts on identifying novel roles of multivalently presented oligosaccharides as they are known to induce more enhanced cellular responses than monovalent oligosaccharides. For this a method was developed, which is suitable to modify whole animal and bacterial cells as well as proteins, with specific oligosaccharides. Briefly, the oligosaccharides 2-fucosyllactose, 3-fucosyllactose, 3-sialyllactose, 6-sialyllactose and 3-fucosyl-3-sialyllactose were modified at their reducing end to contain a cyclic-carbamate group that reacts with primary amine groups. These oligosaccharide derivatives can be used to modify many biological entities including whole cells and proteins. I used this method to coat cells with ligands of the E-selectin receptor that

are known to mediate leukocyte extravasation, and demonstrated that this influences the behavior of the cells in an *in vitro* model for leukocyte extravasation. Furthermore, I coated *Escherichia coli* K-12 cells with sialic acid containing oligosaccharides and demonstrated that these surface glycans emulate immune regulatory roles mediated by certain pathogenic bacteria that present the same glycans. More specifically, these glycans inactivate the complement cascade by recruiting the inhibiting Factor H. Finally, I created custom-made glycoproteins and showed that they enhance the production of inflammatory cytokines by lipopolysaccharide-stimulated dendritic cells in a PI3K dependent manner. These results are presented in the second manuscript of this thesis.

While working on the oligosaccharide-cyclic-carbamate technology, I discovered that coating cells with sialyllactose leads to rapid cell death that was characterized by extensive blebbing and cytoskeleton depolymerization. Cell death could be blocked by using various caspase inhibitors which indicates a form of programmed cell death. Furthermore, the toxicity of the sialyllactose-containing oligosaccharides was dependent on the linkage of the sialic acid, as α2-3 linked sialic acid coating by 3-sialyllactose-cyclic-carbamate ligation, was more potent than α2-6 linked sialic acid coating by 6-sialyllactose-cyclic-carbamate ligation. Intriguingly, incorporating sialyllactose modified 3-sn-phosphatidylethanolamine into the cell membrane did not induce cell death which indicates that the cell death effect depends on the sialyllactose modification of distinct sites that occur in the cell membrane. I identified 23 protein components involved in this novel pathway with a CRISPR-Cas9 based screen and was able to demonstrate that G-protein coupled receptor signaling plays a key role during sialyllactose-coating mediated cell death.

The key contributions of this this work to the scientific community are the establishment of a method that enables the modification of whole cells, proteins and lipids with specific oligosaccharides, and the identification of a new form of cell death that is initiated by sialylated glycans at the cell surface. The oligosaccharide-cyclic-carbamate technique described here can be used to answer many basic biological questions concerning the physiological and pathophysiological functions of specific glycan epitopes.

Zusammenfassung

Glykane sind komplexe biologische Makromoleküle. Ihre Diversität ist viel grösser als jene von anderen biologischen Molekülen wie Proteine. Dazu besitzen sie auch eine grosse funktionelle Diversität und sind in Prozessen wie der Faltung von Proteinen, dem intrazellulärem Transport, der Polarisierung von Immunantworten und vieles mehr involviert. Die Synthese der meisten Glykane findet im endoplasmatischen Retikulum und im Golgi Apparatus statt. Insbesondere der Golgi Apparatus ist für die Diversität der Glykane zuständig. Es beinhaltet eine Vielfalt an Glykosyltransferasen, welche unkonjugierte Glykane, wie humane Milcholigosaccharide, oder Glykokonjugate, wie Glykoproteine oder Glykolipide, aufbauen. Bei der Synthese von Glykanen handelt es sich daher nicht um einen linearen Prozess mit Sequenzvorgabe wie bei der Synthese von Proteinen, sondern eher um einen komplexen Vorgang bei der verschiedenste Reaktionen gleichzeitig stattfinden und sogar miteinander kompetitieren. Die Diversität der generierten Epitope ist daher enorm und es ist schwierig den unterschiedlichen Strukturen Funktionen zuzuordnen. Daher habe ich chemisch hergestellte Oligosaccharide verwendet, um unbekannte Rollen von Glykanen zu entdecken.

In einer vorherigen Studie wurde demonstriert, wie dass in der menschlichen Milch vorkommende Oligosaccharid 3-Sialyllaktose, die Reifung von dendritischen Zellen aus den mesenterischen Lymphknoten vorantreibt. Weiterhin ist bekannt, dass die humanen Milcholigosaccharide Lakto-N-Fukopentaose III und Lakto-N-Neotetraose die Proliferation von peritonealen Makrophagen fördern. Ich habe daher spekuliert, dass auch andere Oligosaccharide, die in menschlicher Milch vorkommen, Antigen-präsentierende Zellen stimulieren können. Monozytäre THP-1 Zellen und dendritische Zellen, die aus mesenterischen Lymphknoten isoliert wurden, habe ich mit chemisch synthetisierten humanen Milch-Oligosacchariden stimuliert. 3-Fucosyl-3-Sialyllaktose und Sialyllakto-N-tetraose c haben eine Zunahme der Laktatproduktion in den Zellen bewirkt, welches zu einem Ansäuern des Mediums geführt hat. Es ist allgemein bekannt, dass Laktat eine M2 Polarisierung von Makrophagen bewirkt, welches zur Produktion von Immun-hemmenden Zytokinen wie IL-10 und TGF-β führt. Die Resultate hierzu sind in Manuskript 1 dieser Arbeit zu finden.

Danach habe ich mich entschieden meine Bestrebungen auf die Entdeckung neuer Funktionen von multivalenten Oligosacchariden zu fokussieren, da diese bekannterweise zu stärkeren Reaktionen führen wie monovalente Oligosaccharide. Dazu wurde eine Methode entwickelt, welches sich dazu eignet tierische und bakterielle Zellen, als auch Proteine mit spezifischen Oligosacchariden zu modifizieren. Dazu wurden die Oligosaccharide 2-Fukosyllaktose, 3-Fukosyllaktose, 3-Sialyllaktose, 6-Sialyllaktose und 3-Fukosyl-3-Sialyllaktose an ihrem reduzierendem Ende so modifiziert, dass sie eine zyklische Carbamat-Gruppe aufweisen, welches in der Lage ist mit primären Aminen eine kovalente

Bindung einzugehen. Diese Methode kann dazu verwendet werden, um viele biologische Entitäten, wie ganze Zellen und Proteine zu modifizieren. Anhand dieser Methode habe ich Zellen mit Oligosacchariden modifiziert, die als Konsequenz an den Rezeptor E-Selektin binden konnten, welches für die Auswanderung von Leukozyten aus den Blutgefässen in das Gewebe verantwortlich ist. Mittels einem *in vitro* Ansatz konnte ich demonstrieren, dass solche Zellen neue Bindungseigenschaften für E-Selektin bekommen. Weiterhin, konnte ich auch *Escherichia coli* K-12 mit sialinsäurehaltigen Oligosacchariden modifizieren, welche daraufhin immunmodulatorische Eigenschaften erhalten haben, die sonst nur bei pathogenen Bakterien beobachtet werden. Die Ursache dafür war, dass die Zellen den Komplement-Kaskade inhibierenden Protein Faktor H an ihre Oberfläche rekrutieren konnten. Zuletzt, habe ich auch künstliche Glykoproteine hergestellt, welche eine PI3K-abhängige Zunahme der Produktion von inflammatorischen Zytokinen, durch Lipopolysaccharid-stimulierte dendritische Zellen, vermittelt haben. Diese Resultate sind im zweiten Manuskript dieser Arbeit beschrieben.

Während meiner Arbeit an der oben beschriebenen Technologie, habe ich entdeckt, dass Zellen, die mit Sialyllaktose modifiziert wurden schnell sterben. Dabei bilden sich an der Membran Bläschen und es kommt zu einem Abbau des Zytoskeletts. Der Zelltod konnte mittels verschiedener Inhibitoren der Caspasen verhindert werden, welches dafür spricht, dass es sich um eine programmierte Form von Zelltod handelt. Weiterhin war die Toxizität von der Bindung der Sialinsäure abhängig, da 3-Sialyllaktose, welches eine α2-3 gebundene Sialinsäure aufweist, bei tieferen Konzentrationen Zelltod hervorgerufen hat als 6-Sialyllaktose, welches eine α2-6 gebundene Sialinsäure aufweist. Interessanterweise, hatte die Inkorporation von Sialyllaktose modifiziertem 3-sn-Phosphatidylethanolamine in die Plasmamembran keinen Einfluss auf das Überleben der Zellen, weshalb ich darauf geschlossen habe, dass die Modifizierung spezifischer Epitope auf der Zelloberfläche mit Sialyllaktose, den Zelltod induzieren. Ich habe dann mittels einem genetischen CRISPR-Cas9-Screen 23 Proteine identifiziert die eine Rolle bei dieser Form des Zelltodes spielen. Auf diesem Screen aufbauend, konnte ich zeigen, dass G-Protein gekoppelte Rezeptoren und ihre Signalwege, eine besonders wichtige Rolle spielen. Diese Resultate sind im dritten Manuskript dieser Doktorarbeit beschrieben.

Die wichtigsten Beiträge dieser Arbeit an die wissenschaftliche Gemeinschaft sind die Etablierung einer Methode, welches die Modifizierung ganzer Zellen, Proteine und Lipide mit spezifischen Oligosacchariden ermöglicht, und die Entdeckung einer neuartigen Art von Zelltod, das durch sialinsäurehaltigen Glykanen initiiert wird. Die hier beschriebene Methode kann benutzt werden, um viele grundlegende biologische Fragestellungen bezüglich den physiologischen und pathophysiologischen Rollen spezifischer Glykane zu beantworten.

Abbreviations

2FL	2-fucosyllactose
3FL	3-fucosyllactose
3SL	3-sialyllactose
6SL	6-sialyllactose
AAL	*Aleuria aurantia* lectin
Appbp2	amyloid beta precursor binding protein 2
BSA	bovine serum albumin
Cul5	cullin 5
DISC	Death-inducing signaling complex
EPO	erythropoietin
ER	endoplasmic reticulum
FCS	fetal calf serum
Ffar4	free fatty acid receptor 4
FSL	3-sialyl-3-fucosyllactose [Sia(α2-3)Gal(β1-4)[Fuc(α1-3)]Glc]
Fuc	Fucose
FUT2	2-α-L-fucosyltransferase 2
Gal	galactose
GalNAc	N-acetylgalactosamine
Glc	glucose
GlcNAc	N-acetylglucosamine
HBSS	Hank's Balanced Salt Solution
HMO	human milk oligosaccharide
IAP	protein that inhibits apoptosis
IL	interleukin
ITIM	immunoreceptor tyrosine-based inhibition motifs

LNFP	lacto-N-fucopentaose
LOS	Lipid bound oligosaccharide
LPS	lipopolysaccharides
LST	sialyllacto-N-tetraose a
MAL	*Maackia amurensis* lectin I
Man	mannose
MLKL	mixed lineage kinase domain-like protein
MurNAc	N-acetlymuramic acid
Olfr	olfactory receptor
PBMC	peripheral blood mononuclear cell
PBS	phosphate buffered saline
PE	phycoerythrin
RIPK	kinase receptor interacting protein
Rnf133	ring finger protein 133
RPMI	Roswell Park Memorial Institute Medium
Sia	sialic acid
Siah2	seven in absentia 2
SMAC	secondary mitochondria-derived activator of caspases
Spn	sialophorin
Surf4	surfeit gene 4
TGF-β	transforming growth factor-β
TLC	thin-layer chromatography
TLR	Toll-like receptor
TNF-α	tumor necrosis factor-α
TRAIL	TNF-related apoptosis-inducing ligand
UEA	*Ulex europaeus* agglutinin I

Introduction

Glycans are structurally diverse [1] and their synthesis is not template-driven [2] such as for proteins. This often impedes the functional characterization of specific glycans because of the deficiency of genetic approaches. Mucins for example are proteins that occur at epithelial surfaces and are heterogenously glycosylated [3]. The glycans on these proteins are immune suppressing but the responsible structures remain unknown [4]. The goal of this project was to tackle this problem and to develop new approaches to functionally characterize glycan structures. I used chemically synthesized oligosaccharides to define the structural-functional relationship of specific oligosaccharides that are secreted as free glycans, such as human milk oligosaccharides, and of glycans coupled to proteins, such as mucins. To study the role of glycans that are conjugated to proteins, I used oligosaccharides derivatized with a cyclic-carbamate group at their reducing end that can bind covalently to primary amines which occur on proteins. During the course of this work I discovered that sialic acid (Sia) containing glycans on the cell surface initiate a previously uncharacterized form of programmed cell death. This introduction offers a brief overview of the diversity that occurs in glycans and the diversity of functions that glycans are involved in. The roles of glycans in cell death are emphasized and the various forms of cell death elaborated.

Glycans and their diversity in structure and function

Glycans can either occur as soluble molecules that are secreted by cells [5, 6] or attached to other biomolecules. When glycans are enzymatically attached to other biomolecules such as proteins, lipids or other non-glycans we speak of glycosylation. The products of such reactions are called glycoconjugates. Modified proteins are known as glycoproteins or proteoglycans [7] while glycosylated lipids are generally classified as glycolipids [8]. Glycosylation is the most common posttranslational modification of proteins and a bioinformatics study demonstrated that 50% of all proteins registered in the SWISS-PROT database are glycosylated [9]. There are three general types of protein-glycosylation which are N-, O- and C-linked glycosylation [10]. Some would also claim that glycosylphosphatidylinositol anchors are a form of protein glycosylation as a phosphoinositide lipid is attached via a glycan linker to the C-terminus of a protein [10].

The structural diversity of glycans

The chemical basis of glycan diversity

Glycan diversity is vast due to the great variabilities in the glycosidic bonds, monosaccharide composition, branching and length of the glycans [11]. A factor contributing to the heterogeneity of glycans is that glycosidic bonds can be made from the reducing end of one monosaccharide to almost

any hydroxyl-group of another monosaccharide or even an aglycone. Maltose for example consists of α1-4 linked glucose (Glc) while trehalose contains an α1-1 linkage between the two Glc residues. On top of this comes the anomerism of the exocyclic oxygen towards the configuration determining C-atom of the sugar, where the prefix α stands for a *cis* orientation while β means there is a *trans* configuration. Starch for instance contains α1-4 linked Glc while cellulose contains β1-4 linked Glc.

Another point of variability, are the monosaccharides that occur in the glycan. The monosaccharides vary in the amount of C atoms and the axial orientation of the hydroxyl groups. Figure 1 demonstrates common monosaccharides that occur in mammalian glycans and introduces the abbreviations for the monosaccharides that shall be used throughout this thesis. Note that in all mammals except humans N-acetyl-D-neuraminic acid is hydroxylated at the acetyl group and is termed N-glycolyl-D-neuraminic acid. Both are classified as Sia residues.

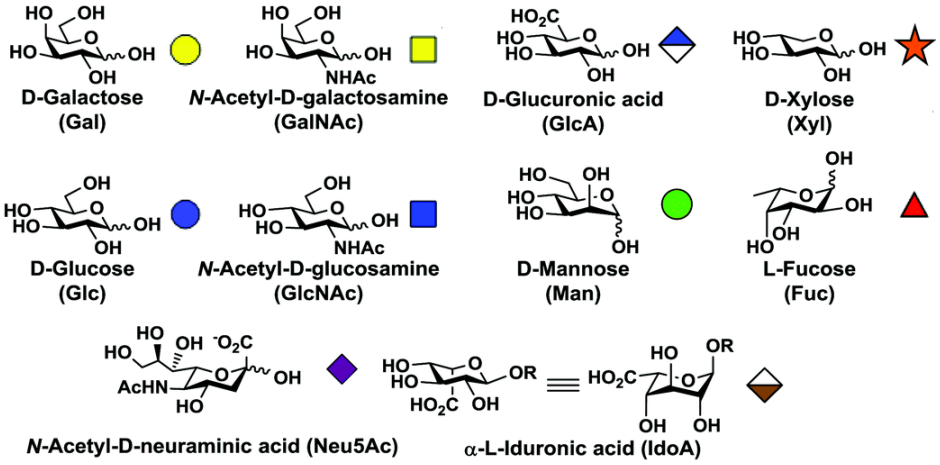

Figure 1: Some common monosaccharides that occur in mammalian glycans. These monosaccharides are attached as oligosaccharides to other biomolecules such as lipids or proteins. Each monosaccharide is labelled with the corresponding symbol that serves as a simplification for further images (modified from [12]).

Branching is also a source of diversity in glycans. An example for this is the branching of N-linked glycans. N-linked glycans are defined by their attachment to asparagines and in mammals they can be biantennary, triantennary or tetraantennary [13]. This is actually of great functional relevance too. Tetraantennary N-linked glycans interact more extensively with galectins, a secreted class of lectins, which is important for membrane stability of proteins [14] and also inhibits spontaneous crosslinking of signaling receptors in T cells [15]. Short and long-chain glycans can also be differentiated. Glycosaminoglycans are large unbranched polysaccharides consisting of repeating disaccharide units and are good examples of large glycans and consist of repeats of possibly thousands of disaccharide repeats [16]. On the other hand glycan-moieties of glycosphingolipids are relatively short and mostly have less than ten monosaccharides in the glycan [17].

N-linked Glycosylation

N-linked oligosaccharides are attached to the asparagine of the tripeptide sequence Asn-X-Thr/Ser whereas X can be any amino acid but proline [18]. There are three major classes of N-linked saccharides: high-mannose (Man), complex and hybrid oligosaccharides (Fig. 2). High-Man is, in essence, just two β1-4-linked N-acetylglucosamine (GlcNACs) with up to nine Man residues in mammals, which is the maximal amount of Man that occur on the precursor oligosaccharide before it is attached to the protein. Complex N-glycans are generated by cleaving away all Man residues but the three closest to the reducing end [13] and they are then extended with other types of monosaccharides which will be discussed briefly further below in this section.

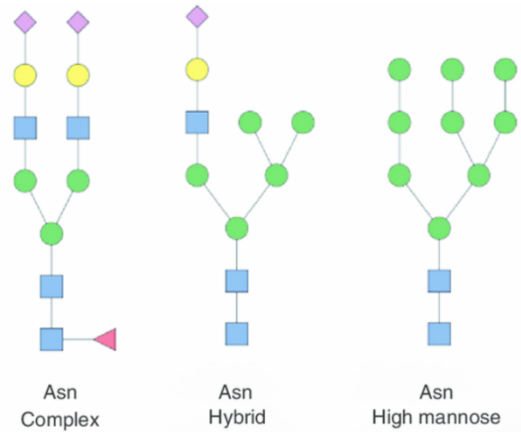

Figure 2: Comparative overview of the major types of vertebrate N-glycan subtypes. Complex-type N-glycans are trimmed high-Man-type N-linked glycans that are extended with GlcNAc, Gal and Sia. Hybrid-type N-linked oligosaccharides have a mixture of high-Man-type and complex-type branches (modified from [19]).

Proteins destined for N-linked glycosylation possess an N-terminal signal sequence consisting of about 5 to 10 hydrophobic amino acids for their transport to the ER lumen [20]. This signal sequence is recognized and bound by a signal recognition particle that mediates the transport of the protein into the endoplasmic reticulum (ER) [20]. The next step in the ER is the addition of the N-linked oligosaccharide (Fig. 3). This process is catalyzed by a membrane protein complex termed oligosaccharyltransferase which transfers the N-glycan precursor, which is linked to dolichol, onto the nascent protein. This enzyme is positioned next to the translocator in the ER membrane [21].

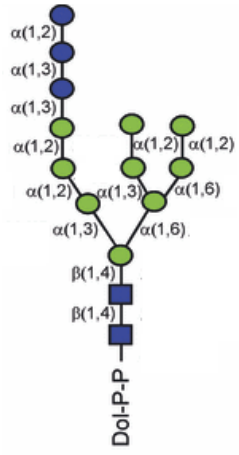

Figure 3: Dolichol-pyrophosphate (PP)-linked precursor for N-linked glycosylation. The precursor is attached to asparagine, which is the first step of N-linked glycosylation. The oligosaccharide can then be processed to create the diversity of N-linked glycans (modified from [22]).

The newly synthesized glycoproteins are transported to the cis-Golgi stack by vesicular transport [23]. The high Man oligosaccharides can be further trimmed by the Golgi α-1,2-mannosidase to yield a $Man_5GlcNAc_2$ structure. In the medial cisternae, further N-glycan heterogeneity is created by the branching of complex-type N-glycans. This is accomplished by the GlcNAc-transferases 1-5 that add the various branches to the three core Man residues (Fig. 4) [24].

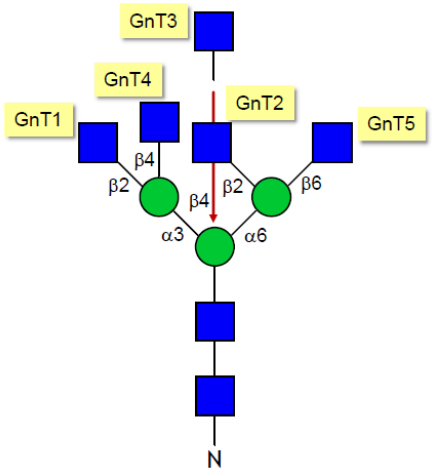

Figure 4: The branching of complex-type N-glycans is accomplished by the GlcNAc-transferases 1-5. The GlcNACs placed by the GlcNAc-transferases are the first monosaccharide of a branch on the N-linked glycan. Commonly, N-linked glycans have about two to four branches. Only the GlcNAc positioned by GlcNAc-transferase 3 is not elongated with further monosaccharides (provided by Thierry Hennet).

The GlcNAc-initiated branches on N-linked glycans, but also GlcNAc residues that occur in O-glycans or glycolipids, can be elongated in different ways. The addition of β1-4 linked galactose (Gal) generates a so called type-2 unit that is also known as N-acetyllactosamine [25]. Alternatively, a β1-4

N-acetylgalactosamine (GalNAc)-transferase may form so called LacdiNAc units [26]. The latter structure is rare in mammals, has however been indicated to play a key role in the capability of mouse embryonic stems cells to divide [27]. Instead of the β1-4 linkage, the Gal may also be attached in a β1-3 linkage. The respective glycans are termed type-1 glycan units or neo-N-acetyllactosamine [28]. The alternating activity of β1-4 Gal-transferases and β1-3 GlcNAc-transferases leads to the synthesis of poly-N-acetyllactosamine [29]. This epitope mainly occurs on multiantennary N-glycans on the β1-6 branch and is a strong ligand for a class of lectins known as galectins [30]. Poly-N-acetyllactosamine can also be branched by the addition of β1-6 linked GlcNAc. Branched and unbranched poly-N-acetyllactosamine are termed as the "I" and "i" antigens respectively as they are also blood groups [31]. Some individuals lack the β1-6 GlcNAc-transferase that is responsible for the formation of the antigen and therefore only have unbranched poly-N-acetyllactosamine [32].

The final steps of complex oligosaccharide synthesis occur in the trans Golgi cisternae and consist of the addition of outer chain Gal and Sia residues [33]. The newly synthesized glycoproteins then exit the Golgi and are transported to their final destination [34]. These final steps of N-linked glycosylation result in a multitude of different epitopes that are terminally presented by the N-glycan chains (Fig. 5).

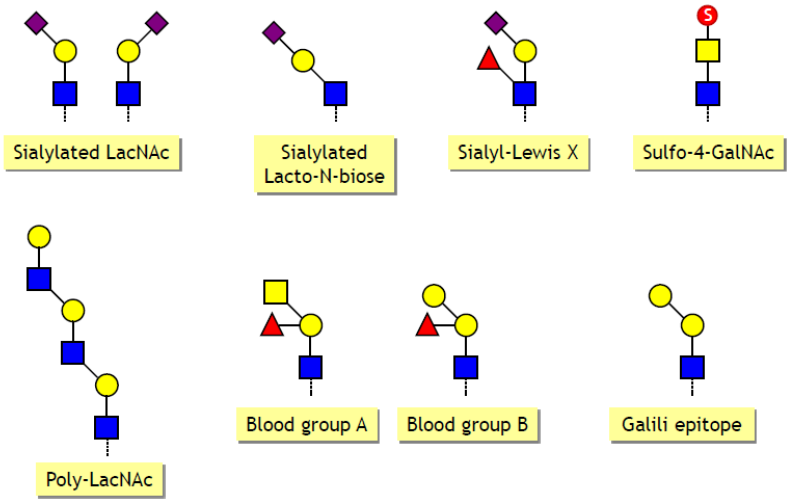

Figure 5: Some typical epitopes found on complex-type N-linked glycans. Sialylated glycan epitopes often play a role in immunological responses as they interact with immune-dampening Siglec receptors or selectins which mediate immune cell extravasation from blood vessels. Poly-N-acetyllactosamine is a potent ligand for galectins that can regulate cell death or stabilize glycosylated proteins at the cell surface. The blood groups A and B occur as epitopes on cells and are the reason for incompatibility between certain blood donors and recipients. The Galili epitope is not presented on human cells and therefore the human body forms antibodies against it (provided by Thierry Hennet).

O-linked Glycosylation

O-linked glycans can be attached to serine, threonine and hydroxylysine [35]. One exception to this is the O-glycosylation of glycogenin, which occurs on tyrosine [36]. Seven different monosaccharides can occur at the reducing end of O-linked glycans which are GalNAc, fucose (Fuc), Glc, Man, Gal, xylose and GlcNAc [35].

O-GalNAcylation is performed in the Golgi apparatus on proteins known as mucins but can occur on other proteins too [37]. O-linked GalNAc can be extended in at least eight different ways, resulting in eight different core structures (Fig. 6) [38]. The cores are then extended with various monosaccharides. The terminal epitopes of O-GalNAc type glycans resemble the ones found on N-linked glycans and their synthesis is actually catalyzed by the same enzymes (Fig. 5) [37]. The placement of an α2-6 linked Sia onto the core GalNAc stops further elongation and results in the so called sialyl-Tn-antigen [39].

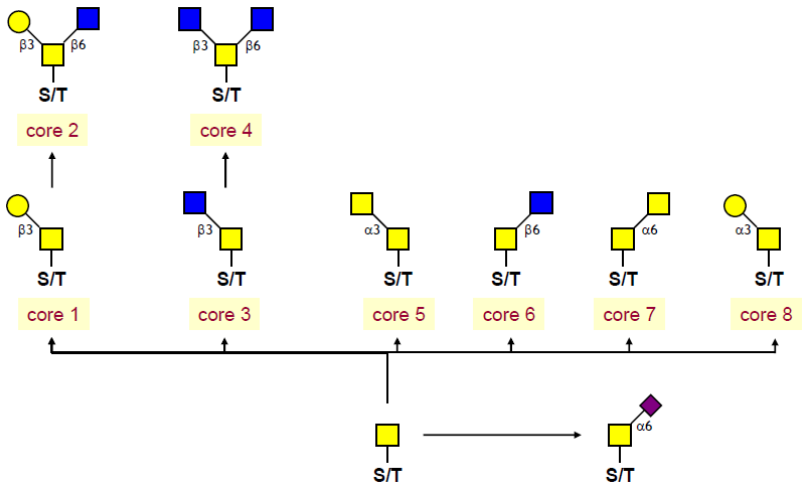

Figure 6: Core structures that occur on O-GalNAc type glycans. The cores 1 to 4 are the most common core structures to be placed on O-GalNAc type glycans. In some cells, especially in cells with tumorigenic properties the core GalNAc is not extended which is known as the Tn-antigen. The core GalNAc can also be elongated by an α2-6 Sia-transferase to the so called sialyl-Tn-antigen (provided by Thierry Hennet).

Another form of O-linked glycosylation is O-linked xylose. This modification is made in the Golgi apparatus on serine residues of so called proteoglycans [40]. Proteoglycans are secreted or membrane bound proteins that are modified with long carbohydrate polymers that consist of disaccharide repeats that belong to the class of the glycosaminoglycans. Due to their modification with sulfate, they are highly polar. The glycosaminoglycans that occur on proteoglycans are heparan-, chondroitin-, and dermatan-sulfate (Fig. 7) [41].

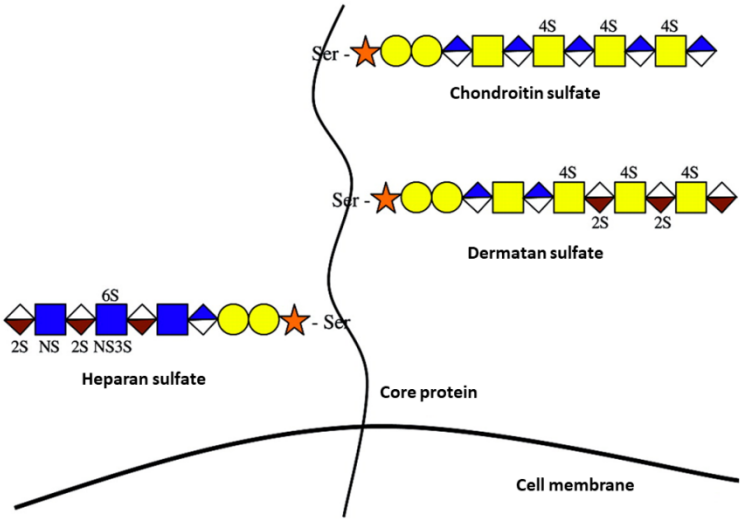

Figure 7: Proteoglycans and the glycosaminoglycans that occur on them. Chondroitin sulfate is the most common glycosaminoglycan. Dermatan sulfate can be distinguished from chondroitin sulfate by the presence of iduronic acid. Heparan sulfate is highly similar to heparin and consists of highly sulfated regions that are interrupted by non-sulfated regions (modified from [42]).

Other O-glycans have Fuc, Gal, Glc or Man as their core at the reducing end. Depending on the core, the synthesis of these glycans is initiated in the ER or the Golgi apparatus. They can all be extended with other monosaccharides and all but O-Gal-type glycans can present terminal Sia [35].

Next to proteins also lipids are modified with glycans. As the glycans are attached to the hydroxyl group of ceramide, this is actually also a form of O-linked glycosylation. Ceramide is synthesized in the ER [17] and can be galactosylated in the ER [43] or glucosylated in the Golgi apparatus [44]. The galactosylated form is hardly extended and can maximally be modified with one more Gal while the glucosylated form can be elongated to form prominent glycosphingolipid classes such as the Globo-, Ganglio- or Lactoseries (Fig. 8). Many of the glycans epitopes can be found on N-linked glycans, on O-GalNAc-linked glycans and on glycosphingolipids too (Fig. 5) [44].

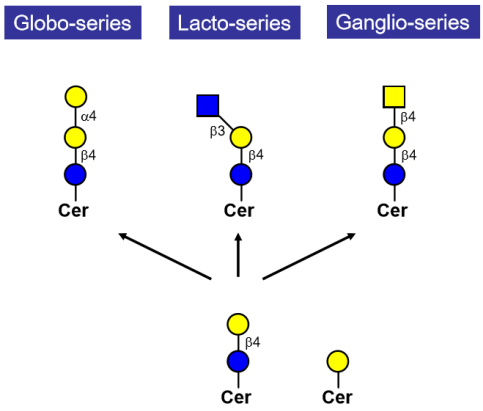

Figure 8: The various classes of glycosphingolipids with Glc at the reducing end of the oligosaccharide component. Globosides are especially common at the cell surface of erythrocytes and present no terminal Sia while gangliosides occur on nerve cells and can be modified with terminal Sia (provided by Thierry Hennet).

Bacterial Glycosylation

Glycosylation in bacteria is even more diverse than in mammals [45]. The outer-membrane of Gram-positive bacteria mainly consists of peptidoglycan, which is a polymer consisting of GlcNAc that is β1-4 linked to N- acetylmuramic acid (MurNAc). MurNAc contains a tri- to pentapeptide at the 2'-acetamido group that is responsible for crosslinking the layers of the carbohydrate polymer (Fig. 9). About every tenth MurNAc also has a teichoic acid attached to it [46]. Teichoic acids protrude from the peptidoglycan layer and consist of ribitol-phosphate or glycerol-phosphate polymers [47]. Alternatively the teichoic acids of certain bacteria are attached to lipids in the plasma membrane [48].

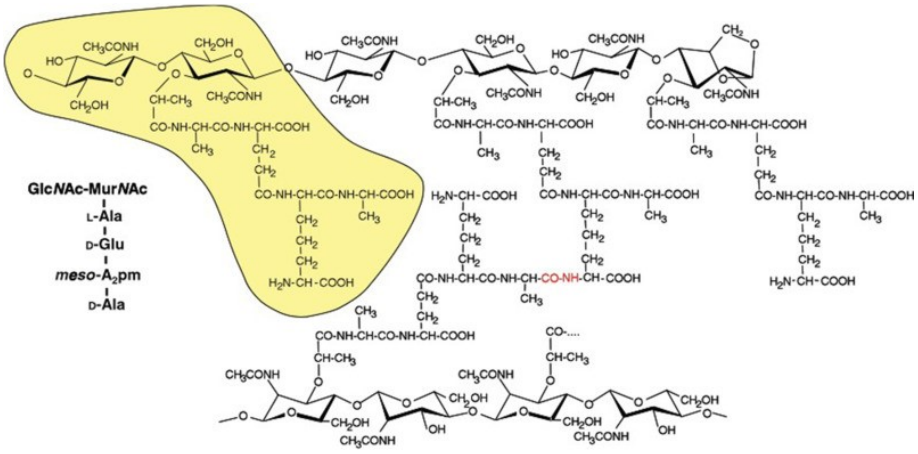

Figure 9: Peptidoglycan consists of repetitive disaccharide repeats of GlcNAc and MurNAc. The monosaccharides are linked by β1-4 linkages and each MurNAc is modified with 4 to 5 amino acids. One disaccharide repeat with the respective amino acid modification on MurNAc is highlighted in yellow (copied from [49]).

The peptidoglycan layer and the teichoic acids associated with it are relatively conserved between bacteria. Therefore, these molecules are also exploited by the immune system as pathogen associated molecular patterns, such as lipoteichoic acid which is recognized by the Toll-like receptor 2 (TLR2) [50] or the GlcNAcβ1-4MurNAc disaccharide derived from peptidoglycan turnover which is also recognized by TLR2 [51]. The intracellular receptors NOD1 and NOD2 that initiate defense reactions against intracellular pathogens via the inflammasome also recognize peptidoglycan fragments that are in the cytoplasm [52, 53].

However many bacteria, including Gram-positive bacteria, also display capsular polysaccharides at their surface and these are highly diverse between bacteria. Such glycans are often produced by pathogenic bacteria and form thick layers that surround the individual bacterium and enable immune evasion. The carbohydrate component of the capsule is commonly acidic and consists of repeating units of 1 to 6 monosaccharides [54]. The structural diversity of the capsule is huge, as for example *E. coli* on its own can synthesize more than 80 different capsular polysaccharides [55]. The most important functions of capsular polysaccharides are to evade phagocytosis [56], protect the bacteria from desiccation by attracting water and also to avoid being infected by bacteriophages [57].

In comparison to Gram-positive bacteria, Gram-negative bacteria only have a thin layer of peptidoglycan that is covered by an outer membrane. This outer membrane has lipopolysaccharides (LPS) incorporated into it. LPS consists of a lipid A moiety that is incorporated into the outer membrane and has a carbohydrate moiety as a head group that protrudes out of the outer membrane (Fig. 10). The carbohydrate component consists of the oligosaccharide-core and the O-antigen. Common monosaccharides in the core-oligosaccharide are 2-keto-3-desoxy-octonat, heptose, Glc, Gal and GlcNAc. During the synthesis of LPS the core oligosaccharide is attached to lipid A inside the cytoplasm before being flipped to face the periplasm where the O-antigen is attached. The O-antigen consists of tandem repeats of tetra- or pentasaccharides, depending on the bacterial species and strain. While the core oligosaccharide is always present, the O-antigen can also be absent in certain strains and species [58]. When the O-antigen is missing, the lipid-A core-oligosaccharide structure is defined as a lipooligosaccharide (LOS) [59].

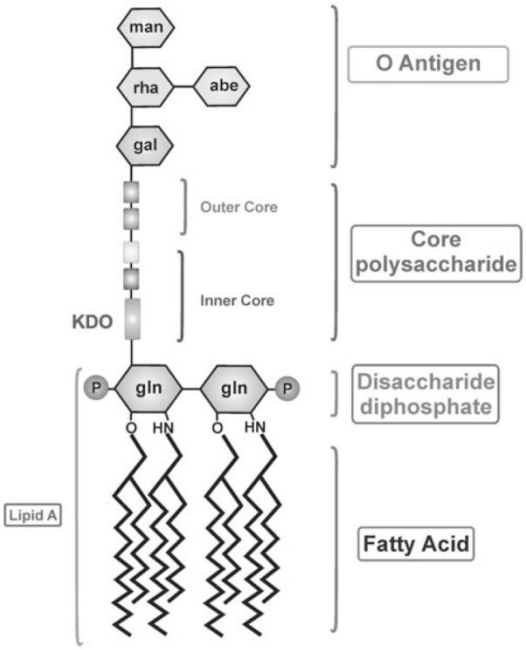

Figure 10: Schematic representation of LPS structure. Lipid A is modified with a disaccharide diphosphate that is elongated with a core saccharide. A polymerase then attaches a defined number of O-antigens that are premade on bactoprenol to the core polysaccharide (copied from [60]).

Bacteria are also capable of performing O- and N-glycosylation of proteins. O-linked glycosylation most commonly occurs on pili and flagella [61, 62]. As in mammals, serine and threonine can be O-glycosylated but also tyrosine is a possible acceptor [62]. The oligosaccharides attached via O-glycosylation are far more diverse in bacteria than in mammals and contain more than the 9 monosaccharides depicted in figure 1 [63-66]. Some bacteria can also O-glycosylate other proteins than pili and flagella such as *Neisseria spp.* and *Bacteroides spp*.

Neisseria gonorrhoeae for instance has *Ngo* glycoproteins that are O-glycosylated. These proteins are likely involved in processes such as the electron transport system and are important redox components [67]. Ng1276 for instance is a copper-containing nitrite reductase that is important for growth during oxygen-limitation and has been proposed to receive electrons from Ng0994 [68]. Ng1371 on the other hand is a multiheme containing c-type cytochrome belonging to the cbb3 oxidase complex which is the predicted terminal oxidase of the *Ngo* proteins [69].

Bacteroides fragilis, serves as another example of a bacterial species that can O-glycosylate other proteins than pili and flagella. *B. fragilis* is a component of the humans gut microbiota [70]. It can O-glycosylate many extracytoplasmic proteins that are of importance for the bacteria's capability to colonize the intestine [71]. *B. fragilis* and also other members of the *Bacteroides* genera are able to

glycosylate proteins that have the three amino acid sequence motif D(S,T)(A,L,V,I,M,T) at the middle serine or threonine [72].

N-glycosylation in bacteria has been best described in the pathogen *Campylobacter jejuni*. The glycan is synthesized on bactoprenol before being flipped to the periplasm where it is attached to an asparagine residue of a carrier protein by the oligosaccharyltransferase PglB [73]. Other bacteria with N-glycosylation are *Desulfovibrio spp., Helicobacter spp., Haemophilus influenza* and *Actinobacillus pleuropneumoniae* [74].

The functional Diversity of common Glycan Epitopes

Here, a few examples, of the functions that glycans are involved in, are provided. This by no means covers the vast diversity of roles that glycans play.

ER quality control

Calnexin and calreticulin are chaperones in the ER that are responsible for the correct folding of glycoproteins. They bind to the conserved oligosaccharide that is attached to N-linked glycans and regulate the folding of the protein [75]. Once the oligosaccharide precursor ($Glc_3Man_9GlcNAc_2$) has been transferred onto asparagine of the target protein, the two outermost Glc residues are removed by the glucosidases I and II [76, 77]. The monoglucosylated oligosaccharide is recognized by the folding assistants' calnexin and calreticulin that both interact with ERp57. ERp57 then forms intermolecular disulfide bonds with the glycoprotein to assist with the formation of disulfide bonds [78]. Once glucosidase II cleaves off the last Glc, calnexin and calreticulin dissociate from the target protein [13]. Correctly folded glycoproteins then enter the secretory pathway. On the other hand, glycoproteins that are not correctly glycosylated can be re-glucosylated by UDP-Glc:glycoprotein Glc-transferase which enables the renewed assembly with calreticulin or calnexin [79]. If however folding cannot be achieved at all, at some time the completely de-glucosylated oligosaccharide will be processed by the ER degradation-enhancing α1,2-mannosidase-like protein which, once it has cleaved its target, will initiate ER-associated degradation [79].

IgG glycosylation

The effector functions of IgG-type antibodies also depend on the N-linked glycan that is attached to the Fc-domain at asparagine-297. Core fucosylation of antibodies for instance has been shown to dampen antibody-dependent, cell-mediated cytotoxicity, a mechanism of cell-mediated immunity whereby natural killer cells actively lyse an antibody covered target cell via the Fcγ-receptor III. This is also the reason why therapeutic antibodies against certain forms of cancer are produced in cells that lack the core fucosylating enzyme Fuc-transferase 8 [80].

Lysosomal trafficking

Another key role that can be mediated by glycans is the trafficking of lysosomal resident proteins to the early endosomes. In vertebrates and some invertebrates this specificity is made possible by a Man-6-phosphate tag that is added to N-linked oligosaccharides of lysosomal resident proteins in the Golgi apparatus [81-83]. In the trans-Golgi network, specific luminal Man-6-phosphate receptors recognize this tag and bind the respective proteins that are packed into clathrin-coated vesicles determined for transport to early endosomes [84, 85].

In total, two enzymes are responsible for the addition of Man-6-phosphate. UDP-GlcNAc 1-phosphotransferase (GlcNAc-1-phosphotransferase) binds to peptides with the recognition sequence in the cis Golgi and adds a GlcNAc-phosphate group to one or two of the Man residues on the N-linked oligosaccharide [86]. A second enzyme, α-GlcNAc-1-phosphodiester α-GlcNAc-aminidase (uncovering enzyme), in the trans-Golgi network removes the GlcNAc residue and uncovers the Man-6-phosphate tag [87, 88].

The A, B and H antigens

In humans, the poly-N-acetyllactosamine chains of N-glycans, O-GalNAc glycans and glycolipids are also modified to form the ABO blood group antigens (Fig. 11).

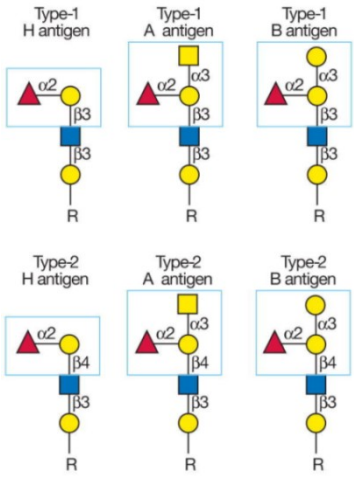

Figure 11: ABO blood group antigens that are attached to the type 1 and type 2 N-acetyllactosamine chains that occur on N- and O-glycans. The A antigen is characterized by a terminal α1-3 linked GalNAc while the B antigen has an α1-3 linked Gal. The H antigen has neither and is found in individuals that have the O blood group (copied from [89]).

All three antigens are modified by the H α1-2 Fuc-transferase in erythrocyte precursors [90]. This modification is also performed on glycans of epithelial cells but by another enzyme called Se α1-2 Fuc-transferase [91]. The A glycan epitope is made by an α1-3 GalNAc transferase that is encoded by

the so called A allele. Another variant of the same gene termed the B allele encodes an α1-3 Gal-transferase [92]. A third dysfunctional H allele has lost its enzymatic activity completely. An individual who is homozygous for one of the A or B genes will have the blood group A or B respectively, as is also the case for individuals that are heterozygous for the A and H or B and H alleles. A heterozygous individual for the A and B allele will have the blood group AB and present both α1-3-linked GalNAc and α1-3-linked Gal on the ABO antigens. The blood group glycan epitopes must be considered when performing blood group transfusions. People of blood group A cannot receive blood from a donor with blood group B and vice versa. Everybody can however receive blood with the group H antigen as anti-H antibodies are not made because the A and B antigens are actually synthesized upon the H antigen. The ABO compatibility is also of great importance for heart, kidney, liver and bone marrow transplantations [93]. There is also one very rare blood type known as the Bombay phenotype. Individuals with this blood type have antigens against the A, B and H antigens because they actually lack the α1-2 Fuc-transferase that is needed to synthesize all three blood group determining antigens [94].

Lewis antigens

The Lewis blood groups are another class of blood group antigens that contain α1-3 and α1-4 Fuc residues. The enzymes Le α1-3/α1-4 Fuc-transferase, that are encoded at the Lewis blood group locus, and Se α1-2 Fuc-transferase are central for the synthesis of the Le^a and Le^b glycan epitopes [95]. Some individuals have an inactive Le locus and are therefore negative for these glycan epitopes [96]. The Le α1-3/α1-4 Fuc-transferases are expressed by the same epithelial cells that express the Se α1-2 Fuc-transferase. As a consequence, the soluble glycans produced by epithelial cells commonly present these Lewis glycan epitopes [97]. Erythrocytes also present the Le^a and Le^b glycan epitopes on their cell surface however this is not because erythrocyte precursor can produce them but rather because erythrocytes acquire them via passive absorption of glycolipids that are in the plasma as components of lipoprotein complexes [98]. The Le^x and Le^y determinants and their sialylated versions are synthesized by α1-3 Fuc-transferases that are distinct from the Le α1-3/α1-4 Fuc-transferase [99].

Sialyl-Lewis X

This glycan epitope mediates cell-cell recognition processes and it's best known role is the regulation of leukocyte extravasation by enabling the tethering of leukocytes to the endothelial layer of blood vessels [100]. Sialyl-Lewis X is recognized by L-, P- and E-selectin [101]. L-selectin is present on lymphocytes and acts as a homing receptor for lymphocytes that enables them to be recruited to the lymph nodes [102]. E-selectin is mainly present on endothelial cells while P-selectin is present on platelets and endothelial cells. E- and P-selectin are both present in Weibel-Palade bodies that can be

found inside endothelial cells. If endothelial cells receive an appropriate signal, such as by recognizing bacterial pathogen-associated molecular patterns like peptidoglycan, the contents of the Weibel-Palade bodies is released and E-and P-selectin are placed on the luminal membrane of the affected endothelial cell. Now the sialyl-Lewis X presenting leukocytes can bind to the endothelial cells, which initiates rolling and extravasation and therefore enables immune responses [103-105]. Some cancer cells that also present sialyl-Lewis X are able to hijack this system and use it to migrate into the underlying tissue therefore making sialyl-Lewis X an important player during metastasis [106, 107].

The Galili epitope

The Galα1-3Gal terminus is synthesized by a specific α1-3 Gal-transferase that is expressed by many mammals but not by Old World primates such as humans. Therefore this epitope is immunogenic in humans. About 1% of human IgG is specific for the terminal Galα1-3Gal epitope [108]. Studies have proposed that this specific antibody may play a role in the removal of normal senescent and pathological human erythrocytes from the circulation [109]. Only 1% of normal human red blood cells were found to bind anti-Galα1-3. These cells had the highest density, and are thought to be the senescent red blood cells. Moreover, much greater proportions of thalassemic and sickle cells interact with anti-Galα1-3. Other studies have also shown that the bacterial lipopolysaccharide from *Salmonella sp*. and *E. coli* contain terminal α-1,3-Gal [110, 111].

α2-3-sialylated glycans

At least six different α2-3 Sia-transferases are responsible for synthesizing α2-3-sialylated glycans in deuterostomes [112]. A good example for an α2-3 sialylated glycan epitope is sialyl-Lewis X, the selectin ligand that was described above. Terminal α2-3-linked sialylation has been suggested to serve as a mask, to cover terminal Gal, that are recognized by the asialoglycoprotein receptor which mediates the removal of glycoproteins from the serum [113]. In $CD8^+$ T cells α2-3 sialylated glycans have been shown to enhance cell survival and act protectively against apoptosis, which serves as a means in lymphocytes to eliminate self-reactive immune responses [114].

As α2-3 sialylated glycans are terminal epitopes that are at the outermost layer on the cell surface, they also play an important role during infections. Hemagglutinin of the avian influenza virus for instance binds to α2-3 sialylated glycans in the avian respiratory tract [115]. For an influenza virus to infect humans however, the specificity of hemagglutinin must be altered to bind α2-6 sialylated glycans as these are more common in the upper human respiratory tract [116]. *Helicobacter pylori* is another pathogen that exploits sialylation for its disease progression by binding to α2-3 sialylated

glycans in the gastrointestinal tract mucosa where it can cause gastritis, gastric ulcers, and lymphomas in the gastrointestinal tract mucosa [117].

α2-6-sialylated glycans

There are also at least six enzymes that are able of catalyzing the transfer of α2-6-linked Sia in vertebrates [118]. St6gal1 is expressed by hepatocytes and lymphocytes [119]. Because mainly St6gal1 is responsible for α2-6 sialylation in lymphocytes, it is not surprising that mice that have a debilitating mutation in St6gal1, have an immune pathology that is characterized by a reduced antibody response to T-cell dependent and independent antigens [120]. B cell proliferation is also strongly reduced in response to CD40 and IgM crosslinking on the cell surface and the IgM serum levels are decreased by 65% [120]. Another very critical role of α2-6 surface sialylation is its dampening role in B cell responses. On the cell surface of B lymphocytes there is a receptor named Siglec-2 which dampens B cell responses when it binds to α2-6 Sia that is presented on the cells own cell surface [121].

α2-8-sialylated glycans

The α2-8 Sia epitope occurs mainly in the nervous system of vertebrates [122]. There are at least five different α2-8-Sia-transferases in deuterostomes [123] and two of them, St8sia2 and St8sia4 are able to synthesize polymers of 200 or more α2-8 linked Sia residues, which are termed poly-Sia [124]. N-glycans with α2-3 linked Sia serve as an acceptor for Sia-transferases capable of synthesizing polysialic acid [123]. An example of such a protein is the embryonic form of NCAM which due to the modification has less homotypic interactions than the adult form of the protein [125-127]. This interferes with cell-adhesion processes in the nerve system and may create a more plastic environment that favors the formation of the nervous system in the early stages [128]. Mice that are deficient for St8sia2 for instance, have misguided migration of a subset of hippocampal neurons [129]. A deficiency for both St8sia2 and St8sia4 leads to a severe impediment of the nervous system and leads to premature death. Interestingly, this phenotype can be rescued by knocking out NCAM which shows that the phenotypes are due to the loss of polysialic acid on NCAM [130].

Glycolipids can also present α2-8 linked terminal Sia. Unlike the large polysialic acid molecules that are observed on NCAM for instance, only oligomeric α2-8 Sia is attached to glycolipids [131]. This is catalyzed by the three enzymes St8sia1, St8sia3 and St8sia5 [123].

Mucins

A prominent class of O-glycoproteins is the mucin-family. Mucins are high-molecular weight proteins and are produced by epithelial cells in animals. The interesting thing about these proteins is that they

are heavily glycosylated (Fig. 12). They are often secreted as a gel-like substance and therefore can serve as lubricants or barriers. They can however also influence cells by binding to receptors on their surface and have attained a reputation as inhibitors of cell signaling. The extensive glycosylation of these proteins has given them a large water-holding capacity and also makes the protein backbone resistant to protease digestion. Especially the latter is of importance in maintaining mucosal barriers that are constantly exposed to proteases such as in the digestive tract [132].

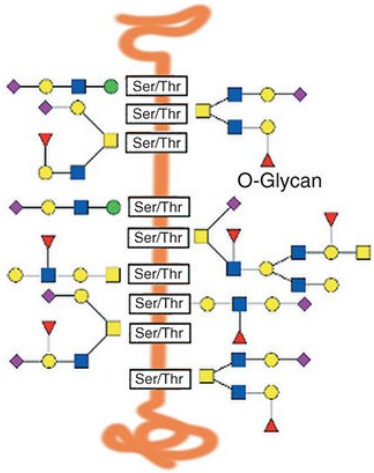

Figure 12: Generic structure of a mucin monomer. Mucins contain repeat structures that have many serine and threonine residues that are O-glycosylated, resulting in dense glycosylation (modified from [133]).

Mucins can either be membrane bound or secreted. Up to now 20 different mucins have been characterized in humans. Secreted mucins consist of a heavily glycosylated central region and flanking cysteine rich regions that can form intermolecular disulfide bonds with other mucin monomers. Due to these intermolecular disulfide bonds, secreted mucins can form massive aggregates with molecular weights that can reach 1 to 10 million Daltons. The oligosaccharides are attached via an O-GalNAc core to either serine or threonine [132].

O-linked GalNAc can be extended in at least eight different ways that result in eight different core structures (Fig.6). The cores 1 and 2 are the most common and are established by the attachment of β1-3 linked galactose to the reducing end GalNAc to make core 1 and an additional β1-6 linked GlcNAc to the reducing end GalNAc to make the second core (Fig. 6). The cores can then be extended with various monosaccharides and often present terminal Sia [134].

Secreted mucins mostly occur at mucosal surfaces such as the lungs or the intestine for example. MUC2 is present at the mucosal surface of the intestine and is produced by secretory goblet cells [135]. The O-linked glycans make up about 80% of MUC2's molecular mass [3, 136]. A monomer of MUC2 is about 2.5 MDa and after polymerization it can be more than 100 MDa in size [136]. MUC2

polymerization most likely occurs as a result of trimers that are formed between MUC2 dimers [136, 137].

Mucin glycosylation has been shown to play a pivotal role in maintaining the intestinal barrier. Mice that are engineered to lack the core 1 Gal-transferase for instance, develop intestinal bowels disease within 2 weeks after birth [138]. Another study has confirmed that the inner layer of the mucous can be penetrated by bacteria more easily in core 1 Gal-transferase lacking mice [139]. Therefore, it is not surprising that if the mice are treated with antibiotics, disease development is ameliorated [138]. Similarly, eliminating the core 3 Gal-transferase in mice leads to disturbed intestinal barrier function although not as extreme as is observed in core 1 Gal-transferase lacking mice [140]. The core 3 Gal-transferase deficient mice have increased permeability and colonization of their colon mucosa. The application of dextran sodium sulfate also leads to an exacerbated onset of colitis in comparison to wild type mice [140].

The glycans presented by mucins also seem to influence the microbial composition. Mice that lack β1-4-GalNAc-transferase 2 for instance have an altered microbiota that is especially noticeable in the ileum [141]. These mutant mice are not able to add GalNAc to Gal residues that are substituted with an α2,3-linked Sia and therefore lack the so called Sd[a]/Cad antigen [141]. Interestingly, these mutant mice have extremely low numbers of *Helicobacter sp.* which indicates that the Sd[a]/Cad glycan epitope is especially important for this particular species to be able to establish itself in the digestive tract [141].

The O-glycans on mucins can also promote the cultivation of beneficial bacteria in the gut. The symbiont *Bacteroides thetaiotaomicron* for instance, stimulates angiogenesis to increase the absorptive capacities of the gut [142], produces short chain fatty acids that can be used for energy when absorbed in the colon, inhibits inflammatory responses in the intestine [143] and induces the production of antimicrobial molecules at the mucosal surface [144]. *B. thetaiotaomicron* has more than 80 polysaccharide utilization loci whereas mucin-type O-glycans induces the expression of 16 of them. Furthermore, if L-Fuc becomes scarce, *B. thetaiotaomicron* can induce the expression of 2-α-L-Fuc-transferase 2 (Fut2) in intraepithelial epithelial cells of the gut which leads to more α1-2 linked fucosylation on mucin-type O-glycans in the gut [145, 146].

The *Bifidobacteria* genus is another example for symbiotic bacteria in the intestinal tract. There is evidence that they can counteract pathogen colonization [147] and inhibit the development of cancer due to colitis [148]. A well-known member of this bacterial genus is *Bifidobacterium bifidum* which is often found in the guts of infants. It possesses many glycosidases that are able to digest the oligosaccharides that occur on mucin-type O-glycans [149, 150]. An example of such a glycosidase is

endo-α-GalNAc-aminidase which can hydrolyze the bond between GalNAc and serine or threonine in O-glycosidic linkages [151]. Also 1,2 α-L-fucosidase, which can cleave off terminally α1-2 linked Fuc, occurs in *B. bifidum* [152]. Interestingly when *Bifidobacteria* bind to mucins, glycosidases such as the ones mentioned above are expressed [153].

Escherichia coli is one of the most common facultative anaerobes in the mammalian gut [154]. Defects in its carbohydrate utilisation locus impact the capability of *E. coli* to colonise and persist in the gut of mice [154]. Interestingly, the dependence of *E. coli* on different mucin-type O-glycans changes during the course of colonisation. During the log phase of colonisation for instance *E. coli* upregulates genes that are necessary for the catabolism of GlcNAc while Sia and Fuc catabolism is required during the stationary phase of gut colonisation [154].

Certain bacteria that colonise the gut don't have the machinery to feed on mucin-type O-glycans. They profit from the hydrolytic activity of other intestine colonising bacteria. *Akkermansia muciniphila* for instance can degrade the glycans on MUC2 but *Bacteroides vulgatus* cannot [155]. Therefore, *B. vulgatus* cannot grow on MUC2 as its sole carbon source. However, when *A. muciniphila* and *B. vulgatus* are co-cultured, the growth of the latter does take place [155].

Another example demonstrating how mucin glycosylation can alter the microbiota in the gut is the influence of the secretor status on the microbial composition. The secretor status depends on the functionality of the galactoside FUT2. FUT2 is responsible for linking L-Fuc to Gal via an α1-2 linkage on mucin-type O-glycans which leads to the formation of the so called H-antigen [156]. The H-antigen itself can be further processed to the blood group A and B antigens or can be modified by the Lewis transferase, resulting in the production of the Lewis determinants Le^b and Le^y [156]. About 20% of the Caucasian population is homozygous for a null allele within the FUT2 gene, resulting in the total absence of the H-antigen on all mucin-type O-glycans [156]. Such individuals are known as non-secretors while people with at least one functional FUT2 allele are known as secretors. The gut microbiota of "non-secretors" is distinctly different from that of secretors. Species of the genus *Prevotella* for instance are enriched within the gut of non-secretors [157]. This genus of bacteria is able to hydrolyze terminal 6-SO3-GlcNAc on mucin-type O-glycans [158]. The desulfation of mucins by *Prevotella* species is a critical observation especially as desulfated mucin O-glycans have been associated with exacerbated inflammation after dextran sodium sulfate treatment [158]. Mice that lack the GlcNAc 6-sulfotransferase for instance have an increased infiltration of $CD45^+$ inflammatory cells, including neutrophils and macrophages, into the colon [159]. Also the absence of the sulfate transporter NaS1, which maintains the levels of circulating sulfate, in knockout mice leads to an exacerbation of colitis in the DSS model [160].

O-glycans on mucins can also influence the immune system directly. Recently, the group of Andrea Cerutti demonstrated that MUC2 can be ingested by antigen-sampling dendritic cells. The glycans presented by MUC2 had an anti-inflammatory effect that is mediated via a galectin-3-Dectin-1-FcγRIIB receptor complex that activates the transcription factor β-catenin. They then showed that β-catenin can block the expression of inflammatory cytokines by inhibiting the nuclear factor κB. Tolerogenic cytokines on the other hand aren't influenced by β-catenin [4].

Some mucins are not secreted but instead are incorporated into the plasma membrane of the expressing cell. Examples for membrane incorporated mucins are MUC1, MUC3A, MUC3B, MUC4, MUC12, MUC13, MUC15, MUC16, MUC17, MUC20 and MUC21. They have a single transmembrane domain, a short intracellular domain (22-80 amino acids) and a large extracellular domain. The major components of the extracellular domain are the tandem-repeat domains which is also the key feature of all proteins that are classified as mucins. As with the secreted mucins these repeats are highly glycosylated. Membrane-bound mucins are highly diverse and involved in many different processes such as modulating immune responses or facilitating adhesion between cells [161].

Soluble Glycans

Not all glycans are attached to another biomolecule. Human milk oligosaccharides (HMOs) and hyaluronan are examples for glycans that are secreted by cells and also have important modulatory functions. HMOs are a structurally highly diverse collection of sugars that occur in human milk. They contain the five monosaccharides Glc, Gal, GlcNAc, Fuc and Sia. The reducing end is always lactose that is elongated with β1-3- or β1-6-linked lacto-*N*-biose (Galβ1-3GlcNAc) or N-acetyllactosamine (Galβ1-4GlcNAc). Lacto-*N*-biose chains cannot be further modified with Gal, Fuc or Sia while N-acetyllactosamine can be modified with one or two further monosaccharides. β1-6-linkages between monosaccharides introduce branching points in the lacto-*N*-biose and N-acetyllactosamine chains (Fig. 13).

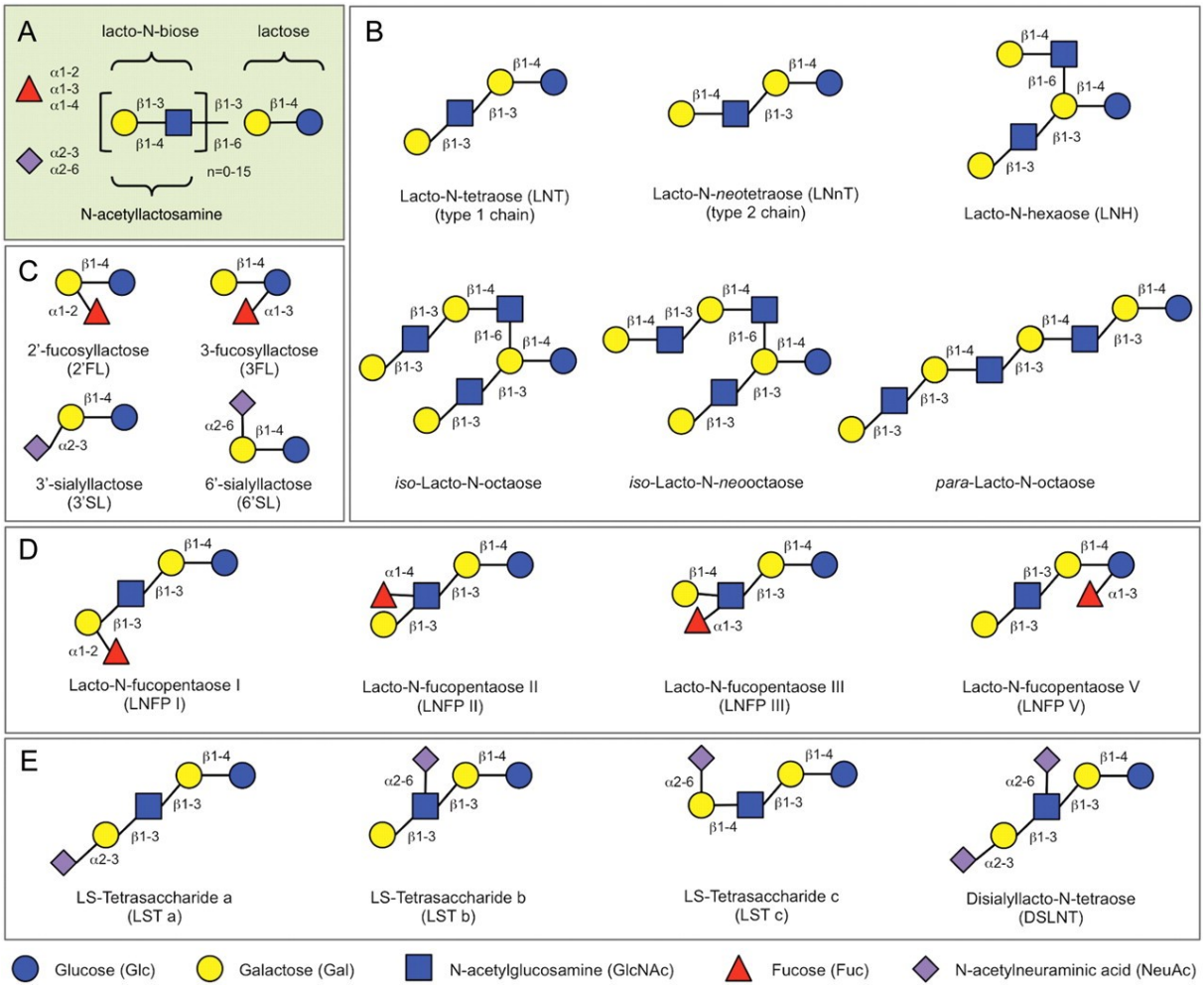

Figure 13: The structural diversity of HMOs. (A) The structure of all HMOs follows the same blueprint with lactose at the core. The elongation of lactose occurs by attaching N-acetyllactosamine or lacto-N-biose repeats. (C) Simple trisaccharides can be established by sialylating or fucosylating lactose. Elongated HMOs can also be (D) fucosylated or (E) sialylated (copied from [5]).

HMOs play an important role for the breastfed infant. Originally, HMOs were discovered as factors that promote the growth of *Bifidobacteria*, which are desirable bacteria that grow in the gut of neonates. Furthermore, HMOs can serve as soluble decoys for pathogens that bind to them, which ultimately displace them from the epithelium. The best example for this role of HMOs was observed in studies with *Campylobacter jejuni* that bind to α1-2-fucosylated surface glycans and can be displaced by soluble α1-2-fucosylated HMOs. Feeding mice with α1-2-fucosylated HMOs lead to reduced colonization by *C. jejuni* [162]. HMOs can also directly interact with epithelial cells to alter their gene expression, leading to changes in the cell's surface glycans which directly affects the adhesion of bacterial subtypes to the guts epithelium. 3'-sialyllactose binding to epithelial cells for instance lowers the expression of the Sia-transferases St3gal1, St3gal2 and St3gal4 which leads to decreased α2-3- and α2-6-sialylation on the cell surface [163]. HMOs are also able to directly affect leukocytes. They can influence the production of cytokines by lymphocytes leading to a more

balanced Th1/Th2 response [164]. This was shown with cord blood T-cells that have been exposed to sialylated HMOs which increases the amount of interferon-γ-producing CD3+CD4+ and interlukin-13 (IL-13) producing CD3+CD8+ lymphocytes [164]. Another study was able to show that human milk oligosaccharides interfere with the interaction of selectins with their ligands, ultimately leading to less leukocyte rolling on activated endothelial cells which is required for leukocyte extravasation and the recruitment of cells to inflamed tissues [165].

Recent results indicate that HMOs may directly regulate antigen presenting cells like dendritic cells. The onset of colitis was delayed in $IL10^{-/-}$ mice that were deficient for the α2-3 Sia-transferase 4 that, among other functions, is responsible for the synthesis of 3-sialyllactose. When these mice were supplemented with 3-sialyllactose the severity of colitis was restored. The authors then demonstrated that 3-sialyllactose was able to directly stimulate lymph node $CD11c^{+}$ dendritic cells via TLR4 signaling [166].

Hyaluronan is another soluble glycan that has many regulatory functions. It consists of the monosaccharides glucuronic acid and GlcNAc that are linked alternately by β1-4- and β1-3-linkages. The polymers can range from 5'000 to 20'000 kDa in size [6]. Hyaluronan binds to membrane proteins such as CD44 and leads to their clustering on the cell surface. This mediates the activation of downstream kinases like c-Src and the focal adhesion kinase. In tumor cells this results in proliferation and invasion while in embryonic cells an epithelial to mesenchymal transition is induced [167]. Surprisingly in light of these results however, high-molecular weight hyaluronan has been shown to be protective against cancer metastasis in naked mole rats which is the reason why these animals don't suffer from cancer although cancer often affects aged rodents [168]. Hyaluronan is also an important component in joints where it acts as a lubricant but also dampens impacts during movement which counteracts degradative processes [169]. Another important role of hyaluronan is the protective layer it forms around the egg cells. To successfully fertilize the egg cell, sperm cells therefore must produce hyaluronidases, so that they can access the plasma membrane [170]. Hyaluronan is also crucial in other processes such as wound repair, inflammation and cell migration [6].

Immune regulatory roles of bacterial glycans

As with mammalian cells the outermost layer of bacterial cells is composed of glycans which form the interface of bacterial cells with their environment and with other bacteria or host cells. The capsules and O-antigens are the outermost glycans of many bacterial cells and they are highly immunogenic and result in strong antibody responses. Bacterial species are often classified into serological groups according to their specific O-antigen. In *E. coli* alone 173 different O-antigens and 103 different

capsular polysaccharides have been identified. The consequence is that contact to one specific serotype does not mean that the immune system can mount a challenge against the pathogen in general but to the specific serotype. Therefore it is possible that the same species can infect a host if it has a serotype that the immune system has not encountered yet [171].

The N- and O-glycosylation machineries also exist in bacterial cells. S layer glycoproteins that occur in the peptidoglycan layer of Gram-positive bacteria were one of the first bacterial protein classes where glycosylation was detected [172, 173]. Later, the pili of *Neisseria gonorrhoeae* and *N. meningitides*, as well as the flagella of *Pseudomonas aeruginosa* and *Helicobacter pylori* were proven to be glycosylated [171]. These glycoproteins are frequently of great relevance for interactions of the host with bacteria. The mannosylated Apa glycoproteins of *Mycobacterium spp.* is able to inflict delayed-type-hypersensitivity reactions in vivo and activate the amplification of T lymphocytes in vitro but these effects are lost when the Apa glycoprotein is chemically or enzymatically deglycosylated [174].

Some bacteria are able to ingest the glycans of their host and present them on their own surface. One example is the pathogen *Haemophilus influenzae* which can scavenge Sia from its environment and activate it to CMP-Sia to attach the monosaccharide to its lipopolysaccharides [175]. Not only pathogens can present host derived glycans on their surface but also commensals such as *B. thetaiotaomicron* for instance can enhance the expression of α1-2 fucosyltransferase by intestinal epithelial cells [176]. This leads to the upregulation of fucosylated glycans on the host's epithelium. These Fuc residues are released and absorbed by *B. thetaiotaomicron* with a Fuc specific permease. Inside the cell the Fuc is metabolized to GDP-Fuc and subsequently incorporated into the capsular polysaccharides and lipopolysaccharides [177]. The surface Fuc is very important for *B. thetaiotaomicron* to colonize the gut of their host as was shown with mutant strains that are not able to incorporate Fuc [178].

The oligosaccharides on the cell surface are also a useful tool for bacteria to evade immune surveillance. *Neisseria meningitidis* for example presents Sia on its surface to evade the complement cascade [179]. Sia is a common terminal monosaccharide on many host glycans in mammals. It has many functions of which one is to hinder the hosts own cells being attacked by the complement system, by recruiting the complement factor H. The central component of the complement cascade is the factor C3 which binds to cell surfaces and via different mechanisms is cleaved to the factors C3a and C3b. The latter of the two acts as an opsonization signal and also initiates cytolysis by initiating the formation of a membrane attack complex [180]. If factor H is recruited to the cell surface however, it mediates the cleavage and deactivation of factor C3b, thereby stopping the complement

system in its track [181]. The production of a hyaluronic acid capsule by group A streptococci is another good example of molecular mimicry by a pathogen to avoid the host's immune system [182].

Another class of polysaccharides that have very interesting immunological properties are so called zwitterionic polysaccharides. These sugars have both a positive and a negative charge. Normally, polysaccharides are T-cell-independent antigens and can therefore not stimulate IgG class switching in B cells or elicit immunologic memory. However, zwitterionic polysaccharides have been shown to be presented on MHC class II. The pathway of presentation remains the same as for protein antigens [183].

Bacterial glycans are also a key class of molecules to establish long-term interactions between commensal bacteria and the host. *Bacteroides fragilis* can produce at least eight capsular polysaccharides [184]. Phase variation between the different capsular polysaccharides is controlled by a DNA inversion based mechanism and enables this commensal species to react to the immune system and phage infections, making it extremely competitive in cultivating the mammalian gut [184]. Some of the capsular polysaccharides of *B. fragilis* are also important in maintaining the health of the host. Polysaccharide A is the most commonly produced capsular polysaccharide produced by *B. fragilis* and it plays an essential role in the maturation of the immune system [185]. It is a well-known fact that mice kept in a germ-free environment have an underdeveloped intestinal immune system [186]. If the mice are mono-associated with *B. fragilis,* immune system maturation is rescued. However, if the bacteria lack the genetic locus that is responsible for the synthesis of polysaccharide A, the maturation of the immune system is not restored. Mice that are cultured with polysaccharide A lacking *B. fragilis* had less $CD4^+$ splenic lymphocytes and these cells produced markedly less interferon-γ. However they produced more IL-4 which lead the authors to speculate that polysaccharide A plays a key role in regulating the homeostasis of the Th1/Th2 response and that this is central for the correct maturation of the guts immune system [187].

The glycans on *Helicobacter pylori* also seem to regulate the host's immunity. Many O-antigens are fucosylated and resemble the Lewis blood group antigens of the host [188]. Similar to the capsular polysaccharides of *B. fragilis*, the antigens presented by *H. pylori* are phase variable which is steered by slip-strand mispairing in the coding regions of the Fuc-transferase genes [189]. This results in a heterogeneous population of *H. pylori*. The Lewis antigen-positive bacteria can bind to the C type lectin DC-SIGN that is expressed by dendritic cells and thereby inhibit the differentiation of T cells into Th1 cells and block immune responses [190]. The Lewis antigen-negative population on the other hand fails to bind to DC-SIGN and promotes the development of Th1 cells and a proinflammatory environment instead. Phase variation therefore enables *H. pylori* to modulate its environment to create an ideal niche to colonize the host [191].

The glycobiology of cell death

In the 1980s researchers were able to show that lectins expressed on the cell surface of macrophages can specifically recognise dead cells. Therefore, dying cells must have their own specific cell surface glycome [192]. This opened up an interface between the fields of cell death biology and glycobiology. Not only is altered glycosylation a consequence of cell death but it also plays a modulating role on programmed cell death. Glycosylation of cell-death receptors for instance can fine tune the sensitivity of cells to death [193]. Certain glycans can also recruit a class of lectins termed galectins that can initiate apoptosis after being recruited to the cell surface [194].

Galectins

Galectins are a family of β-galactoside binding lectins that are atypically secreted into the extracellular space. They are also present in the cytoplasm or in the nucleus. Up to now 15 galectins have been discovered in mammals of which only 13 occur in humans. Galectins are either dimers or have a tandem conformation, except for galectin-3 which has a chimeric shape (Fig. 14). The structure of galectins enables them to crosslink different glycan epitopes [195].

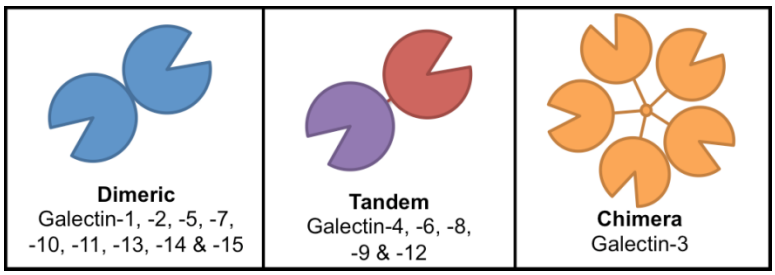

Figure 14: Some galectins form dimers with two equal carbohydrate binding domains (dimeric) while others have two different carbohydrate binding domains (tandem). Galectin-3 is an exception and can form so called chimeras with five equal carbohydrate binding domains (copied from [196]).

The major ligands of the galectins are lactose and N-acetyllactosamine. Tandem repeats of these motifs, like for instance poly-N-acetyllactosamine, lead to increased binding affinities of the galectins due to more Van der Waals interactions taking place between the carbohydrate and carbohydrate binding pocket of the galectin. The binding specificities of the individual galectins to different glycan structures do vary however [197]. The galectins-2 and -3 bind more strongly to fucosylated A and B blood group antigens than galectin-1 while galectin-2 exhibits reduced binding to sialylated glycans compared to the galectins-1 and -3 [198].

Galectins are involved in many processes such as mediating cell-cell interactions, cell-matrix adhesion and transmembrane signaling [196]. Interestingly they can also regulate cell death either from outside or from inside the cell. On the cell surface galectins can initiate cell death by triggering

further downstream signaling processes by crosslinking glycosylated receptors on the cell surface [194]. One example for galectin-mediated cell death is the negative selection of T cells in the thymus. The galectins-1 and -9 are both secreted by epithelial cells in the thymus and can mediate T cell apoptosis. The galectins-1 and -9 are also crucial for the elimination of activated and infected T cells after immune responses in the periphery [194]. Galectin-1 can interact with several receptors on the cell surface but especially its interactions with CD7, CD43 and CD45 are important to induce apoptosis. In keratinocytes the expression of galectin-7 is regulated by p53 and is believed to be necessary to regulate apoptosis after damage by UV-light [194, 196]. Galectin-12 is also apoptosis promoting but in adipocytes [196]. Galectin-3 on the other hand has anti-apoptotic properties. Interestingly it is the intracellular form of galectin-3 that has been shown to have an anti-apoptotic effect. Although the precise mechanism is unclear, it seems to be due to its ability to bind to Bcl-2, an anti-apoptotic, intracellular protein [194]. Extracellular galectin-3 on the other hand can promote cell death as has been observed for T cells and neutrophils [196].

Siglecs

Siglecs are type I membrane proteins that have an extracellular N-terminal and intracellular C-terminal domain. The N-terminus consists of a V-type immunoglobular domain that is responsible for ligand binding. The primary ligands of Siglec proteins are Sia containing glycans. As the most Siglecs have a relatively short stem, they do not usually bind to the glycans on other cells but to the glycans on the own cell surface. The only exception is Siglec-1 which has 16 C2-Ig domains, making it long and capable of binding to glycans on other cells [199].

In primates 17 Siglecs have been identified to date. Mice on the other hand only have 8 Siglecs. Most of them are expressed by immune cells such as Siglec-2 which is expressed by B cells [121, 200]. But some Siglecs, such as Siglec-4 that is present on myelin cells [201], are also expressed by other cells.

The most Siglecs have an intracellular immunoreceptor tyrosine-based inhibition motif (ITIM)-domain. Once a respective Siglec has bound its ligand, a tyrosine residue in the ITIM-domain is phosphorylated which enables the recruitment of SH2 domain-containing proteins such as SHP phosphatases. This leads to the dephosphorylation of several proteins and is responsible for immune dampening reactions [202]. Activated Siglec-7 for example will mediate the dephosphorylation of the activatory nuclear factor ZAP-70 that is downstream of T cell receptor signaling [203]. The Siglecs-14 and -15 in primates and Siglec-H in mice have a positively charged arginine or lysine residue in the cytoplasmic domain that is able to recruit ITAM-containing adapter proteins such as DAP10 or DAP12 that mediate the up-regulation of several phosphorylation cascades and the activation of cellular

signaling cascades [200, 204, 205]. DAP12 for instance is able to phosphorylate Syk in myeloid and NK cells as well as ZAP-70 in NK cells which all mediate proinflammatory signaling [206].

Recently, Siglecs have also been shown to be able to induce cell death. Siglec-8 for instance is present on the surface of eosinophil cells and its ligation leads to apoptosis. In the presence of IL-5 however, the cells undergo caspase-independent necrotic-like cell death that is dependent on the formation of reactive oxygen species and the phosphorylation of ERK1/2 and MEK1 [207].

The clustering of Siglec-7 by specific $F(ab')_2$ fragments also leads to cell death in the monocytic cell line U937. However, the effect is independent of the intracellular ITIM-domain as cells expressing a truncated version of Siglec-7 still underwent cell death when Siglec-7 was clustered. Also the oxygen radical scavenger N-acetyl cysteine completely inhibits this form of Siglec-7 mediated cell death but a pan-caspase inhibitor did not. The authors identified the middle of the membrane-proximal C2-set domain as absolutely required for cell death and therefore concluded that the cell death inducing signal is transduced extracellularly [208]. Human neutrophils can undergo autophagic-type cell death as a consequence to Siglec-9 ligation in the presence of cytokines that are required for neutrophil survival such as GM-CSF. For this type of cell death to occur the inhibition of caspases and the production of reactive oxygen species is required [209].

Death-receptor glycosylation and cell death regulation

The TNF-related apoptosis-inducing ligand (TRAIL) induces cell death by binding and activating the receptors TRAIL-R1 and TRAIL-R2. The ligation of TRAIL to these receptors initiates the formation of the Death-inducing signaling complex (DISC) by recruiting the caspases-8 and -10 together with the adaptor protein FADD [210]. These initiator caspases then mediate the activation of effector caspases such as caspase-3 that cause the dismantling of the cell [211].

The sensitivity of a cell to TRAIL is not only dependent on the expression level of the receptors but also on their post-translational modifications. TRAIL-R2 for example is O-glycosylated which is required for the formation of the DISC and apoptosis as a consequence of TRAIL binding [212]. On the other hand, N-glycosylation regulates TRAIL-R1 as was shown in N-glycosylation-deficient TRAIL-R1 mutants. Cells that express unglycosylated versions of the human TRAIL-R1 or the murine TRAIL-R are less sensitive to TRAIL treatment due to lower TRAIL receptor aggregation and less DISC formation, however the binding affinity of TRAIL to the receptor is not affected [193].

Programmed cell death

Cell death can either be the result of necrosis or due to a form of programmed cell death [213]. Necrosis is a process that is caused by cell injury or infection and is dependent on cell external factors. Programmed cell death however is a regulated process that leads to the death of a cell in a defined manner with a specified outcome. There are several forms of programmed cell death such as apoptosis, pyroptosis and necroptosis. While apoptosis is not inflammatory, necroptosis and pyroptosis are highly inflammatory processes [214].

Necrosis

Necrosis can be viewed as the premature death of a cell caused by cell injury. In contrast to programmed forms of cell death, necrosis is almost always a negative event that is detrimental and can be fatal for the organism. Necrosis is not initiated by a general signaling pathway as apoptosis is, instead it is caused by the loss of membrane integrity and the leakage of cellular components into the extracellular space [215]. This leads to an inflammatory response in the vicinity which attracts leukocytes to the site of damage that eliminate the debris by phagocytosis. Necrosis is characterized by oncosis which is cell swelling. The cell starts to bleb and the nucleus shrinks before dissolving into the cytoplasm [216].

Apoptosis

Apoptosis can be initiated in many different ways. It is characterized by morphological and intracellular changes. First the cells start to shrink and become round because the cytoskeleton is being digested by caspases [217]. The cytoplasm becomes dense and the organelles become tightly packed. The chromatin then starts to become denser and compact patches develop beneath the nuclear envelope, a process that is known as pyknosis [218, 219]. In later stages the DNA starts to fragment [220] and irregular blebs start to occur on the cell membrane. Finally the cell starts to break apart. The fragments that are formed are known as apoptotic bodies [221]. Apoptosis can be initiated by an intrinsic and an extrinsic pathway (Fig. 15). The intrinsic pathway is initiated by cell endogenous stress such as the formation of reactive oxygen species while the extrinsic pathway is initiated by signals derived from other cells such as cell death signaling proteins like TRAIL [222].

Proteases called caspases play a central role during apoptosis. The caspases 8, 9 and 10 are initiator caspases [223] while the caspases 3, 6 and 7 are effector caspases [224]. Initiator caspases require activation by either the intrinsic or extrinsic pathway. They then activate the effector caspases by cleaving them. The effector caspases then start proteolytically digesting an array of intracellular proteins which ultimately leads to cell death [224].

Intrinsic pathway

The intrinsic pathway is initiated via apoptotic proteins that disrupt the mitochondria. This often leads to mitochondrial swelling and increased mitochondrial permeability which causes pro-apoptotic factors to leak into the cytoplasm [225]. Proteins called secondary mitochondria-derived activator of caspases (SMACs) are released into the cytoplasm as a consequence. They can bind to proteins that inhibit apoptosis (IAPs) and block their activity. IAPs normally suppress apoptosis by binding to caspases and inactivating them [226].

Cytochrome c is another component that is released by the mitochondria that plays a central role during apoptosis [227]. In the cytoplasm it binds to the apoptotic protease activating factor-1 and ATP which then associates with the pro-caspase-9 to form a complex known as the apoptosome (Fig. 15). In this complex pro-caspase-9 is cleaved to its active form which can then activate the effector caspase-3 [223].

Extrinsic pathway

TNFR1 stimulation can lead to the activation of caspases through the TNF receptor-associated death domain and the Fas-associated death domain proteins that together with the caspases 8 and 10 assemble to form the DISC (Fig.15). However, usually tumor necrosis factor-α (TNF-α) stimulation does not induce apoptosis due to simultaneous NF-κB signaling that leads to the expression of FLIP, a protein that stops the activation of caspase-8 [228]. Furthermore, the proteins cIAP1 and cIAP2 are upregulated that are able to ubiquitinate an apoptosis promoting protein called the kinase receptor interacting protein 1 (RIPK1). The consequence of RIPK1 ubiquitination is that it associates with the pro-survival kinase TAK3 and becomes deactivated [229]. If cIAP 1 and 2 are depleted, RIPK1 will not be ubiquitinated and will become an essential part of the DISC that ultimately mediates the activation of the caspases 8 and 10 [230].

The Fas pathway is another possibility to extrinsically induce apoptosis. It occurs when the transmembrane protein “Fas ligand” binds to the Fas receptor on the designated target cell [231]. Fas ligand itself is actually a member of the TNF family [231]. The interaction of Fas ligand with the Fas receptor leads to the formation of the DISC which contains the Fas-associated death domain protein, caspase-8 and caspase-10. Activation of the initiators caspases-8 and -10 leads to the activation of the downstream effector caspases [232].

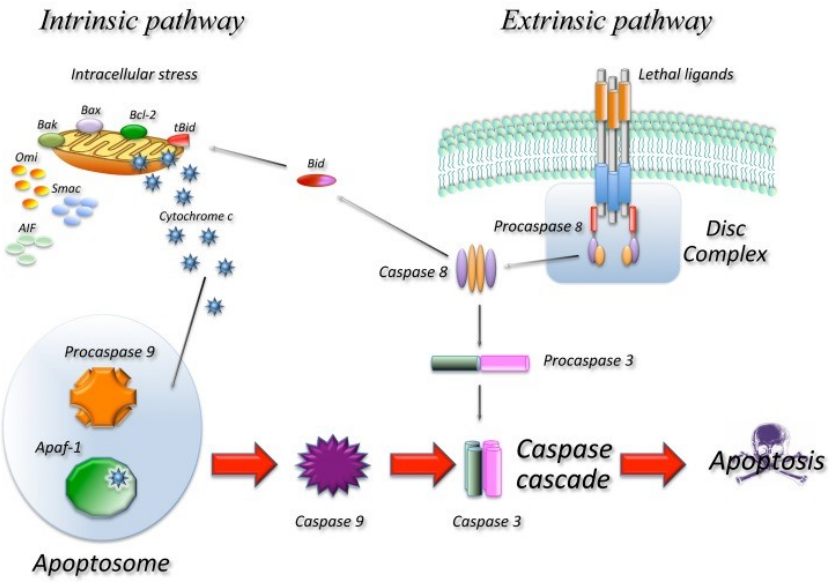

Figure 15: Intrinsic and extrinsic apoptosis inducing pathways. In the intrinsic pathway, cytochrome c is released from the mitochondria, which initiates the formation of the apoptosome that cleaves and activates caspase-9. In the extrinsic pathway the stimulation of a death receptor leads to the intracellular formation of the DISC which mediates the activation of caspase-8 (copied from [233]).

Pyroptosis

Pyroptosis is a form of programmed cell death that mainly occurs in immune cells and is initiated from within the cell itself by the recognition of cell internal pathogens or danger associated molecular patterns. Unlike during apoptosis, the plasma membrane ruptures and damage associated patterns such as ATP, DNA or the adapter protein ASC are released into the extracellular space. The inflammatory cytokines IL-1β and IL-18 are also released. Pore formation which leads to a disrupted cellular ionic gradient, results in disturbed osmotic pressure and the influx of water that ultimately causes the cell to swell and burst [234].

For the initiation of pyroptosis so called NOD-like receptors are required that recognize pathogen- or danger associated molecular patterns inside the cytoplasm. There are more than 20 subsets of NOD-like receptors [235]. The best characterized are NOD1, NOD2, NLRP3 and NLRC4 [236]. They all recognize bacterial, viral and toxic foreign components or danger associated molecular patterns in the cytoplasm. The recognition of ligands by NOD-like receptors leads to the formation of a so called inflammasome which is a single large protein complex that takes shape in the cytoplasm (Fig. 16) [237]. The inflammasome has many protein components but its most important are the respective NOD-like receptor protein, caspase-1 and the adaptor protein ASC [235].

The inflammasome is ultimately responsible for cleaving and activating caspase-1 [238]. Caspase-1 itself initiates pyroptosis and is responsible for cleaving the precursors of IL-1β and IL-18 into their active form. Until recently, caspase-1 was believed to be the only caspase that can initiate pyroptosis. However in 2013 murine caspase-11 and its human homologs caspases-4 and -5 were also proven to cause pyroptosis. For pro-caspase-11 expression, TRIF activation is absolutely necessary which can be caused by TLR3 or TLR4 signaling. Unlike caspase-1 that requires a receptor/scaffold mediator to recognize intracellular pathogen- or danger- associated molecular patterns to be activated, caspase-11 can directly bind to LPS via its caspase recruitment domain and become activated [239]. For pyroptosis to occur, affected cells often require priming by Toll like receptor signaling that leads to NF-κB signaling. The production of pro-IL-1β and pro-IL-18 is actually a consequence of Toll-like receptor signaling [240].

Not so long ago a protein called Gasdermin-D was identified as a substrate of the caspases-1/4/5 and -11. These caspases cleave Gasdermin-D in the middle linker, which releases the N-terminal fragment that perforates the plasma membrane during pyroptosis [241-244]. Recently, Gasdermin-E was shown to be cleaved by caspase-3 in the linker region, establishing an N-terminal fragment that can perforate the cell membrane [245]. Until this discovery, caspase-3 activity had mainly been associated with apoptosis. However, Gasdermin-E activation can direct cell death towards pyroptosis. The ectopic expression of gasdermin E was furthermore shown to be able to redirect TNF-α induced apoptosis to pyroptotic cell death in cultured cancer cells [245].

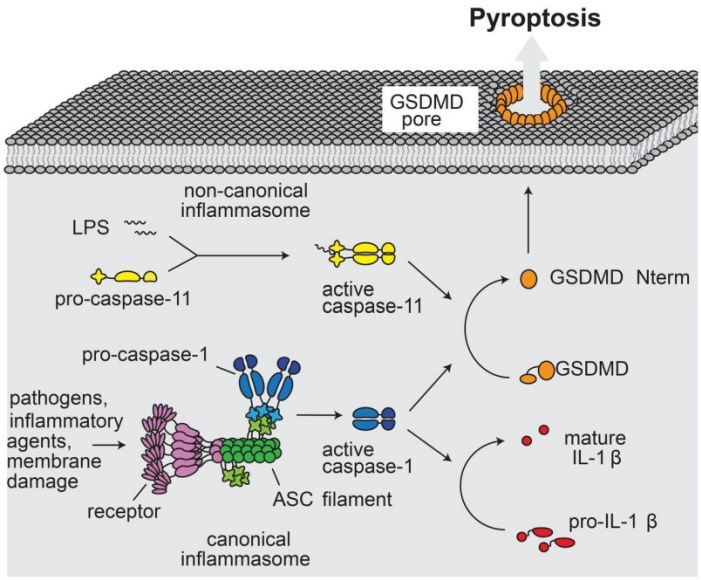

Figure 16: Pyroptosis is executed by Gasdermin-D. NOD receptors act as sensors for intracellular pathogens and danger-associated molecular patterns. The ligation of NOD receptors to a target mediates the formation of the inflammasome. ASC filaments acts as the central scaffold of the inflammasome and recruit pro-caspase-1 which is then activated. Pro-caspase-11 on the other hand does not need to be recruited to the inflammasome and can directly recognize its ligands such as LPS. Caspase-1 mediates the activation of IL-1β and both caspase-1 and -11 can activate gasdermin-D which then incorporates itself into the plasma membrane and forms pores that ultimately kill the cell (copied from [244]).

Necroptosis

Necroptosis is actually a programmed form of necrosis. It is a caspase-independent form of cell death that occurs in response to viral infections but also if cell homeostasis is lost. DNA damage for instance can lead to the downstream phosphorylation of the necroptosis drivers kinase receptor interacting proteins (RIPKs) 1 and 3 [246, 247]. Necroptosis can also be induced by TNF-α via the TNFR1. As with extrinsically induced apoptosis, the TNF-receptor associated death domain is responsible for initiating TNF-α inflicted necroptosis by signaling to RIPK1 which then recruits RIPK3 (Fig. 17) to the so called necrosome. The necrosome is only formed when caspase-8 remains inactive, otherwise DISC assembly and apoptosis will occur [248]. The necrosome is a microfilament-like protein complex that also accommodates the RIPKs 1 and 3 and is responsible for phosphorylating and activating a protein called mixed lineage kinase domain like pseudokinase (MLKL) [249]. Phosphorylation leads to MLKL oligomerization and its incorporation into the plasma membrane (Fig. 17) and the membranes of organelles inside the cell which leads to their permeabilization [250, 251]. This leads to the leakage of damage-associated patterns into the extracellular space which can elicit immune responses [249]. Incorporation of MLKL into the mitochondrial membrane may block the electron transport chain in

the mitochondria which inflicts mitochondrial damage and permeability [252]. The lysosomes are also damaged by MLKL which in response start to leak lysosomal hydrolases into the cytoplasm [253].

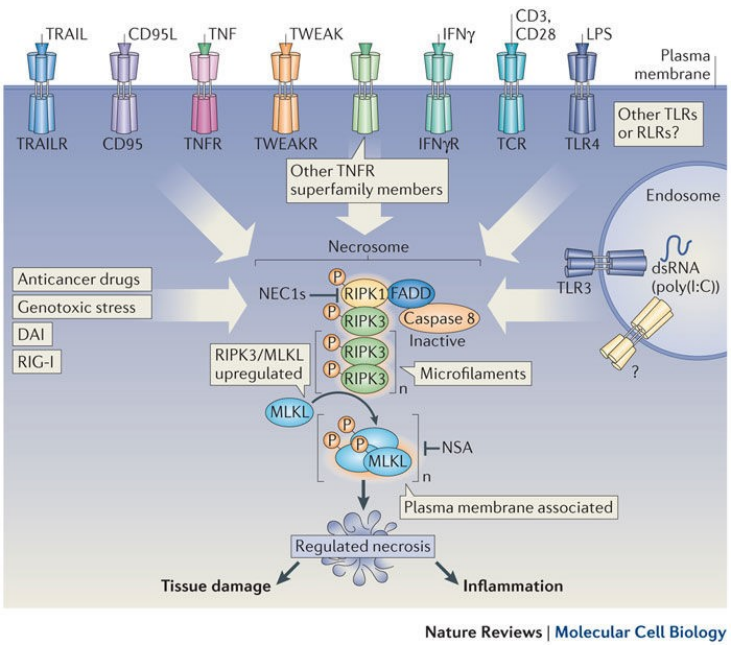

Figure 17: The necroptosis pathway. When caspase-8 is inactive, death receptor signaling leads to the assembly of the necrosome that consists of the RIPKs 1 and 3. The necrosome then phosphorylates MLKL which oligomerizes and is inserted into the plasma membrane. This leads to membrane damage and therefore cell lysis and death. Necroptosis can be inhibited with the small molecules necrostatin-1 (Nec-1) and necrosulfonamide (NSA) (copied from [248]).

The pathways that are involved during necroptosis and apoptosis are highly intervened and share many components. RIPK1 for example has been implicated during apoptosis [254] and necroptosis [255, 256]. RIPK1 interacts with both FADD and caspase-8 and is absolutely required for the induction of apoptosis in the presence of the IAP inhibiting SMAC mimetics [257]. This is evident in mice that lack RIPK1 as they have an increased amount of apoptosis and die at 1 to 3 days of age [258].

RIPK1 has a death domain which enables it to interact with death receptors such as the TNF receptor 1 or the Fas receptor that are required for caspase-8 mediated apoptosis [259, 260]. Furthermore, RIPK1 contains a RIP homotypic domain that is required for its interaction with RIPK3 [261]. The influence of RIPK1 on cell death is also dependent on its posttranslational modifications. RIPK1 can be ubiquitinated at lysine 63 which leads to the downstream activation of mitogen-activated protein kinases as well as NF-κB and the induction of downstream pro-survival genes. The ubiquitination of RIPK1 at lysine 63 is depleted in cells that lack cIAP 1 and 2. Depletion of cIAP 1 and 2 can be achieved by genetic means or by treating cells with so called SMAC mimetics that cause the degradation of IAPs [262, 263]. Deubiquitinated RIPK1 can then mediate apoptosis or necroptosis and is responsible for the formation of the apoptosis or necroptosis promoting signaling complexes

[264]. Caspase activity during apoptosis can inhibit necroptosis by cleaving RIPK1 and 3. If apoptosis is inhibited by applying pan-caspase inhibitors such as benzyloxycarbonyl-Val-Ala-Asp(OMe)-fluoromethylketone, cell death becomes skewed from apoptosis to necroptosis. In the necroptotic pathway, RIPK3 is further downstream of RIPK1 [265]. A-type NIH 3T3 and L929 cells that do not express RIPK3 and have been treated with zVAD, are protected from necroptosis [266].

Surprisingly, the Bcl-2 protein family member Bcl-2 modifying factor is required for necroptosis to take place. Bcl-2 is a protein that is located in the outer membrane of the mitochondria where it plays an important role as an inhibitor of pro-apoptotic proteins. There are however related proteins that fulfil a pro-apoptotic function such as Bax and Bak that are also in the outer mitochondrial membrane and mediate its permeabilization when activated during apoptosis. This results in pro-apoptotic mitochondrial residents, such as cytochrome c or reactive oxygen species, being released into the cytoplasm. Both Bax and Bak are activated by BH3-only proteins and are inhibited by BCL-2 and BCL-XI [267].

References

1. Zhang, L., S. Luo, and B. Zhang, *Glycan analysis of therapeutic glycoproteins.* MAbs, 2016. **8**(2): p. 205-15.
2. Roth, J., *Protein N-glycosylation along the secretory pathway: relationship to organelle topography and function, protein quality control, and cell interactions.* Chem Rev, 2002. **102**(2): p. 285-303.
3. Thomsson, K.A., et al., *Detailed O-glycomics of the Muc2 mucin from colon of wild-type, core 1- and core 3-transferase-deficient mice highlights differences compared with human MUC2.* Glycobiology, 2012. **22**(8): p. 1128-39.
4. Shan, M., et al., *Mucus enhances gut homeostasis and oral tolerance by delivering immunoregulatory signals.* Science, 2013. **342**(6157): p. 447-53.
5. Bode, L., *Human milk oligosaccharides: every baby needs a sugar mama.* Glycobiology, 2012. **22**(9): p. 1147-62.
6. Laurent, T.C. and J.R. Fraser, *Hyaluronan.* FASEB J, 1992. **6**(7): p. 2397-404.
7. Shylaja, M. and H.S. Seshadri, *Glycoproteins - an Overview.* Biochemical Education, 1989. **17**(4): p. 170-178.
8. Law, J.H., *Glycolipids.* Annual Review of Biochemistry, 1960. **29**: p. 131-150.

9. Apweiler, R., H. Hermjakob, and N. Sharon, *On the frequency of protein glycosylation, as deduced from analysis of the SWISS-PROT database.* Biochimica Et Biophysica Acta-General Subjects, 1999. **1473**(1): p. 4-8.

10. Spiro, R.G., *Protein glycosylation: nature, distribution, enzymatic formation, and disease implications of glycopeptide bonds.* Glycobiology, 2002. **12**(4): p. 43r-56r.

11. Marino, K., et al., *A systematic approach to protein glycosylation analysis: a path through the maze.* Nature Chemical Biology, 2010. **6**(10): p. 713-723.

12. Yu, H. and X. Chen, *One-pot multienzyme (OPME) systems for chemoenzymatic synthesis of carbohydrates.* Organic & Biomolecular Chemistry, 2016. **14**(10): p. 2809-2818.

13. Bieberich, E., *Synthesis, Processing, and Function of N-glycans in N-glycoproteins.* Adv Neurobiol, 2014. **9**: p. 47-70.

14. Rabinovich, G.A., et al., *Functions of cell surface galectin-glycoprotein lattices.* Curr Opin Struct Biol, 2007. **17**(5): p. 513-20.

15. Demetriou, M., et al., *Negative regulation of T-cell activation and autoimmunity by Mgat5 N-glycosylation.* Nature, 2001. **409**(6821): p. 733-9.

16. Gandhi, N.S. and R.L. Mancera, *The Structure of Glycosaminoglycans and their Interactions with Proteins.* Chemical Biology & Drug Design, 2008. **72**(6): p. 455-482.

17. Hakomori, S.I., *Structure and function of glycosphingolipids and sphingolipids: recollections and future trends.* Biochim Biophys Acta, 2008. **1780**(3): p. 325-46.

18. Aebi, M., *N-linked protein glycosylation in the ER.* Biochim Biophys Acta, 2013. **1833**(11): p. 2430-7.

19. Sjogren, J. and M. Collin, *Bacterial glycosidases in pathogenesis and glycoengineering.* Future Microbiology, 2014. **9**(9): p. 1039-1051.

20. Akopian, D., et al., *Signal recognition particle: an essential protein-targeting machine.* Annu Rev Biochem, 2013. **82**: p. 693-721.

21. Mohorko, E., R. Glockshuber, and M. Aebi, *Oligosaccharyltransferase: the central enzyme of N-linked protein glycosylation.* J Inherit Metab Dis, 2011. **34**(4): p. 869-78.

22. Farid, A., et al., *Arabidopsis thaliana alpha1,2-glucosyltransferase (ALG10) is required for efficient N-glycosylation and leaf growth.* Plant Journal, 2011. **68**(2): p. 314-325.

23. Nakagawa, H., et al., *ER-resident Gi2 protein controls sar1 translocation onto the ER during budding of transport vesicles.* J Cell Biochem, 2011. **112**(9): p. 2250-6.

24. Kizuka, Y. and N. Taniguchi, *Enzymes for N-Glycan Branching and Their Genetic and Nongenetic Regulation in Cancer.* Biomolecules, 2016. **6**(2).

25. Johnson, J.L., et al., *The regulatory power of glycans and their binding partners in immunity.* Trends in Immunology, 2013. **34**(6): p. 290-298.

26. Kawar, Z.S., et al., *Novel poly-GalNAcbeta1-4GlcNAc (LacdiNAc) and fucosylated poly-LacdiNAc N-glycans from mammalian cells expressing beta1,4-N-acetylgalactosaminyltransferase and alpha1,3-fucosyltransferase.* J Biol Chem, 2005. **280**(13): p. 12810-9.

27. Sasaki, N., et al., *LacdiNAc (GalNAcbeta1-4GlcNAc) contributes to self-renewal of mouse embryonic stem cells by regulating leukemia inhibitory factor/STAT3 signaling.* Stem Cells, 2011. **29**(4): p. 641-50.

28. Choo, M., et al., *Characterization of H type 1 and type 1 N-acetyllactosamine glycan epitopes on ovarian cancer specifically recognized by the anti-glycan monoclonal antibody mAb-A4.* J Biol Chem, 2017. **292**(15): p. 6163-6176.

29. Spillmann, D. and J. Finne, *Poly-N-acetyllactosamine glycans of cellular glycoproteins: predominance of linear chains in mouse neuroblastoma and rat pheochromocytoma cell lines.* J Neurochem, 1987. **49**(3): p. 874-83.

30. Stowell, S.R., et al., *Human galectin-1 recognition of poly-N-acetyllactosamine and chimeric polysaccharides.* Glycobiology, 2004. **14**(2): p. 157-67.

31. Ujita, M., et al., *Poly-N-acetyllactosamine synthesis in branched N-glycans is controlled by complemental branch specificity of i-extension enzyme and beta 1,4-galactosyltransferase I.* Journal of Biological Chemistry, 1999. **274**(24): p. 16717-16726.

32. Inaba, N., et al., *A novel I-branching beta-1,6-N-acetylglucosaminyltransferase involved in human blood group I antigen expression.* Blood, 2003. **101**(7): p. 2870-2876.

33. Stanley, P., *Golgi glycosylation.* Cold Spring Harb Perspect Biol, 2011. **3**(4).

34. Kornfeld, R. and S. Kornfeld, *Assembly of asparagine-linked oligosaccharides.* Annu Rev Biochem, 1985. **54**: p. 631-64.

35. Van den Steen, P., et al., *Concepts and principles of O-linked glycosylation.* Critical Reviews in Biochemistry and Molecular Biology, 1998. **33**(3): p. 151-208.

36. Alonso, M.D., et al., *Tyrosine-194 of glycogenin undergoes autocatalytic glucosylation but is not essential for catalytic function and activity.* FEBS Lett, 1994. **342**(1): p. 38-42.

37. Gill, D.J., H. Clausen, and F. Bard, *Location, location, location: new insights into O-GalNAc protein glycosylation.* Trends in Cell Biology, 2011. **21**(3): p. 149-158.

38. Cummings, R.D. and J.M. Pierce, *Handbook of Glycomics Preface.* Handbook of Glycomics, 2009: p. Xi-Xiii.

39. Munkley, J., *The Role of Sialyl-Tn in Cancer.* International Journal of Molecular Sciences, 2016. **17**(3).

40. Varki, A. and H.H. Freeze, *The major glycosylation pathways of mammalian membranes. A summary.* Subcell Biochem, 1994. **22**: p. 71-100.

41. Iozzo, R.V. and L. Schaefer, *Proteoglycan form and function: A comprehensive nomenclature of proteoglycans.* Matrix Biol, 2015. **42**: p. 11-55.

42. Taylor, K.R. and R.L. Gallo, *Glycosaminoglycans and their proteoglycans: host-associated molecular patterns for initiation and modulation of inflammation.* Faseb Journal, 2006. **20**(1): p. 9-22.

43. Sprong, H., et al., *UDP-galactose : ceramide galactosyltransferase is a class I integral membrane protein of the endoplasmic reticulum.* Journal of Biological Chemistry, 1998. **273**(40): p. 25880-25888.

44. D'Angelo, G., et al., *Glycosphingolipids: synthesis and functions.* FEBS J, 2013. **280**(24): p. 6338-53.

45. Schaffer, C. and P. Messner, *Surface-layer glycoproteins: an example for the diversity of bacterial glycosylation with promising impacts on nanobiotechnology.* Glycobiology, 2004. **14**(8): p. 31R-42R.

46. Vollmer, W. and U. Bertsche, *Murein (peptidoglycan) structure, architecture and biosynthesis in Escherichia coli.* Biochim Biophys Acta, 2008. **1778**(9): p. 1714-34.

47. Brown, S., J.P. Santa Maria, Jr., and S. Walker, *Wall teichoic acids of gram-positive bacteria.* Annu Rev Microbiol, 2013. **67**: p. 313-36.

48. Percy, M.G. and A. Grundling, *Lipoteichoic acid synthesis and function in gram-positive bacteria.* Annu Rev Microbiol, 2014. **68**: p. 81-100.

49. Hsu, Y.P., X. Meng, and M.S. VanNieuwenhze, *Methods for visualization of peptidoglycan biosynthesis.* Imaging Bacterial Molecules, Structures and Cells, 2016. **43**: p. 3-48.

50. Dessing, M.C., et al., *Role played by Toll-like receptors 2 and 4 in lipoteichoic acid-induced lung inflammation and coagulation.* J Infect Dis, 2008. **197**(2): p. 245-52.

51. McDonald, C., N. Inohara, and G. Nunez, *Peptidoglycan signaling in innate immunity and inflammatory disease.* J Biol Chem, 2005. **280**(21): p. 20177-80.

52. Inohara, N., et al., *Human Nod1 confers responsiveness to bacterial lipopolysaccharides.* J Biol Chem, 2001. **276**(4): p. 2551-4.

53. Ogura, Y., et al., *Nod2, a Nod1/Apaf-1 family member that is restricted to monocytes and activates NF-kappaB.* J Biol Chem, 2001. **276**(7): p. 4812-8.

54. Boulnois, G.J. and K. Jann, *Bacterial polysaccharide capsule synthesis, export and evolution of structural diversity.* Mol Microbiol, 1989. **3**(12): p. 1819-23.

55. Whitfield, C., *Biosynthesis and assembly of capsular polysaccharides in Escherichia coli.* Annu Rev Biochem, 2006. **75**: p. 39-68.

56. Daffe, M. and G. Etienne, *The capsule of Mycobacterium tuberculosis and its implications for pathogenicity.* Tuber Lung Dis, 1999. **79**(3): p. 153-69.

57. Willis, L.M. and C. Whitfield, *Structure, biosynthesis, and function of bacterial capsular polysaccharides synthesized by ABC transporter-dependent pathways.* Carbohydr Res, 2013. **378**: p. 35-44.

58. Wang, X. and P.J. Quinn, *Lipopolysaccharide: Biosynthetic pathway and structure modification.* Prog Lipid Res, 2010. **49**(2): p. 97-107.

59. Mandrell, R.E. and M.A. Apicella, *Lipo-oligosaccharides (LOS) of mucosal pathogens: molecular mimicry and host-modification of LOS.* Immunobiology, 1993. **187**(3-5): p. 382-402.

60. Galdiero, S., et al., *Microbe-Host Interactions: Structure and Role of Gram-Negative Bacterial Porins.* Current Protein & Peptide Science, 2012. **13**(8): p. 843-854.

61. Merino, S. and J.M. Tomas, *Gram-negative flagella glycosylation.* Int J Mol Sci, 2014. **15**(2): p. 2840-57.

62. Nothaft, H. and C.M. Szymanski, *Protein glycosylation in bacteria: sweeter than ever.* Nature Reviews Microbiology, 2010. **8**(11): p. 765-778.

63. Thibault, P., et al., *Identification of the carbohydrate moieties and glycosylation motifs in Campylobacter jejuni flagellin.* J Biol Chem, 2001. **276**(37): p. 34862-70.

64. Schirm, M., et al., *Identification of unusual bacterial glycosylation by tandem mass spectrometry analyses of intact proteins.* Anal Chem, 2005. **77**(23): p. 7774-82.

65. Logan, S.M., et al., *Identification of novel carbohydrate modifications on Campylobacter jejuni 11168 flagellin using metabolomics-based approaches.* Febs Journal, 2009. **276**(4): p. 1014-1023.

66. Schirm, M., et al., *Structural and genetic characterization of glycosylation of type a flagellin in Pseudomonas aeruginosa.* J Bacteriol, 2004. **186**(9): p. 2523-31.

67. Vik, A., et al., *Broad spectrum O-linked protein glycosylation in the human pathogen Neisseria gonorrhoeae.* Proceedings of the National Academy of Sciences of the United States of America, 2009. **106**(11): p. 4447-4452.

68. Boulanger, M.J. and M.E.P. Murphy, *Crystal structure of the soluble domain of the major anaerobically induced outer membrane protein (AniA) from pathogenic Neisseria: A new class of copper-containing nitrite reductases.* Journal of Molecular Biology, 2002. **315**(5): p. 1111-1127.

69. Pitcher, R.S. and N.J. Watmough, *The bacterial cytochrome cbb3 oxidases.* Biochim Biophys Acta, 2004. **1655**(1-3): p. 388-99.

70. Wexler, H.M., *Bacteroides: the good, the bad, and the nitty-gritty.* Clin Microbiol Rev, 2007. **20**(4): p. 593-621.

71. Coyne, M.J., et al., *Role of glycan synthesis in colonization of the mammalian gut by the bacterial symbiont Bacteroides fragilis.* Proc Natl Acad Sci U S A, 2008. **105**(35): p. 13099-104.

72. Fletcher, C.M., M.J. Coyne, and L.E. Comstock, *Theoretical and experimental characterization of the scope of protein O-glycosylation in Bacteroides fragilis.* J Biol Chem, 2011. **286**(5): p. 3219-26.

73. Kelly, J., et al., *Biosynthesis of the N-linked glycan in Campylobacter jejuni and addition onto protein through Block transfer.* Journal of Bacteriology, 2006. **188**(7): p. 2427-2434.

74. Nothaft, H. and C.M. Szymanski, *Bacterial Protein N-Glycosylation: New Perspectives and Applications.* Journal of Biological Chemistry, 2013. **288**(10): p. 6912-6920.

75. Williams, D.B., *Beyond lectins: the calnexin/calreticulin chaperone system of the endoplasmic reticulum.* Journal of Cell Science, 2006. **119**(4): p. 615-623.

76. Pelletier, M.F., et al., *The heterodimeric structure of glucosidase II is required for its activity, solubility, and localization in vivo.* Glycobiology, 2000. **10**(8): p. 815-827.

77. Shailubhai, K., et al., *Glucosidase-I, a Transmembrane Endoplasmic Reticular Glycoprotein with a Luminal Catalytic Domain.* Journal of Biological Chemistry, 1991. **266**(25): p. 16587-16593.

78. Ellgaard, L. and E.M. Frickel, *Calnexin, calreticulin, and ERp57 - Teammates in glycoprotein folding.* Cell Biochemistry and Biophysics, 2003. **39**(3): p. 223-247.

79. Hebert, D.N., et al., *The role of UDP-glucose: glycoprotein glucosyltransferase and EDEM in glycoprotein maturation and quality control in the ER.* Faseb Journal, 2006. **20**(5): p. A1307-A1307.

80. Dalziel, M., et al., *Emerging principles for the therapeutic exploitation of glycosylation.* Science, 2014. **343**(6166): p. 1235681.

81. Hickman, S., L.J. Shapiro, and E.F. Neufeld, *A recognition marker required for uptake of a lysosomal enzyme by cultured fibroblasts.* Biochem Biophys Res Commun, 1974. **57**(1): p. 55-61.

82. Natowicz, M.R., et al., *Enzymatic identification of mannose 6-phosphate on the recognition marker for receptor-mediated pinocytosis of beta-glucuronidase by human fibroblasts.* Proc Natl Acad Sci U S A, 1979. **76**(9): p. 4322-6.

83. Nadimpalli, S.K. and P.K. Amancha, *Evolution of mannose 6-phosphate receptors (MPR300 and 46): lysosomal enzyme sorting proteins.* Curr Protein Pept Sci, 2010. **11**(1): p. 68-90.

84. Geuze, H.J., et al., *Possible pathways for lysosomal enzyme delivery.* J Cell Biol, 1985. **101**(6): p. 2253-62.

85. Hasilik, A. and E.F. Neufeld, *Biosynthesis of lysosomal enzymes in fibroblasts. Phosphorylation of mannose residues.* J Biol Chem, 1980. **255**(10): p. 4946-50.

86. Reitman, M.L. and S. Kornfeld, *Lysosomal enzyme targeting. N-Acetylglucosaminylphosphotransferase selectively phosphorylates native lysosomal enzymes.* J Biol Chem, 1981. **256**(23): p. 11977-80.

87. Varki, A. and S. Kornfeld, *Identification of a rat liver alpha-N-acetylglucosaminyl phosphodiesterase capable of removing "blocking" alpha-N-acetylglucosamine residues from phosphorylated high mannose oligosaccharides of lysosomal enzymes.* J Biol Chem, 1980. **255**(18): p. 8398-401.

88. Rohrer, J. and R. Kornfeld, *Lysosomal hydrolase mannose 6-phosphate uncovering enzyme resides in the trans-Golgi network.* Mol Biol Cell, 2001. **12**(6): p. 1623-31.

89. Varki, A., *Essentials of glycobiology*. 2nd ed. 2009, New York: Cold Spring Harbor Laboratory Press. 784 S.

90. Prieto, P.A., et al., *Expression of human H-type alpha1,2-fucosyltransferase encoding for blood group H(O) antigen in Chinese hamster ovary cells. Evidence for preferential fucosylation and truncation of polylactosamine sequences.* J Biol Chem, 1997. **272**(4): p. 2089-97.

91. Lin, B., et al., *Characterization of three members of murine alpha1,2-fucosyltransferases: change in the expression of the Se gene in the intestine of mice after administration of microbes.* Arch Biochem Biophys, 2001. **388**(2): p. 207-15.

92. Meloncelli, P.J. and T.L. Lowary, *Synthesis of ABO histo-blood group type I and II antigens.* Carbohydr Res, 2010. **345**(16): p. 2305-22.

93. Rydberg, L., *ABO-incompatibility in solid organ transplantation.* Transfus Med, 2001. **11**(4): p. 325-42.

94. Yunis, E.J., J.M. Svardal, and R.A. Bridges, *Genetics of the Bombay phenotype.* Blood, 1969. **33**(1): p. 124-32.

95. Mourant, A., *The Nature of Human Genetic-Variation - a Citation Classic Commentary on the Distribution of the Human-Blood Groups and Other Polymorphisms by Mourant,A.E., Kopec,A.C., and Domaniewskasobczak,K.* Current Contents/Clinical Medicine, 1989(28): p. 12-12.

96. Marcus, D.M., *The ABO, Hh, secretor, and Lewis systems.* Immunol Ser, 1989. **43**: p. 685-99.

97. Henry, S., R. Oriol, and B. Samuelsson, *Lewis histo-blood group system and associated secretory phenotypes.* Vox Sang, 1995. **69**(3): p. 166-82.

98. Marcus, D.M. and L.E. Cass, *Glycosphingolipids with Lewis blood group activity: uptake by human erythrocytes.* Science, 1969. **164**(3879): p. 553-5.

99. de Vries, T., et al., *Fucosyltransferases: structure/function studies.* Glycobiology, 2001. **11**(10): p. 119r-128r.

100. Sperandio, M., C.A. Gleissner, and K. Ley, *Glycosylation in immune cell trafficking.* Immunol Rev, 2009. **230**(1): p. 97-113.

101. McEver, R.P., *Selectins: initiators of leucocyte adhesion and signalling at the vascular wall.* Cardiovascular Research, 2015. **107**(3): p. 331-339.

102. Kansas, G.S., *Structure and Function of L-Selectin.* Apmis, 1992. **100**(4): p. 287-293.

103. Kunkel, E.J. and K. Ley, *Distinct phenotype of E-selectin-deficient mice - E-selectin is required for slow leukocyte rolling in vivo.* Circulation Research, 1996. **79**(6): p. 1196-1204.

104. Ley, K., et al., *Getting to the site of inflammation: the leukocyte adhesion cascade updated.* Nature Reviews Immunology, 2007. **7**(9): p. 678-689.

105. Muller, W.A., *Getting Leukocytes to the Site of Inflammation.* Veterinary Pathology, 2013. **50**(1): p. 7-22.

106. Julien, S., et al., *Selectin ligand sialyl-Lewis x antigen drives metastasis of hormone-dependent breast cancers.* Cancer Res, 2011. **71**(24): p. 7683-93.

107. Nakamori, S., et al., *Involvement of carbohydrate antigen sialyl Lewis(x) in colorectal cancer metastasis.* Dis Colon Rectum, 1997. **40**(4): p. 420-31.

108. Galili, U., et al., *Human natural anti-alpha-galactosyl IgG. II. The specific recognition of alpha (1----3)-linked galactose residues.* J Exp Med, 1985. **162**(2): p. 573-82.

109. Galili, U., et al., *A unique natural human IgG antibody with anti-alpha-galactosyl specificity.* J Exp Med, 1984. **160**(5): p. 1519-31.

110. Luderitz, O., D.A. Simmons, and G. Westphal, *The immunochemistry of Salmonella chemotype VI O-antigens. The structure of oligosaccharides from Salmonella group U (o 43) lipopolysaccharides.* Biochem J, 1965. **97**(3): p. 820-6.

111. Springer, G.F., *Blood-group and Forssman antigenic determinants shared between microbes and mammalian cells.* Prog Allergy, 1971. **15**: p. 9-77.

112. Petit, D., et al., *Integrative view of alpha2,3-sialyltransferases (ST3Gal) molecular and functional evolution in deuterostomes: significance of lineage-specific losses.* Mol Biol Evol, 2015. **32**(4): p. 906-27.

113. Schwartz, A.L., *The hepatic asialoglycoprotein receptor.* CRC Crit Rev Biochem, 1984. **16**(3): p. 207-33.

114. Lichtenstein, R.G. and G.A. Rabinovich, *Glycobiology of cell death: when glycans and lectins govern cell fate.* Cell Death and Differentiation, 2013. **20**(8): p. 976-986.

115. Pillai, S.P.S. and C.W. Lee, *Species and age related differences in the type and distribution of influenza virus receptors in different tissues of chickens, ducks and turkeys.* Virology Journal, 2010. **7**.

116. Shinya, K., et al., *Avian flu: influenza virus receptors in the human airway.* Nature, 2006. **440**(7083): p. 435-6.

117. Aspholm, M., et al., *SabA is the H. pylori hemagglutinin and is polymorphic in binding to sialylated glycans.* Plos Pathogens, 2006. **2**(10): p. 989-1001.

118. Teppa, R.E., et al., *Phylogenetic-Derived Insights into the Evolution of Sialylation in Eukaryotes: Comprehensive Analysis of Vertebrate beta-Galactoside alpha 2,3/6-Sialyltransferases (ST3Gal and ST6Gal).* International Journal of Molecular Sciences, 2016. **17**(8).

119. Kitagawa, H. and J.C. Paulson, *Differential expression of five sialyltransferase genes in human tissues.* J Biol Chem, 1994. **269**(27): p. 17872-8.

120. Hennet, T., et al., *Immune regulation by the ST6Gal sialyltransferase.* Proc Natl Acad Sci U S A, 1998. **95**(8): p. 4504-9.

121. Poe, J.C. and T.F. Tedder, *CD22 and Siglec-G in B cell function and tolerance.* Trends Immunol, 2012. **33**(8): p. 413-20.

122. Schnaar, R.L., R. Gerardy-Schahn, and H. Hildebrandt, *Sialic acids in the brain: gangliosides and polysialic acid in nervous system development, stability, disease, and regeneration.* Physiol Rev, 2014. **94**(2): p. 461-518.

123. Harduin-Lepers, A., et al., *Evolutionary history of the alpha2,8-sialyltransferase (ST8Sia) gene family: Tandem duplications in early deuterostomes explain most of the diversity found in the vertebrate ST8Sia genes.* Bmc Evolutionary Biology, 2008. **8**.

124. Angata, K. and M. Fukuda, *Polysialyltransferases: major players in polysialic acid synthesis on the neural cell adhesion molecule.* Biochimie, 2003. **85**(1-2): p. 195-206.

125. Edelman, G.M., *Cell adhesion molecules in the regulation of animal form and tissue pattern.* Annu Rev Cell Biol, 1986. **2**: p. 81-116.

126. Sadoul, R., et al., *Adult and Embryonic Mouse Neural Cell-Adhesion Molecules Have Different Binding-Properties.* Nature, 1983. **304**(5924): p. 347-349.

127. Rutishauser, U., *Specific Alteration of Ncam-Mediated Cell-Adhesion by an Endoneuraminidase.* Federation Proceedings, 1986. **45**(6): p. 1753-1753.

128. Hildebrandt, H., et al., *Dissecting polysialic acid and NCAM functions in brain development.* Journal of Neurochemistry, 2007. **103**: p. 56-64.

129. Angata, K., et al., *Sialyltransferase ST8Sia-II assembles a subset of polysialic acid that directs hippocampal axonal targeting and promotes fear behavior.* Journal of Biological Chemistry, 2004. **279**(31): p. 32603-32613.

130. Weinhold, B., et al., *Genetic ablation of polysialic acid causes severe neurodevelopmental defects rescued by deletion of the neural cell adhesion molecule.* Journal of Biological Chemistry, 2005. **280**(52): p. 42971-42977.

131. Kolter, T., *Ganglioside biochemistry.* ISRN Biochem, 2012. **2012**: p. 506160.

132. Perez-Vilar, J. and R.L. Hill, *The structure and assembly of secreted mucins.* J Biol Chem, 1999. **274**(45): p. 31751-4.

133. Newburg, D.S. and G. Grave, *Recent advances in human milk glycobiology.* Pediatr Res, 2014.

134. Brockhausen, I., H. Schachter, and P. Stanley, *O-GalNAc Glycans*, in *Essentials of Glycobiology*, A. Varki, et al., Editors. 2009: Cold Spring Harbor (NY).

135. Pelaseyed, T., et al., *The mucus and mucins of the goblet cells and enterocytes provide the first defense line of the gastrointestinal tract and interact with the immune system.* Immunological Reviews, 2014. **260**(1): p. 8-20.

136. Johansson, M.E., et al., *Composition and functional role of the mucus layers in the intestine.* Cell Mol Life Sci, 2011. **68**(22): p. 3635-41.

137. Godl, K., et al., *The N terminus of the MUC2 mucin forms trimers that are held together within a trypsin-resistant core fragment.* Journal of Biological Chemistry, 2002. **277**(49): p. 47248-47256.

138. Fu, J., et al., *Loss of intestinal core 1-derived O-glycans causes spontaneous colitis in mice.* J Clin Invest, 2011. **121**(4): p. 1657-66.

139. Johansson, M.E.V., et al., *Bacteria penetrate the normally impenetrable inner colon mucus layer in both murine colitis models and patients with ulcerative colitis.* Gut, 2014. **63**(2): p. 281-291.

140. An, G., et al., *Increased susceptibility to colitis and colorectal tumors in mice lacking core 3-derived O-glycans.* J Exp Med, 2007. **204**(6): p. 1417-29.

141. Staubach, F., et al., *Expression of the blood-group-related glycosyltransferase B4galnt2 influences the intestinal microbiota in mice.* ISME J, 2012. **6**(7): p. 1345-55.

142. Stappenbeck, T.S., L.V. Hooper, and J.I. Gordon, *Developmental regulation of intestinal angiogenesis by indigenous microbes via Paneth cells.* Proceedings of the National Academy of Sciences of the United States of America, 2002. **99**(24): p. 15451-15455.

143. Kelly, D., et al., *Commensal anaerobic gut bacteria attenuate inflammation by regulating nuclear-cytoplasmic shuttling of PPAR-gamma and RelA.* Nat Immunol, 2004. **5**(1): p. 104-12.

144. Hooper, L.V., et al., *Angiogenins: a new class of microbicidal proteins involved in innate immunity.* Nat Immunol, 2003. **4**(3): p. 269-73.

145. Hooper, L.V., et al., *A molecular sensor that allows a gut commensal to control its nutrient foundation in a competitive ecosystem.* Proceedings of the National Academy of Sciences of the United States of America, 1999. **96**(17): p. 9833-9838.

146. Meng, D., et al., *Bacterial symbionts induce a FUT2-dependent fucosylated niche on colonic epithelium via ERK and JNK signaling.* American Journal of Physiology-Gastrointestinal and Liver Physiology, 2007. **293**(4): p. G780-G787.

147. Fanning, S., et al., *Bifidobacterial surface-exopolysaccharide facilitates commensal-host interaction through immune modulation and pathogen protection.* Proceedings of the National Academy of Sciences of the United States of America, 2012. **109**(6): p. 2108-2113.

148. Femia, A.P., et al., *Antitumorigenic activity of the prebiotic inulin enriched with oligofructose in combination with the probiotics Lactobacillus rhamnosus and Bifidobacterium lactis on azoxymethane-induced colon carcinogenesis in rats.* Carcinogenesis, 2002. **23**(11): p. 1953-1960.

149. Turroni, F., et al., *Genome analysis of Bifidobacterium bifidum PRL2010 reveals metabolic pathways for host-derived glycan foraging.* Proceedings of the National Academy of Sciences of the United States of America, 2010. **107**(45): p. 19514-19519.

150. Turroni, F., et al., *Genetic strategies for mucin metabolism in Bifidobacterium bifidum PRL2010: an example of possible human-microbe co-evolution.* Gut Microbes, 2011. **2**(3): p. 183-9.

151. Fujita, K., et al., *Identification and molecular cloning of a novel glycoside hydrolase family of core 1 type O-glycan-specific endo-alpha-N-acetylgalactosaminidase from Bifidobacterium longum.* J Biol Chem, 2005. **280**(45): p. 37415-22.

152. Katayama, T., et al., *Molecular cloning and characterization of Bifidobacterium bifidum 1,2-alpha-L-fucosidase (AfcA), a novel inverting glycosidase (Glycoside hydrolase family 95).* Journal of Bacteriology, 2004. **186**(15): p. 4885-4893.

153. Ruas-Madiedo, P., et al., *Mucin degradation by Bifidobacterium strains isolated from the human intestinal microbiota.* Applied and Environmental Microbiology, 2008. **74**(6): p. 1936-1940.

154. Chang, D.E., et al., *Carbon nutrition of Escherichia coli in the mouse intestine.* Proceedings of the National Academy of Sciences of the United States of America, 2004. **101**(19): p. 7427-7432.

155. Png, C.W., et al., *Mucolytic Bacteria With Increased Prevalence in IBD Mucosa Augment In Vitro Utilization of Mucin by Other Bacteria.* American Journal of Gastroenterology, 2010. **105**(11): p. 2420-2428.

156. Ikehara, Y., et al., *Polymorphisms of two fucosyltransferase genes (Lewis and Secretor genes) involving type I Lewis antigens are associated with the presence of anti-Helicobacter pylori IgG antibody.* Cancer Epidemiol Biomarkers Prev, 2001. **10**(9): p. 971-7.

157. Rausch, P., et al., *Colonic mucosa-associated microbiota is influenced by an interaction of Crohn disease and FUT2 (Secretor) genotype.* Proceedings of the National Academy of Sciences of the United States of America, 2011. **108**(47): p. 19030-19035.

158. Rho, J.H., et al., *A novel mechanism for desulfation of mucin: identification and cloning of a mucin-desulfating glycosidase (sulfoglycosidase) from Prevotella strain RS2.* J Bacteriol, 2005. **187**(5): p. 1543-51.

159. Tobisawa, Y., et al., *Sulfation of colonic mucins by N-acetylglucosamine 6-O-sulfotransferase-2 and its protective function in experimental colitis in mice.* J Biol Chem, 2010. **285**(9): p. 6750-60.

160. Dawson, P.A., et al., *Reduced mucin sulfonation and impaired intestinal barrier function in the hyposulfataemic NaS1 null mouse.* Gut, 2009. **58**(7): p. 910-9.

161. Moniaux, N., et al., *Structural organization and classification of the human mucin genes.* Front Biosci, 2001. **6**: p. D1192-206.

162. Ruiz-Palacios, G.M., et al., *Campylobacter jejuni binds intestinal H(O) antigen (Fuc alpha 1, 2Gal beta 1, 4GlcNAc), and fucosyloligosaccharides of human milk inhibit its binding and infection.* J Biol Chem, 2003. **278**(16): p. 14112-20.

163. Angeloni, S., et al., *Glycoprofiling with micro-arrays of glycoconjugates and lectins.* Glycobiology, 2005. **15**(1): p. 31-41.

164. Eiwegger, T., et al., *Human milk--derived oligosaccharides and plant-derived oligosaccharides stimulate cytokine production of cord blood T-cells in vitro.* Pediatr Res, 2004. **56**(4): p. 536-40.

165. Bode, L., et al., *Inhibition of monocyte, lymphocyte, and neutrophil adhesion to endothelial cells by human milk oligosaccharides.* Thromb Haemost, 2004. **92**(6): p. 1402-10.

166. Kurakevich, E., et al., *Milk oligosaccharide sialyl(alpha2,3)lactose activates intestinal CD11c+ cells through TLR4.* Proc Natl Acad Sci U S A, 2013.

167. Bourguignon, L.Y., et al., *CD44 interaction with c-Src kinase promotes cortactin-mediated cytoskeleton function and hyaluronic acid-dependent ovarian tumor cell migration.* J Biol Chem, 2001. **276**(10): p. 7327-36.

168. Tian, X., et al., *High-molecular-mass hyaluronan mediates the cancer resistance of the naked mole rat.* Nature, 2013. **499**(7458): p. 346-9.

169. Tamer, T.M., *Hyaluronan and synovial joint: function, distribution and healing.* Interdiscip Toxicol, 2013. **6**(3): p. 111-25.

170. Kim, E., et al., *Identification of a hyaluronidase, Hyal5, involved in penetration of mouse sperm through cumulus mass.* Proceedings of the National Academy of Sciences of the United States of America, 2005. **102**(50): p. 18028-18033.

171. Atarashi, K., et al., *Th17 Cell Induction by Adhesion of Microbes to Intestinal Epithelial Cells.* Cell, 2015.

172. Mescher, M.F., J.L. Strominger, and S.W. Watson, *Protein and carbohydrate composition of the cell envelope of Halobacterium salinarium.* J Bacteriol, 1974. **120**(2): p. 945-54.

173. Sleytr, U.B. and K.J. Thorne, *Chemical characterization of the regularly arranged surface layers of Clostridium thermosaccharolyticum and Clostridium thermohydrosulfuricum.* J Bacteriol, 1976. **126**(1): p. 377-83.

174. Romain, F., et al., *Deglycosylation of the 45/47-kilodalton antigen complex of Mycobacterium tuberculosis decreases its capacity to elicit in vivo or in vitro cellular immune responses.* Infect Immun, 1999. **67**(11): p. 5567-72.

175. Vimr, E.R., et al., *Diversity of microbial sialic acid metabolism.* Microbiol Mol Biol Rev, 2004. **68**(1): p. 132-53.

176. Bry, L., et al., *A model of host-microbial interactions in an open mammalian ecosystem.* Science, 1996. **273**(5280): p. 1380-3.

177. Coyne, M.J., et al., *Human symbionts use a host-like pathway for surface fucosylation.* Science, 2005. **307**(5716): p. 1778-1781.

178. Comstock, L.E. and D.L. Kasper, *Bacterial glycans: key mediators of diverse host immune responses.* Cell, 2006. **126**(5): p. 847-50.

179. Lewis, L.A., M. Carter, and S. Ram, *The relative roles of factor H binding protein, neisserial surface protein A, and lipooligosaccharide sialylation in regulation of the alternative pathway of complement on meningococci.* J Immunol, 2012. **188**(10): p. 5063-72.

180. Nesargikar, P.N., B. Spiller, and R. Chavez, *The complement system: history, pathways, cascade and inhibitors.* Eur J Microbiol Immunol (Bp), 2012. **2**(2): p. 103-11.

181. Ferreira, V.P., M.K. Pangburn, and C. Cortes, *Complement control protein factor H: the good, the bad, and the inadequate.* Mol Immunol, 2010. **47**(13): p. 2187-97.

182. Stollerman, G.H. and J.B. Dale, *The importance of the group a streptococcus capsule in the pathogenesis of human infections: a historical perspective.* Clin Infect Dis, 2008. **46**(7): p. 1038-45.

183. Cobb, B.A., et al., *Polysaccharide processing and presentation by the MHCII pathway.* Cell, 2004. **117**(5): p. 677-87.

184. van der Woude, M.W. and A.J. Baumler, *Phase and antigenic variation in bacteria.* Clinical Microbiology Reviews, 2004. **17**(3): p. 581-+.

185. Troy, E.B. and D.L. Kasper, *Beneficial effects of Bacteroides fragilis polysaccharides on the immune system.* Frontiers in Bioscience-Landmark, 2010. **15**: p. 25-34.

186. Grover, M. and P.C. Kashyap, *Germ-free mice as a model to study effect of gut microbiota on host physiology.* Neurogastroenterology and Motility, 2014. **26**(6): p. 745-748.

187. Mazmanian, S.K., et al., *An immunomodulatory molecule of symbiotic bacteria directs maturation of the host immune system.* Cell, 2005. **122**(1): p. 107-18.

188. Appelmelk, B.J., et al., *Why Helicobacter pylori has Lewis antigens.* Trends in Microbiology, 2000. **8**(12): p. 565-570.

189. Sanabria-Valentin, E., M.T. Colbert, and M.J. Blaser, *Role of futC slipped strand mispairing in Helicobacter pylori Lewisy phase variation.* Microbes Infect, 2007. **9**(14-15): p. 1553-60.

190. Bergman, M.P., et al., *Helicobacter pylori modulates the T helper cell 1/T helper cell 2 balance through phase-variable interaction between lipopolysaccharide and DC-SIGN.* J Exp Med, 2004. **200**(8): p. 979-90.

191. Bergman, M., et al., *Helicobacter pylori phase variation, immune modulation and gastric autoimmunity.* Nature Reviews Microbiology, 2006. **4**(2): p. 151-159.

192. Duvall, E., A.H. Wyllie, and R.G. Morris, *Macrophage recognition of cells undergoing programmed cell death (apoptosis).* Immunology, 1985. **56**(2): p. 351-8.

193. Dufour, F., et al., *N-glycosylation of mouse TRAIL-R and human TRAIL-R1 enhances TRAIL-induced death.* Cell Death and Differentiation, 2017. **24**(3): p. 500-510.

194. Hernandez, J.D. and L.G. Baum, *Ah, sweet mystery of death! Galectins and control of cell fate.* Glycobiology, 2002. **12**(10): p. 127R-36R.

195. Barondes, S.H., et al., *Galectins - Structure and Function of a Large Family of Animal Lectins.* Journal of Biological Chemistry, 1994. **269**(33): p. 20807-20810.

196. Yang, R.Y., G.A. Rabinovich, and F.T. Liu, *Galectins: structure, function and therapeutic potential.* Expert Rev Mol Med, 2008. **10**: p. e17.

197. Brewer, C.F., *Thermodynamic binding studies of galectin-1,-3 and-7.* Glycoconjugate Journal, 2002. **19**(7-9): p. 459-465.

198. Stowell, S.R., et al., *Galectin-1, -2, and -3 exhibit differential recognition of sialylated glycans and blood group antigens.* J Biol Chem, 2008. **283**(15): p. 10109-23.

199. Macauley, M.S., P.R. Crocker, and J.C. Paulson, *Siglec-mediated regulation of immune cell function in disease.* Nat Rev Immunol, 2014. **14**(10): p. 653-66.

200. Crocker, P.R., J.C. Paulson, and A. Varki, *Siglecs and their roles in the immune system.* Nat Rev Immunol, 2007. **7**(4): p. 255-66.

201. Quarles, R.H., *Myelin-associated glycoprotein (MAG): past, present and beyond.* J Neurochem, 2007. **100**(6): p. 1431-48.

202. Avril, T., et al., *The membrane-proximal immunoreceptor tyrosine-based inhibitory motif is critical for the inhibitory signaling mediated by Siglecs-7 and-9, CD33-related Siglecs expressed on human monocytes and NK cells.* Journal of Immunology, 2004. **173**(11): p. 6841-6849.

203. von Gunten, S. and B.S. Bochner, *Basic and clinical immunology of Siglecs.* Ann N Y Acad Sci, 2008. **1143**: p. 61-82.

204. Angata, T., et al., *Discovery of Siglec-14, a novel sialic acid receptor undergoing concerted evolution with Siglec-5 in primates.* FASEB J, 2006. **20**(12): p. 1964-73.

205. Angata, T., et al., *Siglec-15: an immune system Siglec conserved throughout vertebrate evolution.* Glycobiology, 2007. **17**(8): p. 838-46.

206. Lanier, L.L., *DAP10- and DAP12-associated receptors in innate immunity.* Immunol Rev, 2009. **227**(1): p. 150-60.

207. Kano, G., et al., *Mechanism of Siglec-8-mediated cell death in IL-5-activated eosinophils: role for reactive oxygen species-enhanced MEK/ERK activation.* J Allergy Clin Immunol, 2013. **132**(2): p. 437-45.

208. Mitsuki, M., et al., *Siglec-7 mediates nonapoptotic cell death independently of its immunoreceptor tyrosine-based inhibitory motifs in monocytic cell line U937.* Glycobiology, 2010. **20**(3): p. 395-402.

209. von Gunten, S. and H.U. Simon, *Autophagic-like cell death in neutrophils induced by autoantibodies.* Autophagy, 2007. **3**(1): p. 67-8.

210. Bodmer, J.L., et al., *TRAIL receptor-2 signals apoptosis through FADD and caspase-8.* Nature Cell Biology, 2000. **2**(4): p. 241-243.

211. Ashkenazi, A., *Directing cancer cells to self-destruct with pro-apoptotic receptor agonists.* Nature Reviews Drug Discovery, 2008. **7**(12): p. 1001-1012.

212. Wagner, K.W., et al., *Death-receptor O-glycosylation controls tumor-cell sensitivity to the proapoptotic ligand Apo2L/TRAIL.* Nat Med, 2007. **13**(9): p. 1070-7.

213. Kerr, J.F., A.H. Wyllie, and A.R. Currie, *Apoptosis: a basic biological phenomenon with wide-ranging implications in tissue kinetics.* Br J Cancer, 1972. **26**(4): p. 239-57.

214. Nagata, S. and M. Tanaka, *Programmed cell death and the immune system.* Nat Rev Immunol, 2017. **17**(5): p. 333-340.

215. Proskuryakov, S.Y., A.G. Konoplyannikov, and V.L. Gabai, *Necrosis: a specific form of programmed cell death?* Exp Cell Res, 2003. **283**(1): p. 1-16.

216. Kroemer, G., et al., *Classification of cell death: recommendations of the Nomenclature Committee on Cell Death 2009.* Cell Death Differ, 2009. **16**(1): p. 3-11.

217. Bohm, I., *Disruption of the cytoskeleton after apoptosis induction with autoantibodies.* Autoimmunity, 2003. **36**(3): p. 183-9.

218. Susin, S.A., et al., *Two distinct pathways leading to nuclear apoptosis.* J Exp Med, 2000. **192**(4): p. 571-80.

219. Imreh, G. and E. Hallberg, *Sequential degradation of proteins from the nuclear envelope during apoptosis.* J Cell Sci, 2001. **114**(Pt 20): p. 3643-53.

220. Nagata, S., *Apoptotic DNA fragmentation.* Exp Cell Res, 2000. **256**(1): p. 12-8.

221. Atkin-Smith, G.K., et al., *Isolation of cell type-specific apoptotic bodies by fluorescence-activated cell sorting.* Sci Rep, 2017. **7**: p. 39846.

222. Elmore, S., *Apoptosis: A review of programmed cell death.* Toxicologic Pathology, 2007. **35**(4): p. 495-516.

223. Chen, M. and J. Wang, *Initiator caspases in apoptosis signaling pathways.* Apoptosis, 2002. **7**(4): p. 313-9.

224. Chang, H.Y. and X. Yang, *Proteases for cell suicide: functions and regulation of caspases.* Microbiol Mol Biol Rev, 2000. **64**(4): p. 821-46.

225. Wang, C. and R.J. Youle, *The role of mitochondria in apoptosis*.* Annu Rev Genet, 2009. **43**: p. 95-118.

226. Yang, Y.L. and X.M. Li, *The IAP family: endogenous caspase inhibitors with multiple biological activities.* Cell Res, 2000. **10**(3): p. 169-77.

227. Dejean, L.M., S. Martinez-Caballero, and K.W. Kinnally, *Is MAC the knife that cuts cytochrome c from mitochondria during apoptosis?* Cell Death Differ, 2006. **13**(8): p. 1387-95.

228. Micheau, O., et al., *NF-kappaB signals induce the expression of c-FLIP.* Mol Cell Biol, 2001. **21**(16): p. 5299-305.

229. Bertrand, M.J.M., et al., *cIAP1 and cIAP2 facilitate cancer cell survival by functioning as E3 ligases that promote RIP1 ubiquitination.* Molecular Cell, 2008. **30**(6): p. 689-700.

230. Graber, T.E. and M. Holcik, *Distinct roles for the cellular inhibitors of apoptosis proteins 1 and 2.* Cell Death & Disease, 2011. **2**.

231. Wajant, H., *The Fas signaling pathway: More than a paradigm.* Science, 2002. **296**(5573): p. 1635-1636.

232. Guicciardi, M.E. and G.J. Gores, *Life and death by death receptors.* FASEB J, 2009. **23**(6): p. 1625-37.

233. Favaloro, B., et al., *Role of apoptosis in disease.* Aging (Albany NY), 2012. **4**(5): p. 330-49.

234. Fink, S.L. and B.T. Cookson, *Caspase-1-dependent pore formation during pyroptosis leads to osmotic lysis of infected host macrophages.* Cellular Microbiology, 2006. **8**(11): p. 1812-1825.

235. Franchi, L., et al., *Function of Nod-like receptors in microbial recognition and host defense.* Immunological Reviews, 2009. **227**: p. 106-128.

236. Kufer, T.A. and P.J. Sansonetti, *Sensing of bacteria: NOD a lonely job.* Current Opinion in Microbiology, 2007. **10**(1): p. 62-69.

237. Fernandes-Alnemri, T., et al., *The pyroptosome: a supramolecular assembly of ASC dimers mediating inflammatory cell death via caspase-1 activation.* Cell Death and Differentiation, 2007. **14**(9): p. 1590-1604.

238. Ogura, Y., F.S. Sutterwala, and R.A. Flavell, *The inflammasome: First line of the immune response to cell stress.* Cell, 2006. **126**(4): p. 659-662.

239. Shi, J., et al., *Inflammatory caspases are innate immune receptors for intracellular LPS.* Nature, 2014. **514**(7521): p. 187-92.

240. Kawai, T. and S. Akira, *TLR signaling.* Cell Death Differ, 2006. **13**(5): p. 816-25.

241. Shi, J., et al., *Cleavage of GSDMD by inflammatory caspases determines pyroptotic cell death.* Nature, 2015. **526**(7575): p. 660-5.

242. Kayagaki, N., et al., *Caspase-11 cleaves gasdermin D for non-canonical inflammasome signalling.* Nature, 2015. **526**(7575): p. 666-71.

243. Liu, X., et al., *Inflammasome-activated gasdermin D causes pyroptosis by forming membrane pores.* Nature, 2016. **535**(7610): p. 153-8.

244. Sborgi, L., et al., *GSDMD membrane pore formation constitutes the mechanism of pyroptotic cell death.* EMBO J, 2016. **35**(16): p. 1766-78.

245. Wang, Y., et al., *Chemotherapy drugs induce pyroptosis through caspase-3 cleavage of a Gasdermin.* Nature, 2017.

246. Jiang, Y., et al., *BaP-induced DNA damage initiated p53-independent necroptosis via the mitochondrial pathway involving Bax and Bcl-2.* Hum Exp Toxicol, 2013. **32**(12): p. 1245-57.

247. Belizario, J., L. Vieira-Cordeiro, and S. Enns, *Necroptotic Cell Death Signaling and Execution Pathway: Lessons from Knockout Mice.* Mediators Inflamm, 2015. **2015**: p. 128076.

248. Vanden Berghe, T., et al., *Regulated necrosis: the expanding network of non-apoptotic cell death pathways.* Nat Rev Mol Cell Biol, 2014. **15**(2): p. 135-47.

249. Vanden Berghe, T., B. Hassannia, and P. Vandenabeele, *An outline of necrosome triggers.* Cell Mol Life Sci, 2016. **73**(11-12): p. 2137-52.

250. Wang, H., et al., *Mixed lineage kinase domain-like protein MLKL causes necrotic membrane disruption upon phosphorylation by RIP3.* Mol Cell, 2014. **54**(1): p. 133-46.

251. Su, L.J., et al., *A Plug Release Mechanism for Membrane Permeation by MLKL.* Structure, 2014. **22**(10): p. 1489-1500.

252. Marshall, K.D. and C.P. Baines, *Necroptosis: is there a role for mitochondria?* Front Physiol, 2014. **5**: p. 323.

253. Repnik, U., M. Hafner Cesen, and B. Turk, *Lysosomal membrane permeabilization in cell death: concepts and challenges.* Mitochondrion, 2014. **19 Pt A**: p. 49-57.

254. Wang, L., F. Du, and X. Wang, *TNF-alpha induces two distinct caspase-8 activation pathways.* Cell, 2008. **133**(4): p. 693-703.

255. Degterev, A., et al., *Identification of RIP1 kinase as a specific cellular target of necrostatins.* Nature Chemical Biology, 2008. **4**(5): p. 313-321.

256. Holler, N., et al., *Fas triggers an alternative, caspase-8-independent cell death pathway using the kinase RIP as effector molecule.* Nature Immunology, 2000. **1**(6): p. 489-495.

257. Wu, H., J. Tschopp, and S.C. Lin, *Smac mimetics and TNFalpha: a dangerous liaison?* Cell, 2007. **131**(4): p. 655-8.

258. Kelliher, M.A., et al., *The death domain kinase RIP mediates the TNF-induced NF-kappaB signal.* Immunity, 1998. **8**(3): p. 297-303.

259. Schutze, S., V. Tchikov, and W. Schneider-Brachert, *Regulation of TNFR1 and CD95 signalling by receptor compartmentalization.* Nature Reviews Molecular Cell Biology, 2008. **9**(8): p. 655-U5.

260. Wilson, N.S., V. Dixit, and A. Ashkenazi, *Death receptor signal transducers: nodes of coordination in immune signaling networks.* Nature Immunology, 2009. **10**(4): p. 348-355.

261. Sun, X., et al., *Identification of a novel homotypic interaction motif required for the phosphorylation of receptor-interacting protein (RIP) by RIP3.* J Biol Chem, 2002. **277**(11): p. 9505-11.

262. Mahoney, D.J., et al., *Both cIAP1 and cIAP2 regulate TNFalpha-mediated NF-kappaB activation.* Proc Natl Acad Sci U S A, 2008. **105**(33): p. 11778-83.

263. Varfolomeev, E., et al., *c-IAP1 and c-IAP2 are critical mediators of tumor necrosis factor alpha (TNFalpha)-induced NF-kappaB activation.* J Biol Chem, 2008. **283**(36): p. 24295-9.

264. Liu, X., et al., *Post-translational modifications as key regulators of TNF-induced necroptosis.* Cell Death & Disease, 2016. **7**.

265. Feng, S., et al., *Cleavage of RIP3 inactivates its caspase-independent apoptosis pathway by removal of kinase domain.* Cell Signal, 2007. **19**(10): p. 2056-67.

266. Zhang, D.W., et al., *RIP3, an energy metabolism regulator that switches TNF-induced cell death from apoptosis to necrosis.* Science, 2009. **325**(5938): p. 332-6.

267. Hardwick, J.M. and L. Soane, *Multiple functions of BCL-2 family proteins.* Cold Spring Harb Perspect Biol, 2013. **5**(2).

3-Sialyl-3-fucosyllactose and Sialyllacto-N-neotetraose Induce Lactate Production and Secretion in Antigen Presenting Cells

Marek W. J. Whitehead[1], Lubor Borsig[1], Thierry Hennet[1,*]

[1]Institute of Physiology, University of Zurich, Winterthurerstrasse 190, 8057 Zurich, Switzerland

[*]Lead contact

(Manuscript in preparation)

Abstract

Human milk oligosaccharides are responsible for maintaining homeostasis in the infants gut such as by promoting the growth of beneficial bacteria like *Bifidobacteria* or by acting as antiadhesives for pathogens. Human milk oligosaccharides can also influence the behavior of leukocytes but relatively little is known about the direct regulatory effects that human milk oligosaccharides have on immunity. This especially applies for antigen presenting cells that play an important role in initiating immune response as the first line of defense. We used a panel of 15 synthesized human milk oligosaccharides to investigate if human milk oligosaccharides are capable of stimulating THP-1 and murine mesenteric lymph node derived dendritic cells. None of the human milk oligosaccharides led to the upregulation of the activation markers CD54 on THP-1 cells or CD80 on mesenteric lymph node derived dendritic cells. However, we were able to show that 3-sialyl-3-fucosyllactose and sialyllacto-N-neotetraose c were able to increase the amount of lactate produced and secreted by these cells. High lactate levels are known to be a mechanism deployed by tumor cells to influence tumor-associated macrophages to gain M2-like characteristics which leads to the greater production of immunosupressive cytokines like IL-10 or the transforming growth factor-β (TGF-β). We therefore suggest that the sialylated human milk oligosaccharides 3-sialyl-3-fucosyllactose and sialyllacto-N-neotetraose c increase the production of lactate by antigen presenting cells which is known to initiate M2-like polarization in macrophages and also inhibit the activation of cytotoxic T-cells as is analogously done by cancer cells.

Introduction

Human milk contains a vast diversity and great abundance of oligosaccharides which makes it almost unique compared to the milk of many other mammalian species such as cows that only have trace amounts of complex milk oligosaccharides [1]. Up to now about 200 different oligosaccharides have been identified in human milk [1]. These oligosaccharides however cannot be metabolized in the

human gut and therefore the question arises what these sugars actually do [2]. Before the human milk oligosaccharides (HMOs) were identified, a fraction of milk was discovered that promotes the growth of bacteria of the genus *Bifidobacteria*. This genus has been shown to be highly beneficial in the human gut and its presence can be correlated with increased rates of remission in patients affected with ulcerative colitis [3]. Later, it was found that this fraction of human milk was actually the HMOs.

Next to this effect on the proliferation of beneficial bacteria in the gut, HMOs have also been shown to support the human infant by other mechanisms too. HMOs act as anti-adhesives for pathogenic bacteria such as *Campylobacter jejuni*. Some studies even claim that HMOs can directly influence the epithelial cells that reside in the gut. Gut epithelial immortalized cell lines such as HT-29, HIEC and Caco-2 cells, were shown to suppress cell cycle progression in response to HMOs and induce apoptosis when treated with 7.5 mg/ml of HMOs [4]. Although it is unlikely that such high concentrations of HMOs actually occur at the gut epithelium. Another study showed with radioactively labelled HMOs, that the oligosaccharides actually pass the epithelial barrier and gain access to the human blood compartment and are then excreted via the urine [5]. That means HMOs could also play roles on the basolateral side of the guts lumen. Certain HMOs for instance can block the adhesion of monocytes, lymphocytes and neutrophils to endothelial cells by interfering with selectin binding [6].

Our interest is how HMOs influence the immune cells at the mucosal surface in the gut. Sialylated HMOs were shown to increase the amount of interferon-γ producing CD3+CD4+ and CD3+CD8+ producing cord blood derived T-cells [7] and sialylated HMOs cause a reduction in IL-4 production in a subset of lymphocytes derived from patients that suffered from peanut allergies [8]. Furthermore, one study demonstrated that pig peripheral blood mononuclear cells that are stimulated with HMOs, secrete more IL-10 [9].

Less is known about the regulatory effects of HMOs on antigen presenting cells such as macrophages or dendritic cells. Lacto-N-fucopentaose III (LNFPIII; Tab. 1) and Lacto-N-neotetraose (Galβ1-4GlcNAcβ1-3Galβ1-4Glc) are able to induce the proliferation of peritoneal macrophages and can suppress naïve CD4+ T-cell responses [10, 11]. LNFPIII stimulation also leads to an increase of prostaglandin E_2, IL-10 and TNFα secretion by peritoneal macrophages [12].

Table 1: Human milk oligosaccharides and their levels of contaminating LPS.

Abbreviation	Full name	Structure	LPS level (pg/mg)
2FL	2-Fucosyllactose	Fuc(α1-2)Gal(β1-4)Glc	n.d.
3FL	3-Fucosyllactose	Gal(β1-4)[Fuc(α1-3)]Glc	n.d.
3SL	3-Sialyllactose	Sia(α2-3)Gal(β1-4)Glc	n.d.
6SL	6-Sialyllactose	Sia(α2-6)Gal(β1-4)Glc	n.d.
FSL	3-Sialyl-3-fucosyllactose	Sia(α2-3)Gal(β1-4)[Fuc(α1-3)]Glc	3.1
DFL	Difucosyllactose	Fuc(α1-2)Gal(β1-4)[Fuc(α1-3)]Glc	n.d.
LNFPI	Lacto-N-fucopentaose	Fuc(α 1-2)Gal(β1-3)GlcNAc (β1-3)Gal(β1-4)Glc	n.d.
LNFPII	Lacto-N-fucopentaose II	Gal(β1-3)[Fuc(α1-4)]GlcNAc (β1-3)Gal(β1-4)Glc	n.d.
LNFPIII	Lacto-N-fucopentaose III	Gal(β1-4)[Fuc(α1-3)]GlcNAc (β1-3)Gal(β1-4)Glc	n.d.
LST-a	Sialyllacto-N-tetraose a	Sia(α2-3)Gal(β1-3)GlcNAc(β1-3) Gal(β1-4)Glc	2.4
LST-c	Sialyllacto-N-neotetraose c	Sia(α2-6)Gal(β1-4)GlcNAc(β1-3) Gal(β1-4)Glc	2.4
LST-d	Sialyllacto-N-neotetraose d	Sia(α2-3)Gal(β1-4)GlcNAc(β1-3) Gal(β1-4)Glc	2.4
Para-LNnH	Para-lacto-N-neohexaose	Gal(β1-4)GlcNAc(β1-3)Gal(β1-4) GlcNAc(β1-3)Gal(β1-4)Glc	4.4
LNnH	Lacto-N-neohexaose	Gal(β1-4)GlcNAc(β1-3)[Gal(β1-4) GlcNAc(β1-6)]Gal(β1-4)Glc	2.2
DSLNT	Disialyllacto-N-tetraose	Sia(α2-3)Gal(α1-3)[Sia(α2-6)] GlcNAc(β1-3)Gal(β1-4)Glc	n.d.

Siglecs are immune-modulating receptors that occur on leukocytes including antigen-presenting cells [13]. Interestingly, sialylated HMOs have been shown to be able to bind to these receptors [14] and also galectins which bind to β1-3 and β1-4 linked galactose are potential receptors for the HMOs [15]. However the precise consequences of HMO binding to these receptors in different cell types remains to be elucidated.

We set out to identify novel roles of HMOs on antigen presenting cells. In the guts lamina propria there are macrophages and dendritic cells that act as sentinels and can take up antigens. Antigen loaded dendritic cells can then migrate into the mesentery lymph nodes to present their cargo to T-cells for example [16]. Both macrophages and dendritic cells are key determinants of the type of immune reaction that is launched because of the amount and types of cytokines that they produce after activation [17, 18]. Previous studies have shown that bacterial glycans and the glycans that

occur on mucins can influence the cytokine response of antigen presenting cells [19-21]. So we asked ourselves if HMOs could actually also regulate the immune responses that are initiated by antigen presenting cells.

For the stimulation experiments we chose to work with the monocytic immortal cell line THP-1 and murine mesenteric lymph node derived dendritic cells from C57BL/6 mice. The prior is a commonly used model system for monocytes derived from an acute monocytic leukemia patient. The cells are often used as they still have the potential to differentiate into macrophages and fulfill functions that are performed by monocytes and macrophages such as phagocytosis, producing inflammatory cytokines or removing cellular debris [22]. Mesenteric lymph node derived dendritic cells on the other hand are in close proximity to the intestinal barrier and are therefore at the actual site that comes into contact with the complex oligosaccharides that occur in milk. Dendritic cells from gut associated lymph nodes react differently to stimuli from the gut such as derived from the commensal gut microbiota compared to dendritic cells that occur in gut distant tissue such as the spleen [23]. While the prior will act immune regulatory the latter will initiate a strong inflammatory response to the same stimulus [23].

Materials and Methods

Human milk oligosaccharides

2-Fucosyllactose (2FL), 3-fucosyllactose (3FL), 3-sialyllactose (3SL), 6-sialyllactose (6SL), 3-sialyl-3-fucosyllactose (FSL), difucosyllactose (DFL), lacto-N-fucopentaose I (LNFPI), lacto-N-fucopentaose II (LNFPII), lacto-N-fucopentaose III (LNFPIII), sialyllacto-N-tetraose a (LST-a), sialyllacto-N-neotetraose c (LST-c), sialyllacto-N-neotetraose d (LST-d), para-lacto-N-neohexaose (Para-LNnH) and disialyllacto-N-tetraose (DSLNT) were all synthesized and supplied by the company Glycom (Tab. 1).

Lipopolysaccharide quantification and removal

Lipopolysaccharide (LPS) levels were determined with the Endotoxin Plus kit 0.03 EU/ml sensitivity (Lonza) according to the provided instructions. If the LPS contamination was above 5 pg per mg oligosaccharide, LPS was removed with Endotoxin Removal Beads (Miltenyi Biotec).

Briefly, the respective oligosaccharide was resuspended in a volume of 500 to 1000 µl of water and 50 µl of the resuspended beads were added to the oligosaccharide solution. This was incubated for 1 h rotating end over end at 4°C. The beads were then centrifuged down at 500 x g for 5 min and the

oligosaccharide containing supernatant was harvested. The LPS levels were determined again to confirm the absence of endotoxins (Tab. 1).

THP-1 cultivation

THP-1 cells were cultured in Roswell Park Memorial Institute (RPMI) medium with 10% fetal calf serum (FCS).

Mesenteric lymph node dendritic cell isolation and cultivation

Mesenteric lymph node derived dendritic cells were harvested and cultured as previously described [24]. Briefly, mesenteric lymph nodes were removed from euthanised mice and incubated in 2.5 mg/ml collagenase D (Roche) in RPMI medium with 10% FCS for 10 min shaking at 150 rounds per minute (rpm) at 37°C. The lymph nodes were then gently homogenized by aspirating them through an 18G syringe. The homogenate was incubated for a further 20 min at 37°C in a water bath. The cells were then pelleted by centrifuging them for 7 min at 300 x g. The pellet was resuspended in 1 ml of 2 mM EDTA and 0.5% bovine serum albumin (BSA) in phosphate buffered saline (PBS; pH 7.2). Clumps were further homogenized by gently aspirating them through an 18G syringe. Next, the cells were passed through a 40 µm cell strainer to remove any cell aggregates. The cells were then centrifuged again and resuspended in 100 µl of 2 mM EDTA and 0.5% bovine serum albumin (BSA) in PBS (pH 7.2). Purified rat anti-mouse CD16/32 (Affymetrix eBioscience) was added at 5 µg/ml and the mix was incubated at 4°C for 10 min to block Fc receptors. Then CD11c beads (Miltenyi Biotec) were added to isolate the $CD11c^+$ cells according to the provided manual with a magnetic separator. The cells were cultivated in RPMI medium with 10% FCS supplemented with penicillin and streptomycin.

Reverse transcription PCR for Siglecs and galectins in THP-1 cells

The reverse transcription step was performed with the Omniscript RT kit (Qiagen) with random hexamers (Qiagen) according to the procedure described by the supplier.

PCRs were performed with Taq polymerase (Sigma Aldrich) according to the protocol provided by the supplier. The following forward (FP) and reverse (RP) primers were designed for the Siglecs -2 (FP: 5'-GAGTGCAACCCTGACCTGTG-3'; RP: 5'-GAGCTTGAGCCCACAGATTG-3'), -3 (FP: 5'-TACTCACTCCTCGGTGCTCA-3'; RP: 5'-TGAGGCAGAGACAAAGAGCG-3'), -14 (FP: 5'-ATGCTCCACAGAACCTCGC-3'; RP: 5'-CCTATGTTAGGCAGCTCCAGG-3'), -15 (FP: 5'-ACCTAGTGACCGCCGAACTG-3'; RP: 5'-GTGTCCGGGGTGTCCAGATG-3') and the galectins -1 (FP: 5'-ATCTCAAACCTGGAGAGTGCC-3'; RP: 5'-CTGGAAGGGAAAGACAGCCTC-3'), -2 (FP: 5'-GGGGTCAACCCTGAAGATCA-3'; RP: 5'-ACCCAGCCTGTTGGGAAAAG-3'), -3 (FP: 5'-

CTTATCCTGGACAGGCACCTC-3'; RP: 5'-CCCAGGCAAAGGCAGGTTAT-3'), -9 (FP: 5'-GGGCTGTACCCATCCAAGTC-3'; RP: 5'-AGGCAGTGAGCTTCACACAA-3'), -10 (FP: 5'-CCACCCAGAAGGAGACAACA-3'; RP: 5'GGCCATCCTGAAAGGGCATA-3').

Flow cytometry

In each experiment 40'000 cells were stained with 5 µg/ml of the anti-murine CD11c-allophycocyanin (APC) (Biolegend), anti-murine CD80-phycoerythrin (PE) (BD Pharmingen), anti-human CD54-PE (Affymetrix eBioscience), anti-human CD107a-PE (Affymetrix eBioscience) and/or anti-human Siglec-1-PE (Affymetrix eBioscience) antibodies in Hank's Balanced Saline Solution (HBSS) at 4°C for 30 min, then washed twice in HBSS before analysis using a FACScanto II flow cytometer (BD Bioscience).

Cell stimulation with human milk oligosaccharides

Generally, THP-1 cells and mesenteric lymph node derived dendritic cells were sawn at 200'000 cells/ml in 200 µl and cultured in 96-well plates unless specified otherwise. Then the cells were stimulated with 1 mM of each HMO. Positive controls were stimulated with 500 ng/ml LPS for mesenteric lymph node derived dendritic cells or 10 ng/ml of LPS for THP-1 cells. Mesenteric lymph node derived dendritic cells were cultivated for 14 h before the cells were used for flow cytometry while THP-1 cells were used 24 h after stimulation. In certain experiments the THP-1 cells were pre-treated with 1 mM of each oligosaccharide before being treated with 10 ng/ml of LPS. If the cells were cultured as drop cultures on Terasaki plates, they were sawn at 800'000 cells/ml and stimulated with 1 mM of the respective HMO for 14 h (dendritic cells) or 24 h (THP-1).

Measuring the pH of cell culture media

These experiments were conducted blinded. For the measurement pH test strips with a resolution of 0.3 to 0.4 pH units between the pH values 6.0 and 7.7 were used (Sigma-Aldrich)

Determination of lactate levels in the culture media

To measure the amount of lactate in the culture media a commercial L-lactate assay (ScienCell) was used according to the provided instructions. The measurement was done with an Infinite® 200 Pro plate reader (Tecan Trading AG, Männerdorf, Switzerland).

3-(4,5-dimethylthiazol-2-yl)-2,5,diphenyltetrazolium bromide assay

The cells were cultured in 100 µl of media and 10 µl of a 12 mM 3-(4,5-dimethylthiazol-2-yl)-2,5,diphenyltetrazolium bromide stock was added. The cells were then incubated at 37°C for 4 h.

Then, all but 25 µl of the media was removed. 50 µl of DMSO was then added to each well and the plates were incubated at 37°C for 10 min. The liquid content of each well was mixed well and the absorption was determined at 540 nm with an Infinite® 200 Pro plate reader (Tecan Trading AG, Männerdorf, Switzerland).

Quantification and statistical analysis

All results are presented as means with their standard deviations unless otherwise indicated. The data was analyzed in GraphPad Prism 5 by ANOVA with Bonferroni's multiple comparison post-testing to determine statistical differences between different experimental groups. A p-value below 0.05 was considered as statistically significant.

Results

Determination of Lipopolysaccharide levels in human milk oligosaccharide preparations

To be able to use the synthesized HMOs in immunological in vitro assays, it was important for us to determine if any of the oligosaccharides were contaminated with LPS as this could lead to the stimulation of immune cells independently of HMOs and enable false conclusions [25, 26]. Therefore we used the Limulus Amebocyte lysate assay to determine the amount of LPS contamination in the HMOs. The LPS in contaminated oligosaccharide preparations was removed by polymyxin B coated agarose beads to achieve an LPS load of maximally 5 pg/mg of oligosaccharide. This threshold was chosen as previously it was shown that LPS can induce the activation of immune cells at concentrations as low as 10 pg/ml in the media [27] (Table 1).

HMOs do not influence THP-1 or mesenteric lymph node derived dendritic cell activation

Dendritic cells express many lectins that may be able to bind human milk oligosaccharides such as C-type lectins [28], galectins [29, 30] or Siglecs [31, 32]. We demonstrated that THP-1 cells highly express the Siglecs -3 and -14 (bands at 260 bp and 229 bp respectively) and the galectins 1, 2 and 3 (bands at 212 bp, 289 bp and 215 bp) (Fig. 1A). The expression of Siglec-2 was very low (band at 295 bp) while Siglec-15 (band expected at 238 bp) and the galectins-9 and -10 (bands expected at 251 bp and 279 bp) were not expressed (Fig. 1A). On protein level Siglec-1 was shown to be present on the surface of THP-1 cells by flow cytometry (Fig. 1B). That means THP-1 cells as well as mesenteric lymph node derived dendritic cells express proteins that can bind HMOs which may lead to intracellular signaling for instance via the intracellular ITIM-domain that that many Siglecs have [13]. Alternatively galectins have also been shown to be able to modulate immune reactions such as when

galectin-3 binds to the glycans on the intestinal mucin MUC2 and then forms a complex with dectin-1 and FcγRIIB which activates β-catenin and influences the production of cytokines [21].

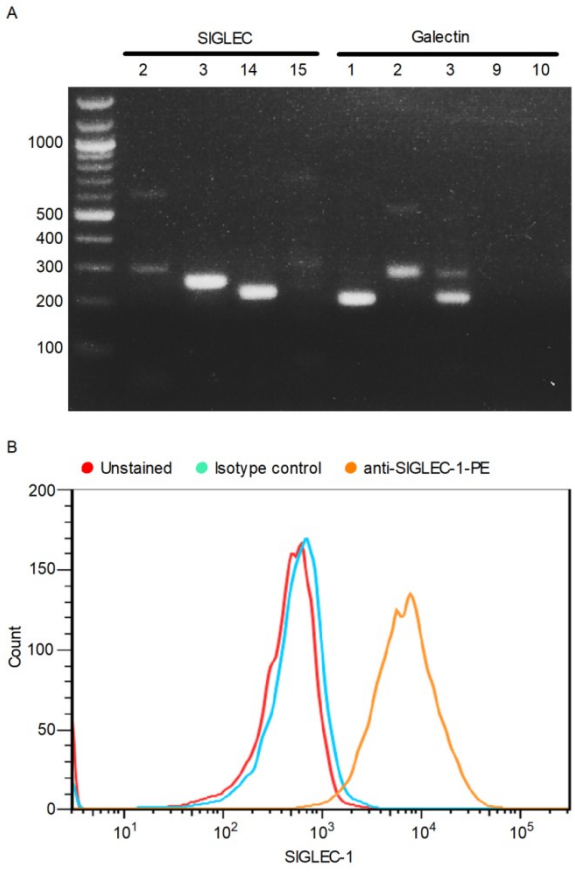

Figure 1: Expression of Siglec and galectins by THP-1 cells. (A) RT-PCR was performed for the Siglecs -2, -3, -14, -15 and the galectins -1, -2, -3, -9, -10. The expected band sizes are 295bp, 260 bp, 229 bp, 238 bp, 212 bp, 289 bp, 215 bp, 251 bp and 279 bp in that order. (B) THP-1 cells were stained with an antibody targeting Siglec-1 to show that it is present on the surface of THP-1 cells by flow cytometry. Unstained cells (red lines), isotype control (blue lines), anti-Siglec-1-PE stained (orange lines). The presented data is representative for three independent experiments.

The stimulation of mesenteric lymph node derived dendritic cells with LPS lead to a two fold increase of the costimulatory activation marker CD86 on the surface of the cells. The HMOs on the other hand did not lead to a further increase in CD86 surface levels (Fig. 2A). Similarly, LPS stimulation induced a 60 fold increase of the integrin CD54 on the surface of THP-1 cells but HMOs did not lead to an increase of CD54 (Fig. 2B). CD54 is an integrin that appears on the cell surface of THP-1 cells when they have been activated and plays a role during the extravasation of monocytes into inflamed tissues in vivo [33].

Next, we examined if pre-stimulating THP-1 monocytes with HMOs could influence the degree of CD54 surface presentation of LPS stimulated cells. However none of the HMOs influenced the amount of CD54 presented on the cell surface (Fig. 2C).

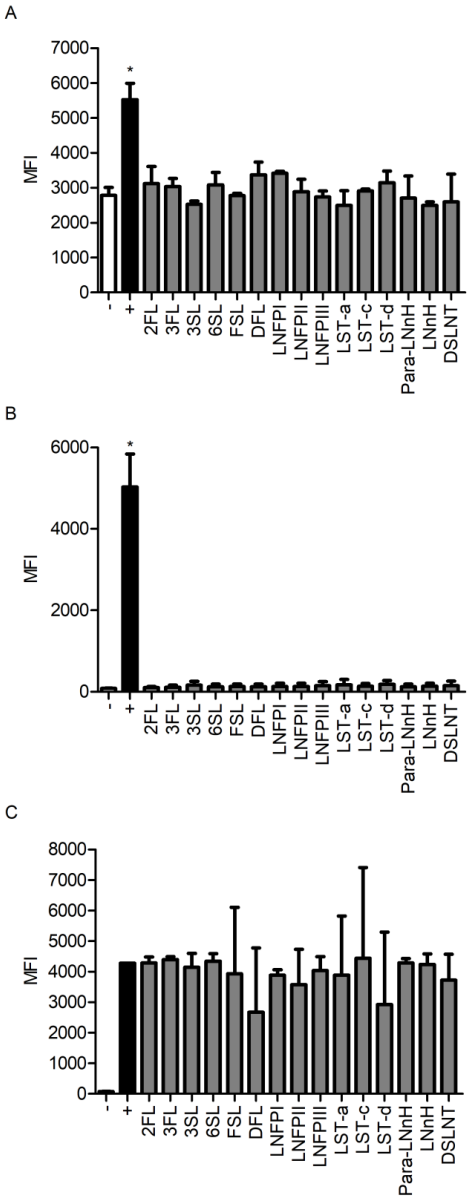

Figure 2: Stimulation of mesenteric lymph node derived dendritic cells and THP-1 cells with HMOs (A) Mesenteric lymph node derived dendritic cells were stimulated with HMOs for 14 h and then the cells were stained with anti-CD80-PE to determine the amount of the activation marker CD80 on their surface by flow cytometry. (B) THP-1 cells were stimulated with HMOs for 24 h and then the cells were stained with anti-CD54-PE to determine the amount of the activation marker CD54 on their surface by flow cytometry. (C) THP-1 cells were pre-treated with 1 mM of the respective HMO and then stimulated with LPS for a further 24 h. The cells were harvested and stained with anti-CD54-PE to determine the amount of the activation marker CD54 on their surface. -, no treatment; +, 10 ng/ml LPS (THP-1) or 500 ng/ml LPS (mesenteric lymph node derived dendritic

cells); MFI, median fluorescence intensity. The median fluorescence intensity is plotted in a bar graph and the error bar is the standard deviation of three independent samples. The statistical significance was calculated by ANOVA with Bonferroni post-testing in all three graphs.

FSL, LST-c and LST-d stimulation of THP-1 cells leads to acidification of the surrounding media

When THP-1 cells were cultured in drop cultures on Terasaki plates, the addition of FSL, LST-c and LST-d lead to a visible acidification of the phenol-red containing media which turns yellow when it becomes more acidic. We measured the pH of these drops after 24 h of cultivation and determined that there was a pH of 7.15 in the media of cells treated with the oligosaccharides FSL and LST-c and a pH of 7.3 in the media of cells treated with LST-d while all other HMOs did not cause this pH shift and the pH was at 7.7 as the untreated control was (Fig. 3A). The same effect could also be obtained by culturing the cells at high density (1'000'000 cells per ml) in round bottom 96-well plates (data not shown) in comparison to the low densities that we typically used (200'000 cells per ml).

We then tracked the dynamics of the pH change in FSL, LST-c and LST-d treated cells over a period of 24 h. As a control we treated cells with 3SL, which did not lead to a decrease of the pH after 24 h compared to untreated cells. Both the FSL and LST-c treated cells had a clearly lower pH of 7.3 after 6 h of cultivation compared to 3SL treated cells that remained at pH 7.7. The pH dropped to 7.15 between 12 and 24 h of cultivation (Figs. 3B, C). The pH of LST-d treated cells also dropped to 7.3 between 12 and 24 h of cultivation (Fig. 3D).

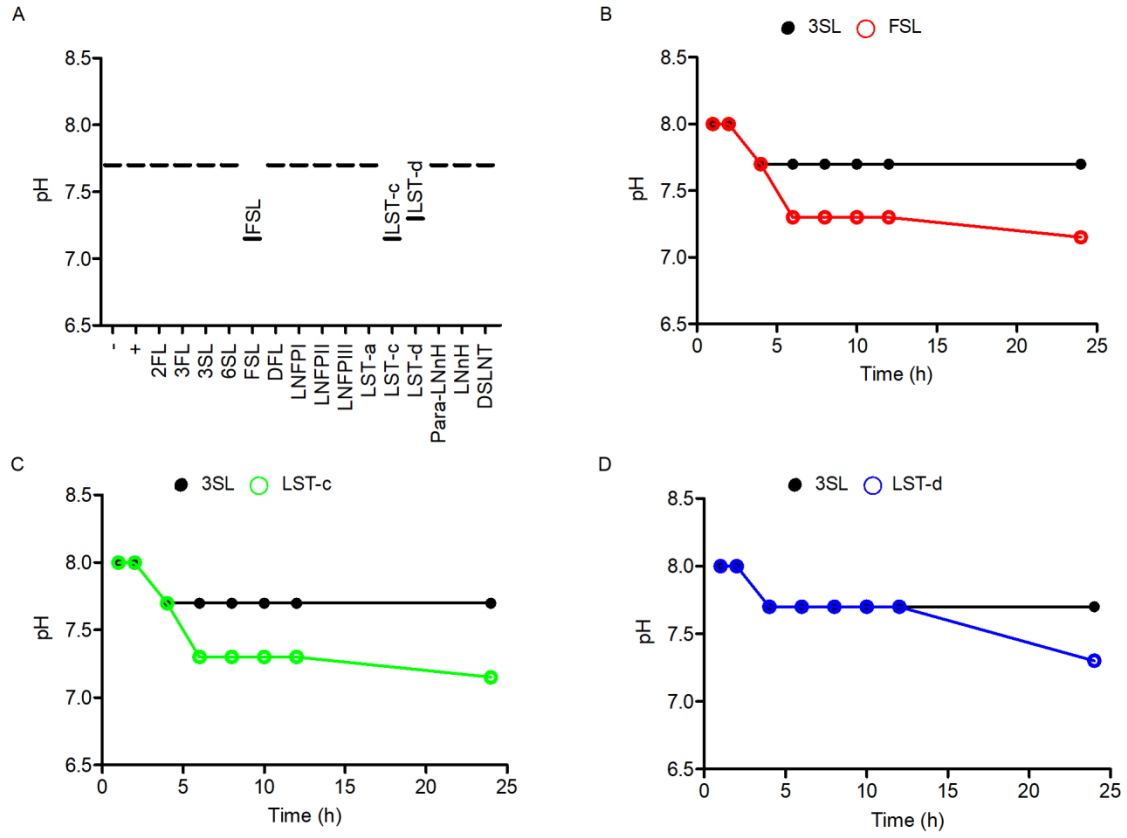

Figure 3: FSL, LST-c and LST-d induced THP-1 cells to acidify the media. (A) THP-1 cells were cultivated in drop cultures on Terasaki plates and 1 mM of each human milk oligosaccharide was added. 24 h later the pH of the cell culture media was determined by high resolution pH strips. All data points represent triplicates. (B, C, D) THP-1 cells were cultured in Terasaki plates and stimulated with 1 mM of 3SL, FSL, LST-c or LST-d for 24 h. The pH was measured after 1, 2, 4, 6, 8, 10, 12 and 24 h. Black, 3SL; red, FSL; green, LST-c; blue, LST-d. For each measurement a single drop was used and per time point three independent measurements were made. The pH determination occurred blinded.

Increased production of lactate explains the drop in pH of FSL and Lst-c treated THP-1 cells

The decrease of the pH in the media of FSL, LST-c and LST-d treated cells could be due to several mechanisms. One possibility is the release of the acidic lysosomal interior liquid into the extracellular space via secretion. This occurs in macrophages for instance that use secretory lysosomes to transport MHC-II to the cell surface to present antigens [34]. Another example for cells that secrete their lysosomes, are osteoclasts which secrete enzymes for bone resorption enabling the remodeling of bones [35, 36]. A marker of lysosomal fusion with the plasma membrane is the presence of the lysosomal membrane protein CD207a at the plasma membrane so we tested if the treatment of THP-1 cells with FSL and LST-c lead to increased staining of CD207a compared to 3SL treated cells, however no increase was observed (Fig. 4A).

We next asked ourselves if the increased pH may be due to increased metabolic activity of the cells as a consequence of the treatment with FSL, LST-c or LST-d. Increased levels of soluble CO_2 and lactic acid may cause the media to turn acidic [37-39]. Therefore we used the 3-(4,5-dimethylthiazol-2-yl)-2,5,diphenyltetrazolium bromide assay, which is a colorimetric assay, to assess the metabolic activity of cells. In this assay the dye 3-(4,5-dimethylthiazol-2-yl)-2,5,diphenyltetrazolium bromide is reduced to it insoluble form formazan by the activity of NAD(P)H-dependent oxidoreductase enzymes [40]. The FSL, LST-c and LST-d treated cells had no increased absorption at 540 nm compared to untreated and 3SL treated cells (Fig. 4B) and the number of living cells remained equal between all the treatments at around $3x10^5$ to $4x10^5$ cells per ml (Fig. 4C, D) which, taken together, indicates that the metabolic rate remains the same between the cells.

A further possibility however, is that there is no change in the overall metabolic rate but rather that there is reprogramming of the metabolism such as occurs in cancer cells that are often characterized by the Warburg effect where the metabolism is redirected towards more glycolysis at the cost of oxidative phosphorylation, leading to the greater production of lactate which causes media acidification [41-43]. This effect has also been observed in antigen presenting cells such as dendritic cells or macrophages and has been shown to be of great importance for the activation of T cells for instance [44, 45]. Indeed, we were able to show that THP-1 cells treated with FSL and LST-c have about 3 times more lactate in their surrounding media than untreated or 3SL treated THP-1 cells (Fig. 4E). However LST-d treated cells don't have significantly more lactate in their surrounding media (Fig. 4E).

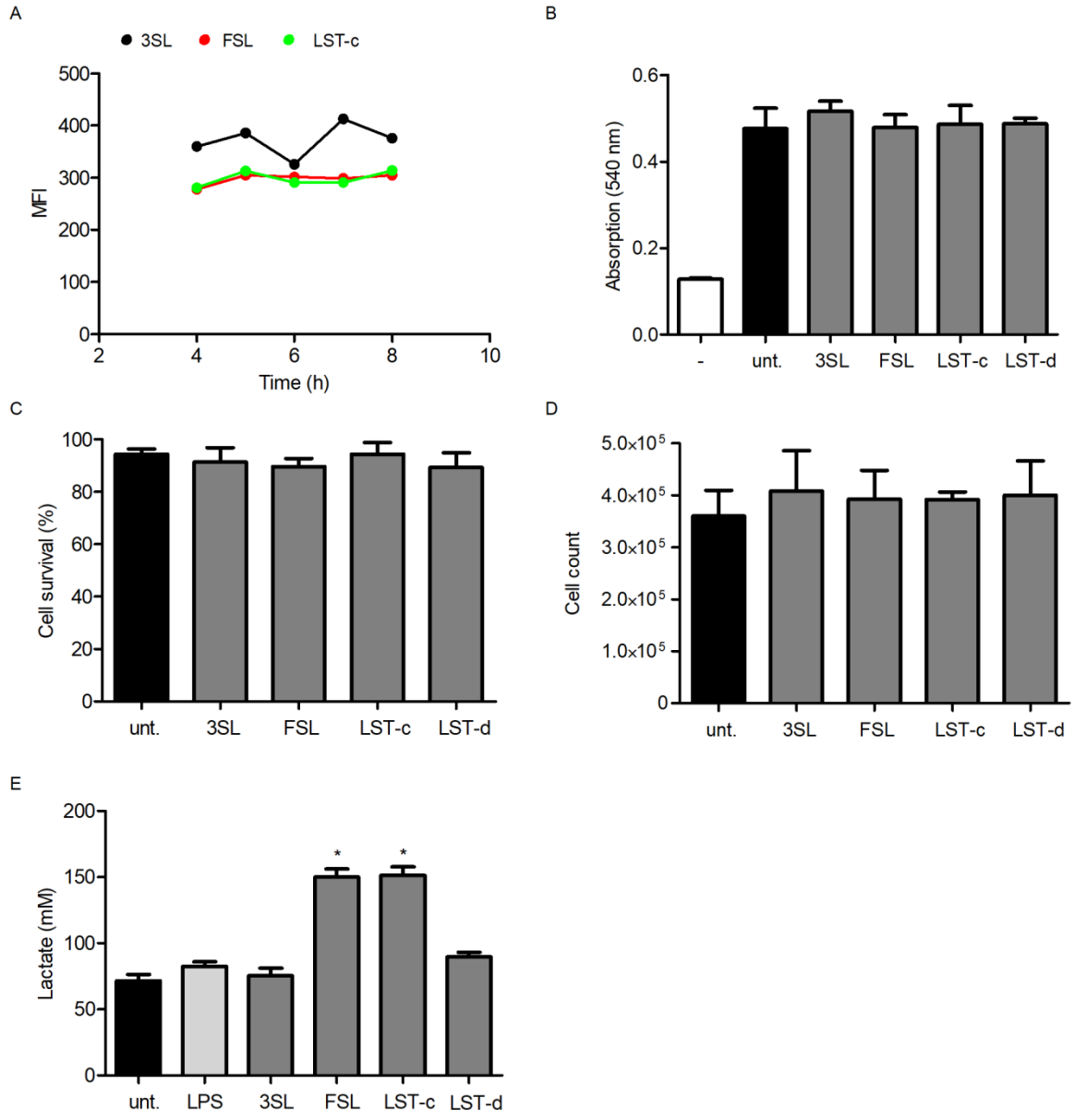

Figure 4: FSL and LST-c treated THP-1 cells secrete lactate. (A) Flow cytometry was performed with THP-1 cells that were treated with 3SL, FSL or LST-c and stained with a PE labelled antibody targeting CD207a. Measurements were conducted 4, 5, 6, 7 and 8 hours after the addition of the respective HMO and the median fluorescence intensity was determined and plotted on the y-axis. Black, 3SL; red, FSL; green, LST-c. (B) THP-1 cells were either untreated or treated with 3SL, FSL, LST-c or LST-d for 5 h. Then the 3-(4,5-dimethylthiazol-2-yl)-2,5,diphenyltetrazolium bromide assay was performed over a duration of 4 h prior to dissolving the produced formazan with DMSO and measuring the absorption at 540 nm. -, control without cells; unt., untreated. The experiment was performed in triplicate and the error bars indicate the standard deviation. The absence of statistical significance was determined by ANOVA with Bonferroni post-testing. (C, D) To count the amount of cells, a Neubauer improved cytometer was used and the amount of dead cells was determined by staining dead cells with trypan blue. Unt., untreated. The experiments were performed in triplicates and the

absence of statistical significance was determined by ANOVA and Bonferroni post-testing. (E) The cells were either untreated or stimulated with 3SL, FSL or LST-c for 24 h. Then the media was collected and the amount of lactate was determined in the supernatant. Unt., untreated. The experiments were performed in triplicates and the statistical significance was determined with ANOVA and Bonferroni post-testing.

Media acidification occurs in FSL and LST-c treated mesenteric lymph node derived dendritic cells

The next question that we asked ourselves was if the same effect could also be observed in mesenteric lymph node derived dendritic cells. To determine this we also incubated the cells in drop cultures on Terasaki plates and stimulated the cells with the two stronger acting HMOs FSL and LST-c but also 3SL as a negative control. As with the THP-1 cells, mesenteric lymph node derived dendritic cells made the media more acidic when treated with FSL or LST-c, resulting in a pH of 7.3 after 24 h (Figs. 5A, B). 3SL on the other hand did not induce this change of pH. Instead, the pH remained at 7.7 (Figs. 5A, B). We also measured the lactate levels, and although the mean levels were increased from the baseline of around 10 mM in untreated cells to around 25 mM in FSL and LST-c treated cells, it was not statistically significant.

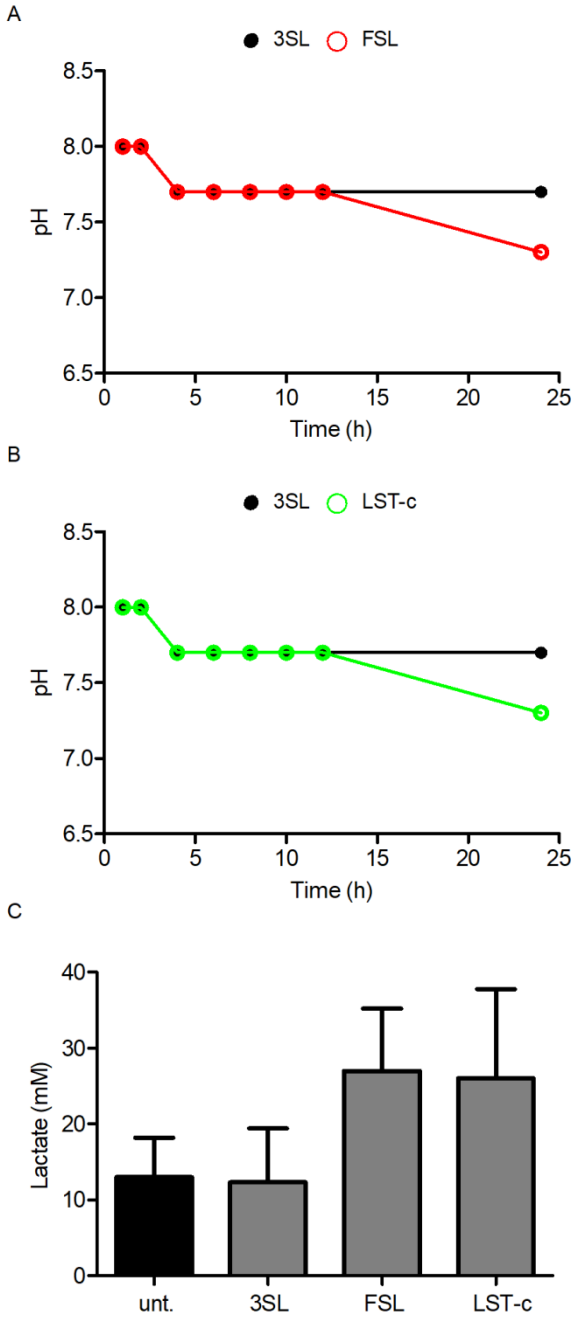

Figure 5: FSL and LST-c stimulation lead to the acidification of the media of mesenteric lymph node derived dendritic cells. (A, B) Mesenteric lymph node derived dendritic cells were cultured in Terasaki plates and stimulated with 1 mM of 3SL, FSL, LST-c or LST-d for 24 h. The pH was measured after 1, 2, 4, 6, 8, 10, 12 and 24 h. Black, 3SL; red, FSL; green, LST-c; blue, LST-d. For each measurement a single drop was used and per time point three independent measurements were made. The pH determination occurred blinded. (C) The cells were either untreated or stimulated with 3SL, FSL or LST-c for 24 h. Then the media was collected and the amount of lactate was determined in the supernatant. Unt., untreated. The experiments were performed in triplicates and the statistical significance was determined by ANOVA with Bonferroni post-testing.

Discussion

To generate energy, mammalian cells catabolize glucose into pyruvate and the most of it is then directed into the tricarboxylic acid (TCA) cycle. Only some of the pyruvate is fermented into lactate. However in 1929, Otto Warburg discovered that in tumor cells, pyruvate fermentation predominates despite the availability of oxygen [46]. 20 years later, activated macrophages were discovered to have increased rates of glycolysis and reduced oxygen consumption [47]. As a consequence, most of the glucose is metabolized into lactate at the cost of oxidative phosphorylation [48].

Dendritic cells as well as macrophages react by reducing oxidative phosphorylation and increasing glycolysis when they are stimulated with activating stimulants such as LPS, interferon-γ or the Toll-like receptor 3 (TLR3) ligand poly(I:C) [49, 50]. Analogous to the Warburg effect there is also increased flux through the pentose phosphate pathway which means increased production of purines and pyrimidines that are available for biosynthesis and also an increase in the amount of NADPH that can be used by NADPH oxidases to generate reactive oxygen species [51]. This metabolic switch is essential for the maturation of macrophages and dendritic cells and inhibition of this process, such as by using inhibitors of glycolysis like 2-deoxy-D-glucose, leads to decreased antigen presenting cell maturation as is evident by the reduced amounts of the costimulatory proteins CD80 and CD86 on the cell surface [52].

Interestingly, in our experiments, no observable pH decrease occurs in LPS treated THP-1 cells or mesenteric lymph node derived dendritic cells, and the lactate amount in the media is not increased after 24 h either, although LPS stimulation has been shown to lead to the metabolic switch from the TCA cycle to glycolysis. This indicates that the lactate remains intracellular after the treatment with LPS. There are two control points that can influence the increase in extracellular lactate concentrations, one is the activity of lactate dehydrogenase which is responsible for the regeneration of pyruvate from lactate and the other is the transport of lactate through specific monocarboxylate transporters [53]. Both checkpoints may be involved as regulators of lactate secretion and the HMOs FSL, LST-c and LST-d may serve as switches that initiate lactate production and secretion. The precise mechanism leading to this switch still remains to be identified. Both THP-1 cells and mesenteric lymph node derived dendritic cells have many lectins on their cell surface such as Siglecs [31, 32], galectins [29, 30] or C-type lectins [28] which could initiate the described process (Fig. 1).

The secretion of lactate is actually something that is done by cancer cells and the increased lactate levels in the surrounding media have been shown to have a profound influence on the surrounding antigen presenting cells. Another study was able to show that lactate is the component in tumor conditioned media that is able to activate HIF1α in macrophages, ultimately leading to an M2-like

transcriptional profile [54]. In tumors this is critical, as it leads to the production of immunosuppressive cytokines like IL-10 and TGF-β and less inflammatory cytokines like IL-12, IL-1β, TNF-α or IL-6 [55]. Furthermore lactate is able to suppress the proliferation and cytokine production by human cytotoxic T lymphocytes [56]. We therefore propose that FSL and LST-c can reprogram antigen presenting cells to be more immunomodulatory than inflammatory which makes sense when considering that the gut lumen, where these oligosaccharides occur in the suckling after breastfeeding, is rich in external stimuli from food and the microbiota that should not induce an inflammatory immune response in the healthy state.

Acknowledgments

We thank Glycom A/S for supplying us with the human milk oligosaccharides. This research was supported by the Zurich Center for Integrative Human Physiology (ZIHP) and by the Swiss National Science Foundation grant 314730_172880.

Author Contributions

M.W.J.W., L.B., and T.H. planned the experiments. M.W.J.W. performed the experiments. M.W.J.W wrote the manuscript.

References

1. Hennet, T., A. Weiss, and L. Borsig, *Decoding breast milk oligosaccharides.* Swiss Med Wkly, 2014. **144**: p. w13927.

2. German, J.B., et al., *Human milk oligosaccharides: evolution, structures and bioselectivity as substrates for intestinal bacteria.* Nestle Nutr Workshop Ser Pediatr Program, 2008. **62**: p. 205-18; discussion 218-22.

3. Ghouri, Y.A., et al., *Systematic review of randomized controlled trials of probiotics, prebiotics, and synbiotics in inflammatory bowel disease.* Clin Exp Gastroenterol, 2014. **7**: p. 473-87.

4. Kuntz, S., S. Rudloff, and C. Kunz, *Oligosaccharides from human milk influence growth-related characteristics of intestinally transformed and non-transformed intestinal cells.* Br J Nutr, 2008. **99**(3): p. 462-71.

5. Obermeier, S., et al., *Secretion of 13C-labelled oligosaccharides into human milk and infant's urine after an oral [13C]galactose load.* Isotopes Environ Health Stud, 1999. **35**(1-2): p. 119-25.

6. Bode, L., et al., *Inhibition of monocyte, lymphocyte, and neutrophil adhesion to endothelial cells by human milk oligosaccharides.* Thromb Haemost, 2004. **92**(6): p. 1402-10.

7. Eiwegger, T., et al., *Human milk--derived oligosaccharides and plant-derived oligosaccharides stimulate cytokine production of cord blood T-cells in vitro.* Pediatr Res, 2004. **56**(4): p. 536-40.

8. Eiwegger, T., et al., *Prebiotic oligosaccharides: in vitro evidence for gastrointestinal epithelial transfer and immunomodulatory properties.* Pediatr Allergy Immunol, 2010. **21**(8): p. 1179-88.

9. Comstock, S.S., et al., *Select human milk oligosaccharides directly modulate peripheral blood mononuclear cells isolated from 10-d-old pigs.* Br J Nutr, 2014. **111**(5): p. 819-28.

10. Atochina, O., et al., *A schistosome-expressed immunomodulatory glycoconjugate expands peritoneal Gr1(+) macrophages that suppress naive CD4(+) T cell proliferation via an IFN-gamma and nitric oxide-dependent mechanism.* J Immunol, 2001. **167**(8): p. 4293-302.

11. Terrazas, L.I., et al., *The schistosome oligosaccharide lacto-N-neotetraose expands Gr1(+) cells that secrete anti-inflammatory cytokines and inhibit proliferation of naive CD4(+) cells: a potential mechanism for immune polarization in helminth infections.* J Immunol, 2001. **167**(9): p. 5294-303.

12. Atochina, O. and D. Harn, *LNFPIII/LeX-stimulated macrophages activate natural killer cells via CD40-CD40L interaction.* Clin Diagn Lab Immunol, 2005. **12**(9): p. 1041-9.

13. Crocker, P.R., J.C. Paulson, and A. Varki, *Siglecs and their roles in the immune system.* Nat Rev Immunol, 2007. **7**(4): p. 255-66.

14. Koliwer-Brandl, H., et al., *Lectin inhibition assays for the analysis of bioactive milk sialoglycoconjugates.* International Dairy Journal, 2011. **21**(6): p. 413-420.

15. Rabinovich, G.A., et al., *Galectins and their ligands: amplifiers, silencers or tuners of the inflammatory response?* Trends Immunol, 2002. **23**(6): p. 313-20.

16. Pabst, O. and G. Bernhardt, *The puzzle of intestinal lamina propria dendritic cells and macrophages.* Eur J Immunol, 2010. **40**(8): p. 2107-11.

17. Banchereau, J. and R.M. Steinman, *Dendritic cells and the control of immunity.* Nature, 1998. **392**(6673): p. 245-52.

18. Arango Duque, G. and A. Descoteaux, *Macrophage cytokines: involvement in immunity and infectious diseases.* Front Immunol, 2014. **5**: p. 491.

19. Bergman, M.P., et al., *Helicobacter pylori modulates the T helper cell 1/T helper cell 2 balance through phase-variable interaction between lipopolysaccharide and DC-SIGN.* J Exp Med, 2004. **200**(8): p. 979-90.

20. Tailleux, L., et al., *DC-SIGN is the major Mycobacterium tuberculosis receptor on human dendritic cells.* J Exp Med, 2003. **197**(1): p. 121-7.

21. Shan, M., et al., *Mucus enhances gut homeostasis and oral tolerance by delivering immunoregulatory signals.* Science, 2013. **342**(6157): p. 447-53.

22. Bosshart, H. and M. Heinzelmann, *THP-1 cells as a model for human monocytes.* Ann Transl Med, 2016. **4**(21): p. 438.

23. Fink, L.N. and H. Frokiaer, *Dendritic cells from Peyer's patches and mesenteric lymph nodes differ from spleen dendritic cells in their response to commensal gut bacteria.* Scand J Immunol, 2008. **68**(3): p. 270-9.

24. Kurakevich, E., et al., *Milk oligosaccharide sialyl(alpha2,3)lactose activates intestinal CD11c+ cells through TLR4.* Proc Natl Acad Sci U S A, 2013.

25. Alexander, C. and E.T. Rietschel, *Bacterial lipopolysaccharides and innate immunity.* J Endotoxin Res, 2001. **7**(3): p. 167-202.

26. Nerurkar, S.S., et al., *Lipopolysaccharide (LPS) contamination plays the real role in C-reactive protein-induced IL-6 secretion from human endothelial cells in vitro.* Arterioscler Thromb Vasc Biol, 2005. **25**(9): p. e136.

27. Schwarz, H., et al., *Residual endotoxin contaminations in recombinant proteins are sufficient to activate human CD1c+ dendritic cells.* PLoS One, 2014. **9**(12): p. e113840.

28. van Kooyk, Y., *C-type lectins on dendritic cells: key modulators for the induction of immune responses.* Biochem Soc Trans, 2008. **36**(Pt 6): p. 1478-81.

29. Fulcher, J.A., et al., *Galectin-1 co-clusters CD43/CD45 on dendritic cells and induces cell activation and migration through Syk and protein kinase C signaling.* J Biol Chem, 2009. **284**(39): p. 26860-70.

30. Thiemann, S., et al., *Galectin-1 regulates tissue exit of specific dendritic cell populations.* J Biol Chem, 2015. **290**(37): p. 22662-77.

31. Lock, K., et al., *Expression of CD33-related Siglecs on human mononuclear phagocytes, monocyte-derived dendritic cells and plasmacytoid dendritic cells.* Immunobiology, 2004. **209**(1-2): p. 199-207.

32. Izquierdo-Useros, N., et al., *Siglec-1 is a novel dendritic cell receptor that mediates HIV-1 trans-infection through recognition of viral membrane gangliosides.* PLoS Biol, 2012. **10**(12): p. e1001448.

33. Mustjoki, S., et al., *Intercellular adhesion molecule-1 in extravasation of normal mononuclear and leukaemia cells.* Br J Haematol, 2001. **113**(4): p. 989-1000.

34. Peters, P.J., et al., *Segregation of MHC class II molecules from MHC class I molecules in the Golgi complex for transport to lysosomal compartments.* Nature, 1991. **349**(6311): p. 669-76.

35. Mulari, M., J. Vaaraniemi, and H.K. Vaananen, *Intracellular membrane trafficking in bone resorbing osteoclasts.* Microsc Res Tech, 2003. **61**(6): p. 496-503.

36. Toyomura, T., et al., *From lysosomes to the plasma membrane: localization of vacuolar-type H+ -ATPase with the a3 isoform during osteoclast differentiation.* J Biol Chem, 2003. **278**(24): p. 22023-30.

37. Arnett, T.R., et al., *Effects of medium acidification by alteration of carbon dioxide or bicarbonate concentrations on the resorptive activity of rat osteoclasts.* J Bone Miner Res, 1994. **9**(3): p. 375-9.

38. Omasa, T., et al., *Effects of lactate concentration on hybridoma culture in lactate-controlled fed-batch operation.* Biotechnol Bioeng, 1992. **39**(5): p. 556-64.

39. Patel, S.D., et al., *The lactate issue revisited: novel feeding protocols to examine inhibition of cell proliferation and glucose metabolism in hematopoietic cell cultures.* Biotechnol Prog, 2000. **16**(5): p. 885-92.

40. Mosmann, T., *Rapid colorimetric assay for cellular growth and survival: application to proliferation and cytotoxicity assays.* J Immunol Methods, 1983. **65**(1-2): p. 55-63.

41. Alfarouk, K.O., et al., *Glycolysis, tumor metabolism, cancer growth and dissemination. A new pH-based etiopathogenic perspective and therapeutic approach to an old cancer question.* Oncoscience, 2014. **1**(12): p. 777-802.

42. Alfarouk, K.O., *Tumor metabolism, cancer cell transporters, and microenvironmental resistance.* J Enzyme Inhib Med Chem, 2016. **31**(6): p. 859-66.

43. Alfarouk, K.O., A.K. Muddathir, and M.E. Shayoub, *Tumor acidity as evolutionary spite.* Cancers (Basel), 2011. **3**(1): p. 408-14.

44. O'Neill, L.A. and E.J. Pearce, *Immunometabolism governs dendritic cell and macrophage function.* J Exp Med, 2016. **213**(1): p. 15-23.

45. Pearce, E.L. and E.J. Pearce, *Metabolic pathways in immune cell activation and quiescence.* Immunity, 2013. **38**(4): p. 633-43.

46. Warburg, O., F. Wind, and E. Negelein, *The Metabolism of Tumors in the Body.* J Gen Physiol, 1927. **8**(6): p. 519-30.

47. Hard, G.C., *Some biochemical aspects of the immune macrophage.* Br J Exp Pathol, 1970. **51**(1): p. 97-105.

48. Newsholme, P., et al., *Metabolism of glucose, glutamine, long-chain fatty acids and ketone bodies by murine macrophages.* Biochem J, 1986. **239**(1): p. 121-5.

49. Krawczyk, C.M., et al., *Toll-like receptor-induced changes in glycolytic metabolism regulate dendritic cell activation.* Blood, 2010. **115**(23): p. 4742-9.

50. Pantel, A., et al., *Direct type I IFN but not MDA5/TLR3 activation of dendritic cells is required for maturation and metabolic shift to glycolysis after poly IC stimulation.* PLoS Biol, 2014. **12**(1): p. e1001759.

51. Bedard, K. and K.H. Krause, *The NOX family of ROS-generating NADPH oxidases: physiology and pathophysiology.* Physiol Rev, 2007. **87**(1): p. 245-313.

52. Jantsch, J., et al., *Hypoxia and hypoxia-inducible factor-1 alpha modulate lipopolysaccharide-induced dendritic cell activation and function.* J Immunol, 2008. **180**(7): p. 4697-705.

53. Draoui, N. and O. Feron, *Lactate shuttles at a glance: from physiological paradigms to anti-cancer treatments.* Dis Model Mech, 2011. **4**(6): p. 727-32.

54. Colegio, O.R., et al., *Functional polarization of tumour-associated macrophages by tumour-derived lactic acid.* Nature, 2014. **513**(7519): p. 559-63.

55. Sica, A., et al., *Autocrine production of IL-10 mediates defective IL-12 production and NF-kappa B activation in tumor-associated macrophages.* J Immunol, 2000. **164**(2): p. 762-7.

56. Fischer, K., et al., *Inhibitory effect of tumor cell-derived lactic acid on human T cells.* Blood, 2007. **109**(9): p. 3812-9.

Custom Glycosylation of Cells and Proteins Using Cyclic-carbamate-Derivatized Oligosaccharides

Marek W.J. Whitehead,[1] Nikolay Khanzhin,[2] Lubor Borsig,[1] and Thierry Hennet[1,3,*]

[1]Institute of Physiology, University of Zurich, Winterthurerstrasse 190, 8057 Zurich, Switzerland

[2]Glycom A/S, Kogle Alle 4, 2970 Hørsholm, Denmark

[3]Lead Contact

*Correspondence: thierry.hennet@uzh.ch http://dx.doi.org/10.1016/j.chembiol.2017.08.012

(Manuscript published on the 06.09.2017 in Cell Chemical Biology)

Graphical Abstract

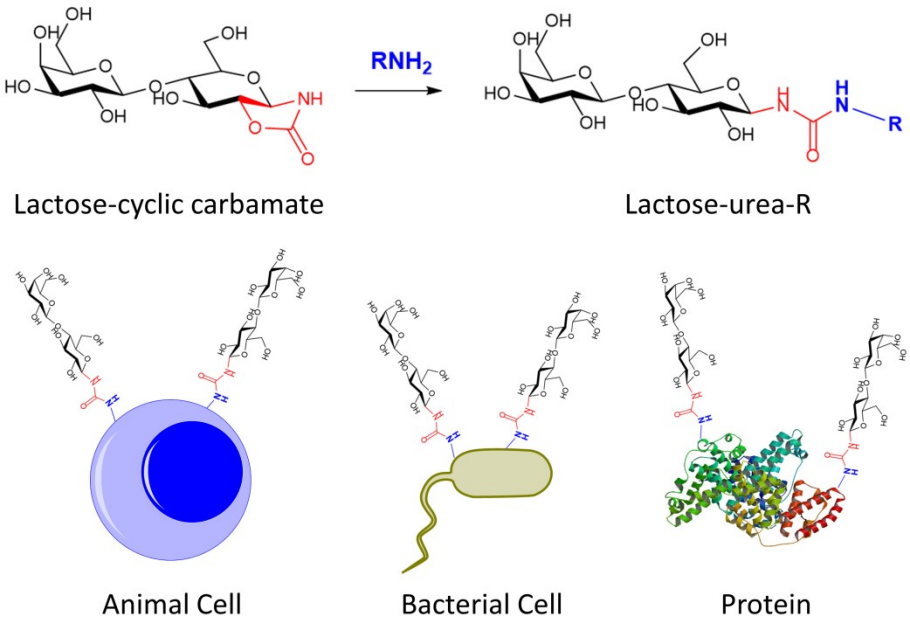

Highlights

- Custom glycosylation of proteins and bacterial and animal cells
- Presentation of E-selectin ligands on cells by 3-fucosyl-3-sialyllactose coating
- Complement factor H binds α2-3 but not α2-6 linked sialic acid on coated E. coli
- Custom glycoproteins stimulate PI3K regulated inflammatory cytokine production

In Brief

The structural heterogeneity impairs the functional characterization of glycan epitopes. Whitehead et al. use cyclic-carbamate-derivatized oligosaccharides to glycosylate proteins and bacterial and animal cells to examine the biological roles of such oligosaccharide epitopes.

Summary

The structural complexity of glycosylation restrains the functional characterization of glycans. We present a versatile carbohydrate ligation technique based on the reaction of cyclic-carbamates with primary amines. Cyclic-carbamate-derivatized carbohydrates can be added to primary amine-containing molecules in aqueous solution to yield glycoconjugates. This method enabled the presentation of carbohydrate epitopes on live animal cells, as shown by the acquisition of E-selectin binding sites on mouse MC-38 cells decorated with 3-fucosyllactose or 3-fucosyl-3-sialyllactose. Ligation of 3- and 6-sialyllactose to Escherichia coli demonstrated the importance of sialic acid linkages in regulating complement factor H binding. Proteins were modified with oligosaccharides to study their role in stimulating cytokine secretion by dendritic cells, thus pointing to interactions between glycoproteins and phosphoinositide 3-kinase signaling in controlling IL-12, tumor necrosis factor alpha and IL-1β release. Overall, cyclic-carbamate-mediated ligation is useful to study the biology of carbohydrate epitopes on proteins and on cell membranes.

Introduction

Unlike nucleic acids and polypeptides, complex carbohydrates do not follow a template-driven assembly. The lack of blueprints hampers the large-scale production of pure glycoconjugates given that enzymatic biosynthesis often yields a large heterogeneity of products. Various strategies have been designed over the past years to facilitate the production of uniformly glycosylated proteins and

lipids. For example, lectin-resistant Chinese hamster ovary (CHO) cells harbor limited glycosylation pathways, which enables the expression of glycoproteins of low glycan complexity [1]. More recently, targeted gene inactivation has been applied to generate CHO cell lines that produce glycoproteins decorated with specific glycan structures [2]. Chemical approaches have also been developed to generate uniformly glycosylated glycoconjugates, such as glycolipids [3], mucin-type glycoproteins [4], and glycopolymers [5]. Whereas chemical synthesis enables large-scale production of homogeneous glycoconjugates, the synthesis reactions applied are often specifically tailored to each glycan produced, thereby restricting the portability of established procedures to multiple structures. A simplified approach consists of ligating specific complex carbohydrates to carrier molecules. Such a strategy has been described recently, taking advantage of coupling pre-assembled glycans to phospholipids [6]. This method applies aminooxy glycans condensed to a polymethyl vinyl ketone scaffold via the formation of oximes. The resulting artificial glycolipids were incorporated into cell membranes and used successfully to assess the role of the sialic-acid-binding lectin Siglec-7 in cancer-cell immune evasion [6]. Other conjugation approaches, such as the succinimidyl ester coupling method, are broadly used for the preparation of conjugated molecules, but are usually unsuited for the glycosylation of viable cells due to their significant cytotoxicity [7-9].

Homogeneous glycoconjugates are valuable to investigate the functional significance of specific glycan epitopes in the context of natural carrier molecules. The ligand properties of carbohydrate-binding proteins can be analyzed quantitatively using arrays of immobilized glycans [10]. However, arrays do not replicate the natural context and density of glycan chains on glycoconjugates. Also, the immobilization of glycans on solid surfaces sometimes shortens the reducing end of glycans, as for example achieved after reductive amination reactions [11, 12]. Whereas glycan arrays can be used to delineate the carbohydrate-binding specificity of lectins, such as selectins and Siglecs [13-15], signaling cascades and cell responses induced by lectin-glycan interactions cannot be addressed using such tools. Selectin binding for instance regulates leukocyte adhesion [16] and chemotaxis [17], which cannot be studied on glass slides covered with glycans. Similarly, Siglecs are signaling molecules that stimulate or repress cell activation through immunoreceptor tyrosine-based activation motifs and immunoreceptor tyrosine-based inhibition motifs [18]. Methods mediating the attachment of glycans to cellular surface proteins are useful to change the surface glycosylation of bacterial and eukaryotic cell membranes.

The pathogenicity of Neisseria gonorrhoeae has been related to its surface sialylation, which mimics host cells [19]. Surface sialylation has been shown to dampen complement activation through the recruitment of factor H, which directly interacts with surface-bound sialic acid [20]. The selective decoration of bacterial membranes with animal glycans featuring sialylated and fucosylated epitopes

would for example allow the importance of molecular mimicry in bacterial pathogenicity to be addressed. The selective glycosylation of polypeptides would also be of interest to study the role of specific glycan epitopes in activating lectin proteins of unclear ligand specificity, such as the broad family of C-type lectins expressed on macrophages and dendritic cells [21].

We present here a carbohydrate ligation technique that is suitable to modify primary amines as found on proteins. Specific oligosaccharides were synthesized to include a strained cyclic-carbamate functional group, which can covalently react with primary amines in aqueous solution [22] and in conditions suitable for labeling living cells at physiological pH and temperatures. This technique enables the rapid and efficient engineering of cells and glycoproteins to study carbohydrate-lectin interactions in natural settings.

STAR methods

Key resources table

REAGENT or RESOURCE	SOURCE	IDENTIFIER
Antibodies		
Anti-IgG-Fc-domain antibody labelled with biotin	Sigma-Aldrich	B3773
Complement factor H antibody (OX-24)	Life Technologies	MA1-70057
Alexa488 labelled anti-mouse-IgG-Fc-domain targeting antibody	Sigma-Aldrich	M0284
Bacterial and Virus Strains		
Escherichia coli K-12	Thermo Fisher Scientific	18265017
Chemicals, Peptides, and Recombinant Proteins		
Ficoll-Paque PLUS	GE Healthcare Life Sciences	17-1440-02
Human GM-CSF, research grade	MACS Miltenyi Biotec	130-093-862
Human IL-4, research grade	MACS Miltenyi Biotec	130-093-917
3-sialyl-3-fucosyllactose	Glycom A/S	N/A
6-sialyllactose	Glycom A/S	N/A
3-fucosyllactose	Glycom A/S	N/A
3-sialyllactose	Glycom A/S	N/A
2-fucosyllactose	Glycom A/S	N/A
Albumin bovine, fraction V from bovine	MP Biomedicals	0216006910
Staphylococcus aureus protein A	Sigma-Aldrich	P6031
Fluorescein isothiocyanate labelled *Ulex Europaeus* agglutinin	Vector Laboratories	FL-1061
Fluorescein isothiocyanate labelled *Aleuria aurantia* agglutinin	Vector Laboratories	FL-1391
E-selectin-human IgG Fc domain probe	Borsig et al. 2002	N/A
P-selectin-human IgG Fc domain probe	Borsig et al. 2002	N/A
L-selectin-human IgG Fc domain probe	Borsig et al. 2002	N/A
Strepatavidin-PE-Cy5	BD Bioscience	554062
Complement factor H	Complement Technology Inc.	A137
Fluorescein isothiocyanate labelled *Sambucus nigra* agglutinin	Vector Laboratories	FL-1301
Fluorescein isothiocyanate labelled *Maackia amurensis* agglutinin I	Vector Laboratories	FL-1311
Lipopolysaccharide	Sigma-Aldrich	L2630
Wortmannin	Enzo Life Sciences	BML-ST415
Critical Commercial Assays		
ProcartaPlex Human Th1/Th2/Th9/Th17/Th22/Treg Cytokine Panel (18plex)	Affymetrix eBioscience	EPX-180-12165-901
Experimental Models: Cell Lines		
MC-38 cells (C57BL6 murine colon adenocarcinoma)	Kerafast	ENH204
RAW264.7	ATCC	TIB-71™
B16-F0	ATCC	CRL-6322™
THP-1	ATCC	TIB-202™
Jurkat, Clone E6-1	ATCC	TIB-152™
Human: PBMC derived dendritic cells	University of Zurich according to O'Neil and Bhardwaj, 2005	N/A
Green fluorescent protein-expressing MC-38 cells	Borsig et al., 2002	N/A
Software and Algorithms		
GraphPad Prism 5	GraphPad Software	http://www.graphpad.com

Contact for reagent and resource sharing

Further information and requests for resources and reagents should be directed to and will be fulfilled by the Lead Contact, Thierry Hennet (thierry.hennet@uzh.ch).

Experimental model and subject details

Cell lines

Mouse colon carcinoma MC-38 cells [23], mouse macrophage RAW264.7 cells and B16 melanoma cells were cultured in Dulbecco's Modified Eagle medium with 10% fetal calf serum. Human monocytic THP-1 cells and human lymphoma Jurkat cells were cultured in RPMI medium with 10% fetal calf serum.

Dendritic Cell Cultivation

Peripheral blood mononuclear cells (PBMCs) were isolated with Ficoll-Paque PLUS (GE Healthcare) according to the procedure described by the manufacturer. Dendritic cells were obtained by culturing the PBMCs as described by O'Neill and Bhardwaj [24]. Briefly, PBMCs were cultured in RPMI medium with 10% fetal calf serum for 2 h. Non-adherent cells were removed by two washes with RPMI medium. Adherent monocytes were further cultured in RPMI medium with 10% FBS supplemented with 100 IU/ml GM-CSF and 200 IU/ ml IL-4 for five days to induce the differentiation of monocytes to immature dendritic cells.

Method details

Oligosaccharide ligation

Human THP-1 cells, mouse MC-38, RAW264.7 and B16 adherent cells were detached with 2 mM EDTA solution in phosphate buffered saline (PBS), pH 7.4 for 10 min then washed twice with PBS. Cells were resuspended at 4 x 10^5 cells/ml in HBSS supplemented with 1 - 20 mM of oligosaccharide-cyclic-carbamate and incubated at 20 C for 3 h. *Escherichia coli* K-12 was grown to an OD_{600} value of 1.0. Bacteria were fixed in acetone:methanol (1:1, v:v) at -20 C for 15 min, then washed twice with 10 mM borate buffered saline, pH 10. Fixed bacteria were resuspended in 5-15 mM of oligosaccharide-cyclic-carbamate in borate buffered saline and incubated at 20° C for 4 h. BSA fraction V (MP Biomedicals) and *Staphylococcus aureus* protein A (Sigma-Aldrich) were solubilized at 1 mg/ml in borate buffered saline, pH 10 containing 20 mM of oligosaccharide-cyclic-carbamate and incubated at 4 C for 30 h. Unreacted oligosaccharide-cyclic-carbamates were removed by dialysis using a molecular weight cut-off of 1'000 Da.

Flow cytometry

Bacterial and animal cells were stained with 5 µg/ml fluorescein isothiocyanate labelled *Ulex europaeus* agglutinin I (UEA) and fluorescein isothiocyanate labelled *Aleuria Aurantia* lectin (AAL) (Vector Laboratories) in HBSS at 4° C for 20 min, then washed twice in HBSS before analysis using a FACScanto II flow cytometer (BD Bioscience). To detect E-, P- and L-selectin ligands on human and mouse cell lines, 10 mg/ml of each selectin probe, that consist of the carbohydrate binding domain of the respective murine selectin fused to an IgG Fc domain [25], were used. These selectin probes were pre-complexed with an anti-IgG-Fc-domain antibody labelled with biotin (Sigma-Aldrich) before being used to stain the cells for 50 min. Afterwards the cells were incubated for another 20 min with streptavidin-PE-Cy5 (BD Bioscience). Before the measurement, the cells were washed one time with HBSS. Images of single cells analyzed during flow cytometry were recorded using an ImageStream Mark II Imaging Flow Cytometer (Merck).

E-selectin adhesion assay

Microtiter plates were coated with 4 µg/ml of *Staphylococcus aureus* protein A (Sigma Aldrich) in 50 mM Na_2CO_3/$NaHCO_3$, pH 9.5 at 4° C for 14 h and washed twice with HBSS. After blocking with 1% BSA in HBSS at 25° C for 30 min, the wells were coated with 6 µg/ml of E-selectin-IgG-Fc-domain in 1% BSA in HBSS for 1 h. The wells were washed twice with 1% BSA in HBSS and 6 x 10^4 green fluorescent protein-expressing MC-38 cells [25] were added in 1% BSA in HBSS. The plate was incubated at 4° C for 1 h while being shaken at 80 rounds per minute. Non-adherent cells were removed by washing the wells with HBSS. Fluorescence was measured using a Genios Spectra Fluor Plus fluorescence plate reader (Tecan Trading AG, Männerdorf, Switzerland) at 509 nm.

Selectin Blot

BSA and its glycosylated variants were dotted at 500, 250, 125 or 60.5 ng onto nitrocellulose membranes. Membranes were blocked with 5% BSA in PBS for 1 h at 20° C. E-, P- or L-selectin human Fc-domain chimeras were pre-complexed with anti-IgG-Fc-domain antibodies labelled with biotin (Sigma-Aldrich) in PBS with 0.1 mM calcium chloride and this mix was added to the membranes for 14 h at 4° C. Membranes were washed 3-times with PBS, 0.05% Tween20 for 5 min and then incubated with streptavidin-HRP (Sigma-Aldrich) for 1 h at 20° C before developing blots with an X-OMAT 2000 Processor (Kodak) using Hyperfilms for enhanced chemiluminescence (Amersham).

Factor H binding assay

About 10^9 *E. coli* K-12 cells were incubated in HBSS with 25% human serum (Sigma-Aldrich) at 37° C for 30 min. Bacteria were washed twice with HBSS then incubated for 50 min at 20° C in HBSS, 1 mM $CaCl_2$, 1 mM $MgCl_2$ and 20 µg/ml factor H (Complement Technology, Inc.) [26, 27]. Bound Factor H was detected using a complement factor H antibody (OX-24, Life Technologies) and an Alexa488 labelled anti-mouse-IgG-Fc-domain targeting antibody (Sigma-Aldrich).

Fluorescence and confocal microscopy

E. coli K-12 cells were stained with 5 µg/ml of fluorescein isothiocyanate labelled UEA or fluorescein isothiocyanate labelled AAL at 4 C for 20 min. Alternatively bacteria were stained with 20 µg/ml of fluorescein isothiocyanate labelled *Sambucus nigra* agglutinin (SNA) or 20 µg/ml fluorescein isothiocyanate labelled MAL (Vector Laboratories) at 25° C for 1 h. Fluorescence was recorded using an Axiovert 200M fluorescence microscope (Zeiss). To visualize 2FL coating on MC-38 cells using confocal microscopy, cells were cultured on coverslips for 2 days to a confluency of 50%. Cells were incubated with 4 mM 2FL-cyclic-carbamate for 30 min prior to fixation with 3% formalin for 20 min at 20° C. The cells were washed three times with PBS, permeabilized with 0.1% saponin in PBS, and incubated in 20 mM glycine for 15 min at 20° C to quench unreacted formalin. Cells were stained for 30 min at 20° C with 10 µg/ml UEA-biotin (Vector Laboratories) in PBS with 0.1 mM calcium chloride. After 3 washes in PBS, cells were stained with 10 µg/ml streptavidin-Alexa647 (Thermo Fisher Scientific), 10 µg/ml wheat germ agglutinin-Alexa488 (Thermo Fisher Scientific) and 500 µg/ml 4'6-diamidin-2-phenylindol (Biotium) in PBS with 0.1 mM calcium chloride for 1 h at 20 C. The cells were then washed 3 times in PBS before being mounted in ProLong™ Gold Antifade Mountant (Thermo Fisher Scientific). Confocal microscopy was performed with an SP5 microscope (Leica).

Dendritic cell stimulation

Aliquots of 1.5 x 10^5 human PBMC-derived dendritic cells were incubated with *E. coli* K-12 cells at a 1:1 ratio. Alternatively, 1.5 x 10^5 human PBMC-derived dendritic cells were incubated with 250 µg/ml of custom-glycosylated BSA for 3 h at 37 C, followed by stimulation with 500 ng/ml of lipopolysaccharide (Sigma-Aldrich). In some experiments 300 nM Wortmannin (Enzo Life Sciences, Lausen, Switzerland) was added to the cells 3 h before incubation with custom-glycosylated BSA. Cell supernatants were collected 24 h later for cytokine determination.

Cytokine determination

Supernatants of PBMC-derived dendritic cells were used undiluted for the determination of the concentrations of IL-10, IL-6, IL-12p70, TNF-α, IL-1β, interferon-γ, IL-18, and IL-23. The ProcartaPlex Human Th1/Th2/Th9/Th17/Th22/Treg Cytokine Panel (18plex, Affymetrix eBioscience) was applied according to the standard procedure of the manufacturer.

Compound preparation

Details of compound preparation and characterization are given in Methods S1.

NMR and mass spectrometry

Proton and carbon nuclear magnetic resonance (^{1}H and ^{13}C NMR) spectra were recorded on a Bruker Advance-400 (400 MHz and 100 MHz, respectively) at the Department of Chemistry of the Danish Technical University (DTU). Chemical shifts are reported in ppm (parts per million) with reference to residual solvent signal as indicated. ^{1}H NMR data are reported in the following order: chemical shift, multiplicity, coupling constant(s) (J) in Hz, integration, and assignment if available. Multiplicity is indicated as s (=singlet), d (=doublet), t (=triplet), q (=quartet), quint (=quinted), dd (=doublet of doublets), dt (doublet of triplets), td (triplet of doublets), br (=broadened), m (=multiplet). ^{13}C NMR data are extracted from APT (attached proton test) spectra and reported as chemical shifts with key assignments. High-resolution mass spectra (HRMS) were recorded on a Bruker microQTof II MS coupled to a Dionex Ultimate 3000 UHPLC at Glycom A/S with electrospray ionization method (ESI) either in negative or positive mode and calibrated by sodium formate cluster ions; or on a QExactive instrument (Thermo Fisher Scientific, Bremen, Germany) equipped with a heated electrospray ionization (ESI) source and connected to a Dionex Ultimate 3000 UHPLC system with the same method. Reactions were followed by thin-layer chromatography (TLC) on silica gel 60 F_{254} coated on aluminum plates (MERCK 1.05554.0001). Eluted TLC plates were developed by carbonisation at ca. 300° C after treatment with 10% H_2SO_4 in ethanol. The starting oligosaccharides 6SL (Na-salt), 2FL, and 3FL were previously synthesized at Glycom A/S in multi-kg quantities. 3SL (Na-salt) was purchased from GeneChem Inc. (http://genechem.co.kr/index_e.php, catalog No. BCBO0007, Lot No. BO 07KI30-2, NMR assay 85.7% (calc. for the free acid), 88.6% (Na-salt)). 2FL cyclic-carbamate and lactose cyclic-carbamate were prepared previously at Glycom A/S from 2FL and lactose, respectively, as described in WO2009/040363. The general procedures for preparation of novel cyclic-carbamates and corresponding intermediates are exemplified for 3SL. Other cyclic-carbamates (3FL, 6SL, FSL) were prepared analogously.

Quantification and statistical analysis

All results are presented as means with their standard deviations unless otherwise indicated. The data was analyzed in GraphPad Prism 5 by one-way analysis of variance with Bonferroni's multiple comparison post-testing to determine statistical differences between different experimental groups. A p-value below 0.05 was considered as statistically significant.

Results

Oligosaccharide-cyclic-carbamate synthesis

The synthesis of oligosaccharide-cyclic-carbamates and their ligation with primary amino groups are depicted in Figure 1. The synthesis was performed based on the adapted procedures described in WO2009/040363. Most of the starting oligosaccharides were available in kilogram quantities. The corresponding unprotected oligosaccharides (2a-e) except 3-sialyl-3-fucosyllactose [Sia(α2-3)Gal(β1-4)[Fuc(α1-3)]Glc] (FSL) (2f) were peracetylated (3a-e) under standard conditions with acetic anhydride in pyridine followed by anomeric bromination with 30% HBr in acetic acid (compounds 4a-e). The peracetylated α-bromides obtained were inverted into β-azides 5a-e with NaN3 in aqueous acetone. Then, unprotected β-azides 6a-e were prepared by Zemplén deacetylation with MeONa in methanol. The precipitated β-azides were of sufficient purity and were converted into β-cyclic-carbamate derivatives 1a-e in anhydrous dimethylformamide with Ph3P saturated with CO2 and were isolated from the reaction mixture by precipitation with acetone or an acetone-hexane mixture. The initial attempt to convert unprotected 6-sialyllactose [Sia(α2-6)Gal(β1-4)Glc] (6SL)-azide 6e in the free acid form into cyclic-carbamate was not successful. Later, all the unprotected sialylated azides 6d-f as Na salts were smoothly converted into cyclic-carbamates under anhydrous conditions. FSL-azide (6f) was prepared from 3-fucosyllactose [Gal(β1-4)[Fuc(α1-3)]Glc] (3FL)-azide (6c) and 3-sialyllactose [Sia(α2-3)Gal(β1-4)Glc] (3SL) by trans-sialylation catalyzed by trans-sialidase isolated from Trypanosoma cruzi according to a general method described in patent WO2013/ 190531 A1. The FSL-azide (6f) was isolated as a mixture with unreacted 3SL after ion-exchange chromatography and converted into a mixture of FSL-cyclic-carbamate and 3SL, which was used in the following derivatization without further purification. The structural integrity of oligosaccharide-cyclic-carbamate products was confirmed by high-resolution electrospray-ionization mass spectrometry and routine nuclear magnetic resonance (see Supplemental Information).

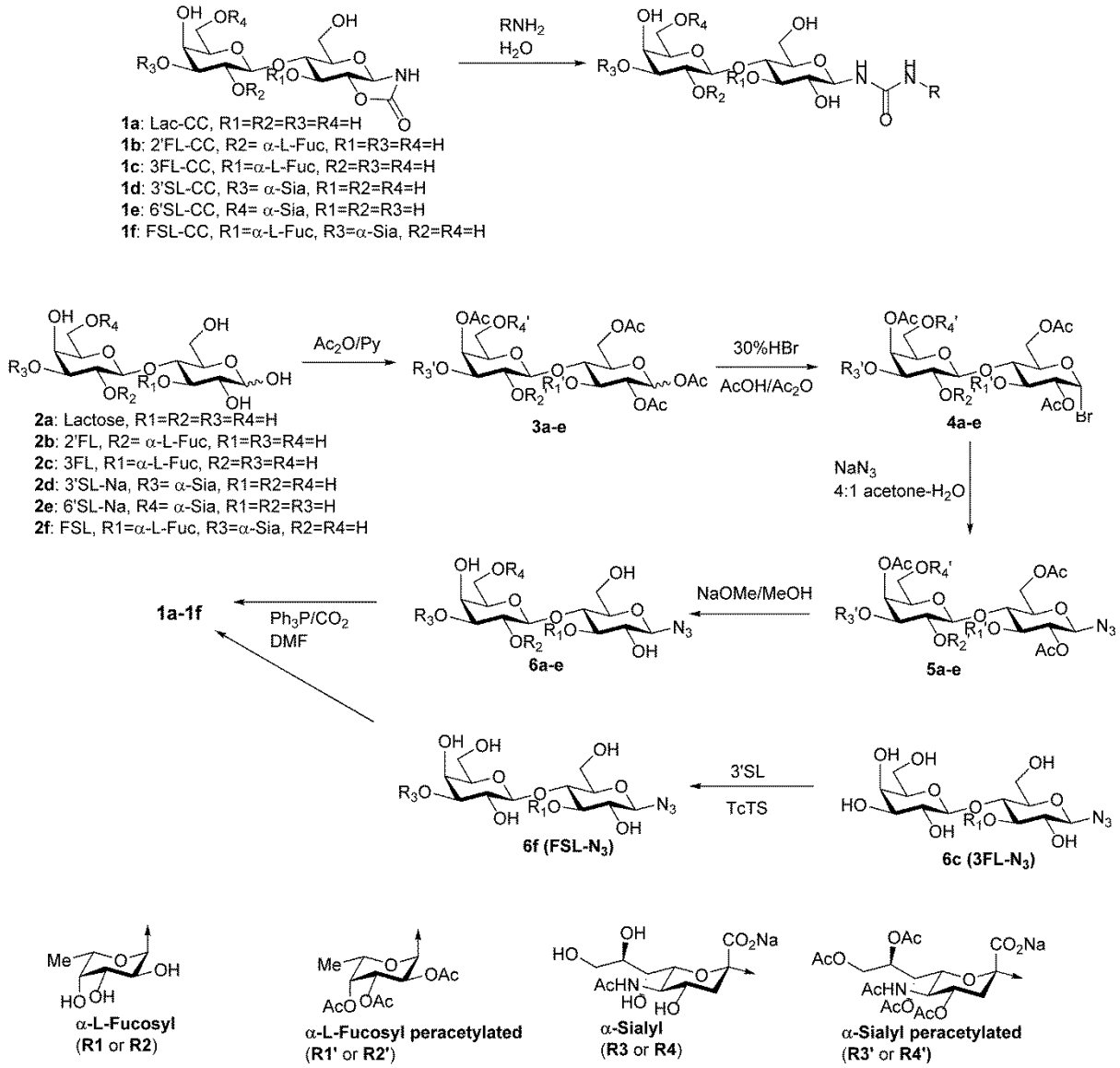

Figure 1: Synthesis of Oligosaccharide-cyclic-carbamates The oligosaccharides 2-fucosyllactose, 3-fucosyllactose, 3-sialyllactose, and 6-sialyllactose were peracetylated and then anomerically brominated. The resulting peracetylated α-bromides were then inverted into β-azides, which could then be converted into β-cyclic-carbamate derivatives. 3-Sialyl-3-fucosyllactose-cyclic-carbamate was synthesized by *trans*-sialylating the unprotected 3-fucosyllactose-azide with the *trans*-sialidase from *Trypanosoma cruzi* before converting it to the β-cyclic-carbamate derivative.

Custom glycosylation of cell membranes

The ligation of oligosaccharide-cyclic-carbamates to biological surfaces was first tested on the murine MC-38 cell line. The covalent attachment of the oligosaccharide 3FL-cyclic-carbamate to MC-38 cells was concentration and time dependent, showing a linear increase of surface α1,3-fucosylation as measured by AAL staining (Fig. S1). Reaction times longer than 3 h decreased cell viability, probably because of the absence of serum and nutrients in Hank's balanced salt solution. Similarly, 3FL-cyclic-

carbamate concentrations above 20 mM decreased cell viability as assessed by Trypan blue exclusion (data not shown). We then ligated oligosaccharide-cyclic-carbamates to murine MC-38 and RAW264.7 cells, and human THP-1 and Jurkat cells to assess the feasibility of the method to increase surface α1,2-fucosylation and α1,3-fucosylation. The incubation of MC-38 cells with 14 mM 2-fucosyllactose [Fuc(α1-2)Gal(β1-4)Glc] (2FL)-cyclic-carbamate yielded an increase in α1,2-fucosylation as measured by *Ulex europaeus* agglutinin I (UEA) staining, which was 7.5-fold increased (Fig. 2A).

Under the same conditions, the staining of α1,3-fucosylation increased by 2.5-fold after incubating MC-38 cells with 3FL-cyclic-carbamate (Fig. 2B). The increase in α1,3-fucosylation staining was more moderate than the increase in α1,2-fucosylation staining because of elevated AAL binding to uncoated MC-38 cells, which indicates high levels of surface α1,3-fucosylation for this cell line. Treatment of additional mouse and human cell lines with 2FL-and 3FL-cyclic-carbamate (Fig. S2A–S2F) confirmed the general applicability of the oligosaccharide ligation technique to increase surface α1,2-fucosylation and α1,3-fucosylation. Coating RAW264.7 and Jurkat cells with 3FL-cyclic-carbamate did not lead to increased staining by AAL due to high background levels of already present surface α1,3-fucosylation. We furthermore confirmed the localization of oligosaccharide-cyclic-carbamate to the surface of MC-38 cells by coating adherent MC-38 cells with 2FL-cyclic-carbamate and staining with UEA. As shown by confocal microscopy, UEA staining co-localized with the cell membrane staining wheat germ agglutinin (Figure S3A). The cell-surface localization of 2FL-cyclic-carbamate was also confirmed by recording fluorescence images of UEA-stained MC-38 cells analyzed by flow cytometry using ImageStream technology (Figure S3B).

The addition of fucosylated epitopes to MC-38 cells also increased binding of members of the selectin family to the cells. The best known ligand of the selectins is the carbohydrate epitope sialyl-Lewis X, which includes α1-3 linked fucose [28]. We observed that ligating 3FL-cyclic-carbamate to MC-38 cells increased E-selectin binding, whereas ligation with 2FL-cyclic-carbamate had no effect (Fig. 2C). Coating MC-38 cells with FSL-cyclic-carbamate, which has a Sia(α2-3)Gal(β1-4)[Fuc(α1-3)]Glc epitope similar to sialyl-Lewis X, led to even stronger binding of E-selectin (Fig. 2C). This result was replicated using B16 melanoma cells, which also showed the strongest E-selectin binding to FSL, followed by 3FL and no effect for 2FL (Fig. 2D). The impact of coating MC-38 cells with fucosylated oligosaccharides on E-selectin-mediated adhesion under rotational stress was also assessed. Only cells presenting 3FL and FSL adhered to E-selectin-coated plates, whereas the presentation of 2FL did not increase adhesion (Fig. 2E). The adhesion of 3FL- and FSL-coated cells was eliminated upon incubation with 5 mM EDTA, thus confirming the Ca^{2+}-dependency of selectin binding. Fluorescence intensities in wells of 3FL- or FSL-coated cells were approximately three to four times higher than for uncoated and 2FL-coated cells, or 3FL- and FSL-coated cells treated with EDTA (Fig. 2E). The addition of 3FL and FSL

epitopes to MC-38 cells, however, did not further increase adhesion to L- and P-selectin, which was already strong in untreated cells (Fig. 2F and 2G).

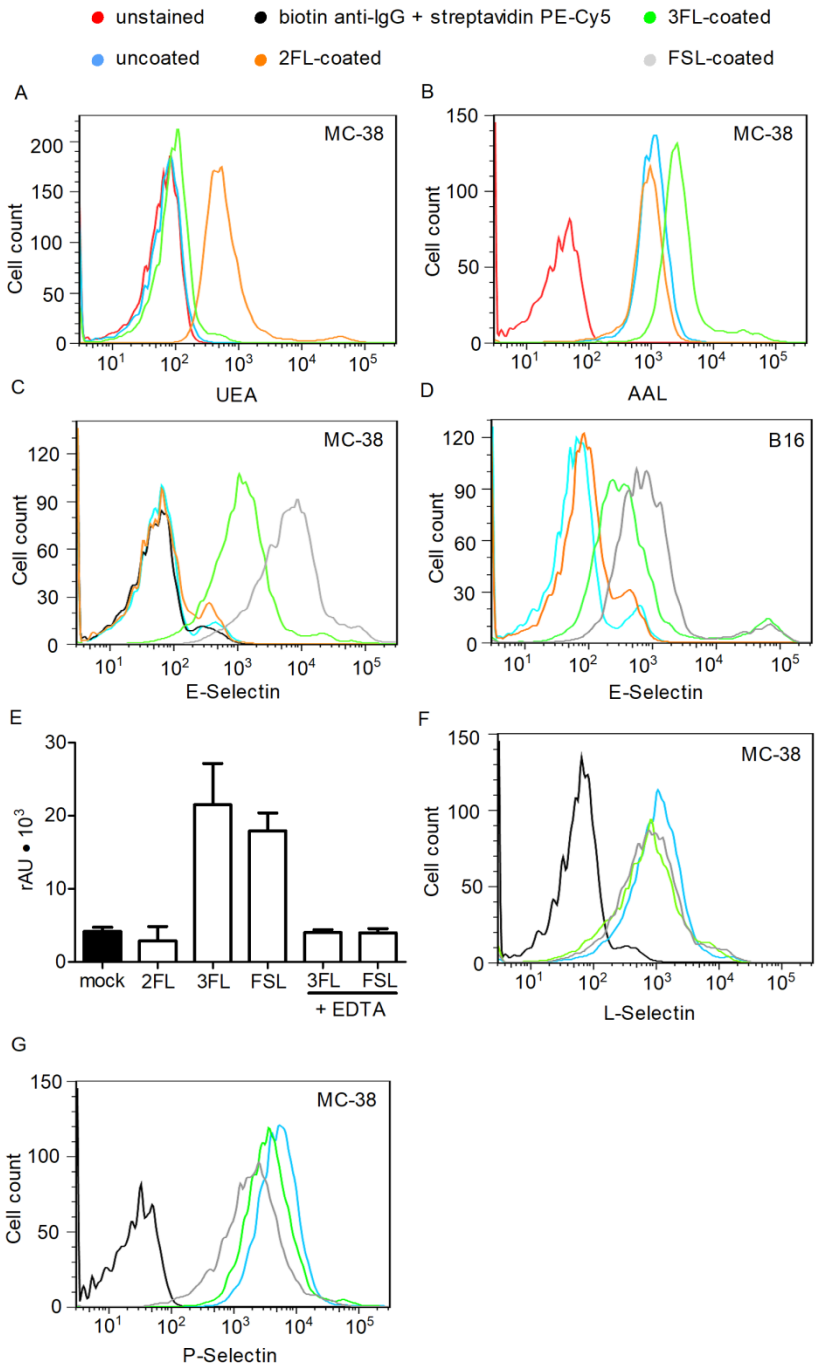

Figure 2: Coating Cells with Oligosaccharide-Cyclic-carbamates. (A and B) MC-38 cells were coated with 2FL- or 3FL-cyclic-carbamate or left uncoated, then stained with fluorescein-isothiocyanate-labeled UEA (A) or AAL (B) before being analyzed by flow cytometry. Unstained cells (red lines), uncoated cells (blue lines), 2FL-coated cells (orange lines), 3FL-coated cells (green lines). (C, D, F, and G) MC-38 (C, F, G) and B16 melanoma cells (D) were coated with fucosyllactose-cyclic-carbamates or left uncoated. The cells were then labeled with an E-selectin (C, D), L-selectin (F), or P-selectin (G) probe with a human Fc domain, which was detected with a biotin-

labeled antibody and streptavidin PE-Cy5 in flow cytometry. Negative control MC-38 cells were not coated or stained with the respective selectin probe. Instead they were stained directly with the Fc domain targeting biotinylated antibody and PE-Cy5-labeled streptavidin. Uncoated cells (blue lines), biotin anti-IgG + streptavidin PE-Cy5 (black lines), 2FL-coated cells (orange lines), 3FL-coated cells (green lines), FSL-coated cells (grey lines). E-selectin mediated adhesion of MC-38 cells coated with 2FL, 3FL, or FSL after 2 h agitation at 80 rounds per minute. Data are shown as average and SD of three samples analyzed.

Custom glycosylation of bacterial membranes

We next tested the possibility to glycosylate bacterial membranes with oligosaccharide-cyclic-carbamates. We coated *Escherichia coli* K-12 with the four oligosaccharides 2FL, 3FL, 3SL, and 6SL. The presentation of the corresponding oligosaccharides was assessed by staining decorated *E. coli* with the lectins UEA and AAL for α1,2-fucose and α1,3-fucose, respectively. Membrane sialylation was detected using the *Maackia amurensis* lectin I (MALI) [29] for α2,3-sialic acid and the SNA [30] for α2,6-sialic acid. Untreated *E. coli* remained unstained by the four lectins, while ligation with oligosaccharide-cyclic-carbamates yielded strong staining for the respective lectins (Fig. 3A).

The addition of specific oligosaccharide structures to bacterial membranes enabled the investigation of these epitopes in the context of immune recognition. Some pathogenic bacteria, such as *N. gonorrhoeae* [20], evade recognition from host immunity by exposing sialylated glycans on their membranes. Sialylated membranes, for example, recruit factor H, which prevents C3 activation and subsequent C3b opsonization [31]. Whereas *N. gonorrhoeae* mainly presents α2,3-sialic acid on lipooligosaccharides [32], it is unclear whether factor H binding solely depends on the negative charge of sialic acid or whether the glycosidic linkage influences binding as well. To address this point, we labeled *E. coli* with increasing concentrations of 3SL- or 6SL-cyclic-carbamate. We found that only the presentation of α2,3-linked sialic acid increased factor H recruitment as assessed by flow cytometry (Fig. 3B). Coating *E. coli* with 20 mM 3SL-cyclic-carbamate yielded a 3-fold increase of factor H staining, whereas 6SL-cyclic-carbamate had no effect up to a concentration of 25 mM (Fig 3C).

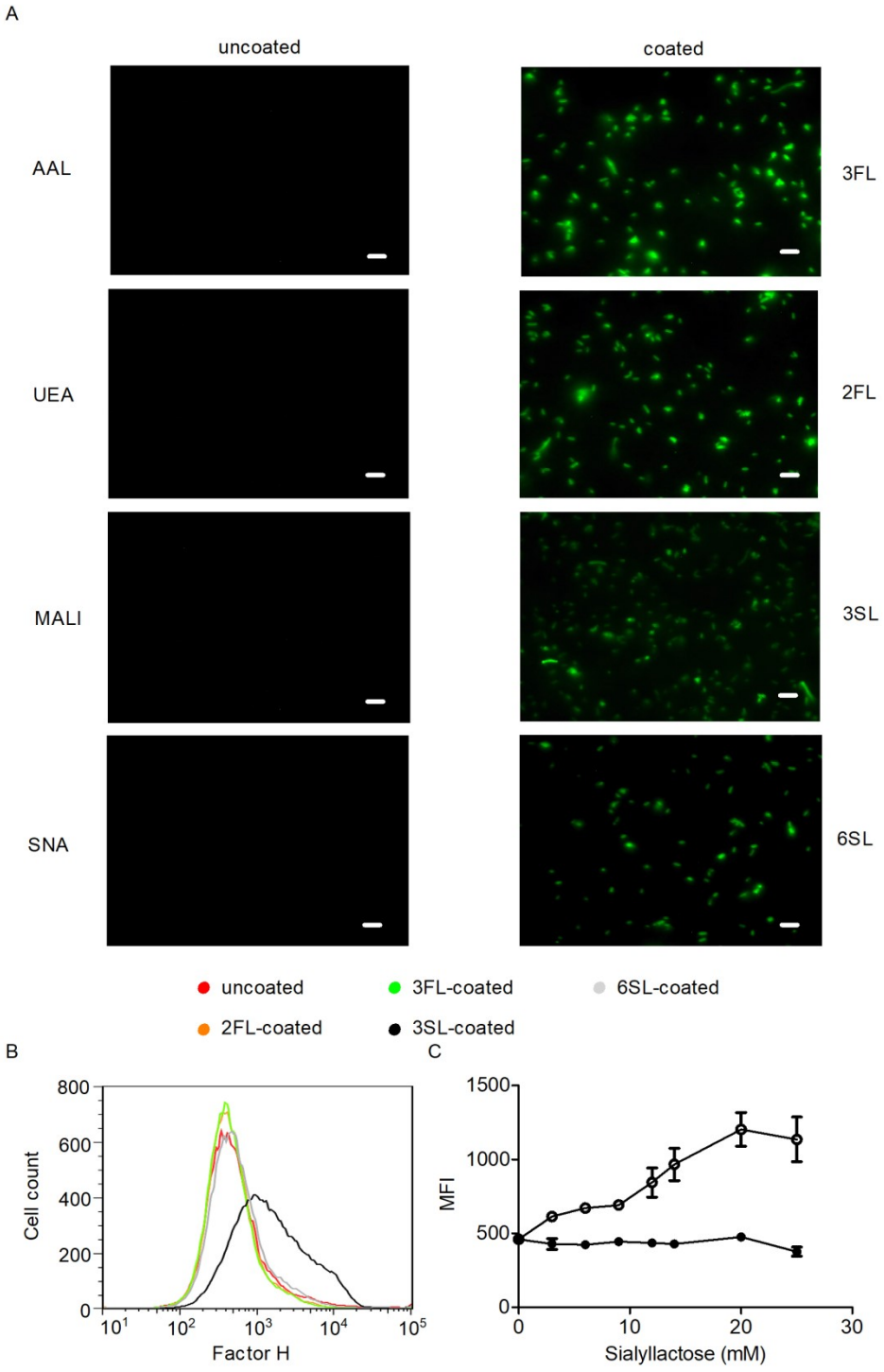

Figure 3: Oligosaccharide Coating of E. coli K-12 and Complement Factor H Recruitment by 3SL. (A) Fixed *E. coli* K-12 coated with 3FL, 2FL, 3SL, and 6SL or left uncoated were stained with fluorescein-isothiocyanate-labeled AAL, UEA, MALI, and SNA and examined by fluorescence microscopy. Scale bar, 10 µm. (B) Binding of complement factor H to fixed *E. coli* K-12 coated with 2FL, 3FL, 3SL, or 6SL detected by anti-factor H IgG and anti-heavy chain binding antibody coupled to Alexa 488. Uncoated (red lines), 2FL-coated cells (orange lines), 3FL-coated cells (green lines), 3SL-coated cells (black lines), 6SL-coated cells (grey lines). (C) Titration of *E. coli* K-12 cells coated with increasing amounts of 3SL (open circles) or 6SL (closed circles) and detection of

complement factor H binding. MFI, median fluorescence intensity. Data are shown as averages and SD of three values.

Previous studies have shown that bacterial glycans influence the pattern of cytokines released by dendritic cells upon stimulation [33, 34]. To determine if the coating of bacteria with different oligosaccharides leads to changes in the cytokine response of dendritic cells, we incubated human PBMC-derived dendritic cells with *E. coli* K-12 cells labeled with lactose [Gal(β1-4)Glc] (Lac), 2FL, 3FL, 3SL, and 6SL derivatized to cyclic-carbamates. The stimulation of dendritic cells by oligosaccharide-coated bacteria differentially affected the production of several cytokines investigated. Whereas the release of IL-6 and IL-10 remained insensitive to oligosaccharide coating, the levels of interferon (IFN)-γ, IL-1β, IL-12p70, IL-18, TNF-α, and IL-23 by dendritic cells increased after coating of *E. coli* with 3FL, 3SL, and 6SL but not after coating with 2FL and Lac (Fig. 4). These results demonstrate that bacterial glycosylation is a critical factor that influences the pattern of cytokines produced by dendritic cells. Dendritic cells express many C-type lectins [35], such as dectins and DC-SIGN, which coordinate the recognition of carbohydrate epitopes and trigger different signaling pathways resulting in various cytokine responses. By enabling the display of unique carbohydrate structures on bacterial membranes, oligosaccharide-cyclic-carbamates represent valuable tools to dissect the pathways involved in the recognition of bacterial glycans by immune cells.

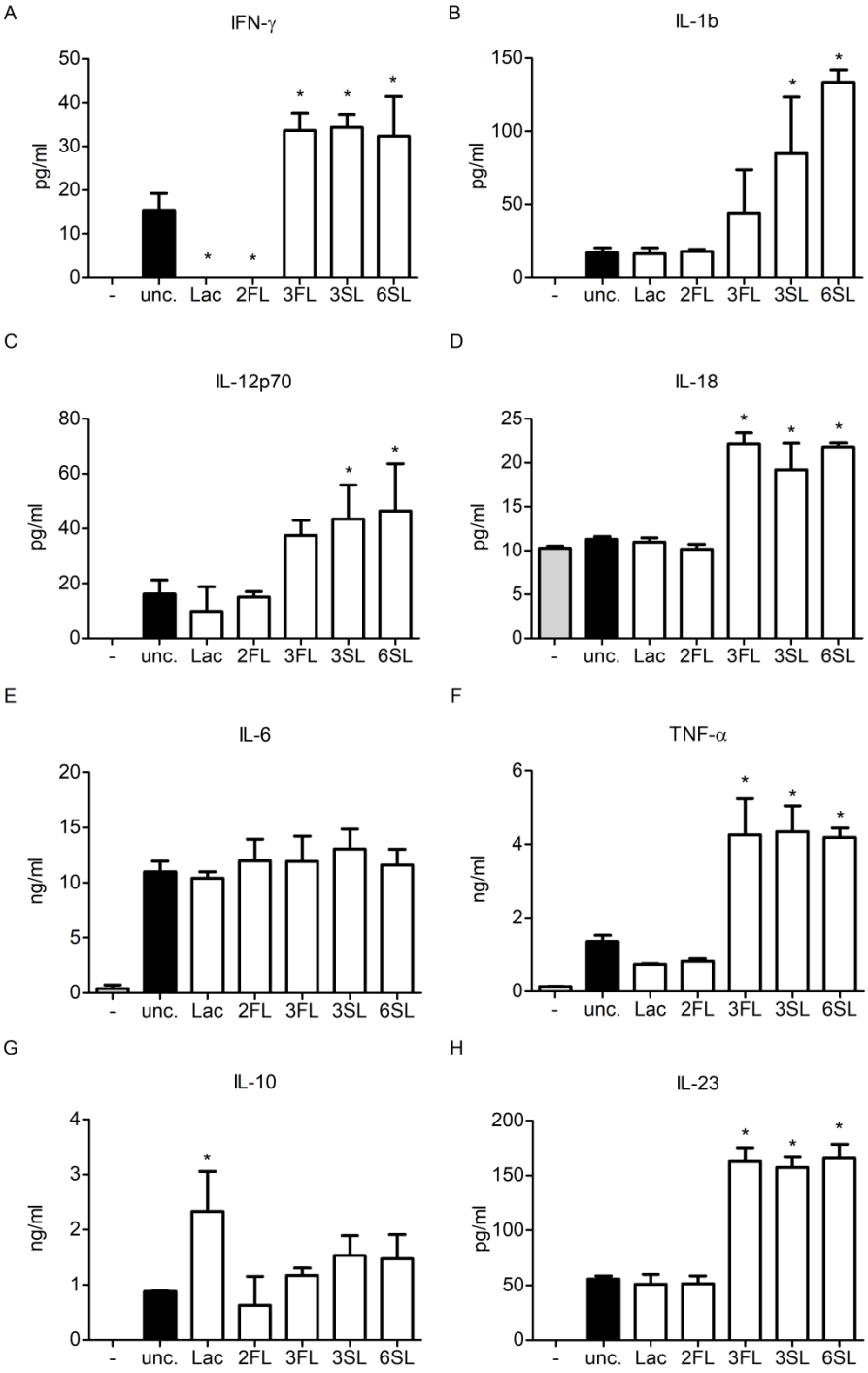

Figure 4: Cytokine Response of Human Dendritic Cells to Oligosaccharide-Coated E. coli. Cytokine response of human PBMC-derived dendritic cells to oligosaccharide-cyclic-carbamate-coated *E. coli* K-12 at a ratio of 1:1. (A) interferon-γ; (B) IL-1β; (C) IL-12p70; (D) IL-18; (E) IL-6; (F) TNF-α; (G) IL-10; (H) IL-23. Cytokines were measured after 24 h. Unc, uncoated. Data represent averages and SD of three experiments. *$p < 0.05$.

Custom glycosylation of proteins

Beside animal and bacterial cells, oligosaccharide-cyclic-carbamates can also be ligated directly to primary amines on proteins. Such modified proteins can then be used as customized glycoproteins to study the roles of multivalent glycans on protein backbones. For example, we modified BSA and *Staphylococcus aureus* protein A with 2FL, 3FL, 3SL, and 6SL. BSA has 59 lysine residues, and their complete modification with each trisaccharide tested would result in a mass in-crease from 69 kDa to about 100 kDa. The molecular mass shift observed ranged between 10 kDa for 6SL and 20 kDa for 3SL (Fig. 5A), which was expected considering that BSA includes 17 disulfide bridges [36], which decrease the accessibility of some lysine residues for oligosaccharide-cyclic-carbamates. Denaturing BSA by adding thiol reducing agents was not an option, given that cyclic-carbamates can react with thiols [22]. *Staphylococcus aureus* protein A, on the other hand, has no disulfide bridges and can therefore be completely denatured by heat treatment. After incubation with oligosaccharide-cyclic-carbamates, the molecular mass of *Staphylococcus aureus* protein A increased from 42 kDa to up to 80 kDa, which indicated a nearly complete glycosylation of its 58 lysine residues (Fig. 5B). As expected, heat-denatured protein A, with and without oligosaccharide modification, did not retain its IgG-binding activity, as demonstrated by ELISA (data not shown). Given that the ligation of MC-38 cells with fucosylated oligosaccharides increased E-selectin binding, we also tested the affinity of glycosylated BSA for E-, P-, and L-selectin.

BSA decorated with 3SL, 6SL, and 2FL remained unbound by the three selectin proteins, whereas decoration with 3FL and FSL increased selectin binding as assessed by dot blotting (Fig. 5C–5E). In this setting, 3FL-BSA and FSL-BSA were equally recognized by E-selectin (Fig. 5C) and P-selectin (Fig. 5D). Recognition by L-selectin was weaker for 3FL-BSA but equally strong for FSL-BSA (Fig. 5E). These findings are compatible with data obtained from glycan arrays showing that selectins mainly bind to glycans carrying sialyl-Lewis A and sialyl-Lewis X epitopes [15, 37-39].

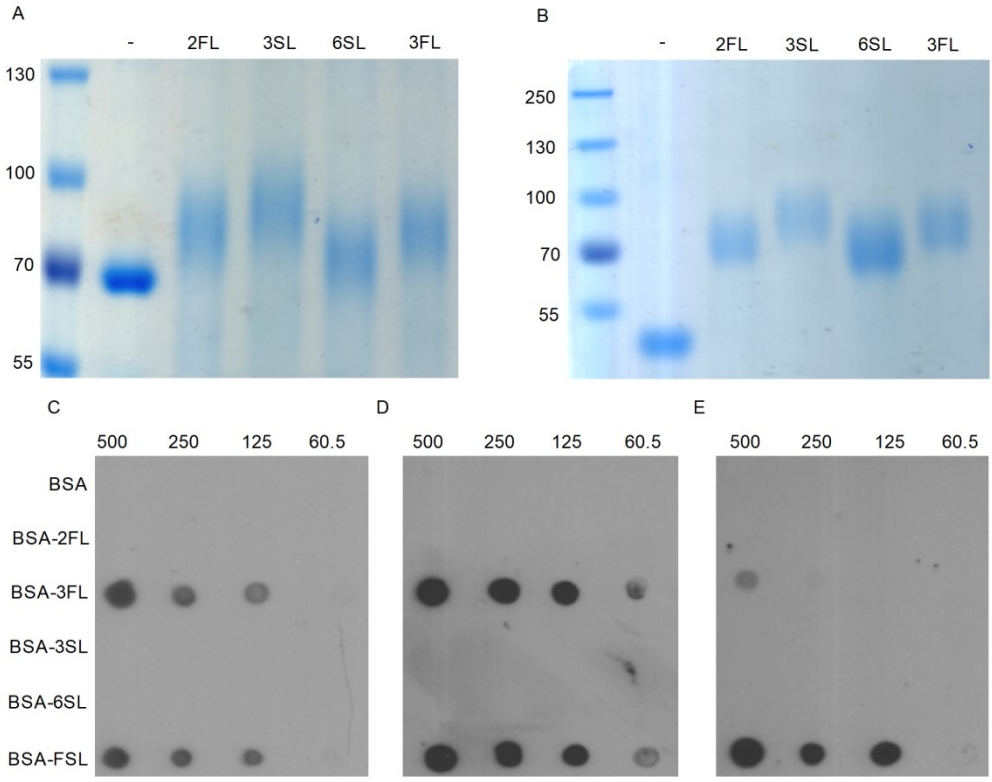

Figure 5: Gel Electrophoresis of Oligosaccharide-Coated Proteins and Selectin Binding (A and B) The oligosaccharides 2FL, 3FL, 3SL, 6SL were coupled to (A) BSA and (B) *Staphylococcus aureus* protein A. Custom-glycosylated proteins were stained using Coomassie blue. Molecular weight markers are indicated in kDa at the left of each panel. (C–E) BSA coated with 2FL, 3FL, 3SL, 6SL, FSL was dotted onto nitrocellulose membranes at the indicated amounts (ng). (C) E-selectin binding, (D) P-selectin binding, and (E) L-selectin binding was assessed using selectin probes fused to a human Fc domain, detected by a biotinylated anti-Fc antibody and streptavidin-linked horseradish peroxidase.

Previous studies have shown that the glycan moiety of mucins regulate the production of the cytokines IL-10 and IL-12 by dendritic cells [40]. We therefore applied glycosylated BSA to determine the impact of different glycans on cytokine secretion by human PBMC-derived dendritic cells. We tested the tetrasaccharide FSL and its related trisaccharides 3FL and 3SL at 10, 50, and 250 μg/ml. Pre-incubating dendritic cells with 3FL- and FSL-BSA decreased IL-10 production after lipopolysaccharide (LPS) stimulation. By contrast, pre-incubation with 3SL-BSA had no effect on IL-10 production (Fig. S4A). The pre-treatment of dendritic cells with glycosylated BSA had no impact on IL-6 and IL-12p70 production (Fig. S4B and S4C). To identify the mechanisms causing the effect of FSL-BSA on cytokine release, we pre-treated dendritic cells with the dectin-1 inhibitor laminarin [41, 42], a DC-SIGN inhibiting antibody [43, 44], the SHP1/2 PTPase inhibitor NSC-87877 [45], and the phosphatidylinositol 3-kinase (PI3K) inhibitor wortmannin [46]. Whereas pre-treatments with laminarin, the DC-SIGN inhibiting antibody, and NSC-87877 had no impact on the regulatory effect of FSL-BSA toward the

release of IL-10 (data not shown), we found that blocking PI3K with wortmannin strongly increased the levels of the pro-inflammatory cytokines TNF-α, IL-12p70, and IL-1β produced by dendritic cells after FSL-BSA pre-incubation and LPS stimulation (Fig. 6A–6C). By contrast, the inhibition of PI3K had no effect on the production of IL-6 (Fig. 6D) and IL-10 (Fig. 6E), indicating that FSL-BSA pre-treatment enhanced TNF-α, IL-12p70, and IL-1β secretion through a mechanism that is normally suppressed by PI3K. PI3K is known to negatively regulate TLR signaling [47], suggesting that lectins involved in the recognition of FSL-BSA are also suppressed in a PI3K-dependent manner. We next addressed whether the stimulatory effect of glycosylated BSA was restricted to the FSL epitope by also testing Lac-BSA, 3FL-BSA, and 3SL-BSA.

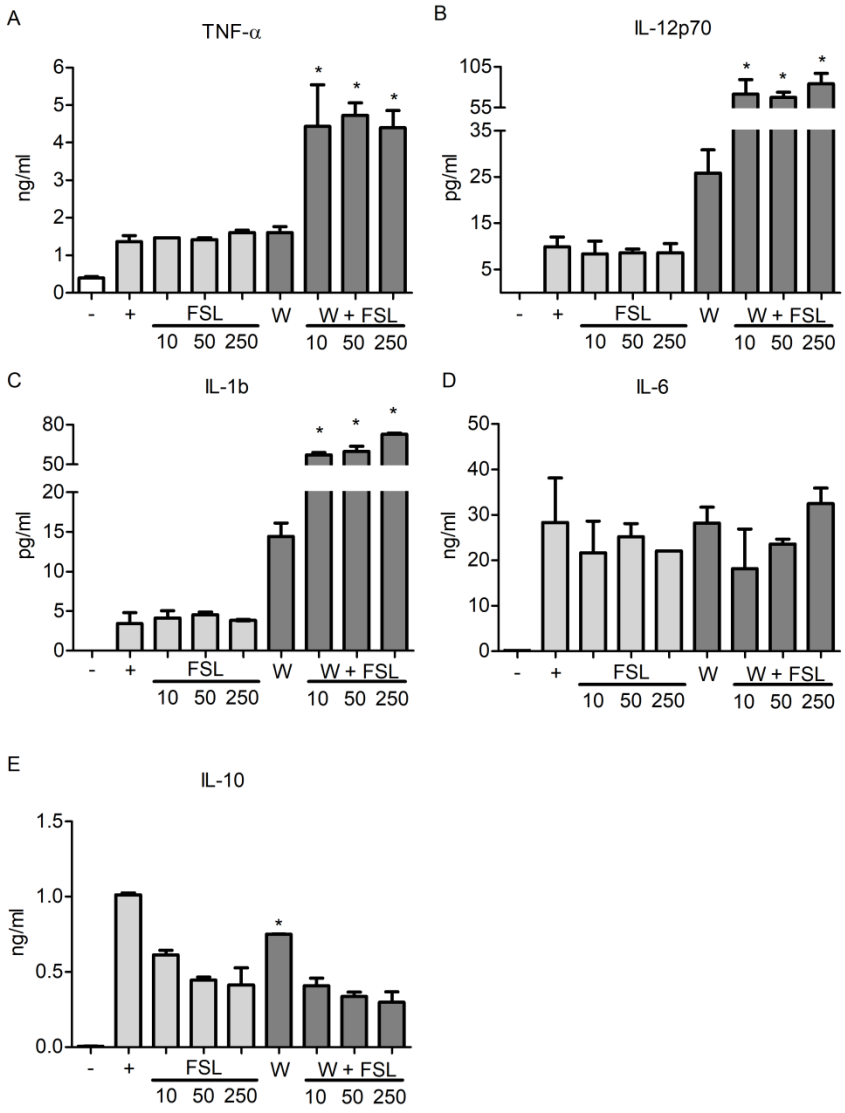

Figure 6: Effect of PI3K Inhibition on Cytokine Production in LPS Stimulated Dendritic Cells Pre-treated with Glycosylated BSA. FSL-modified BSA was added to PBMC-derived human dendritic cells at the indicated concentrations (μg/mL). Some cells were treated with wortmannin (labeled with W) before the addition of FSL-

modified BSA. Finally the cells were stimulated with LPS. The medium was collected and (A) TNF-α, (B) IL-12p70, (C) IL-1β, (D) IL-6, and (E) IL-10 levels were determined. W, wortmannin; -, untreated; +, stimulated with 500 ng/mL LPS. Data represent averages and SD of three experiments. *p < 0.05.

We compared IL-12p70 and IL-6 as these two cytokines were either sensitive or insensitive to wortmannin-mediated PI3K inhibition. The same stimulatory effect was observed for all forms of glycosylated BSA, whereas non-glycosylated BSA was inactive (Fig. 7A). As noticed for FSL-BSA before, any type of glycosylated BSA failed to influence IL-6 in dendritic cells stimulated with LPS (Fig. 7B). These experiments showed that custom-glycosylated proteins such as BSA can be applied to investigate the regulatory effects of endogenous lectins on immune cell activation.

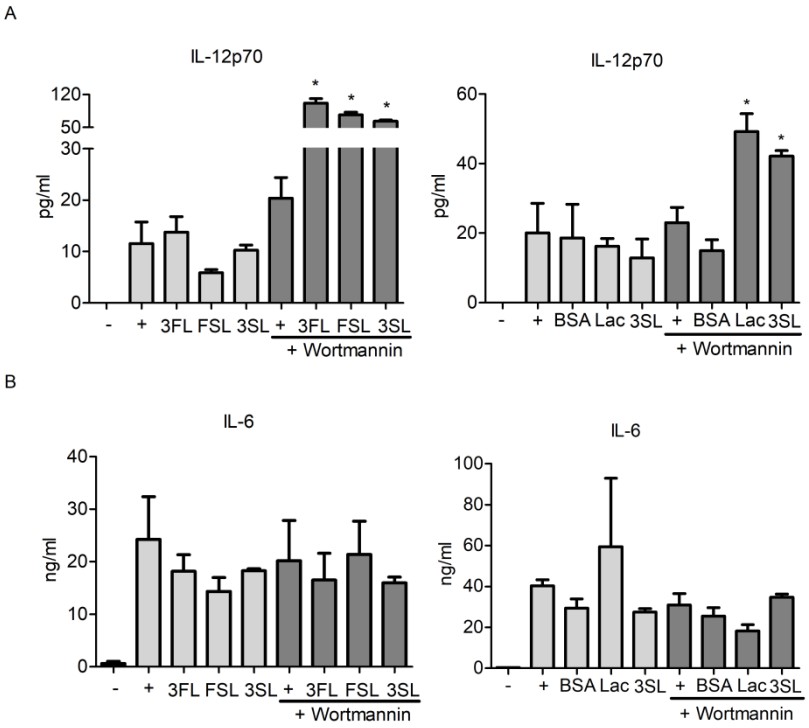

Figure 7: Effect of PI3K Inhibition on Cytokine Production Depends on Glycan Chains. Native and glycosylated BSA was added to PBMC-derived human dendritic cells at 250 µg/mL with or without pre-treatment with wortmannin. (A) IL-12p70, (B) IL-6 levels in cell supernatants after 24 h incubation. -, untreated; +, stimulated with 500 ng/mL LPS. Data represent averages and SD of three experiments. *p < 0.05.

Discussion

We present a method with which whole cells and any molecule containing primary amines can be modified to expose specific oligosaccharide structures. The simplicity and the lack of toxicity of the cyclic-carbamate-mediated ligation technique enable its application under physiological conditions at neutral pH and over a broad range of temperatures. The versatility of the technique was illustrated

by investigating selectin binding to glycan-decorated murine MC-38 cells, factor H binding to decorated *E. coli*, and dendritic cell activation by custom-glycosylated proteins.

As shown through the ligation of fucosylated oligosaccharides to MC-38 cells, the technique enables the study of carbohydrate-binding proteins in the context of cellular membranes. The sialyl-Lewis X epitope is the generally accepted ligand for selectins, implying that α2-3 linked sialic acid linked to galactose increases the binding affinity to selectins [48-50]. Sulfated Lewis X has also been reported to be a selectin ligand, which implies that the negative charge facilitates selectin binding [51, 52]. Our comparative study of selectin binding demonstrated that α1-3 fucosylation without sialylation mediates strong E-selectin binding to mouse cells. These results confirm the previous observation that α1-3-fucosyltransferase overexpression is sufficient to enable cells to roll on E-selectin [53]. However, increasing α1-3 fucosylation of MC-38 cells by decorating them with 3FL did not increase the binding to P- and L-selectin, although significant binding to P- and L-selectin was observed when α1-3 fucosylated epitopes were exposed on glycosylated BSA spotted on nitrocellulose membranes. This illustrates that the context of epitope presentation, either on a cell membrane or on a solid surface, affects the binding specificity of selectin isoforms. Such differences in carbohydrate-binding behavior indicate that results obtained with glycans spotted on glass arrays may diverge from the binding properties to the same epitopes presented on glycoconjugates inserted in cell membranes.

The application of the cyclic-carbamate ligation technology to coat *E. coli* demonstrated its value as a tool to study the role of specific bacterial glycan structures and their interaction with host proteins. Whereas membrane sialylation was previously shown to interfere with complement activation [20, 54], the importance of the glycosidic linkage of sialic acid remained unclear. The decoration of bacterial membranes with α2-3 and α2-6 linked sialic acid using cyclic-carbamate ligation clearly demonstrated the preferential binding of complement factor H to α2-3 linked sialic acid. In pathogenic bacteria, sialic acid either occurs in the context of lipooligosaccharides that are incorporated into the outer membrane of Gram-negative bacteria or in capsular polysaccharides [55, 56]. *N. gonorrhoeae* and *N. meningitidis* sialylate their lipooligosaccharides with an outer-membrane α2-3 sialyltransferase. Gonococcal sialylated lipooligosaccharides have been shown to recruit factor H to the bacterial cell surface and protect the cell from C3 attack as observed for mammalian cell membranes [20]. *Haemophilus influenzae* expresses the α2-3 sialyltransferase Lic3A that is absolutely required for its survival in the middle ear of a mouse model for otitis media [57]. Up to now, *Streptococcus agalactiae* is the only Gram-positive bacterium that has been shown to have sialic acid in its capsule, and the responsible sialyltransferase has been shown to catalyze an α2-3 linkage [58]. Interestingly, capsule sialylation of *S. agalactiae* has been associated with the prevention of complement activation [59]. Accordingly, the experimental evidence gained from *E. coli* coating

confirmed the critical importance of α2-3 sialylation on bacterial surfaces to mediate factor-H-dependent complement inhibition.

The heterogeneous glycosylation of mucins renders the assignment of functions to specific glycan structures on these proteins difficult. The dense glycosylation of mucins occurs on serine and threonine residues, which offer poor reactivity for chemical ligations. Lysine-rich polypeptides can therefore be used as backbones for modification using the oligosaccharide-cyclic-carbamate ligation technique to mimic heavily glycosylated mucins. Recently, a method enabling the production of multivalent glycoproteins presenting carbohydrates on serine has been developed [4]. Although this method generates polypeptides including α-GalNAc-modified serines, the procedure has not been advanced to yield proteins carrying complex oligosaccharide epitopes yet. In our work, we used BSA as a backbone to investigate the role of specific glycan epitopes during dendritic cell activation. Our results clearly showed that glycan moieties have an impact on the activation of dendritic cells as exemplified by differential regulation of cytokine expression. Interestingly, glycosylated BSA affected cytokine production in a PI3K-regulated manner. The PI3K is known to downregulate Toll-like receptor signaling [46, 60, 61]. The release of the cytokines IL-1, IL-12, and TNF-α was strongly induced in LPS stimulated dendritic cells that were pre-treated with glycosylated BSA once PI3K was blocked by wortmannin. The carbohydrate-binding receptors involved in sensing of glycosylated BSA are currently unknown, but dendritic cells express a multitude of C-type lectins [35], which contribute to the regulation of immune reactions by recognizing glycoconjugates. C-type lectins, such as the macrophage mannose receptor and DC-SIGN, influence cytokine production in dendritic cells [62, 63]. The availability of uniformly glycosylated proteins will be helpful in delineating ligand specificity and the signaling properties of C-type lectin family members in the context of living cells.

In addition to the direct glycosylation of cell membranes and the production of custom glycoproteins as outlined in the present study, other carrier molecules, such as the phospholipid phosphatidylethanolamine, are suitable supports to produce specific glycolipids. In conclusion, the cyclic-carbamate ligation technique introduces a simple and versatile method to generate specific glycoconjugates by modifying primary amines.

Significance

We have developed a glycan conjugation method based on the derivatization of oligosaccharides with cyclic-carbamates. The resulting compounds enabled the targeted glycosylation of live cells with specific oligosaccharide epitopes. This approach opens the way to engineering rapid and specific changes in cell-surface glycosylation, which for example enables the characterization of carbohydrate ligands presented in the context of cell membranes rather than solid surfaces such as oligosaccharide

arrays on glass slides. We illustrated this concept here by coating multiple mouse and human cell lines with fucosylated oligosaccharides, thereby increasing E-selectin binding. The same approach could be applied to prokaryotic cells to, for example, to study their interactions with proteins from the innate immune system.

The decoration of E. coli with sialylated oligosaccharides demonstrated the specific requirement for α2,3-linked sialic acid for the binding of complement factor H to the bacterial membrane. The technology also allows the study of signaling cascades activated by the recognition of specific oligosaccharide epitopes presented on glycoproteins. Here, we showed that proteins such as BSA can be glycosylated uniformly to address the carbohydrate ligand specificity of cytokine production in stimulated dendritic cells, which express a large number of C-type lectins. Altogether, cyclic-carbamate-derivatized oligosaccharides represent a fast and efficient resource enabling the selective glycosylation of cell surfaces and proteins.

Acknowledgments

We thank Glycom A/S for supplying us with the oligosaccharide-cyclic-carbamates and Dora Molnar-Gabor for the mass spectrometry analysis. Special thanks go to the Chemistry Department of the Danish Technical University (DTU) for enabling us to access their NMR instruments. N.K. is an employee of Glycom A/S, which holds the patent WO2009/040363 on the glycosylcarbamoylation methodology. This research was supported by the Zurich Center for Integrative Human Physiology (ZIHP) and by the Swiss National Science Foundation grant 314730_172880.

Author contributions

M.W.J.W., N.K., L.B., and T.H. planned the experiments. M.W.J.W. and N.K. performed the experiments. M.W.J.W., T.H., and N.K. wrote the manuscript.

References

1. Patnaik, S.K. and P. Stanley, *Lectin-resistant CHO glycosylation mutants.* Methods Enzymol, 2006. **416**: p. 159-82.

2. Yang, Z., et al., *Engineered CHO cells for production of diverse, homogeneous glycoproteins.* Nat Biotechnol, 2015. **33**(8): p. 842-4.

3. Danishefsky, S.J., et al., *Development of Globo-H cancer vaccine.* Acc Chem Res, 2015. **48**(3): p. 643-52.

4. Kramer, J.R., et al., *Chemically tunable mucin chimeras assembled on living cells.* Proc Natl Acad Sci U S A, 2015. **112**(41): p. 12574-9.

5. Kiessling, L.L. and J.C. Grim, *Glycopolymer probes of signal transduction.* Chem Soc Rev, 2013. **42**(10): p. 4476-91.

6. Hudak, J.E., S.M. Canham, and C.R. Bertozzi, *Glycocalyx engineering reveals a Siglec-based mechanism for NK cell immunoevasion.* Nat Chem Biol, 2014. **10**(1): p. 69-75.

7. Anjaneyulu, P.S.R. and J.V. Staros, *Reactions of N-Hydroxysulfosuccinimide Active Esters.* International Journal of Peptide and Protein Research, 1987. **30**(1): p. 117-124.

8. Hermanson, G.T., *Bioconjugate Techniques, 3rd Edition.* Bioconjugate Techniques, 3rd Edition, 2013: p. 1-1146.

9. Jonkheijm, P., et al., *Chemical Strategies for Generating Protein Biochips.* Angewandte Chemie-International Edition, 2008. **47**(50): p. 9618-9647.

10. Feizi, T., et al., *Carbohydrate microarrays - a new set of technologies at the frontiers of glycomics.* Current Opinion in Structural Biology, 2003. **13**(5): p. 637-645.

11. de Boer, A.R., et al., *General microarray technique for immobilization and screening of natural glycans.* Analytical Chemistry, 2007. **79**(21): p. 8107-8113.

12. Song, X.Z., et al., *Novel Fluorescent Glycan Microarray Strategy Reveals Ligands for Galectins.* Chemistry & Biology, 2009. **16**(1): p. 36-47.

13. Blixt, O., et al., *Sialoside analogue arrays for rapid identification of high affinity Siglec ligands.* J Am Chem Soc, 2008. **130**(21): p. 6680-1.

14. Bochner, B.S., et al., *Glycan array screening reveals a candidate ligand for Siglec-8.* J Biol Chem, 2005. **280**(6): p. 4307-12.

15. Preston, R.C., et al., *Implications of the E-selectin S128R mutation for drug discovery.* Glycobiology, 2014. **24**(7): p. 592-601.

16. Bevilacqua, M.P., et al., *Identification of an inducible endothelial-leukocyte adhesion molecule.* Proc Natl Acad Sci U S A, 1987. **84**(24): p. 9238-42.

17. Subramanian, H., et al., *Signaling through L-Selectin Mediates Enhanced Chemotaxis of Lymphocyte Subsets to Secondary Lymphoid Tissue Chemokine.* Journal of Immunology, 2012. **188**(7): p. 3223-3236.

18. Crocker, P.R., J.C. Paulson, and A. Varki, *Siglecs and their roles in the immune system.* Nat Rev Immunol, 2007. **7**(4): p. 255-66.

19. Parsons, N.J., et al., *Cytidine 5'-Monophospho-N-Acetyl Neuraminic Acid and a Low-Molecular Weight Factor from Human-Blood Cells Induce Lipopolysaccharide Alteration in Gonococci When Conferring Resistance to Killing by Human-Serum.* Microbial Pathogenesis, 1988. **5**(4): p. 303-309.

20. Ram, S., et al., *A novel sialic acid binding site on factor H mediates serum resistance of sialylated Neisseria gonorrhoeae.* J Exp Med, 1998. **187**(5): p. 743-52.

21. Banchereau, J. and R.M. Steinman, *Dendritic cells and the control of immunity.* Nature, 1998. **392**(6673): p. 245-52.

22. Ichikawa, Y., Y. Matsukawa, and M. Isobe, *Synthesis of urea-tethered neoglycoconjugates and pseudooligosaccharides in water.* J Am Chem Soc, 2006. **128**(12): p. 3934-8.

23. Rosenberg, S.A., P. Spiess, and R. Lafreniere, *A new approach to the adoptive immunotherapy of cancer with tumor-infiltrating lymphocytes.* Science, 1986. **233**(4770): p. 1318-21.

24. O'Neill, D.W. and N. Bhardwaj, *Differentiation of peripheral blood monocytes into dendritic cells.* Curr Protoc Immunol, 2005. **Chapter 22**: p. Unit 22F 4.

25. Borsig, L., et al., *Synergistic effects of L- and P-selectin in facilitating tumor metastasis can involve non-mucin ligands and implicate leukocytes as enhancers of metastasis.* Proc Natl Acad Sci U S A, 2002. **99**(4): p. 2193-8.

26. Lewis, L.A., et al., *The meningococcal vaccine candidate neisserial surface protein A (NspA) binds to factor H and enhances meningococcal resistance to complement.* PLoS Pathog, 2010. **6**(7): p. e1001027.

27. Ram, S., L.A. Lewis, and S. Agarwal, *Meningococcal group W-135 and Y capsular polysaccharides paradoxically enhance activation of the alternative pathway of complement.* J Biol Chem, 2011. **286**(10): p. 8297-307.

28. Foxall, C., et al., *The three members of the selectin receptor family recognize a common carbohydrate epitope, the sialyl Lewis(x) oligosaccharide.* J Cell Biol, 1992. **117**(4): p. 895-902.

29. Geisler, C. and D.L. Jarvis, *Letter to the Glyco-Forum: Effective glycoanalysis with Maackia amurensis lectins requires a clear understanding of their binding specificities.* Glycobiology, 2011. **21**(8): p. 988-993.

30. Shibuya, N., et al., *The elderberry (Sambucus nigra L.) bark lectin recognizes the Neu5Ac(alpha 2-6)Gal/GalNAc sequence.* J Biol Chem, 1987. **262**(4): p. 1596-601.

31. Weiler, J.M., et al., *Control of the amplification convertase of complement by the plasma protein beta1H.* Proc Natl Acad Sci U S A, 1976. **73**(9): p. 3268-72.

32. Gilbert, M., et al., *Cloning of the lipooligosaccharide alpha-2,3-sialyltransferase from the bacterial pathogens Neisseria meningitidis and Neisseria gonorrhoeae.* J Biol Chem, 1996. **271**(45): p. 28271-6.

33. Bergman, M., et al., *Helicobacter pylori phase variation, immune modulation and gastric autoimmunity.* Nature Reviews Microbiology, 2006. **4**(2): p. 151-159.

34. Tailleux, L., et al., *DC-SIGN is the major Mycobacterium tuberculosis receptor on human dendritic cells.* J Exp Med, 2003. **197**(1): p. 121-7.

35. Figdor, C.G., Y. van Kooyk, and G.J. Adema, *C-type lectin receptors on dendritic cells and Langerhans cells.* Nat Rev Immunol, 2002. **2**(2): p. 77-84.

36. Jordan, G.M., S. Yoshioka, and T. Terao, *The aggregation of bovine serum albumin in solution and in the solid state.* J Pharm Pharmacol, 1994. **46**(3): p. 182-5.

37. Barthel, S.R., et al., *Targeting selectins and selectin ligands in inflammation and cancer.* Expert Opin Ther Targets, 2007. **11**(11): p. 1473-91.

38. Mitsuoka, C., et al., *Sulfated sialyl Lewis X, the putative L-selectin ligand, detected on endothelial cells of high endothelial venules by a distinct set of anti-sialyl Lewis X antibodies.* Biochem Biophys Res Commun, 1997. **230**(3): p. 546-51.

39. Rodgers, S.D., R.T. Camphausen, and D.A. Hammer, *Sialyl Lewis(x)-mediated, PSGL-1-independent rolling adhesion on P-selectin.* Biophys J, 2000. **79**(2): p. 694-706.

40. Shan, M., et al., *Mucus enhances gut homeostasis and oral tolerance by delivering immunoregulatory signals.* Science, 2013. **342**(6157): p. 447-53.

41. Adams, E.L., et al., *Differential high-affinity interaction of dectin-1 with natural or synthetic glucans is dependent upon primary structure and is influenced by polymer chain length and side-chain branching.* Journal of Pharmacology and Experimental Therapeutics, 2008. **325**(1): p. 115-123.

42. Herre, J., et al., *Dectin-1 uses novel mechanisms for yeast phagocytosis in macrophages.* Blood, 2004. **104**(13): p. 4038-4045.

43. Baribaud, F., et al., *Quantitative expression and virus transmission analysis of DC-SIGN on monocyte-derived dendritic cells.* Journal of Virology, 2002. **76**(18): p. 9135-9142.

44. Wu, L., et al., *Functional evaluation of DC-SIGN monoclonal antibodies reveals DC-SIGN interactions with ICAM-3 do not promote human immunodeficiency virus type 1 transmission.* J Virol, 2002. **76**(12): p. 5905-14.

45. Chen, L.W., et al., *Discovery of a novel Shp2 protein tyrosine phosphatase inhibitor.* Molecular Pharmacology, 2006. **70**(2): p. 562-570.

46. Powis, G., et al., *Wortmannin, a Potent and Selective Inhibitor of Phosphatidylinositol-3-Kinase.* Cancer Research, 1994. **54**(9): p. 2419-2423.

47. Fukao, T. and S. Koyasu, *PI3K and negative regulation of TLR signaling.* Trends in Immunology, 2003. **24**(7): p. 358-363.

48. Somers, W.S., et al., *Insights into the molecular basis of leukocyte tethering and rolling revealed by structures of P- and E-selectin bound to SLe(X) and PSGL-1.* Cell, 2000. **103**(3): p. 467-479.

49. Sperandio, M., C.A. Gleissner, and K. Ley, *Glycosylation in immune cell trafficking.* Immunol Rev, 2009. **230**(1): p. 97-113.

50. Yago, T., et al., *Core 1-derived O-glycans are essential E-selectin ligands on neutrophils.* Proc Natl Acad Sci U S A, 2010. **107**(20): p. 9204-9.

51. Green, P.J., et al., *High affinity binding of the leucocyte adhesion molecule L-selectin to 3'-sulphated-Le(a) and -Le(x) oligosaccharides and the predominance of sulphate in this interaction demonstrated by binding studies with a series of lipid-linked oligosaccharides.* Biochem Biophys Res Commun, 1992. **188**(1): p. 244-51.

52. Yuen, C.T., et al., *Novel Sulfated Ligands for the Cell-Adhesion Molecule E-Selectin Revealed by the Neoglycolipid Technology among O-Linked Oligosaccharides on an Ovarian Cystadenoma Glycoprotein.* Biochemistry, 1992. **31**(38): p. 9126-9131.

53. Lowe, J.B., et al., *ELAM-1--dependent cell adhesion to vascular endothelium determined by a transfected human fucosyltransferase cDNA.* Cell, 1990. **63**(3): p. 475-84.

54. Meri, S. and M.K. Pangburn, *Regulation of alternative pathway complement activation by glycosaminoglycans: specificity of the polyanion binding site on factor H.* Biochem Biophys Res Commun, 1994. **198**(1): p. 52-9.

55. Mandrell, R.E., et al., *Lipooligosaccharides (Los) of Some Haemophilus Species Mimic Human Glycosphingolipids, and Some Los Are Sialylated.* Infection and Immunity, 1992. **60**(4): p. 1322-1328.

56. Vimr, E.R., et al., *Diversity of microbial sialic acid metabolism.* Microbiol Mol Biol Rev, 2004. **68**(1): p. 132-53.

57. Severi, E., D.W. Hood, and G.H. Thomas, *Sialic acid utilization by bacterial pathogens.* Microbiology-Sgm, 2007. **153**: p. 2817-2822.

58. Chaffin, D.O., L.M. Mentele, and C.E. Rubens, *Sialylation of group B streptococcal capsular polysaccharide is mediated by cpsK and is required for optimal capsule polymerization and expression.* J Bacteriol, 2005. **187**(13): p. 4615-26.

59. Marques, M.B., et al., *Prevention of C3 Deposition by Capsular Polysaccharide Is a Virulence Mechanism of Type-Iii Group-B Streptococci.* Infection and Immunity, 1992. **60**(10): p. 3986-3993.

60. Fukao, T., et al., *PI3K-mediated negative feedback regulation of IL-12 production in DCs.* Nature Immunology, 2002. **3**(9): p. 875-881.

61. Guha, M. and N. Mackman, *The phosphatidylinositol 3-kinase-Akt pathway limits lipopolysaccharide activation of signaling pathways and expression of inflammatory mediators in human monocytic cells.* Journal of Biological Chemistry, 2002. **277**(35): p. 32124-32132.

62. Geijtenbeek, T.B.H., et al., *Mycobacteria target DC-SIGN to suppress dendritic cell function.* Journal of Experimental Medicine, 2003. **197**(1): p. 7-17.

63. Yamamoto, Y., T.W. Klein, and H. Friedman, *Involvement of mannose receptor in cytokine interleukin-1beta (IL-1beta), IL-6, and granulocyte-macrophage colony-stimulating factor responses, but not in chemokine macrophage inflammatory protein 1beta (MIP-1beta), MIP-2, and KC responses, caused by attachment of Candida albicans to macrophages.* Infect Immun, 1997. **65**(3): p. 1077-82.

Cell Chemical Biology, Volume 24

Supplemental Information

Custom Glycosylation of Cells and Proteins Using Cyclic-carbamate-Derivatized Oligosaccharides

Marek W.J. Whitehead, Nikolay Khanzhin, Lubor Borsig, and Thierry Hennet

Supporting Information

Supplemental Figures

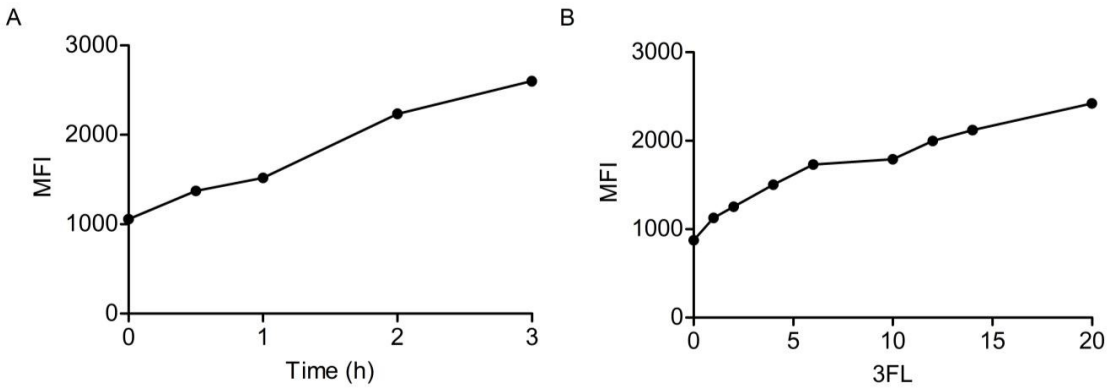

Figure S1: Optimization of cell surface coating with oligosaccharide-cyclic-carbamate, related to Figure 2. (A) MC-38 cells were incubated with 14 mM 3FL-cyclic-carbamate from 0.5 to 3 h before determining the extent of surface coating with FITC labelled AAL by flow cytometry. (B) MC-38 cells were incubated with 0 - 20 mM of 3FL-cyclic-carbamate and surface fucosylation was measured by flow cytometry using FITC labelled AAL. MFI, median fluorescence intensity; 3FL, 3-fucosyllactose.

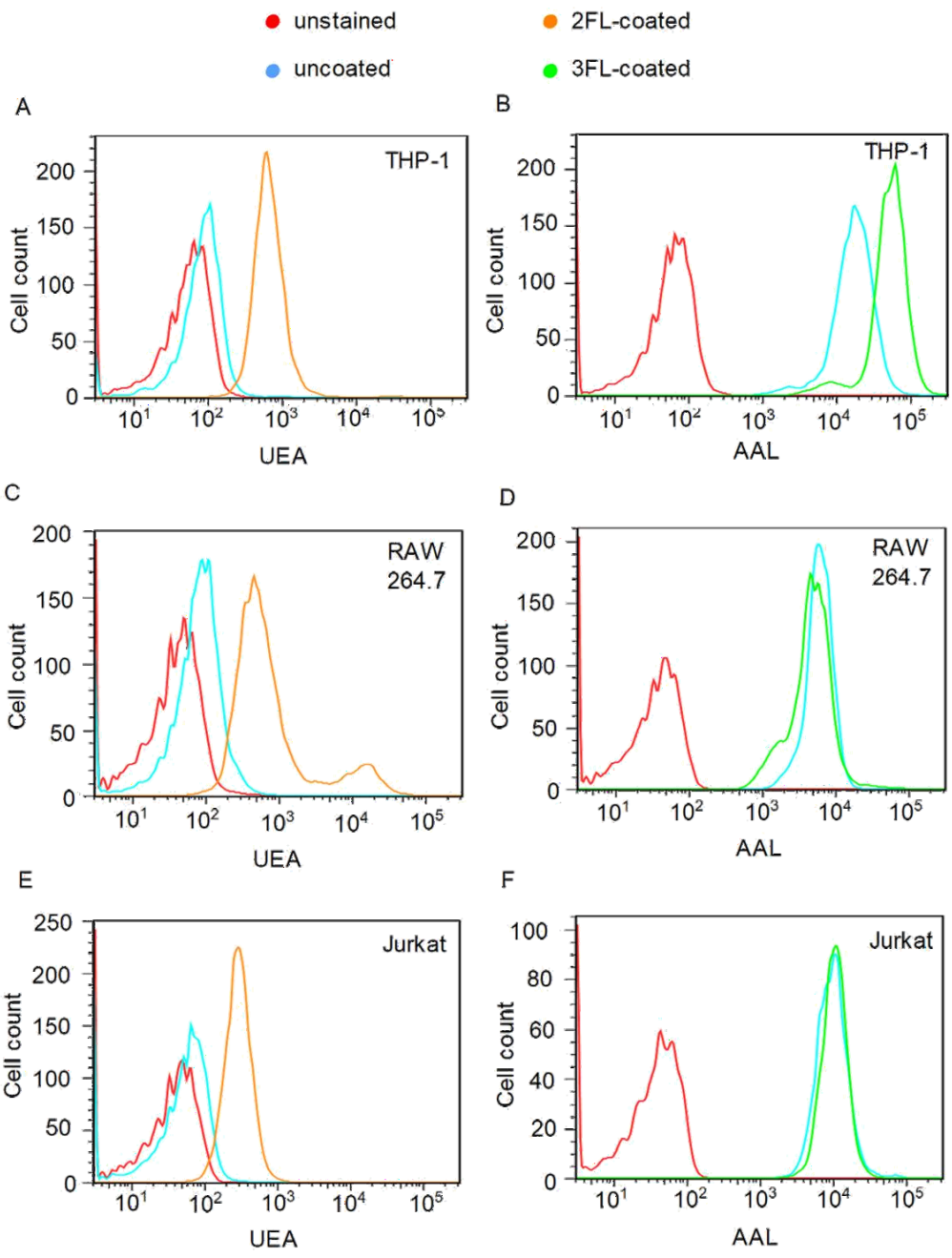

Figure S2: Coating cells with oligosaccharide-cyclic-carbamates, related to Figure 2. (A, B) THP-1, (C, D) RAW264.7 and (E, F) Jurkat cells were coated with 2FL- or 3FL-cyclic-carbamate or left uncoated, then stained with FITC labelled UEA or AAL before being analyzed by flow cytometry. Unstained cells (red lines), uncoated cells (blue lines), 2FL-coated cells (orange lines), 3FL-coated cells (green lines).

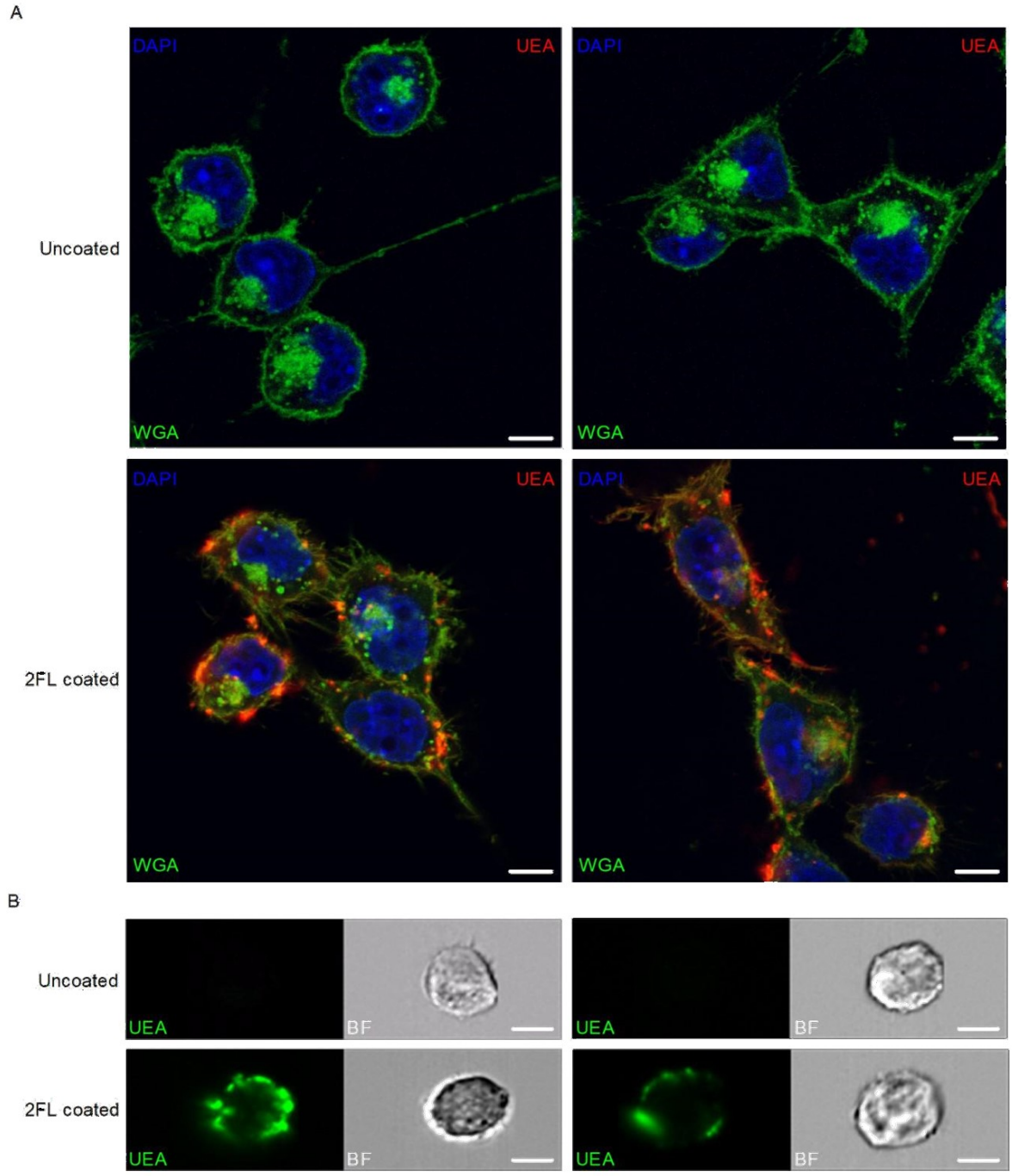

Figure S3: Surface coating of MC-38 cells with 2FL, related to Figure 2. (A) MC-38 cells were coated with 2FL, fixed with formaldehyde (3%), permeabilized with 0.1 % saponin and stained with UEA. Cell membranes and Golgi apparatus were stained using wheat germ agglutinin, and nuclei were stained using 4',6-diamidino-2-phenylindole. (B) Cells coated with 2FL or left uncoated were stained with FITC-labeled UEA and analyzed by flow cytometry. Single cell images were captured using ImageStream® technology. UEA, *Ulex Europaeus* Agglutinin; WGA, wheat germ agglutinin; BF, brightfield. Scale bars: 5 µm.

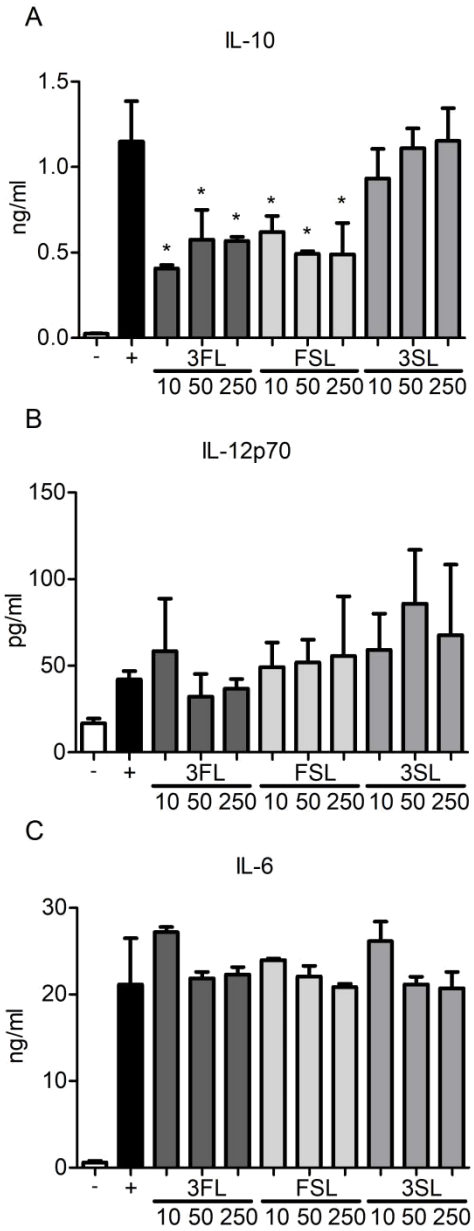

Figure S4: Cytokine response of lipopolysaccharide stimulated dendritic cells pre-treated with glycosylated bovine serum albumin, related to Figure 6. Bovine serum albumin decorated with the oligosaccharides 3FL, FSL, 3SL were added to PBMC-derived human dendritic cells at the indicated concentrations (µg/ml) for 3 h, and then stimulated with lipopolysaccharide at 500 ng/ml. The cytokines (A) IL-10, (B) IL-12p70 and (C) IL-6 were determined in the cell supernatants after 24 h incubation. -, untreated; +, stimulated with 500 ng/ml LPS. Data represent average and standard deviation of three experiments. *, p-value < 0.05.

Methods S1, related to STAR Methods

β-D-**Galactopyranosyl-(1–4)**-β-D-**glucopyranosyl azide (Lactosyl azide, 6a)**

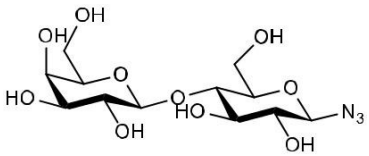

It was prepared previously at Glycom as described in WO2009/040363.

^{1}H NMR (400 MHz, DMSO-d_6, δ DMSO-d_5=2.50) δ 5.65 (d, *J* = 5.5 Hz, 1H), 5.09 (d, *J* = 4.0 Hz, 1H), 4.79 (d, *J* = 4.7 Hz, 1H), 4.77 (d, *J* = 1.6 Hz, 1H), 4.66 (dt, *J* = 8.2, 5.6 Hz, 2H), 4.57 (d, *J* = 8.7 Hz, 1H), 4.52 (d, *J* = 4.6 Hz, 1H), 4.19 (d, *J* = 7.3 Hz, 1H), 3.76 (ddd, *J* = 12.0, 5.5, 2.3 Hz, 1H), 3.66 – 3.57 (m, 2H), 3.56 – 3.40 (m, 4H), 3.39 – 3.24 (m, 4H, overlapping with H_2O), 3.04 (td, *J* = 8.5, 5.4 Hz, 1H).

^{13}C APT NMR (101 MHz, DMSO, δ DMSO-d_5=39.52) δ 103.80 (CH-1'), 89.72 (CH-1), 79.92, 77.02, 75.58, 74.84, 73.25, 73.14, 70.55, 68.18, 60.45 (CH_2OH), 60.12 (CH_2OH).

β-D-**Galactopyranosyl-(1–6)**-β-D-**glucopyrano[2,3-*d*]oxazolidin-2-one (cyclic-carbamate of Lactose, 1a)**

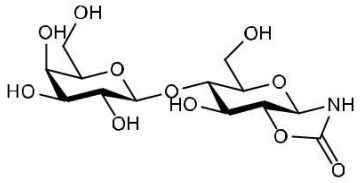

It was prepared previously at Glycom as described in WO2009/040363.

^{1}H NMR (400 MHz, DMSO-d_6, δ DMSO-d_5=2.50) δ 8.49 (br d, *J* = 2.2 Hz, 1H, NHCO), 5.10 (d, *J* = 1.8 Hz, 1H, OH), 5.06 (d, *J* = 4.6 Hz, 1H), 4.86 (dd, *J* = 8.8, 2.1 Hz, 1H, H-1), 4.77-4.82 (m, 2H), 4.75 (t, *J* = 5.0 Hz, 1H), 4.53 (d, *J* = 4.6 Hz, 1H), 4.25 – 4.07 (m, 1H), 3.91 (ddd, *J* = 10.7, 7.1, 1.9 Hz, 1H), 3.74 (ddd, *J* = 12.0, 5.4, 2.2 Hz, 1H), 3.65 (ddd, *J* = 11.8, 6.7, 4.7 Hz, 1H), 3.61 – 3.38 (m, 7H), 3.34 – 3.27 (m, 2H).

^{13}C APT NMR (101 MHz, DMSO-d_6, δ DMSO-d_5=39.52) δ 157.70 (-OCONH-), 104.20 (CH-1'), 84.27 (CH-1), 82.35, 81.22, 79.37, 75.66, 73.24, 71.70, 70.55, 68.22, 60.60 (CH_2OH), 59.93 (CH_2OH).

HRMS (ESI(-)): *m/z* calc. for $[C_{13}H_{20}NO_{11}]^-$ 366.1042 ($[M-H]^-$), found 366.1053.

α-L-**Fucopyranosyl-(1–2)**-β-D-**Galactopyranosyl-(1–6)**-β-D-**glucopyrano[2,3-*d*]oxazolidin-2-one (cyclic-carbamate of 2FL, 1b)**

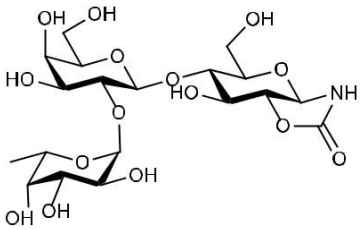

It was prepared previously at Glycom as described in WO2009/040363.

HRMS (ESI(-)): *m/z* calc. for $[C_{19}H_{30}NO_{15}]^-$ ($[M-H]^-$) 512.1620, found 512.1582.

4,7,8,9-tetra-*O*-acetyl-*N*-acetyl-α-neuraminosyl-(2–3)-2,4,6-tri-*O*-acetyl-β-D-galactopyranosyl-(1–4)-1,2,3,6-tetra-*O*-acetyl-α,β-D-glucopyranose (Peracetylated 3SL, 3d)

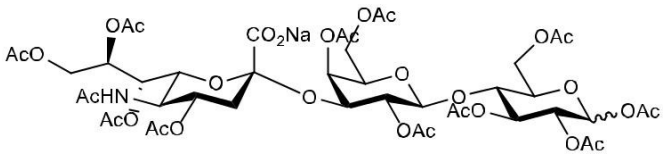

3SL-Na salt **2d** (10.00 g, 15.3 mmol, GeneChem) was suspended in a mixture of pyridine (80 mL) and acetic anhydride (40 mL) and stirred overnight at r.t. followed by stirring at 40°C for 3 days until all dissolved. The obtained reaction mixture was evaporated *in vacuo* and co-evaporated with toluene (4x50 mL) at 50°C/<1 mbar to give 18.73 g of a pale brown foam which was used in the next step directly without further purification. ^{1}H NMR (400 MHz, $CDCl_3$): ca 60:40 mixture of β- and α- anomers.

4,7,8,9-tetra-*O*-acetyl-*N*-acetyl-α-neuraminosyl-(2–3)-2,4,6-tri-*O*-acetyl-β-D-galactopyranosyl-(1–4)-2,3,6-tri-*O*-acetyl-α-D-glucopyranosyl bromide (peracetylated 3SL-bromide, 4d)

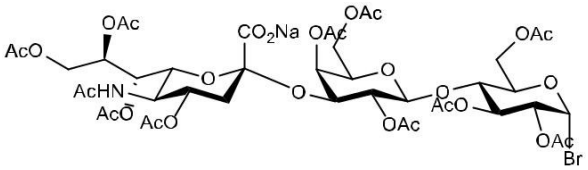

The crude peracetylated 3SL **3d** (ca. 15 mmol) was dissolved in anhydrous CH_2Cl_2 (80 mL) followed by addition of acetic anhydride (6 mL, 63.5 mmol). The obtained mixture was allowed to cool by stirring on an ice bath and followed by addition of 33% (w/w) HBr in acetic acid (30 mL). The ice bath was removed and stirring continued for 2 h at r.t. The obtained solution was cooled again on an ice bath, then it was extracted with ice-cold water (4x100 mL). The combined aqueous phase was re-extracted with CH_2Cl_2 and the obtained organic phase was washed with water (3x50 mL) and brine (50 mL). The combined organic phase was dried (Na_2SO_4) and evaporated *in vacuo* at <20°C to give pale yellow-brown foam (17.37 g, at <1 mbar), which was used in the next step directly.

^{1}H NMR (400 MHz, $CDCl_3$, δ ($CHCl_3$)=7.26 ppm) δ 6.53 (d, *J* = 3.9 Hz, 1H, CH-1 of Glc-Br), 5.66 (t, *J* = 9.7 Hz, 1H), 5.58 (d, *J* = 9.8 Hz, 1H, NH), 5.47 – 5.35 (m, 2H), 5.30 (dd, *J* = 7.2, 2.0 Hz, 1H), 5.08 (ddd, *J* = 7.1, 5.9, 2.9 Hz, 1H), 4.78 (dd, *J* = 9.8, 3.9 Hz, 1H), 4.71 (dd, *J* = 10.6, 7.7 Hz, 1H), 4.64 (d, *J* = 7.7 Hz, 1H), 4.56 – 4.45 (m, 2H), 4.32 (m, 2H), 4.21 – 3.93 (m, 6H), 3.66 (dd, *J* = 10.5, 2.0 Hz, 1H), 2.43 (dd, *J* = 13.5, 5.5 Hz, 1H), 2.21 (s,

3H), 2.13 – 2.04 (m, 21H), 2.00 (s, 3H), 1.88 (s, 3H), 1.85 (dd, *J* = 13.4, 11.1 Hz, 1H).

^{13}C APT NMR (101 MHz, $CDCl_3$, δ ($CDCl_3$)=77.16 ppm) δ 171.03, 170.74, 170.63, 170.56, 170.54, 170.03,

169.74, 169.54, 163.25 (impurity), 98.99 (CH-1 of Gal), 97.11 (C-2 of αDNeuAc 2-3), 86.98 (CH-1 of Glc-N_3),

75.22, 73.72, 73.36, 73.10, 72.91, 71.44, 71.16, 69.82, 69.52, 68.97, 67.29, 66.05, 62.14 (CH_2O), 61.66 (CH_2O),

61.40 (CH_2O), 49.17 (CH-5 of NeuAc), 43.58 (impurity), 37.70 (CH_2-3 of NeuAc), 23.26, 21.00, 20.84, 20.83,

20.80, 20.77, 20.71, 20.57.

4,7,8,9-tetra-*O*-acetyl-*N*-acetyl-α-neuraminosyl-(2–3)-2,4,6-tri-*O*-acetyl-β-D-galactopyranosyl-(1–4)-2,3,6-tri-O-acetyl-β-D-glucopyranosyl azide, Na-salt (peracetylated 3SL-azide, 5d)

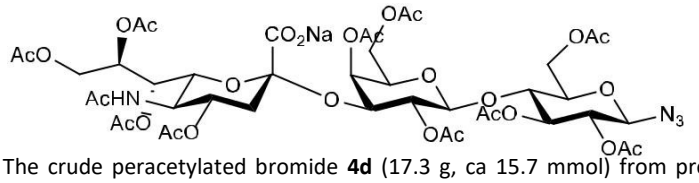

The crude peracetylated bromide **4d** (17.3 g, ca 15.7 mmol) from previous step was dissolved in acetone (100 mL) and allowed to stir on an ice bath. To the obtained cold solution NaN_3 (3.06 g, 47 mmol) in water (20 mL) was added. The cold bath was removed and the stirring continued for 1 h. It was quenched with 80 mL H_2O and most of acetone was removed under reduced pressure at ambient temperature, extracted with EtOAc (100 mL) and washed with brine (3x50 mL). The residual amount of product was re-covered by additional extraction with EtOAc and washing with brine. The combined organic solution was dried (Na_2SO_4) and evaporated in vacuo to give 15.75 g of nearly colorless foam, which was used in the next step directly.

^{1}H NMR (400 MHz, $CDCl_3$, δ ($CHCl_3$)=7.26 ppm) δ 5.65 (d, *J* = 10.2 Hz, 1H, NH), 5.42 (dd, *J* = 3.2, 1.3 Hz, 1H),

5.38 (dt, *J* = 10.9, 5.5 Hz, 1H), 5.26 (dd, *J* = 6.8, 1.9 Hz, 1H), 5.23 (t, *J* = 9.3 Hz, 1H), 5.11 (td, *J* = 6.4, 3.0 Hz,

1H), 4.84 (t, *J* = 9.1 Hz, 1H), 4.73 (dd, *J* = 10.8, 7.7 Hz, 1H), 4.67 (d, *J* = 8.8 Hz, 1H, H-1 of Glc-N_3), 4.56 (d, *J* =

7.9 Hz, 1H, H-1 of Gal), 4.53 (dd, *J* = 12.7, 2.0 Hz, 1H), 4.44 (dd, *J* = 12.4, 4.3 Hz, 1H), 4.24 (dd, *J* = 12.4, 3.0 Hz,

1H), 4.20 – 4.01 (m, 3H, overlapping with EtOAc), 3.97 (dd, *J* = 7.9, 2.9 Hz, 1H), 3.95 – 3.89 (m, 2H), 3.81 (ddd, *J*

10.0, 4.3, 2.2 Hz, 1H), 3.64 (dd, *J* = 10.5, 1.9 Hz, 1H), 2.42 (dd, *J* = 13.5, 5.4 Hz, 1H), 2.11 (s, 3H), 2.09 – 2.00 (m, 27H), 2.00 (s, 3H), 1.87 (s, 3H), 1.84 (dd, *J* = 13.4, 11.1 Hz, 1H), contains ca 1 eq. of EtOAc.

^{13}C NMR (101 MHz, $CDCl_3$, δ ($CDCl_3$)=77.16 ppm) δ 171.01, 170.73, 170.70, 170.54, 170.48, 169.84, 169.79,

169.77, 169.73, 169.59, 163.25 (impurity), 99.93 (CH-1 of Gal), 97.13 (C-2 of αDNeuAc 2-3), 87.75 (CH-1 of Glc-N_3), 76.17, 74.79, 73.71, 73.49, 72.95, 72.35, 71.41, 71.22, 69.72, 69.50, 67.38, 65.94, 62.29 (CH_2O), 62.07 (CH_2O), 61.17 (CH_2O), 60.51 (CH_2O of EtOAc), 49.19 (CH-5 of NeuAc), 37.66 (CH_2-3 of NeuAc), 23.23, 21.16, 21.02, 21.00, 20.85, 20.77, 20.76, 20.74, 20.70, 20.55.

***N*-Acetyl-α-neuraminosyl-(2–3)-β-D-galactopyranosyl-(1–4)-β-D-glucopyranosyl azide, Na-salt (3SL-azide, 6d)**

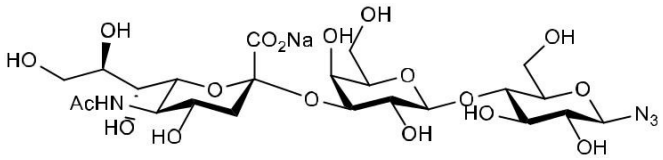

Peracetylated azide **5d** from previous step (15.5 g, ca 15.7 mmol) was dissolved in MeOH (250 mL) followed by addition of MeONa (25% in MeOH, 5.5 mL, 24 mmol) while stirred on an ice bath. After stirring for 22 h at +3°C, extra 2 mL of MeONa solution was added and stirred for extra 19 hrs. TLC indicated the presence of intermediates. It was concentrated under reduced pressure at 0°C with the removal of ca. 150 mL MeOH and MeOAc followed by addition of water (100 mL, pH=13). TLC after 30 min at 0°C indicated a full conversion. It was neutralized with Amberlite IR-120 (H^+ form, 20 g, pH=3), filtered, concentrated under reduced pressure at 0°C to a small volume, then pH was adjusted to 7.0 with 1 M NaOH (12 mL). The obtained solution was freeze-dried to give 9.57 g of very pale yellow solid. TLC Rf=0.46 (SiO_2, eluent 5:4:1:0.1 EtOAc-MeOH-H_2O-AcOH) indicated ca 90% purity with ca 5% 3SL (Rf=0.25) and unidentified impurity (Rf=0.31). The solid was dissolved in MeOH (40 mL) and precipitated with 200 mL iPrOH, stirred for 1 h, filtered, washed with iPrOH, acetone, hexane, dried in vacuo (<1 mbar, r.t.) to give 9.86 g of white solid. NMR indicated ca 95% purity containing ca. 2% 3SL and residual solvents.

^{1}H NMR (400 MHz, D_2O, δ DHO=4.79) δ 4.78 (d, overlapping with DHO, 1H, H-1 of Glc-N_3), 4.54 (d, *J* = 7.9 Hz, 1H, H-1 of Gal), 4.12 (dd, *J* = 9.9, 3.2 Hz, 1H), 4.06 – 3.53 (m, 17H), 3.32 (t, *J* = 8.9 Hz, 1H, H-2 of Gal), 2.77 (dd, *J* = 12.5, 4.6 Hz, 1H), 2.04 (s, 3H), 1.81 (t, *J* = 12.1 Hz, 1H).

^{13}C APT NMR (101 MHz, D_2O) δ 175.00, 173.87, 102.60 (CH-1 of Gal), 99.79 (C-2 of αDNeuAc 2-3), 89.95 (CH-1 of Glc-N_3), 77.56, 76.70, 75.47, 75.18, 74.31, 72.88, 72.52, 71.77, 69.35, 68.34, 68.09, 67.46, 62.58 (CH_2OH of NeuAc), 61.04 (CH_2OH), 59.82 (CH_2OH), 51.68 (CH-5 of NeuAc), 39.64 (CH_2-3 of NeuAc), 22.05 (Ac of NeuAc).

***N*-Acetyl-α-neuraminosyl-(2–3)-β-D-galactopyranosyl-(1–6)-β-D-glucopyrano[2,3-*d*]oxazolidin-2-one, Na-salt (cyclic-carbamate of 3SL, 1d)**

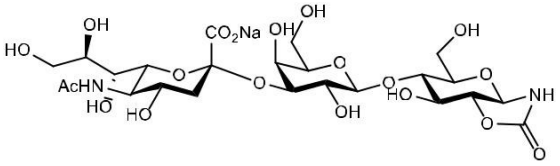

3SL-azide **6d**, Na-salt (9.86g, 14.5 mmol) was dissolved in 600 mL DMF (anhydrous) and dehydrated by co-evaporation with toluene (100 mL, gelly suspension after addition) at 25°C to 3 mbar. The obtained solution was saturated with CO_2 by passing the gas through the solution via cannula connected to a round bottom flask filled with excess of dry ice. Solution of Ph_3P (7.63 g, 29.0 mmol, 2.0 eq.) in anhydrous DMF (20 mL) was dehydrated by co-evaporation with toluene (10 mL) as above and added dropwise with stirring under constant flow of CO_2 in 30 min. After addition was completed, the mixture was allowed to stir under flow of CO_2 for 2.5 hrs. TLC (5:4:1:0.1 EtOAc-MeOH-H_2O-AcOH) indicated no difference after 40 min and 2 h, since the product had the same Rf as starting azide. It was poured slowly into vigorously stirred 1:1 acetone-hexane mixture (1 L). After 30 min it was filtered, washed with acetone, hexane (3x), dried in vacuo (<1 mbar, r.t., o.n.) to give 9.62 g of white solid. NMR indicated >95% purity with ca 30 mol% residual DMF and traces of Ph_3P/Ph_3PO (ca 1 mol%

only), traces of hexane and acetone. ^{1}H and ^{13}C NMR of the same sample in D_2O was re-measured after 3 days and 11 days indicating ca 30% and 80% hydrolysis, respectively. NMR sample in CD_3OD was decomposing much faster: by 80% after ca 5 hrs.

^{1}H NMR (400 MHz, D_2O, δ DHO=4.79) δ 5.06 (d, *J* = 9.0 Hz, 1H, H-1 of Glc-CC), 4.54 (d, *J* = 7.8 Hz, 1H, H-1 of Gal), 4.22 (dd, *J* = 11.0, 7.1 Hz, 1H), 4.14 (dd, *J* = 9.8, 3.2 Hz, 1H), 4.05 – 3.52 (m, 17H), 2.77 (dd, *J* = 12.4, 4.7 Hz, 1H, H-3''$_{eq.}$), 2.04 (s, 3H), 1.81 (t, *J* = 12.1 Hz, 1H, H-3''$_{ax}$).

^{13}C NMR (101 MHz, D_2O) δ 175.00 (Ac of NeuAc), 173.86 (CO_2^-), 159.99 (OCONH), 103.10 (CH-1 of Gal), 99.81 (C-2 of αDNeuAc 2-3), 84.82 (CH-1 of Glc-CC), 80.98, 80.50, 79.26, 75.38, 75.22, 72.87, 71.80, 71.76, 69.24, 68.35, 68.08, 67.32, 62.57 (CH_2OH of NeuAc), 60.87 (CH_2OH), 59.89 (CH_2OH), 51.68 (CH-5 of NeuAc), 39.62 (CH_2-3 of NeuAc), 22.05 (Ac of NeuAc).

HRMS (ESI(-), done at U. of Zurich): *m/z* calc. for $[C_{24}H_{37}O_{19}N_2]^-$ ([M-H]$^-$) 657.19960, found 657.20024.

4,7,8,9-tetra-*O*-acetyl-*N*-acetyl-α-neuraminosyl-(2–6)-2,3,4-tri-*O*-acetyl-β-D-galactopyranosyl-(1–4)-2,3,6-tri-O-acetyl-α-D-glucopyranosyl bromide (peracetylated 6SL-bromide, 4e)

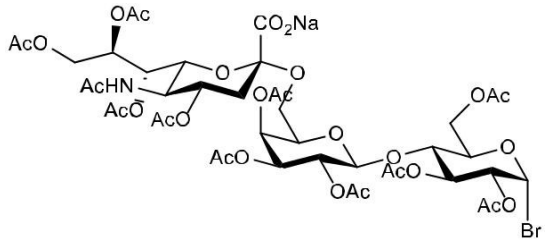

15 g and then 30 g of 6SL-Na salt was converted into 20.8 g and 50.32g, respectively, of bromide **4e** as nearly colorless solid.

^{1}H NMR (400 MHz, $CDCl_3$, δ ($CHCl_3$)=7.26 ppm) δ 6.55 (d, *J* = 4.0 Hz, 1H, H-1 of Glc-Br), 5.98 (d, *J* = 9.8 Hz, 1H, NH), 5.52 (t, *J* = 9.7 Hz, 1H, H-3 of Glc), 5.38 (d, *J* = 3.4 Hz, 1H), 5.33 – 5.25 (m, 2H), 5.11 (dd, *J* = 10.3, 7.9 Hz, 1H), 5.05 – 4.94 (m, 2H), 4.77 (dd, *J* = 10.0, 4.1 Hz, 1H, H-2 of Glc), 4.54 (d, *J* = 7.9 Hz, 1H, H-1 of Gal), 4.52 – 4.45 (m, 1H, CH_2O), 4.29 (dd, *J* = 11.8, 1.7 Hz, 1H, CH_2O), 4.25 – 4.17 (m, 2H), 4.14 (dd, *J* = 10.8, 1.6 Hz, 1H),

4.09 – 3.97 (m, 2H), 3.95 – 3.82 (m, 3H), 3.50 (td, *J* = 9.6, 6.0 Hz, 1H, CH_2O), 2.55 (dd, *J* = 12.8, 4.7 Hz, 1H),

2.17 (s, 3H), 2.15 (s, 3H), 2.12 (s, 3H), 2.10 (s, 3H), 2.09 (s, 3H), 2.05 (s, 3H), 2.05 (s, 3H), 2.03 (s, 3H), 2.02 (s,

3H), 1.95 (s, 3H), 1.89 (overlapping s, 3H), 1.85 (overlapping t, *J* = 12.5 Hz, 1H). ^{13}C NMR (101 MHz, $CDCl_3$, δ ($CDCl_3$)=77.16 ppm) δ 171.44, 171.19, 171.05, 170.90, 170.45, 170.37, 170.20, 170.14, 169.93, 169.90, 169.40, 169.20, 101.08 (CH-1 of Gal), 98.71 (C-2 of αDNeuAc 2-6), 86.62 (CH-1 of Glc-Br), 75.33, 73.29, 72.71, 72.19, 71.33, 70.94, 69.87, 69.27, 69.21, 68.47, 67.43, 67.39, 62.88 (CH_2O), 62.70 (CH_2O), 61.28 (CH_2O), 37.69 (CH_2-3 of NeuAc), 23.09, 21.09, 21.06, 21.04, 20.93, 20.91, 20.86 (three overlapping Ac), 20.80, 20.67.

4,7,8,9-tetra-*O*-acetyl-*N*-acetyl-α-neuraminosyl-(2–6)-2,3,4-tri-*O*-acetyl-β-D-galactopyranosyl-(1–4)-2,3,6-tri-O-acetyl-β-D-glucopyranosyl azide, Na-salt (peracetylated 6SL-azide, 5e)

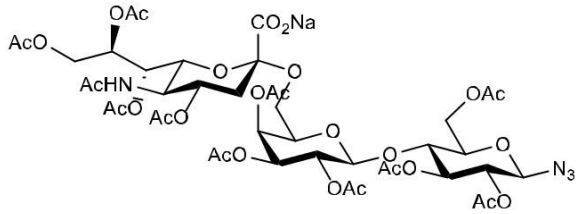

50.2 g of crude bromide **4e** was converted into crude azide **5e** (50.5 g).

^{1}H NMR (400 MHz, $CDCl_3$, δ ($CHCl_3$)=7.26 ppm) δ 6.01 (d, *J* = 9.8 Hz, 1H, NH), 5.39 (dd, *J* = 3.4, 1.1 Hz, 1H),

5.35 – 5.25 (m, 2H), 5.19 (t, *J* = 9.4 Hz, 1H), 5.07 (dd, *J* = 10.3, 7.7 Hz, 1H), 5.04 – 4.94 (m, 2H), 4.86 (dd, *J* =

9.6, 8.8 Hz, 1H), 4.62 (d, *J* = 8.8 Hz, 1H, H-1 of Glc-N_3), 4.55 (d, *J* = 7.8 Hz, 1H, H-1 of Gal), 4.50 (dd, 1H, *J* =

11.9, 1.9 Hz, CH_2-O), 4.31 (dd, *J* = 12.3, 2.2 Hz, 1H), 4.20 – 3.96 (m, 4H), 3.93 – 3.85 (m, 2H), 3.81 (dd, *J* = 10.4,

6.1 Hz, 1H, CH_2O), 3.73 (ddd, *J* = 10.0, 5.7, 2.0 Hz, 1H), 3.51 (dd, *J* = 10.4, 7.2 Hz, 1H, CH_2O), 2.55 (dd, *J* =

12.8, 4.7 Hz, 1H), 2.17 (s, 3H), 2.15 (s, 3H), 2.11 (s, 4H), 2.06 (s, 7H), 2.05 (s, 3H), 2.04 (s, 3H), 2.031 (s, 3H),

2.027 (s, 3H), 1.94 (s, 3H), 1.89 (s, 3H), 1.86 (t, overlapping, *J* = 12.5 Hz, 1H).

^{13}C NMR (101 MHz, $CDCl_3$, δ ($CDCl_3$)=77.16 ppm) δ 171.44, 171.13, 171.01, 170.97, 170.61, 170.53, 170.16, 170.12 (two Ac), 169.67, 169.37, 169.34, 100.82 (CH-1 of Gal), 98.81 (C-2 of αDNeuAc 2-6), 87.80 (CH-1 of Glc-N_3), 75.83, 75.14, 72.73, 72.39, 72.07, 71.26, 71.12, 69.34, 69.17, 68.61, 67.43, 67.34, 62.77 (CH_2O), 62.67 (CH_2O), 62.12 (CH_2O), 49.22 (CH-5 of NeuAc), 37.63 (CH_2-3 of NeuAc), 23.08, 21.08 (two Ac), 20.92 (three Ac), 20.86, 20.85, 20.77, 20.74, 20.66.

***N*-Acetyl-α-neuraminosyl-(2–6)-β-D-galactopyranosyl-(1–4)-β-D-glucopyranosyl azide, Na-salt (6SL-azide, 6e)**

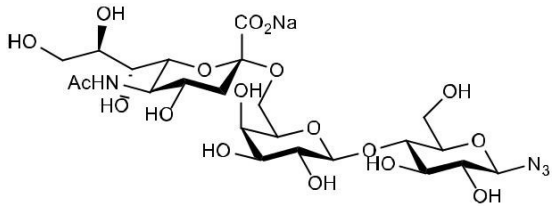

50.5 g of peracetylated azide **5e** was converted into 27.3 g of azide **6e**.

^{1}H NMR (400 MHz, D_2O, δ DHO=4.79) δ 4.77 (d, 1H, overlapping with DHO, H-1 of Glc-N_3), 4.44 (d, *J* = 7.8 Hz,

1H, H-1 of Gal), 4.08 – 3.77 (m, 7H), 3.77 – 3.48 (m, 11H), 3.36 (m, 1H), 2.72 (dd, *J* = 12.4, 4.7 Hz, 1H, H-3''$_{eq}$),

2.04 (s, 3H), 1.74 (t, *J* = 12.2 Hz, 1H, H-3''$_{ax}$).

^{13}C NMR (101 MHz, D_2O) δ 174.89, 173.46, 103.16 (CH-1 of Gal), 100.26 (C-2 of αDNeuAc 2-3), 89.75 (CH-1 of Glc-N_3), 78.98, 76.54, 74.57, 73.71, 72.51, 72.45, 72.34, 71.81, 70.76, 68.51, 68.38 (two overlapping CH-OH), 63.60 (CH_2OH), 62.64 (CH_2OH), 60.02 (CH_2OH), 51.78 (CH-5 of NeuAc), 40.10 (CH_2-3 of NeuAc), 22.07 (Ac of NeuAc).

***N*-Acetyl-α-neuraminosyl-(2–6)-β-D-galactopyranosyl-(1–6)-β-D-glucopyrano[2,3-*d*]oxazolidin-2-one, Na-salt (cyclic-carbamate of 6SL, 1e)**

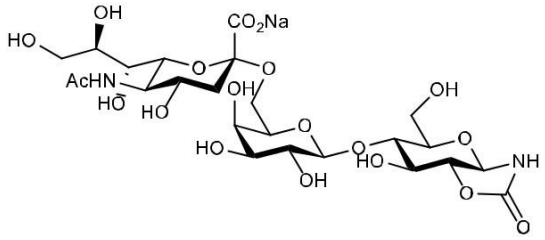

5.00 g of azide **6e** was converted into crude cyclic-carbamate **1e** (5.22 g), contaminated with ca. 10% 6SL.

^{1}H NMR (400 MHz, D_2O, δ DHO=4.79) δ 5.06 (d, *J* = 9.0 Hz, 1H, H-1 of Glc-CC), 4.44 (d, *J* = 7.8 Hz, 1H, H-1 of Gal, 4.29 (dd, *J* = 11.0, 7.1 Hz, 1H), 4.13 – 3.78 (m, 10H), 3.49-3.78 (m, 8H), 2.72 (dd, *J* = 12.4, 4.8 Hz, 1H, H-3''$_{eq}$), 2.04 (s, 3H), 1.74 (t, *J* = 12.2 Hz, 1H, H-3''$_{ax}$).

^{13}C NMR (101 MHz, D_2O) δ 174.96 (Ac of NeuAc), 173.41 (CO_2^-), 159.91 (OCONH), 103.49 (CH-1 of Gal), 100.20 (C-2 of αDNeuAc 2-6), 84.68 (CH-1 of Glc-CC), 81.64, 80.88, 79.12, 73.76, 72.58, 72.25, 71.87, 71.67, 70.61, 68.40 (two overlapping CH-OH), 68.19, 63.75 (CH_2OH), 62.62 (CH_2OH), 60.05 (CH_2OH), 51.79 (CH-5 of NeuAc), 40.16 (CH_2-3 of NeuAc), 21.99 (Ac of NeuAc).

HRMS (ESI(-)) *m/z* calc for $C_{24}H_{37}N_2O_{19}$ ($[M-H]^-$) 657.1996, found 657.2003

2,3,4-tri-*O*-acetyl-α-L-fucopyranosyl-(1–3)-[2,3,4,6-tetra-*O*-acetyl-β-D-galactopyranosyl-(1–4)]-β-D-glucopyranosyl bromide (peracetylated 3FL-bromide, 4c)

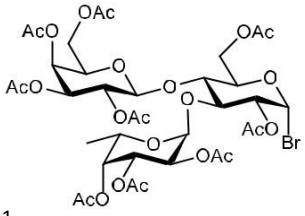

^{1}H NMR (400 MHz, $CDCl_3$, δ ($CHCl_3$)=7.26 ppm): δ 6.47 (d, *J* = 4.1 Hz, 1H, H-1 of Glc-Br), 5.46 (d, *J* = 4.0 Hz, 1H, H-1 of Fuc), 5.42 (dd, *J* = 3.6, 1.1 Hz, 1H), 5.38 (dd, *J* = 3.4, 1.2 Hz, 1H), 5.18 (dd, *J* = 10.9, 3.3 Hz, 1H), 5.11 (dd, *J* = 10.4, 8.1 Hz, 1H), 5.04 (dd, *J* = 10.9, 4.0 Hz, 1H), 4.98 (dd, *J* = 10.4, 3.5 Hz, 1H), 4.91 (q, *J* = 6.6 Hz, 1H), 4.76 (dd, *J* = 9.6, 4.1 Hz, 1H), 4.60 (dd, *J* = 12.6, 1.9 Hz, 1H), 4.55 (dd, *J* = 11.4, 6.1 Hz, 1H), 4.50 (d, *J* = 8.1 Hz, 1H, H-1 of Gal), 4.29 (dd, *J* = 11.5, 8.1 Hz, 1H), 4.20 (t, *J* =

9.4 Hz, 1H), 4.13 (dd, *J* = 12.6, 3.6 Hz, 1H), 4.04 (ddd, *J* = 10.1, 3.6, 1.9 Hz, 1H), 3.96 (dd, *J* = 10.1, 9.1 Hz, 1H), 3.86 (ddd, *J* = 8.3, 6.0, 1.1 Hz, 1H), 2.19 (s, 3H), 2.15 (s, 3H), 2.15 (s, 3H), 2.10 (s, 3H), 2.08 (s, 3H), 2.07 (s, 3H), 1.99 (s, 3H), 1.97 (s, 3H), 1.96 (s, 3H), 1.25 (d, *J* = 6.5 Hz, 3H, Me of Fuc).

^{13}C APT NMR (101 MHz, $CDCl_3$, δ ($CDCl_3$)=77.16 ppm) δ 170.91, 170.70, 170.67, 170.50, 170.21, 170.14 (overlapping two Ac), 169.97, 169.11, 100.66 (CH-1 of Gal), 95.61 (CH-1 of Fuc), 87.35 (CH-1 of Glc-Br), 73.69, 73.49, 72.83, 71.89, 71.39, 71.17, 71.10, 68.95, 68.29, 68.17, 66.67, 64.38, 60.79 (CH_2OH), 60.63 (CH_2OH),

20.91 (overlapping three Ac), 20.87, 20.81, 20.78, 20.75, 20.74, 20.65, 15.93 (Me of Fuc).

2,3,4-tri-*O*-acetyl-α-L-**fucopyranosyl-(1–3)-[2,3,4,6-tetra-*O*-acetyl-**β-D-**galactopyranosyl-(1–4)]-**β-D-**glucopyranosyl azide (peracetylated 3FL-azide, 5c)**

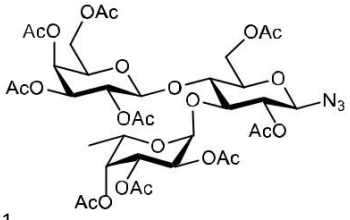

^{1}H NMR (400 MHz, $CDCl_3$, δ ($CHCl_3$)=7.26 ppm): δ 5.41 (dd, *J* = 3.5, 1.0 Hz, 1H), 5.38 (dd, *J* = 3.4, 1.2 Hz, 1H), 5.32 (d, *J* = 4.0 Hz, 1H, H-1 of Fuc), 5.16 (dd, *J* = 10.9, 3.3 Hz, 1H), 5.12 – 4.89 (m, 5H), 4.65 (dd, *J* = 12.4, 2.1 Hz, 1H), 4.53 (dd, *J* = 11.4, 6.1 Hz, 1H), 4.47 (d, *J* = 8.1 Hz, 1H, H-1 of Gal), 4.33 (d, *J* = 8.9 Hz, 1H, H-1 of Glc-N_3), 4.30 (dd, *J* = 11.5, 8.0 Hz, 1H), 4.09 (dd, *J* = 12.3, 4.4 Hz, 1H), 3.99 – 3.83 (m, 3H), 3.55 (dp, *J* = 6.5, 2.9, 2.0 Hz, 1H), 2.19 (s, 3H), 2.15 (s, 3H), 2.14 (s, 3H), 2.08 (s, 3H), 2.07 (s, 3H), 2.05 (s, 3H), 2.05 (s, 3H), 1.97 (s, 3H), 1.95 (s, 3H), 1.23 (d, *J* = 6.5 Hz, 3H).

^{13}C APT NMR (101 MHz, $CDCl_3$, δ ($CDCl_3$)=77.16 ppm): δ 171.27, 170.85, 170.68, 170.51, 170.29, 170.07, 169.90, 169.70, and 169.09 (nine Ac), 100.81 (CH-1 of Gal), 95.70 (CH-1 of Fuc), 87.99 (CH-1 of Glc-N_3), 75.50, 74.17, 73.85, 72.99, 71.40, 71.22, 71.02, 69.00, 68.05, 67.95, 66.68, 64.42, 61.32 (CH_2O), 60.68 (CH_2O), 20.98 (Ac), 20.91 (two Ac), 20.89 (Ac), 20.85 (Ac), 20.77 (Ac), 20.72 (two Ac), 20.64 (Ac), 15.90 (Me of Fuc).

α-L-**Fucopyranosyl-(1–3)-[**β-D-**galactopyranosyl-(1–4)]-**β-D-**glucopyranosyl azide (3FL-azide, 6c)**

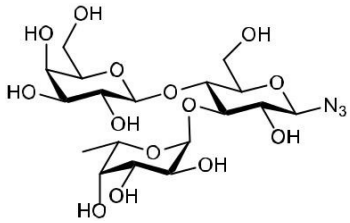

^{1}H NMR (400 MHz, D_2O, δ DHO=4.79) δ 5.44 (d, *J* = 4.0 Hz, 1H, H-1 of Fuc), 4.82 (q, *J* = 6.9 Hz, overlapping with DHO, 1H, H-5 of Fuc), 4.76 (d, *J* = 8.8 Hz, overlapping with DHO, 1H, H-1 of Glc-N_3), 4.44 (d, *J* = 7.7 Hz, 1H, H-1 of Gal), 4.05 – 3.62 (m, 12H), 3.59 (dd, *J* = 7.8, 4.4 Hz, 1H), 3.52 (t, *J* = 9.0 Hz, 1H), 3.50 (dt, *J* = 13.3, 9.4 Hz, 2H), 3.48 (dd, *J* = 9.9, 7.7 Hz, 1H), 1.19 (d, *J* = 6.8 Hz, 3H).

^{13}C APT NMR (101 MHz, D_2O) δ 101.74 (CH-1 of Gal), 98.39 (CH-1 of Fuc), 90.00 (CH-1 of Glc-N_3), 77.26, 76.83, 74.92, 74.19, 72.39, 72.21, 71.92, 71.10, 69.18, 68.29, 68.00, 66.50 (CH-5 of Fuc), 61.46 (CH_2OH), 59.53 (CH_2OH), 15.20 (CH_3 of Fuc).

α-L-**Fucopyranosyl-(1–3)-**[β-D-**galactopyranosyl-(1–6)]-**β-D-**glucopyrano[2,3-*d*]oxazolidin-2-one (cyclic-carbamate of 3FL, 1c)**

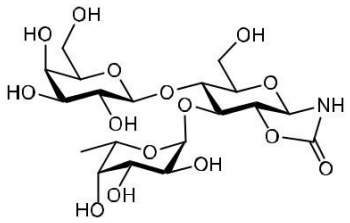

^{1}H NMR (400 MHz, D_2O, δ DHO=4.79) δ 5.14 (d, *J* = 3.9 Hz, 1H, H-1 of Fuc), 5.06 (d, *J* = 9.0 Hz, 1H, H-1 of Glc-CC), 4.67 (q, *J* = 6.7 Hz, 1H, H-5 of Fuc), 4.44 (d, *J* = 7.7 Hz, 1H, H-1 of Gal), 4.28 (dd, *J* = 10.8, 8.0 Hz, 1H), 4.12 (t, *J* = 8.7 Hz, 1H), 4.09 – 3.95 (m, 3H), 3.95 – 3.70 (m, 7H), 3.64 (ddd (two dd), *J* = 19.0, 8.7, 4.1 Hz, 2H),

3.48 (dd, *J* = 9.9, 7.6 Hz, 1H, H-2'), 1.22 (d, *J* = 6.6 Hz, 3H, CH_3).

^{13}C APT NMR (101 MHz, D_2O) δ 159.96 (OCONH), 101.97 (CH-1 of Gal), 97.19 (CH-1 of Fuc), 84.91 (CH-1 of Glc-CC), 81.76, 79.89, 75.04, 74.21, 73.43, 72.38, 71.84, 71.31, 69.19, 68.19, 67.78, 66.77 (CH-5 of Fuc), 61.22 (CH_2OH), 59.62 (CH_2OH), 15.08 (CH_3 of Fuc).

HRMS (ESI(+), done at U. of Zurich): *m/z* calc. for $[C_{19}H_{31}O_{15}NNa]^+$ ($[M+Na]^+$) 536.1586, found 536.1587.

***N*-Acetyl-α-neuraminosyl-(2–3)-β-D-galactopyranosyl-(1–4)-[α-L-fucopyranosyl-(1–3)]-β-D-glucopyranosyl azide (FSL-azide, 6f)**

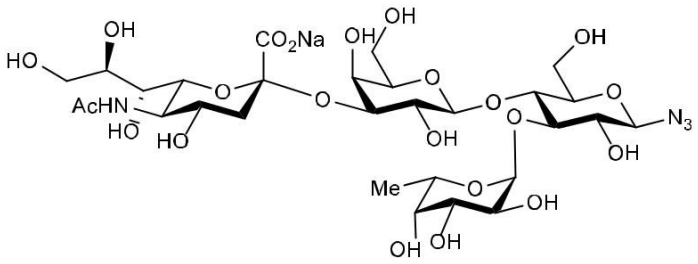

3FL-azide **6c** (1.00 g), 3SL **2d** (1.20 g, Genentech) and trans-sialidase from *Trypanosoma cruzi* (TcTS, 20.5 mg, c-Lecta, 11301-2, ca 61 U/g) were stirred in water (5 mL) at r.t. and pH=6.0 for 24 h and monitored by TLC (6:3:1 MeCN-H_2O-25% aq.NH_3). Ca. 40% conversion was observed with only lactose formed as the side product. The reaction mixture was quenched with methanol and absorbed on silica gel (5.0 g) after evaporation in vacuo. The resulting solid was chromatographed on silica gel (50 g, 0.040-0.063 mm particle size) with 75:15:10 MeCN-H_2O-25% aq. NH_3 (100 mL) then 70:20:10 MeCN-H_2O-25% aq. NH_3 (300 mL) mixture as eluents. The purest fractions were evaporated and freeze-dried to give 24 mg of product, which was used as analytical sample. The remaining fractions containing product together with unreacted 3SL and 3FL-azide were evaporated, re-dissolved in 3 mL H_2O and passed through Dowex 1x4 resin (HCO_3^- form) and eluted with water to give unreacted 3FL-N_3 (452 g). The product was eluted together with 3SL with 60 mM $NaHCO_3$, fractions were combined, acidified with Amberlite IR120 (H^+ form, pH=3), then filtered and the pH was adjusted to 6.0 with 1 M NaOH, followed by freeze-drying to give 504 mg of product contaminated with ca. 30% 3SL.

^{1}H NMR (400 MHz, D_2O, δ DHO=4.79) δ 5.43 (d, *J* = 4.0 Hz, 1H, H-1 of αFuc), 4.76 (d, overlapping with DHO, *J* = 10.6 Hz, 1H, H-1 of $GlcN_3$), 4.50 (d, *J* = 7.8 Hz, 1H, H-1 of Gal), 4.08 (dd, *J* = 9.9, 3.2 Hz, 1H), 4.01 (dd, *J* = 12.5, 2.2 Hz, 1H), 3.97 – 3.45 (m, 20H), 2.76 (dd, *J* = 12.5, 4.6 Hz, 1H, H-3_{eq} of NeuAc), 2.03 (s, 3H), 1.80 (t, *J* = 12.1 Hz, 1H, H-3_{ax} of NeuAc), 1.18 (d, *J* = 6.6 Hz, 3H, Me of Fuc).

^{13}C NMR (101 MHz, D_2O) δ 174.97, 173.84, 101.53 (CH-1 of Gal), 99.61 (C-2 of NeuAc), 98.36 (CH-1 of Fuc),

90.00 (CH-1 of Glc-N_3), 77.17, 76.71, 75.56, 74.90, 74.22, 72.85, 72.18, 71.91, 71.82, 69.34, 69.15, 68.27, 68.06,

67.99, 67.23, 66.46, 62.54 (CH_2OH), 61.44 (CH_2OH), 59.42 (CH_2OH), 51.65 (CH-5 of NeuAc), 39.73 (CH_2-3 of NeuAc), 22.00 (Me of Ac), 15.16 (Me of Fuc).

***N*-Acetyl-α-neuraminosyl-(2–3)-β-D-galactopyranosyl-(1–6)-[α-L-fucopyranosyl-(1–7)]-β-D-glucopyrano[2,3-*d*]oxazolidin-2-one, Na-salt (cyclic-carbamate of FSL, 1f)**

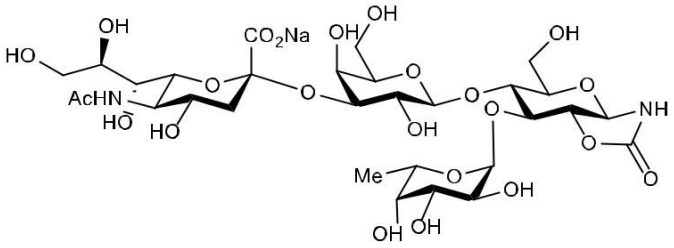

Crude FSL-azide **6f** (480 mg, contaminated with ca 30% 3SL) was dissolved in DMF (5 mL) and dehydrated by co-evaporation with toluene (2x2 mL, 40°C, P=10 mbar). It was saturated with CO_2 generated from dry ice followed by addition of Ph_3P (457 mg, 1.74 mmol, 3 eq.) in DMF (1.5 mL) at +10°C. The cold bath removed and stirring continued for 2 h under CO_2 atmosphere. The obtained solution was added dropwise into stirred acetone-hexane mixture (80 mL, 1:1), filtered, dried in vacuo at r.t. to give 496 mg of white hydroscopic solid contaminated with ca. 30% 3SL.

^{1}H NMR (400 MHz, D_2O, δ DHO=4.79), selected resonances: δ 5.12 (d, *J* = 3.8 Hz, 1H, H-1 of αFuc), 5.06 (d, *J* = 9.0 Hz, 1H, H-1 of Glc-CC), 2.77 (dd, *J* = 12.5, 4.6 Hz, 1H, H-3_{eq} of NeuAc), 1.80 (t, *J* = 12.1 Hz, 1H, H-3_{ax} of NeuAc), 1.21 (d, *J* = 6.6 Hz, 3H, Me of Fuc).

^{13}C NMR (101 MHz, D_2O) δ 174.99, 173.84, 159.97 (OCONH), 101.72 (CH-1 of Gal), 99.70 (C-2 of NeuAc), 97.19 (CH-1 of Fuc), 84.93 (CH-1 of Glc-CC), 81.75, 79.84, 75.56, 75.00, 74.19, 73.32, 72.87, 71.82 (two overlapping CH), 69.63, 69.17, 68.29, 68.06, 67.78, 67.15, 66.77, 62.55 (CH_2O), 61.23 (CH_2O), 59.58 (CH_2O), 51.66 (CH-5 of NeuAc), 39.70 (CH_2-3 of NeuAc), 22.02, 15.05.

HRMS (ESI (-)) *m/z* calc. for $C_{30}H_{47}N_2O_{23}$ ($[M-H]^-$) 803.2575, found 803.2551

Surface Sialylation Mediated Programmed Cell Death

Marek W. J. Whitehead[1], Thierry Hennet[1,*]

[1]Institute of Physiology, University of Zurich, Winterthurerstrasse 190, 8057 Zurich, Switzerland

[*]Lead contact

(Manuscript in preparation)

Abstract

Cells that are undergoing programmed cell death are characterized by changes in their surface glycosylation. Often it is unclear whether these changes are a cause or consequence of programmed cell death. Therefore, we coated cells with oligosaccharides using the cyclic-carbamate method and were able to demonstrate that sialyllactose coating induces rapid, caspase-dependent programmed cell death. We performed a CRISPR-Cas9 screen using the murine GeCKO v2 gRNA library to identify the genetic components of this novel form of programmed cell death. The screen revealed the involvement of the three G-protein coupled receptors free fatty acid receptor 4, the olfactory receptor 1537, the olfactory receptor 310 and the downstream signaling protein adenylate cyclase 7. Sialyllactose-coating led to increased concentrations of the secondary messenger calcium and rapid degradation of microtubules and actin. Here we have demonstrated for the first time a fast and novel form of cell surface sialylation mediated cell death. The speed of cell death and the possibility to inhibit cell death with pertussis toxin as well as the results of our screen indicates that G-protein coupled receptor signaling plays a key role in sialyllactose-coating induced cell death.

Introduction

There are different types of programmed cell death such as apoptosis, pyroptosis and necroptosis as examples of the more well-known types. During programmed forms of cell death the cell initiates a defined process leading to its demise. The outcome is defined such as pyroptosis and necroptosis that lead to an inflammatory response and apoptosis on the other hand which avoids inflammatory responses [1].

Glycans are highly enriched on the cell surface and they mediate many cellular processes such as leukocyte extravasation by the sialyl-Lewis X epitope [2] and the dampening of immune reactions by sialylated glycans [3, 4]. Each cell type has a unique repertoire of glycans and the decoding of the information that every cell has on its surface occurs via lectins that also occur at cell surfaces [5, 6]. The interest in the roles that glycans play during cell death arose due to studies that were conducted

in the 1980s when lectins were constitutively expressed on macrophages and these macrophages were able to selectively recognize apoptotic thymocytes [7]. This indicates that dying cells have a specific surface glycosylation pattern. Through different mechanisms therefore lectin-glycan interactions at the cell surface may regulate or even initiate cell death [8]. Glycosylation of the death receptor CD95 and the tumor necrosis factor-related apoptosis-inducing ligand receptors (TRAIL-R1 and TRAIL-R2) for instance can influence their signaling by enhancing or sterically inhibiting the access of the receptors to their ligands Fas ligand and TNF respectively. Fucosylated core-2 O-glycans for instance on TRAIL-R1 and TRAIL-R2 enhance TRAIL-induced apoptosis [9]. Sialylation on the other hand often protects the cell from cell death receptor-mediated apoptosis. The sialylation of N-linked glycans on Fas ligand reduces the sensitivity of B-cell lymphomas to Fas ligand-induced cell death [10, 11]. TNFR1, a receptor that can also induce cell death in macrophages, has an increased sensitivity towards TNF and the Fas ligand when it lacks α2-6-linked sialic acid and as a consequence induces more cell death [12].

Galectins, a family of soluble lectins that preferentially bind to β-galactoside sugars, frequently play a key role in the initiation of cell death. Galectin-1 binding to the surface of T cells is known to initiate apoptosis and play an important role in the negative selection of self-antigen recognizing T cells [5, 13]. The clustering of CD45, CD3 and CD7 with the mucin-like protein sialophorin at the cell surface has been shown to be involved during galectin-1 mediated cell death [14].

To discover new roles that glycans fulfill during programmed cell death, we coated cells with oligosaccharide-cyclic-carbamates as previously described [15]. Interestingly, coating cells with sialyllactose-cyclic-carbamates induced rapid programmed cell death. Sialylation in relation to galectin and death-receptor mediated cell death has previously only been associated with a protective function [12, 16-18]. However, we describe a novel role of sialic acid containing surface glycans as drivers of a previously unknown from of programmed cell death.

Materials and Methods

Cell culture

MC-38, RAW264.7, L929, HEK293T and HT-29 cells were cultured in Dulbecco's Modified Eagle's Medium supplemented with 10% FCS. THP-1 and Jurkat cells were cultured in RPMI-1640 medium supplemented with 10% FCS.

Oligosaccharide cyclic-carbamates

Lactose- [Gal(β1-4)Glc], 3SL- [Sia(α2-3)Gal(β1-4)Glc] and 6SL- [Sia(α2-6)Gal(β1-4)Glc] cyclic-carbamates were provided by Glycom A/S.

Cell coating with oligosaccharide-cyclic-carbamates

The cell coating procedure was performed as has been previously described [15]. Briefly, the cells were detached from the culture dish with 2 mM EDTA in PBS for 10 min. The cells were washed once and resuspended at 400'000 cells/ml in Hank's balanced saline solution (HBSS). Next, the cells were coated with 8 mM of the respective oligosaccharide-cyclic-carbamate for 10 min, unless otherwise specified. Before further processing the cells were washed 2 times with HBSS.

Quantification of cell death

The cells were stained with 200 ng/ml of propidium iodide for 5 min at 20°C before determining the relative amount of propidium iodide positive cells by flow cytometry with a FACScanto II (Becton Dickinson). Propidium iodide positive cells were considered to be dead. Jurkat cells were stained with 20 µg/ml of 7-Aminoactinomycin D. The analysis was performed by flow cytometry with a FACScanto II (Becton Dickinson). 7-Aminoactinomycin D positive cells were considered not to be viable.

6-sialyllactose-cyclic-carbamate coupling to 3-sn-phosphatidylethanolamine and purification

3-sn-phsopatidylethanolamine (Sigma-Aldrich) was homogenized by sonication for 15 min with a bath sonicator in borate buffered saline, pH 10. A 5 fold molar excess of 6SL-cyclic-carbamate was added to the 3-sn-phsophatidylethanolamine and the reaction mix was incubated at 20°C for 4 h rotating. Afterwards the reaction mix was applied to a DC Kieselgel 60 thin-layer chromatography (TLC) membrane and detection of the educts and products was done by staining with p-anisaldehyde. The product (6SL-3-sn-phosphatidylethanolamine) was separated from the educts with a mobile phase consisting of chloroform:methanol:water (65:25:4). The product (Fig. 3A; arrow) was scraped off the TLC plate and extracted with chloroform:methanol (2:1). Next, the chloroform:methanol was evaporated and phosphate buffered saline (PBS) was used to make a 6SL-3-sn-phosphatidylethanolamine homogenate. The phenol-sulfuric acid assay was performed to determine the amount of purified 6-sialyllactose-3-sn-phosphatidylethanolamine [19].

6-sialyllactose-3-sn-phosphatidylethanolamine incorporation into Jurkat cell membranes

1 mM of 6-sialyllacotse-3-sn-phophatidylethanolamine was added to 400'000 Jurkat cells/ml in HBSS and the cells were incubated for 4 h rotating at 20°C. The cells were washed two times with HBSS before further processing.

Siglec-3 and sialophorin staining for flow cytometry

A Siglec-3 probe with a human Fc-domain (R&D Research) was pre-complexed for 10 min with a biotinylated anti-IgG-Fc-domain antibody labelled with biotin (Sigma-Aldrich). The cells were stained with the pre-complexed Siglec-3 probe for 50 min and then stained with PerCP-Cy5.5 labelled streptavidin (Becton Dickinson) for 20 min before analysing the cells by flow cytometry with a FACScanto II (Becton Dickinson).

A PE labelled antibody targeting sialophorin (Affymetrix eBioscience) was used to stain the cells that were analysed by flow cytometry with a FACScanto II (Becton Dickinson).

Cell death inhibitors

10 µM Q-VD-OPH (Sigma-Aldrich), 100 µM Z-IETD-FMK (Enzo Life Sciences), 20 µM Z-WEHD-FMK (Enzo Life Sciences) or 100 µM Necrostatin-1 (Enzo Life Sciences) were added to the cells media for 4 h. Then, the cells were washed twice with HBSS and coated as described above.

Production of lentivirus particles for the CRISPR-Cas9 screen with the murine GeCKO v2 library

Virus production took place in HEK293T cells that were sawn on 2 T-75 plates so that they would be 70-90% confluent the next day. The following procedure was performed separately for each of the two half-libraries A and B. 1'200 µl of Opti-MEM was mixed with 48 µl of Lipofectamine2000 (Life Technologies). 1'400 µl of Opti-MEM was mixed with 11.5 µg of the lentivirus packaging plasmid psPAX2, 6.4 µg of the lentivirus packaging plasmid pMD2.G and 10.2 µg the murine GeCKO v2 half-library A or B [20]. 1'200 µl of the Lipofectamine2000 mix and 1'200 µl of the plasmid mix were combined and left to incubate at 20°C for 5 min. Then 2000 µl of the Lipofectamine2000-plasmid mixture was applied to the cells together with 13 ml of Dulbecco's Modified Eagle's Medium with 10% FCS. After 6 h the media was replaced with fresh Dulbecco's Modified Eagle's Medium with 10% FCS. The lentiviral particles were harvested 24 h, 48 h and 72 h after the previous media change. The media was centrifuged at 500 x g for 5 min and the supernatant which includes the lentivirus particles was collected and stored at -80°C before being used for infections.

CRISPR-Cas9 screen with murine GeCKO v2 library in L929 and MC-38 cells

The CRISPR-Cas9 screen was performed with the mouse CRISPR Knockout Pooled Library (GeCKO v2) according to a protocol adapted from the originally published research article [20]. Cas9 expressing L929 or MC-38 cells were passaged one day before initiating the screen so that the cells would be 20 – 30% confluent the next day on 10 T-150 plates per half-library A or B and 1 negative control T-150 plate. That means 1'500'000 cells were seeded per plate and 15'000'000 in total per half-library A or B. After 1 day the media was removed and 4 ml of lentivirus containing media for half-library A or B were added to each T-150 plate with 8 μg/ml polybrene (Sigma-Aldrich). The cells were incubated for 2 h and then 14 ml of Dulbecco's Modified Eagle's Medium with 10% FCS was added per plate and the cells were incubated for a further 24 h. Then, the media was removed and selection was initiated with 23 μg/ml of puromycine (InvivoGen) for the L929 cells and 10 μg/ml for the MC-38 cells. The cells were incubated for 72 h which was the time it took for the cells on the negative control plate to die. All surviving cells were collected and treated with 8 mM of 3SL-cyclic-carbamate for 10 min in 10 ml HBSS and plated onto 10 T-75 plates per half-library A or B. The cells were kept for a duration of 4 weeks and clones were picked and cultured in 24-well plate culture dishes. To eliminate false-positive clones, the cells were re-treated with 8 mM 3SL-cyclic-carbamate when they reached confluency.

Sequencing the gRNA encoding sequence and genomic verification

All PCRs were done with Taq polymerase (Sigma-Aldrich).

The gRNA encoding sequence was sequenced with the flanking primers 5'-GGACTATCATATGCTTACCG-3' and 5'-TGCTGTCCCTGTAATAAACC-3'.

Verification PCRs were done with the primers listed in the tables 1 and 2.

Table 1: CRISPR-Cas9 screen L929 cells: gRNAs and genotyping primer sequences.

Gene abbreviation	gRNA	Forward primer	Reverse primer
Ang3	GATCACAACTTGCAAGCACA	TGAAGAAAAGAAAGCTAACCTCACC	GAGGGGAGATAAAAAGCAAACAGAC
Appbp2	TACATGATGAGATGCTCCAC	AGTGATTTAGTGTAAGCGTGTCTCT	CAAGGACAGAATTCTAAGCCCAAAG
Aqp7	GGCATCCTTGTTACCGTCCT	GGATCGTACCAAGACACATCTCTG	GACTTCATAAGACTTCTGTGCACCC
CbrI	CCCCTTCCACATTCAAGCAG	GTGGTGTCTTTCAAGCACAATAGAA	AGAAAGTCAATGGCCACAAAAGAAT
Cisd2	CCAGAAGCGCAAGTACCCCG	TTGGGTCTGCTGTGTATATGGTTTA	CTACAATAAGCTGCTTTGGTGAGAC
Cul5	ACGTCGCCATGTTCTCAACT	TACTACCTCTTCCCGGTCTGGTC	GAACCGCTCTCCTCATACACATC
Ercc6	GTTATACTTCTGTCGCTTCA	CAACATCCCTGAGGCAAATCAATAA	TATTACCCATAGCATGTGTACCCTC
Ffar4	CTCTAGTGCTCGTCGTGCGC	n.a.	n.a.
Galnt13	ACTGGAAGCTAAATTTCCGA	TCTATAATCAACTTGGAGAGCTAATGT	AACACACACAAAGTATCCAAAACTA
Gata 6	TCTACACAAGCGACCACCTC	TCCGGTAAGTATGATAAAATGCCCT	AAATATTCTTAGGTGCCAATTCACT
Mark1	TTCATCTGTCGCTGACGTAA	ACTCCCCAATATCAACCATGAGAAA	ATTGTCTAAGTGACTGTGAGCTCTT
Mtm1	TAAGTATAATTCACACTCCT	TGTTCTGTTGAGCCATAGGAAGTAA	ACAAGGTGGGACGGTAAATAAAATG
Olfr1537	AAGCATGAAGCCAGTGTTAA	n.a.	n.a.
Olfr310	TGTGCACACTTGCAATGACA	n.a.	n.a.
Pptc7	GCCTGATTACATGATCCTCC	TGACATTGTAAAATGCAGGTAGCAG	TAATGTTCCCAATTGTAATCGCCTG
Rnf133	GACATCGTTGTAGTTATGAT	TCAAAATGCTTGTGATCCCAATACC	TGGTGACGATCATAAAGGAGACAAA
Siah2	TTTCAAGTACCAGCATGAAG	GAATACCGTCCTTATTCCTGTCCTT	CATCATGAATGGACCGAGGTGTG
Surf4	GTTTGGAATCATCGCACTGC	AGCAGCATTGGAATAAAGGTGTTTT	TGGCCACTTCTCCAAAAAGAAAAAT

Table 2: CRISPR-Cas9 screen MC-38 cells: gRNAs and genotyping primer sequences

Gene abbreviation	gRNA	Forward primer	Reverse primer
Adcy7	CATCATTGAGCGCCTCAAAG	GTAGATATAAACGCGCAGGAAACAA	CAGTGAACTATCTCCCTAGAACCAG
Anxa8	TCCTACAGGAACCAATGAGC	AGCCATACCCAACACTATGTAAGTT	GCCCTATGTACACATTTCCATTCTG
Cnot8	ACCCGTCTGGAATCAACACA	n.a.	n.a.
Fam3b	AAGTACTTTGATATGTATGA	AGTCACTTAGAGGTAATGTGACCAA	ACAGACCCTGTACTCAATAAACACA
Spn	GAGTCCATGCATCTCACTCG	GGAACTGCAGCATCTACATCTATCT	CAGTAACATGCCACTTGATTCTTGG
Zc3hav1	TCATCCATCCTAGGAGATAC	CTTGAGTGCATAGGGAAAGACAAAC	CAGCAAGAGGAAAGAGGGAGTATAG

Microscopy

For differential interference contrast imaging to record cell death in L929 cells, cultivation was performed in µ-Slide 8 well plates for live cell imaging (Ibidi). The cells were cultivated so that they would be 70% confluent after 2 days of cultivation, so 15'000 cells were seeded per well. On the day of recording the adherent cells were incubated with 8 mM of 3SL-cyclic-carbamate in HBSS just before commencing with the recording. Imaging was performed on the widefield microscope LX (Leica).

For imaging the cytoskeleton, L929 cells were grown on coverslips in 24-well plates for 2 days so that they reached 50% confluency on the day of staining. To achieve this, 20'000 cells were seeded per well. On the day of the experiment, 8 mM 3SL-cyclic-carbamate was added directly to the adherent cells for 0 – 15 min. The cells were washed twice in HBSS and then fixed with 3% formalin in water for 20 min. The cells were permeabilised in PBS with 0.1% saponin and 20 mM glycine. In a first step, staining was performed with a β-tubulin targeting primary murine antibody (Sigma-Aldrich), followed by staining with an Alexa647 labelled anti-mouse Fc-domain targeting antibody (Abcam) and further staining of actin with Alexa488 labelled phalloidin (Abcam) and 4',6-diamidino-2-phenylindole (Biotium) to stain the nucleus. Imaging was conducted on an SP5 confocal microscope (Leica).

Mitochondrial imaging was performed with living L929 cells. The cells were seeded into µ-Slide 8 well plates for live cell imaging (Ibidi) so that they would be 50% confluent in 2 days. Therefore, 10'000 cells were seeded per well. Before microscopy the cells were incubated in growth media supplemented with 25 nM CMXRos (Thermo Fisher Scientific) for 15 min. Then, the cells were washed 3 times with growth media before adding PBS supplemented with 5 µg/ml Hoechst® 33342 (Thermo Fisher Scientific) for 10 min. The cells were washed 3 times with PBS and then Live Cell Imaging Solution (Thermo Fisher Scientific) was added to the cells. Imaging was conducted on an SP5 confocal microscope (Leica).

Cytoplasmic calcium determination

To determine the intracellular calcium concentration of MC-38 and L929 cells the FLUOFORTE® Calcium assay kit (Enzo Life Sciences) was used according to the provided instructions. The measurement was done on an Infinite® 200 Pro plate reader (Tecan Trading AG, Männerdorf, Switzerland).

Results

3-Sialyllactose and 6-Sialyllactose cell coating initiates cell death

Our initial goal was to coat different types of cells with various oligosaccharides using the cyclic-carbamate approach that we recently described to identify novel functions of cell surface oligosaccharides [15]. This was possible with the lactose-, 2-fucosyllatose- (2FL), 3-fucosyllactose- (3FL) and 3-fucosyl-3-sialyllactose- (FSL) cyclic-carbamates [15] however we found that coating MC-38 and L929 cells with 3-sialyllactose- (3SL) or 6-sialyllactose- (6SL) cyclic-carbamate lead to cell death after initiating cell coating (Fig. 1).

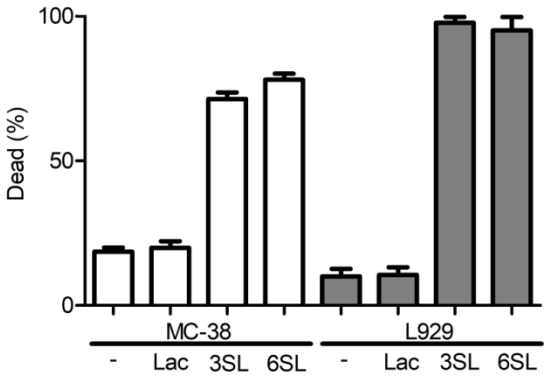

Figure 1: Cell death by coating MC-38 and L929 cells with 3SL- or 6SL-cyclic-carbamates. MC-38 cells were either left uncoated, coated with lactose-, 3SL- or 6SL-cyclic-carbamate for 10 min and then stained with propidium iodide to determine the relative amounts of dead cells by flow cytometry. -, uncoated. The experiment was performed in triplicates and statistical significance was determined by ANOVA and Bonferroni post-testing. The error bars indicate the standard deviation.

When visualized by differential interference contrast microscopy we noticed that 15 minutes after initiating L929 cell coating with 3SL-cyclic-carbamate, the plasma membranes of the cells started to bleb (Fig. 2D-G). After 30 minutes some of the cells had undergone secondary necrosis (black arrows). Cells that were coated with lactose cyclic-carbamate remained viable during 30 minutes of coating (Fig. 2A-C).

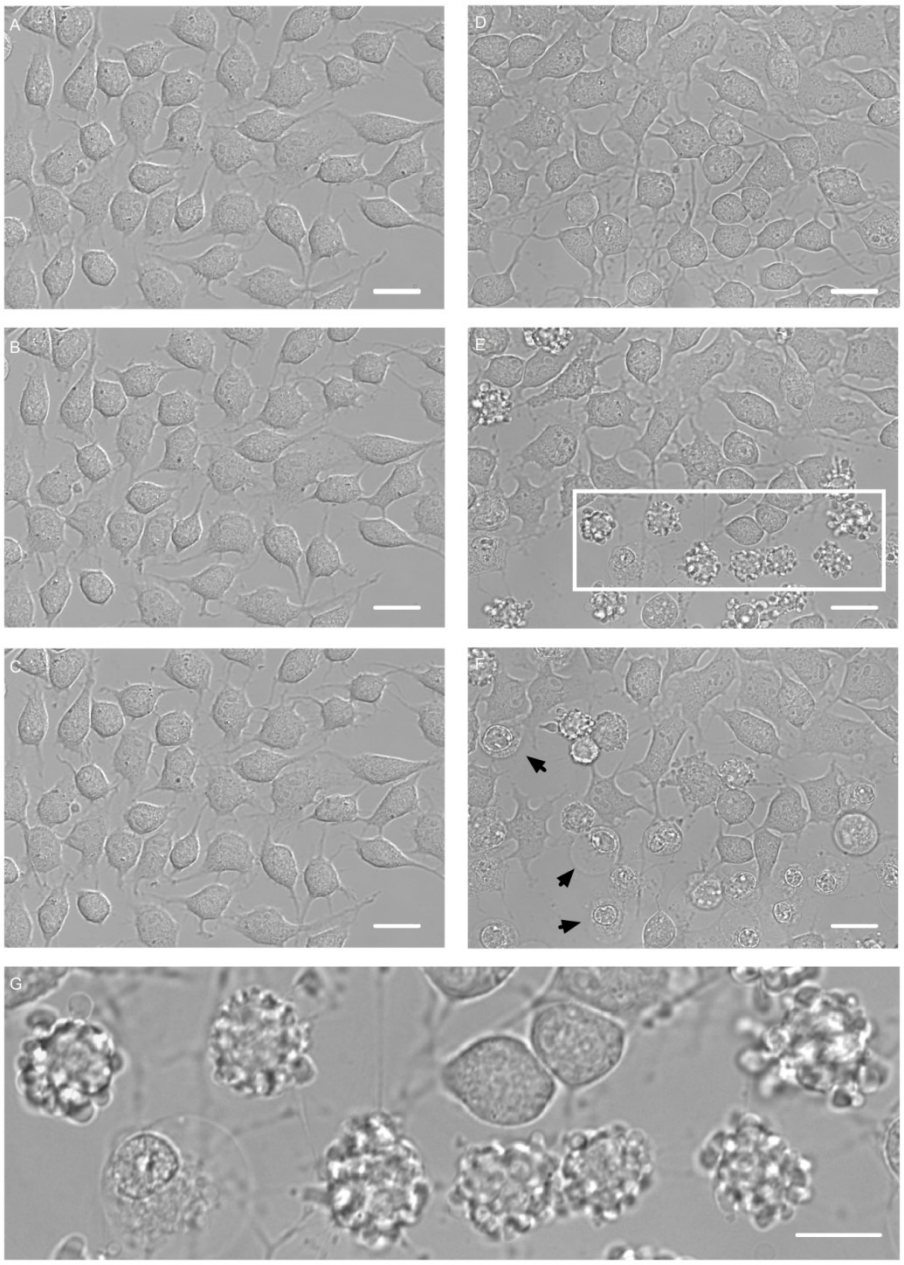

Figure 2: DIC microscopy to visualize 3SL-cyclic-carbamate coating mediated cell death in L929 cells. Adherently growing L929 cells were coated with (A-C) lactose-cyclic-carbamate and images were made after (A) 0 min, (B) 15 min and (C) 30 min. Alternatively, the L929 cells were coated with (D-F) 3SL-cyclic-carbamate and images were made after (D) 0 min, (E) 15 min and (F) 30 min. (G) The marked region in (E) was enlarged to show cells with blebs on their membrane. The white arrow marks cells that have gone through secondary necrosis. Scale bar: 5 µm. These images are representative for three independent experiments.

Oligosaccharide-cyclic-carbamates have been derivatized to have a cyclic-carbamate group at their reducing end which can bind covalently to primary amines that occur on proteins and lipids such as phosphatidylethanolamines [21]. We asked ourselves if cell death primarily occurs due to the coupling of oligosaccharide-cyclic-carbamates to specific epitopes on the cell surface or due to

general surface glycosylation. To answer this question we coupled 6SL-cyclic-carbamate to 3-sn-phosphatidylethanolamine and incorporated the custom-made glycolipids into the membrane of Jurkat cells as has been done with aminooxy glycans condensed to a polymethyl vinyl ketone scaffold via the formation of oximes [22]. Beforehand, we demonstrated by thin-layer chromatography, with chloroform:methanol:water (65:25:4) as the mobile phase, that 6SL-cyclic-carbamate is successfully attached to 3-sn-phosphatidylethanolamine (Fig. 3A; black arrow). 6SL coupled to 3-sn-phosphatidylethanolamine was isolated from the educts by scraping the product off the membrane and extracting the custom-made glycolipid with chloroform:methanol (2:1) (Fig. 3B). Incorporation of 6SL-3sn-phosphatidylethanolamine into Jurkat cell membranes was shown by increased staining with SIGLEC-3 which was increased by the factor 3.5 (Fig. 3C). 6SL-3-sn-phosphatidylethanolamine incorporation into the cell membrane of Jurkat cells did not induce cell death while direct coating with 6SL-cyclic-carbamate lead to 80% cell death (Fig. 3D). This implies that the modification of certain sites leads to cell death and not the general coating of the cells with sialyllactose.

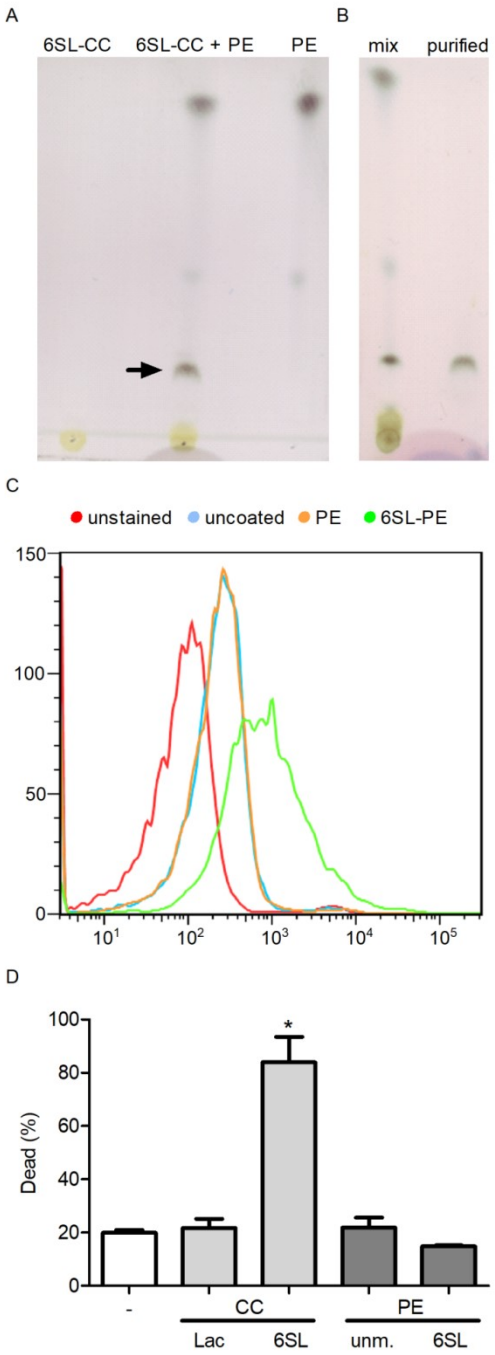

Figure 3: Incorporating 6SL coupled to 3-sn-phospathidylethanolamine into the plasma membrane of Jurkat cells does not induce cell death. (A) 6SL-cyclic-carbamate was attached to the amine group on 3-sn-phosphatidylethanolamine and successful coupling was shown by TLC (black arrow). The presented image is representative of three independent experiments. (B) The product from (A) was scraped off the membrane and Folch extracted from the Kieselgel residue. Successful purification of the product was shown by TLC. The presented image is representative of three independent experiments. (C) The incorporation of 6SL-3-sn-phosphatidylethanolamine into the plasma membrane of Jurkat cells was shown by staining the cells with a Siglec-3 probe. The presented image is representative of three independent experiments. (D) On one hand 6SL-

3-sn-phsophatidylethanolamine was incorporated into Jurkat cells and on the other hand 6SL-cyclic-carbamate was coupled directly to the membrane of Jurkat cells. The extent of cell death was determined by propidium iodide staining and flow cytometry. The experiment was performed in triplicate and statistical significance was determined by ANOVA and Bonferroni post-testing. The error bars indicate the standard deviation. CC, cyclic-carbamate; PE, 3-sn-phosphatidylethanolamine; unm., unmodified.

We next showed that sialyllactose-coating induced cell death occurs in multiple cell lines such as MC-38, RAW264.7, L929, HEK293T, HT-29 and THP-1 cells (Fig. 4A-F). In all the tested cell lines, except RAW264.7, the dose-kill curve was sigmoid with a sharp increase of the extent of cell death (Fig. 4A-F). In RAW264.7 cells the relationship was linear with a gradual increase of cell death with the sialyllactose-cyclic-carbamate dose (Fig. 4B). In all cell lines, except RAW264.7, 3SL-cyclic-carbamate was also more potent than 6SL-cyclic-carbamate with the LD_{50} of 3SL-cyclic-carbamate being lower than the LD_{50} of 6SL-cyclic-carbamate (Fig. 4A-F; Tab. 3).

Table 3: LD_{50} 3SL-cyclic-carbamate and 6SL-cyclic-carbamate in 6 different cell lines.

Cell Line	**LD_{50}(3SL-CC)**	**LD_{50}(6SL-CC)**
MC-38	0.8 mM	3.1 mM
RAW264.7	5.9 mM	6.0 mM
L929	2.2 mM	5.5 mM
HEK293T	1.6 mM	6.7 mM
HT-29	3.5 mM	7.8 mM
THP-1	5.9 mM	7.7 mM

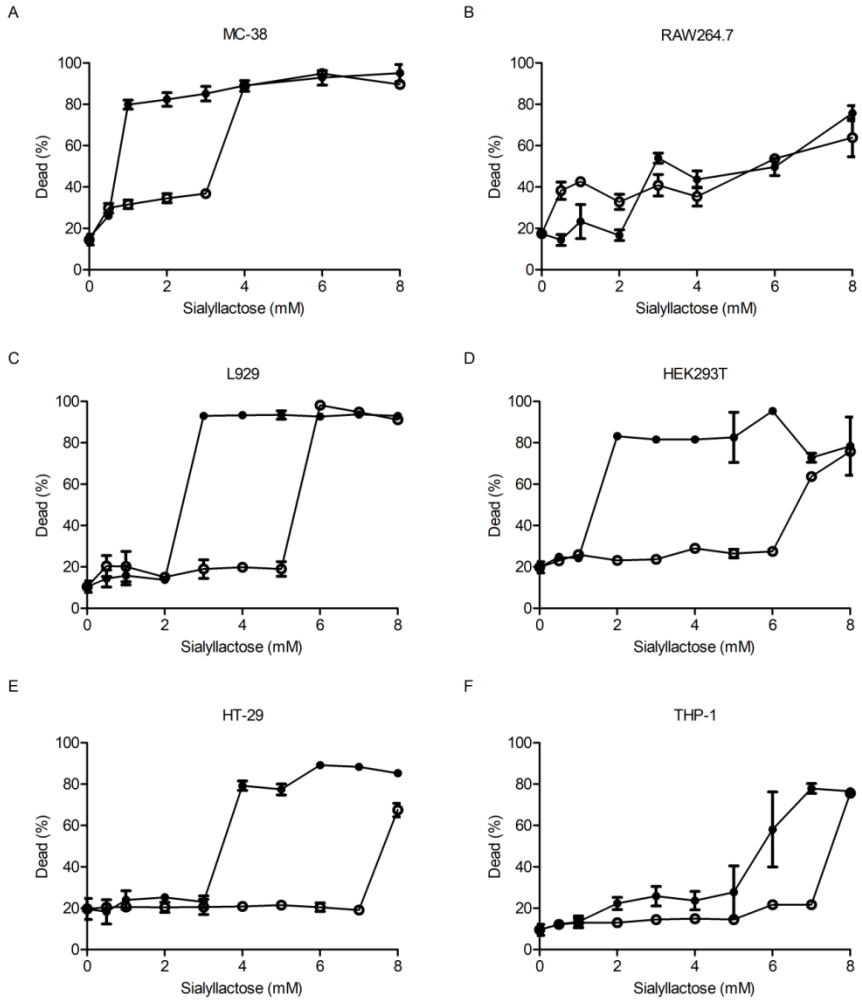

Figure 4: Comparison of cell death inducing potency of 3SL- and 6SL-cyclic-carbamate in six different cell lines. (A) MC-38, (B) RAW264.7, (C) L929, (D) HEK293T, (E) HT-29 and (F) THP-1 cells were coated with increasing concentrations of 3SL- or 6SL-cyclic-carbamate for 10 min. Then, the cells were stained with propidium iodide and the relative amount of dead cells was determined by flow cytometry. -, uncoated; ●, 3SL-cyclic-carbamate; ○, 6SL-cyclic-carbamate. The experiment was performed in triplicate and the error bars indicate the standard deviation.

Sialyllactose coating initiated cell death inhibition by caspase antagonists

The pan-caspase inhibitor Q-VD-OPH [23] lead to a 50% decreased amount of cell death in MC-38 cells (Fig. 5A), a 30% decrease in RAW264.7 cells (Fig. 5B), a 40% decrease in HEK293T cells (Fig. 5D) and a 10 % decrease in THP-1 cells (Fig. 5F). In L929 and HT-29 cells no decrease in cell death was evident (Fig. 5C, E). As the pan-caspase inhibitor counteracted cell death, we decided to test more specific caspase inhibitors such as the caspase-8 inhibitor Z-IETD-FMK [24, 25] and the caspase-1 inhibitor Z-WEHD-FMK [26-28]. We also tested the necroptosis inhibitor necrostatin-1 which inhibits RIPK1 [29, 30]. Z-IETD-FMK decreased cell death by 40% in MC-38 cells (Fig. 5A), 50% in RAW264.7

cells (Fig. 4B), 50% in HEK293T cells (Fig. 5D) but failed to decrease cell death in L929 (Fig. 5C), HT-29 (Fig. 5E) and THP-1 cells (Fig. 5F). Z-WEHD-FMK lead to a decrease of cell death by 40% in MC-38 cells (Fig. 5A), 50% in RAW264.7 cells (Fig. 5B), 20% in L929 cells (Fig. 5C), 50% in HEK293T cells (Fig. 5D) and no decrease in HT-29 and THP-1 cells (Fig. 5E, F). Necrostatin-1 only slightly decreased sialyllactose coating mediated cell death in THP-1 cells by 10% (Fig. 5F) but did not influence the extent of cell death in any of the other cell lines (Fig. 5A-E).

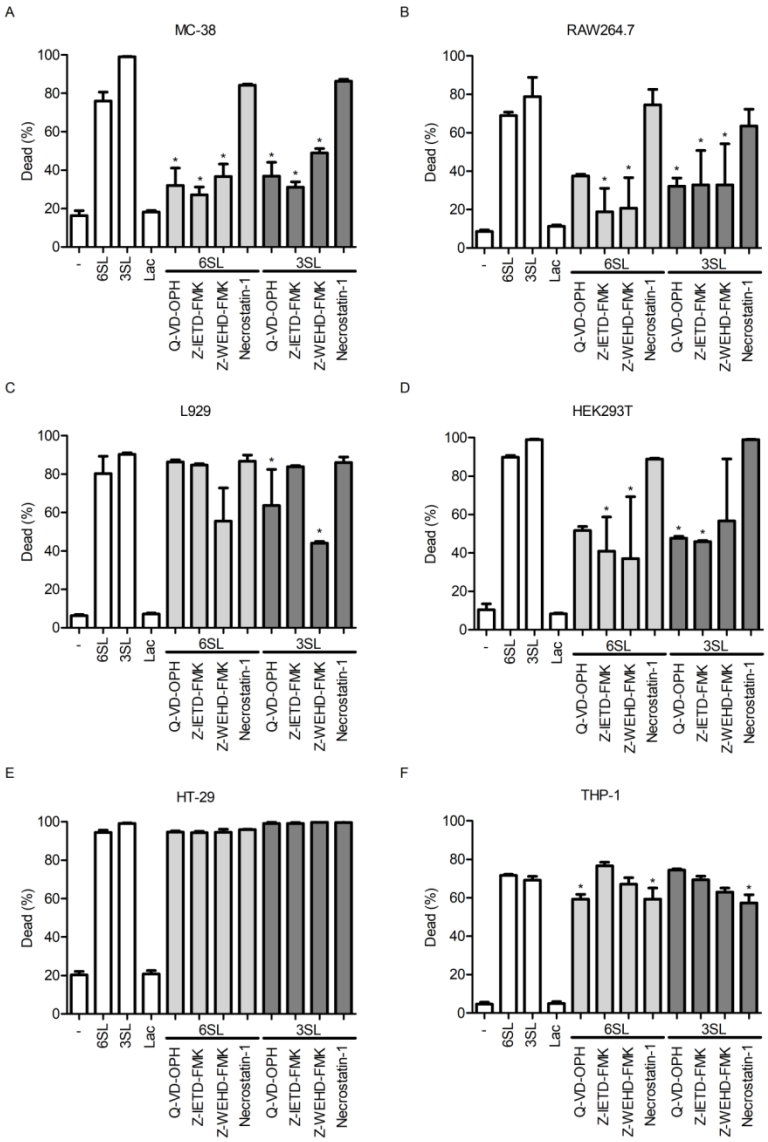

Figure 5: Influence of programmed cell death inhibitors on sialyllactose-cyclic-carbamate mediated cell death. (A) MC-38, (B) RAW264.7, (C) L929, (D) HEK293T, (E) HT-29 and (F) THP-1 cells were cultured in the presence of Q-VD-OPH, Z-IETD-FMK, Z-WEHD-FMK or necrostatin-1 for 4 h. The cells were then coated with 3SL- or 6SL-cyclic-carbamate for 10 min and stained with propidium iodide to determine the amount of dead cells by flow cytometry. The experiments were performed in triplicate and the error bars indicate the standard deviation. The statistical significance was determined by ANOVA and Bonferroni post-testing.

CRISPR-Cas9 screen to identify genes involved during sialyllactose-coating induced cell death

As cell death by 3SL- and 6SL-cyclic-carbamate coating could be inhibited by caspase inhibitors, we concluded that sialyllactose coating induced a programmed form of cell death. Interestingly, this form of cell death is caspase-8 as well as caspase-1 dependent in MC-38, RAW264.7 and in HEK293T cells. In L929 cells, cell death was only dependent on caspase-1. We decided to perform a genetic screen on the MC-38 cells and on the L929 cells to find the pathway involved during sialyllactose coating induced cell death. Both cell lines were transformed to express Cas9 and then infected with lentiviruses containing the murine GeCKO v2 gRNA library which targets 20'611 genes in the murine genome [20]. Then the cells were coated with 3SL-cyclic-carbamate to select the clones that are resistant towards sialyllactose-coating mediated programmed cell death.

In the L929 cell line we identified 18 genes that are involved during 3SL-cyclic-carbamate coating mediated cell death (Tab. 4). These genes could be chiefly classified as G-protein coupled receptors, cytoskeleton interacting proteins, protein degrading proteins, phosphatases, kinases and channel proteins (Tab. 4). The three G-protein coupled receptors free fatty acid receptor 4 (Ffar4), olfactory receptor 1537 (Olfr1537) and olfactory receptor 310 (Olfr310) were interesting candidates to obtain in this screen as G-protein coupled receptors are known for their fast signaling [31]. All three proteins have accessible lysines in their extracellular domains (Fig. 6A-C) and Ffar4 has an N-glycosylation site at position 21 that is only 11 amino acids away from a lysine residue that is potentially accessible for oligosaccharide-cyclic-carbamates (Fig. 6A). Furthermore, cell death could be ameliorated by pre-incubating the cells for 1.5 h with Pertussis toxin (Fig. 6D) which catalyzes ADP-ribosylation of the G-proteins α-subunit, which stops G-proteins from interacting with the G-protein coupled receptors [32]. In the MC-38 cells we identified six genes that were involved in sialyllactose-mediated cell death (Tab. 5). Here, we found proteins involved in cell adhesion and signaling, trafficking and also G-protein coupled receptor signaling (Tab. 5). The presence of deletory mutations in the identified genes were confirmed by genomic PCRs with primers that flank the gRNA targeted sequence (Tab. 1, 2). Some of the clones have not been sequenced due to redundancies of the flanking sequences that make PCRs in these regions difficult such as the genes for Olfr1537 and Olfr310 (Tab. 1, 2). With the flanking primers, it was possible to genotype most of the mutations in the isolated clones (Tab. 6, 7). Some alleles were not possible to decipher from the chromatograms and are annotated as "unknown (not WT)" as wildtype sequences were generally easy to recognize despite more than two alleles being present.

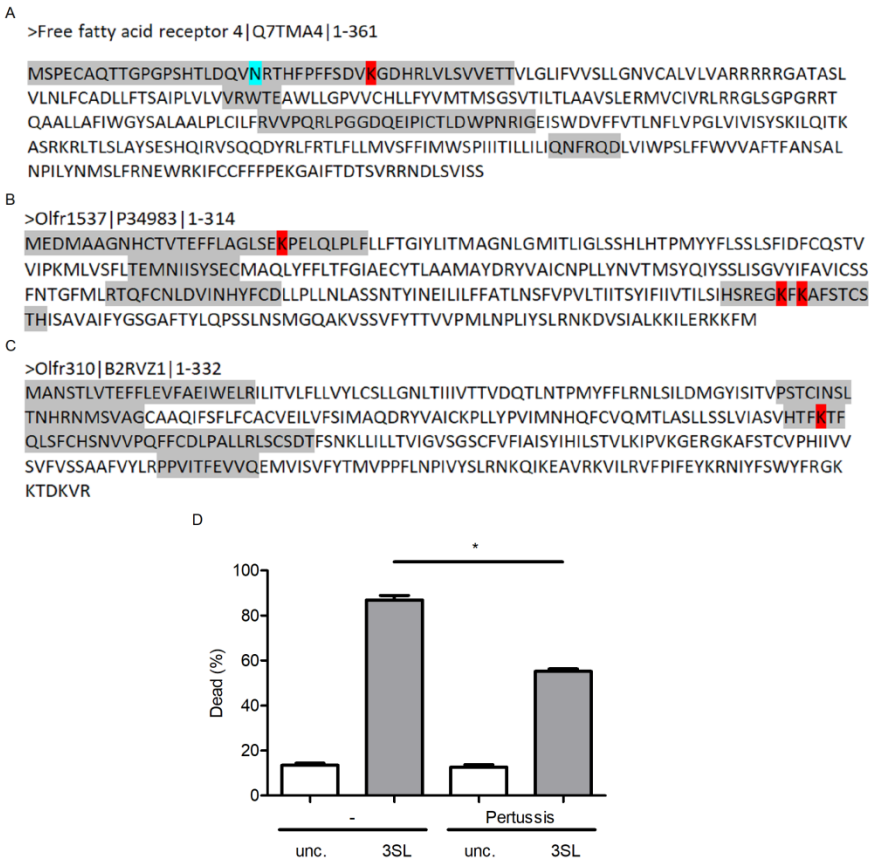

Figure 6: (A-C) Amino acid sequences of Ffar4, Olfr1537 and Olfr310. The sequences with grey highlighting are the extracellular domains of these 7 pass transmembrane proteins. The characterized N-glycosylation sites have been indicated in blue and the accessible lysines for oligosaccharide-cyclic-carbamate ligation are highlighted in red. (D) Pertussis toxin was used to inhibit G-protein-coupled receptor signaling prior to coating cells with 3SL-cyclic-carbamate.

Table 4: Candidates from CRISPR-Cas9 screen in L929 cells

Class	Abbreviation	Gene ID	Full name
Transcription factors	Gata 6	14465	GATA binding protein 6
GPCR	Ffar4	107221	free fatty acid receptor 4
	Olfr1537	257959	olfactory receptor 1537
	Olfr310	258222	olfactory receptor 310
Cytoskeleton	Appbp2	66884	Amyloid beta precursor protein binding protein 2
	Mark1	226778	MAP/microtubule affinity regulating kinase 1
Protein degradation	Cul5	75717	Cullin 5
	Rnf133	386611	ring finger protein 133
	Siah2	20439	Seven in absentia 2
Phosphatase/kinase	Mtm1	17772	X-linked myotubular myopathy gene 1
	Pptc7	320717	PTC7 protein phosphatase homolog
Channel proteins	Aqp7	11832	Aquaporin 7
Intracellular localisation	Surf4	20932	Surfeit gene 4
Translocation regulation	Ang3	11730	Angiogenin, ribonuclease A family, member 3
NADPH metabolism	CbrI	12408	Carbonyl reductase I
Iron binding	Cisd2	67006	CDGSH iron Sulphur domain 2
DNA repair	Ercc6	319955	excision repair cross-complementing rodent repair deficiency, complementation group 6
Glycosylation	Galnt13	271786	UDP-N-acetyl-alpha-D-galactosamine:polypeptide N-acetylgalactosaminetransferase 13

Table 5: Candidates from CRISPR-Cas9 screen in MC-38 cells

Class	Abbreviation	Gene ID	Full name
mRNA stability	Cnot	69125	CCR4-NOT transcription complex, subunit 8
Cells signalling: Ribosylation	Zc3hav1	78781	zinc finger CCCH type, antiviral 1
Cell adhesion and signalling	Spn	20737	sialophorin
GPCR signalling	Adcy7	11513	adenylate cyclase 7
Trafficking	Anxa8	11752	annexin A8

Table 6: Genotyping of mutations from CRISPR-Cas9 screen in L929 cells

Gene	Wildtype allele	Clone allele 1	Clone allele 2	Clone allele 3
Ang3	AAGTTGTGATCTGGAA	AAGTTGTGATCTGGAA	AAGTTGTGATCTGGAA	n.a.
Appbp2	TCCACTG	TCCACTG	unknown (not WT)	unknown (not WT)
Aqp7	GGCATCCTTGTTACCGTCCT	GGCATCCTTGTTACCGTCCT	GGCATCCTTGTTACCGTCCT	n.a.
CbrI	CCCCCCCGAAAGTCAAT	CCCCCCCGAAAGTCAAT	CCCCCCCGAAAGTCAAT	CCCCCCCGAAAGTCAAT
Cisd2	GGGGTACTTGC	GGGGTACTTGC	GGGGTACTTGC	n.a.
Cul5	ACGTCGCCATGTTCTCAACT	n.a.	n.a.	n.a.
Ercc6	AAGCGAC	AAGCGAC	unknown (not WT)	unknown (not WT)
Ffar4	CTCTAGTGCTCGTCGTGCGC	n.a.	n.a.	n.a.
Galnt13	CTAAATTTCCCGATGGTATCC	CTAAATTTCCCGATGGTATCC	WT	n.a
Gata6	CCTTCTACACAAGCGACCACCTCA	CCTTCTACACAAGCGACCACCTCA	n.a.	n.a.
Mark1	TGACGTAATGG	TGACGTAATGG	TGACGTAATGG	n.a.
Mtm1	TCTAAGTATAATTCACACTCCTTGGAGAATGAATC CATTAAGAAAGTAAGTTGAGTTTTTACACG	TCTAAGTATAATTCACACTCCTTGGAGAATGAATC CATTAAGAAAGTAAGTTGAGTTTTTACACG	TCTAAGTATAATTCACACTCCTTGGAGAATGAATC CATTAAGAAAGTAAGTTGAGTTTTTACACG	n.a.
Olfr1537	AAGCATGAAGCCAGTGTTAA	n.a.	n.a.	n.a.
Olfr310	TGTGCACACTTGCAATGACA	n.a.	n.a.	n.a.
Pptc7	CCTCCAGGAG	CCTCCAGGAG	unknown (not WT)	unknown (not WT)
Rnf133	GACATCGTTGTAGTTATGAT	unknown (not WT)	unknown (not WT)	unknown (not WT)
Siah2	CTTCATGCTGGTACTTGAAA	unknown (not WT)	unknown (not WT)	unknown (not WT)
Surf 4	TCGCACTGC	TCGCACTGC	WT	n.a.

Table 7: Genotyping of mutations from CRISPR-Cas9 screen in MC-38 cells

Gene	Wildtype allele	Clone allele 1	Clone allele 2	Clone allele 2
Adcy7	CATCATTGAGCGCCTCAAAGA	CATCATTGAGCGCCTCAAAGA	CATCATTGAGCGCCTCAAAGA	n.a.
Anxa8	AGGACCAATGAGCAGGCCATCA	AGGACCAATGAGCAGGCCATCA	unknown (not WT)	unknown (not WT)
Cnot8	ACCCGTCTGGAATCAACACA	n.a.	n.a.	n.a.
Spn	CCCTCGAGTGAGATG	CCCTCGAGTGAGATG	unknown (not WT)	unknown (not WT)
Zc3hav1	GTATCTCCTAGGATGGATGA	WT	unknown (not WT)	unknown (not WT)

3-sialyllactose coating leads to extensive cytoskeleton depolymerization

In L929 cells we discovered that the amyloid beta precursor binding protein 2 (Appbp2) and MAP/microtubule affinity regulating kinase 1 (Mark1) were important for sialyllactose-coating mediated cell death. Interestingly, both genes are microtubule binding proteins and have previously been associated with regulating cell death [33, 34]. Mark1 is known to phosphorylate the protein tau [35] which when it is not phosphorylated binds to microtubules and stabilizes them [36]. Once tau is phosphorylated, it dissociates from the microtubules which ultimately destabilizes the microtubule fibers [37]. The depolymerization of microtubule fibers would also require the protein degrading machinery which interestingly also was identified in our screen with the genes for cullin 5 (Cul5), ring finger protein 133 (Rnf133) and seven in absentia 2 (Siah2) in the CRISPR-Cas9 screen in L929 cells. Therefore we decided to test if 3SL-cyclic-carbamate coating leads to the degradation of the cytoskeleton. We used confocal microscopy to visualize actin and microtubules. Actin was stained with Alexa488 labelled phalloidin and the microtubules were stained with an antibody that recognizes β-tubulin and a secondary antibody labelled with Alexa647. Lactose coating did not influence the cytoskeleton which remained intact after initiating lactose-cyclic-carbamate coating (Fig. 7A, B, E, F, I, J, M, N). 3SL-cyclic-carbamate coating on the other hand lead to rapid loss of actin and microtubule fibers within 15 minutes whereas a clear loss of fibers can already be seen as soon as 5 min after initiating 3SL-cyclic-carbamate coating (Fig. 7C, D, G, H, K, L, O, P). As a consequence the cytoplasm retracts towards the nucleus (Fig. 7O, P).

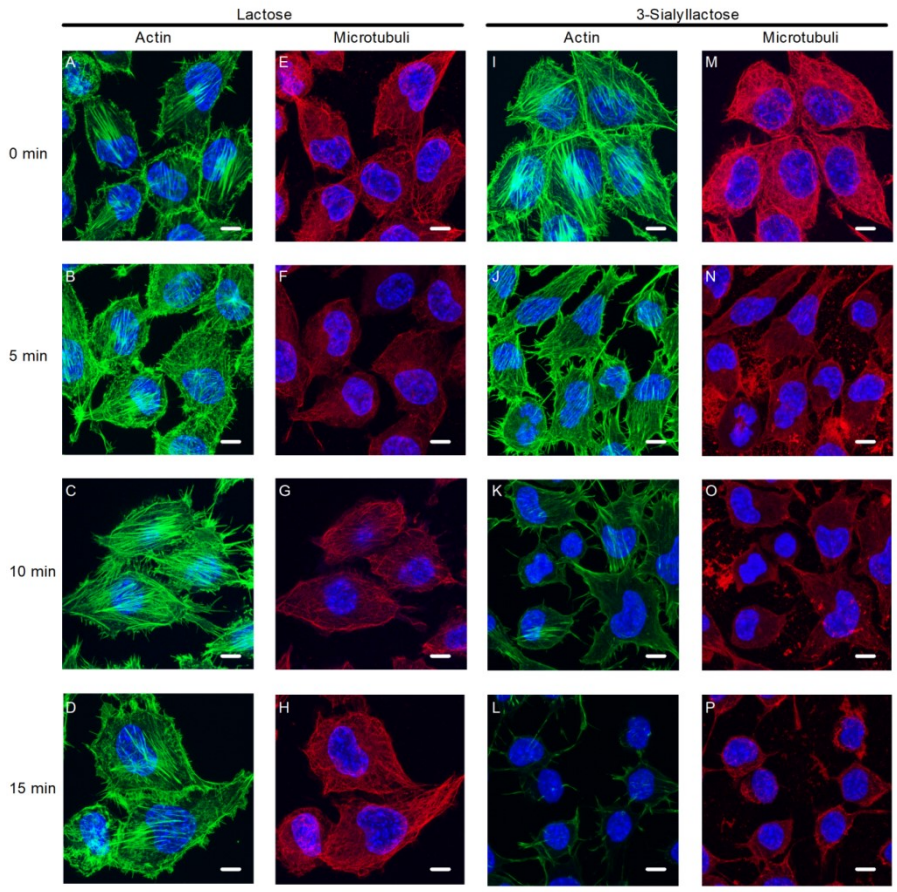

Figure 7: Cytoskeleton depolymerization during 3SL-cyclic-carbamate coating of L929 cells. L929 cells were coated with (A-H) lactose-cyclic-carbamate or (I-P) 3SL-cyclic-carbamate for (A, E, I, M) 0 min, (B, F, J, N) 5 min, (C, G, K, O) 10 min, (D, H, L, P) 15 min. These cells were fixed in formalin and stained with (A-D, I-L) actin staining phalloidin or (E-H, M-P) an antibody that stains β-tubulin. The cells were visualized by confocal microscopy. Scale bar: 5 µm. The experiment was performed three times and these are representative images.

Loss of mitochondrial membrane potential and integrity

Cell death is often associated with a loss of mitochondrial membrane potential [38, 39]. We analyzed the membrane potential with the mitochondrial stain CMXRos which has decreased intensity when the membrane potential is lost [40]. We recorded living L929 cells stained with CMXRos. Lactose-cyclic-carbamate coating lead to no loss in CMXRos staining during live cell imaging (Fig. 8) but 3SL-cyclic-carbamate staining lead to a loss of mitochondrial membrane integrity as soon as 2 min after initiating 3SL-cyclic-carbamate coating (Fig. 8). The imaging also reveals a loss of mitochondrial membrane integrity (white arrow) as can be seen by the bleb that grows and then bursts between 10 and 12 min after initiating 3SL-cyclic-carbamate coating (Fig. 8). That means mitochondrial components such as cytochrome c are being leaked into the cytoplasm which often drive programmed forms of cell death [41].

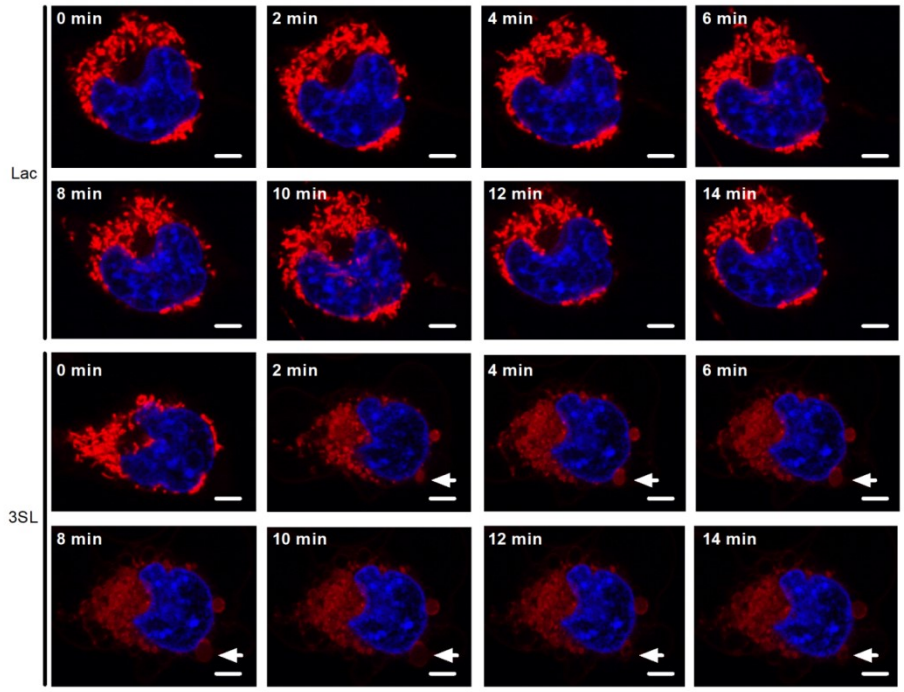

Figure 8: Loss of mitochondrial membrane potential and integrity due to 3SL-cyclic-carbamate coating. L929 cells were loaded with the membrane potential indicating dye CMXRos and coated with lactose- or 3SL-cyclic-carbamate. Single cells were observed for 14 min by live-confocal microscopy. Pictures were made every 2 min. The white arrow indicates a swelling bleb that bursts. Scale bar: 5 µm. The experiment was repeated 3 times and these are representative images.

Increased levels of cytoplasmic calcium during 3SL-coating mediated cell death

Programmed cell death is characterized by a surplus of the second messenger calcium in the cytoplasm [42]. Interestingly, our CRISPR-Cas9 screen in L929 cells revealed the involvement of the 3 G-protein coupled receptors Ffar4, olfactory receptor 1537 (Olfr1537) and olfactory receptor 310 (Olfr301) (Tab. 4). G-protein coupled receptor signaling is of especial interest for this study as they are known to initiate fast signaling events which would be necessary to drive the cell death procedure described here [31]. Calcium is actually also a second messenger that can be released into the cytoplasm after G-protein coupled receptor activation [43].

Another candidate that the CRISPR-Cas9 screen in L929 cells revealed is the surfeit gene 4 (Surf4). The encoded protein is localized to the membrane of the ER and is known to be relevant for the correct localization of the protein STIM-1 in the ER membrane. STIM-1 plays a key role regulating store-operated Ca^{2+} entry [44].

We therefore decided to assess the intracellular calcium concentration during 3SL-cyclic-carbamate mediated cell death in MC-38 and L929 cells with the intracellular FluoForte AM dye which fluoresces green when it associates with calcium ions [45, 46]. In both MC-38 and L929 cells, increased intracellular concentrations of calcium were observed (Fig. 9). In MC-38 cells, green fluorescence remained 2 times higher than the baseline throughout the whole period of 300 s that was recorded (Fig. 9A). In the L929 cells, a 3.5 fold increase was observed just after measuring the green fluorescence after having initiated the 3SL-cyclic-carbamate coating procedure but it rapidly declined back to baseline levels within 100 s of the recording (Fig. 9B).

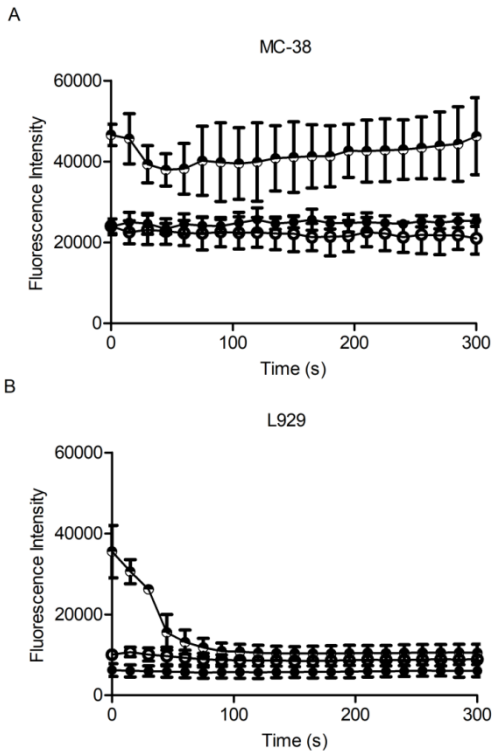

Figure 9: Tracking intracellular calcium levels during 3SL-cyclic-carbamate coating. MC-38 and L929 cells were loaded with the intracellular calcium sensor FLUOFORTE® AM and then coated with lactose-, 3SL-cyclic-carbamate or left uncoated. Fluorescence derived from the FLUOFORTE® AM dye was recorded on a plate reader for 300 s. ◓, 3SL-cyclic-carbamate; ●, uncoated; ○, lactose-cyclic-carbamate. Each data point represents the mean of three independent experiments and the error bars indicate the standard deviation.

Sialophorin and its role during sialyllactose-coating mediated cell death

Sialophorin (Spn) is a highly glycosylated mucin-like protein that occurs on the cell surface of many immune cells [47]. In the CRISPR-Cas9 screen with the MC-38 cells, Spn was one of the identified candidates. We were able to show that MC-38 cells express sialophorin by staining them with a PE

labelled antibody for sialophorin and then performing flow cytometry. Sialophorin staining was 3.5 times more intense in wildtype cells than in the isotype control (Fig. 10A). The isolated MC-38 clone that contained the sialophorin targeting gRNA had no increased staining with the sialophorin targeting antibody compared to the isotype control which demonstrates that the clone has a complete sialophorin knockout (Fig. 10B). Next, we performed a bioinformatics analysis of the extracellular domain of sialophorin and identified the lysines-23, -34, -81, -160 and -207 as possible acceptors for 3SL- or 6SL-cyclic-carbamate (Fig. 10C). In total the extracellular domain of sialophorin has 25 O-GalNAc- and 1 N-GlcNAc-glycosylation site that have been characterized (Fig. 10C).

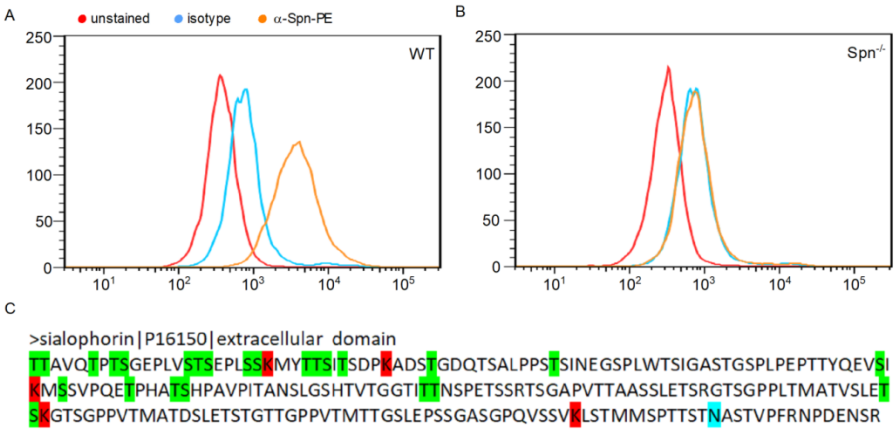

Figure 10: Sialophorin null mutant. (A) Wildtype MC-38 cells and (B) sialophorin gRNA containing MC-38 cells were stained with a sialophorin staining antibody and analyzed by flow cytometry. Red, unstained; blue, isotype control; orange, α-Spn-PE. The experiment was performed three times independently and these are representative images. (C) Amino acid sequence of sialophorin's extracellular domain. Green, O-glycosylation sites; blue, N-glycosylation sites; red, lysines for potential oligosaccharide-cyclic-carbamate coupling.

Discussion

Characteristic for sialyllactose-cyclic-carbamate mediated cell death is the speed at which it takes place. That means cell death must be rapidly initiated. Interestingly, the CRISPR-Cas9 screen we performed with L929 cells revealed the 3 G-protein coupled receptors Ffar4, Olfr1537 and Olfr301. In the MC-38 cell CRISPR-Cas9 screen we revealed the adenylate cyclase 7 as a candidate, a protein which is downstream of G-protein coupled receptors and is responsible for metabolizing ATP into cAMP [48]. These are interesting candidates as G-protein coupled receptors are known to initiate fast signaling responses that take place in seconds [31]. We also demonstrated in silico that all three G-protein coupled receptors have accessible lysines in their extracellular domains that can be coupled to sialyllactose-cyclic-carbamate and that the general G-protein coupled receptor signaling inhibitor

Pertussis toxin is able to decrease the amount of cell death. Ffar4 actually has an N-linked glycosylation site at position 21 that is only 11 amino acids away from a lysine that is accessible for sialyllactose-cyclic-carbamate coupling (Fig. 6). Previous reports have actually strongly indicated that G-protein coupled receptor signaling could play a key role in programmed cell death signaling. The overexpression of the $G\alpha_s$ protein in the SH-SY5Y cell line leads to increased sensitivity of the cells to apoptotic stimuli [49]. Also in cardiomyocytes the activation of $G\alpha_s$ by the β_1- and β_2-adrenergic receptors was able to drive the cells towards a pre-apoptotic state [50].

One possibility is that sialylation on some surface proteins such as G-protein coupled receptors, such as Ffar4, may serve as a molecular switch to initiate cell death in circumstances that require the rapid induction of cell death such as virus infection or the acquisition of cancer cell properties. Sialyltransferases have been shown to be present at the cell surface and are also still functional although the biological relevance of them is still disputed [51]. The cell surface sialyltransferase CMP-NeuAc:GM3 is capable of sialylating the ganglioside GM3 at the plasma membrane [52, 53]. St6gal1 has also been reported to be secreted and able to catalyze sialylation outside the cell [54]. Additionally, dendritic cells have been claimed to have active cell surface sialyltransferases [55].

Another surface protein revealed in our CRISPR-Cas9 screen in MC-38 cells was sialophorin. This protein is well known to be involved during cell death in thymocytes by forming aggregate with other surface protein like CD3, CD7 and CD45 which is galectin-1 dependent [14]. Sialophorin directly interacts with galectin-1 during the formation of this complex and its absence leads to 50 % less galectin-1 binding to the cell surface and reduced cell death in thymocytes exposed to galectin-1 [56]. In thymocytes, the actual signaling of cell death occurs due to the clustering of CD45, which has an intracellular phosphatase that then becomes active leading to caspase-3 activation [57]. Maybe sialophorin can interact with other proteins such as G-protein coupled receptors and also lead to their clustering on the cell surface and enhance their activity.

We demonstrated that sialyllactose coating initiated cell death was caspase dependent (Fig. 5). Caspase activity has been shown to initiate apoptosis via caspase-8 [58] or caspase-9 [59] and pyroptosis via caspase-1 [60]. Caspase-8 and caspase-9 both lead to the activation of caspase-3 which initiates classical apoptosis [59]. Recently however, caspase-3 has been shown to be capable of initiating a pyroptosis-like phenotype by cleaving the protein gasdermin-E which once activated starts creating membrane pores [61]. This shows that it is not possible to rigidly categorize cell death into different types. Sialyllactose-coating induced cell death is dependent on caspase-8 such as MC-38, RAW264.7 and HEK293T cells but still there is rapid formation of pores which makes it possible to stain the cells with propidium iodide. Furthermore, sialyllactose-coating initiated cell death in MC-38

and HEK293T depends on both caspase-8 and caspase-1 activity. In fact, caspase-8 has previously been shown to be involved during pro-IL-1β processing to mature IL-1β and this was NLRP3-inflammasome dependent [62]. In the absence of caspase-1, caspase-8 actually induces apoptosis instead [62]. It still remains to be shown how the caspase interplay unfolds precisely during sialyllactose-coating mediated cell death.

Here, we have discovered a novel form of cell death that is dependent on cell surface sialic-acid. It is extremely rapid and requires the activity of G protein receptor coupled signaling and may present a fast way to remove cells and induce inflammation. The precise epitopes that are modified by sialyllactose-cyclic-carbamate ligation and what occurs to induce programmed cell death, still remain to be identified. However the discovery of cell death mediated by surface sialylation represents a mile-stone in cell death and glycobiology research. A fitting name for this process may be glycoptosis or sialoptosis in contemplation of the many forms of programmed cell death that have already been discovered.

Acknowledgments

We thank Glycom A/S for supplying us with the oligosaccharide-cyclic-carbamates. The plasmids psPAX2 (Addgene plasmid #12260) and pMD2.G (Addgene plasmid #12259) were a gift from Didier Trono. This research was supported by the Zurich Centre for Integrative Human Physiology (ZIHP) and by the Swiss National Science Foundation grant 314730_172880.

Author Contributions

M.W.J.W and T.H. planned the experiments. M.W.J.W. performed the experiments. M.W.J.W wrote the manuscript.

References

1. Kolb, J.P., et al., *Programmed Cell Death and Inflammation: Winter Is Coming.* Trends Immunol, 2017.
2. Bevilacqua, M., et al., *Selectins: a family of adhesion receptors.* Cell, 1991. **67**(2): p. 233.
3. Avril, T., et al., *The membrane-proximal immunoreceptor tyrosine-based inhibitory motif is critical for the inhibitory signaling mediated by Siglecs-7 and-9, CD33-related Siglecs expressed on human monocytes and NK cells.* Journal of Immunology, 2004. **173**(11): p. 6841-6849.

4. Lewis, L.A., M. Carter, and S. Ram, *The relative roles of factor H binding protein, neisserial surface protein A, and lipooligosaccharide sialylation in regulation of the alternative pathway of complement on meningococci.* J Immunol, 2012. **188**(10): p. 5063-72.

5. Hernandez, J.D. and L.G. Baum, *Ah, sweet mystery of death! Galectins and control of cell fate.* Glycobiology, 2002. **12**(10): p. 127R-36R.

6. Fuster, D.G., et al., *Characterization of the regulation of renal Na+/H+ exchanger NHE3 by insulin.* Am J Physiol Renal Physiol, 2007. **292**(2): p. F577-85.

7. Morris, R.G., et al., *Hormone-induced cell death. 2. Surface changes in thymocytes undergoing apoptosis.* Am J Pathol, 1984. **115**(3): p. 426-36.

8. Lichtenstein, R.G. and G.A. Rabinovich, *Glycobiology of cell death: when glycans and lectins govern cell fate.* Cell Death and Differentiation, 2013. **20**(8): p. 976-986.

9. Wagner, K.W., et al., *Death-receptor O-glycosylation controls tumor-cell sensitivity to the proapoptotic ligand Apo2L/TRAIL.* Nat Med, 2007. **13**(9): p. 1070-7.

10. Peter, M.E., et al., *Cell surface sialylation plays a role in modulating sensitivity towards APO-1-mediated apoptotic cell death.* Cell Death Differ, 1995. **2**(3): p. 163-71.

11. Keppler, O.T., et al., *Differential sialylation of cell surface glycoconjugates in a human B lymphoma cell line regulates susceptibility for CD95 (APO-1/Fas)-mediated apoptosis and for infection by a lymphotropic virus.* Glycobiology, 1999. **9**(6): p. 557-69.

12. Liu, Z., et al., *ST6Gal-I regulates macrophage apoptosis via alpha2-6 sialylation of the TNFR1 death receptor.* J Biol Chem, 2011. **286**(45): p. 39654-62.

13. Matarrese, P., et al., *Galectin-1 sensitizes resting human T lymphocytes to Fas (CD95)-mediated cell death via mitochondrial hyperpolarization, budding, and fission.* J Biol Chem, 2005. **280**(8): p. 6969-85.

14. Pace, K.E., et al., *Restricted receptor segregation into membrane microdomains occurs on human T cells during apoptosis induced by galectin-1.* J Immunol, 1999. **163**(7): p. 3801-11.

15. Whitehead, M.W.J., et al., *Custom Glycosylation of Cells and Proteins Using Cyclic-carbamate-Derivatized Oligosaccharides.* Cell Chem Biol, 2017.

16. Van Dyken, S.J., R.S. Green, and J.D. Marth, *Structural and mechanistic features of protein O glycosylation linked to CD8+ T-cell apoptosis.* Mol Cell Biol, 2007. **27**(3): p. 1096-111.

17. Zhuo, Y. and S.L. Bellis, *Emerging role of alpha2,6-sialic acid as a negative regulator of galectin binding and function.* J Biol Chem, 2011. **286**(8): p. 5935-41.

18. Zhuo, Y., R. Chammas, and S.L. Bellis, *Sialylation of beta1 integrins blocks cell adhesion to galectin-3 and protects cells against galectin-3-induced apoptosis.* J Biol Chem, 2008. **283**(32): p. 22177-85.

19. DuBois, M., et al., *Colorimetric Method for Determination of Sugars and Related Substances.* Analytical Chemistry, 1956. **28**(3): p. 350-356.

20. Sanjana, N.E., O. Shalem, and F. Zhang, *Improved vectors and genome-wide libraries for CRISPR screening.* Nat Methods, 2014. **11**(8): p. 783-4.

21. Vance, J.E., *Phosphatidylserine and phosphatidylethanolamine in mammalian cells: two metabolically related aminophospholipids.* J Lipid Res, 2008. **49**(7): p. 1377-87.

22. Hudak, J.E., S.M. Canham, and C.R. Bertozzi, *Glycocalyx engineering reveals a Siglec-based mechanism for NK cell immunoevasion.* Nat Chem Biol, 2014. **10**(1): p. 69-75.

23. Caserta, T.M., et al., *Q-VD-OPh, a broad spectrum caspase inhibitor with potent antiapoptotic properties.* Apoptosis, 2003. **8**(4): p. 345-52.

24. Lawrence, C.P. and S.C. Chow, *Suppression of human T cell proliferation by the caspase inhibitors, z-VAD-FMK and z-IETD-FMK is independent of their caspase inhibition properties.* Toxicol Appl Pharmacol, 2012. **265**(1): p. 103-12.

25. Meguro, T., et al., *Oxyhemoglobin induces caspase-mediated cell death in cerebral endothelial cells.* J Neurochem, 2001. **77**(4): p. 1128-35.

26. Newman, Z.L., S.H. Leppla, and M. Moayeri, *CA-074Me protection against anthrax lethal toxin.* Infect Immun, 2009. **77**(10): p. 4327-36.

27. Chae, J.J., et al., *The B30.2 domain of pyrin, the familial Mediterranean fever protein, interacts directly with caspase-1 to modulate IL-1beta production.* Proc Natl Acad Sci U S A, 2006. **103**(26): p. 9982-7.

28. Naito, T., et al., *Anticancer mechanisms of 1-(3-C-ethynyl-beta-D-ribo-pentofuranosyl) cytosine (ECyd, TAS-106).* Nucleic Acids Res Suppl, 2002(2): p. 241-2.

29. Vandenabeele, P., et al., *Necrostatin-1 blocks both RIPK1 and IDO: consequences for the study of cell death in experimental disease models.* Cell Death Differ, 2013. **20**(2): p. 185-7.

30. Cho, Y., et al., *RIP1-dependent and independent effects of necrostatin-1 in necrosis and T cell activation.* PLoS One, 2011. **6**(8): p. e23209.

31. Lohse, M.J., et al., *Kinetics of G-protein-coupled receptor signals in intact cells.* Br J Pharmacol, 2008. **153 Suppl 1**: p. S125-32.

32. Burns, D.L., *Subunit structure and enzymic activity of pertussis toxin.* Microbiol Sci, 1988. **5**(9): p. 285-7.

33. Briand, S., et al., *PAT1 induces cell death signal and SET mislocalization into the cytoplasm by increasing APP/APLP2 at the cell surface.* Neurobiol Aging, 2011. **32**(6): p. 1099-113.

34. Wu, P.R., et al., *DAPK activates MARK1/2 to regulate microtubule assembly, neuronal differentiation, and tau toxicity.* Cell Death Differ, 2011. **18**(9): p. 1507-20.

35. Yoshida, H. and M. Goedert, *Phosphorylation of microtubule-associated protein tau by AMPK-related kinases.* J Neurochem, 2012. **120**(1): p. 165-76.

36. Kadavath, H., et al., *Tau stabilizes microtubules by binding at the interface between tubulin heterodimers.* Proc Natl Acad Sci U S A, 2015. **112**(24): p. 7501-6.

37. Johnson, G.V. and J.A. Hartigan, *Tau protein in normal and Alzheimer's disease brain: an update.* J Alzheimers Dis, 1999. **1**(4-5): p. 329-51.

38. Gottlieb, E., et al., *Mitochondrial membrane potential regulates matrix configuration and cytochrome c release during apoptosis.* Cell Death Differ, 2003. **10**(6): p. 709-17.

39. Thornton, C. and H. Hagberg, *Role of mitochondria in apoptotic and necroptotic cell death in the developing brain.* Clin Chim Acta, 2015. **451**(Pt A): p. 35-8.

40. Poot, M., L.L. Gibson, and V.L. Singer, *Detection of apoptosis in live cells by MitoTracker red CMXRos and SYTO dye flow cytometry.* Cytometry, 1997. **27**(4): p. 358-64.

41. Liu, X., et al., *Induction of apoptotic program in cell-free extracts: requirement for dATP and cytochrome c.* Cell, 1996. **86**(1): p. 147-57.

42. Orrenius, S., B. Zhivotovsky, and P. Nicotera, *Regulation of cell death: the calcium-apoptosis link.* Nat Rev Mol Cell Biol, 2003. **4**(7): p. 552-65.

43. Kiselyov, K., D.M. Shin, and S. Muallem, *Signalling specificity in GPCR-dependent Ca2+ signalling.* Cell Signal, 2003. **15**(3): p. 243-53.

44. Fujii, Y., et al., *Surf4 modulates STIM1-dependent calcium entry.* Biochem Biophys Res Commun, 2012. **422**(4): p. 615-20.

45. Li, X., et al., *NecroX-5 suppresses IgE/Ag-stimulated anaphylaxis and mast cell activation by regulating the SHP-1-Syk signaling module.* Allergy, 2016. **71**(2): p. 198-209.

46. Vassallo, I., et al., *WIF1 re-expression in glioblastoma inhibits migration through attenuation of non-canonical WNT signaling by downregulating the lncRNA MALAT1.* Oncogene, 2016. **35**(1): p. 12-21.

47. Shelley, C.S., et al., *Molecular characterization of sialophorin (CD43), the lymphocyte surface sialoglycoprotein defective in Wiskott-Aldrich syndrome.* Proc Natl Acad Sci U S A, 1989. **86**(8): p. 2819-23.

48. Jiang, L.I., et al., *Regulation of cAMP responses by the G12/13 pathway converges on adenylyl cyclase VII.* J Biol Chem, 2008. **283**(34): p. 23429-39.

49. Zhao, C., et al., *Galpha(s) sensitizes human SH-SY5Y cells to apoptosis independently of the protein kinase A pathway.* J Neurosci Res, 2006. **84**(2): p. 389-97.

50. Zhu, W.Z., et al., *Dual modulation of cell survival and cell death by beta(2)-adrenergic signaling in adult mouse cardiac myocytes.* Proc Natl Acad Sci U S A, 2001. **98**(4): p. 1607-12.

51. Bernal, A., et al., *Microsomal and plasma membrane sialyltransferase activity in rat epididymis.* Arch Androl, 1983. **11**(1): p. 33-8.

52. Crespo, P.M., V.T. Demichelis, and J.L. Daniotti, *Neobiosynthesis of glycosphingolipids by plasma membrane-associated glycosyltransferases.* J Biol Chem, 2010. **285**(38): p. 29179-90.

53. Vilcaes, A.A., V.T. Demichelis, and J.L. Daniotti, *Trans-activity of plasma membrane-associated ganglioside sialyltransferase in mammalian cells.* J Biol Chem, 2011. **286**(36): p. 31437-46.

54. Schwartz-Albiez, R., et al., *Cell surface sialylation and ecto-sialyltransferase activity of human CD34 progenitors from peripheral blood and bone marrow.* Glycoconj J, 2004. **21**(8-9): p. 451-9.

55. Cabral, M.G., et al., *Human dendritic cells contain cell surface sialyltransferase activity.* Immunol Lett, 2010. **131**(1): p. 89-96.

56. Hernandez, J.D., et al., *Galectin-1 binds different CD43 glycoforms to cluster CD43 and regulate T cell death.* J Immunol, 2006. **177**(8): p. 5328-36.

57. Desharnais, P., et al., *Involvement of CD45 in DNA fragmentation in apoptosis induced by mitochondrial perturbing agents.* Apoptosis, 2008. **13**(2): p. 197-212.

58. Varfolomeev, E.E., et al., *Targeted disruption of the mouse Caspase 8 gene ablates cell death induction by the TNF receptors, Fas/Apo1, and DR3 and is lethal prenatally.* Immunity, 1998. **9**(2): p. 267-76.

59. Slee, E.A., et al., *Ordering the cytochrome c-initiated caspase cascade: hierarchical activation of caspases-2, -3, -6, -7, -8, and -10 in a caspase-9-dependent manner.* J Cell Biol, 1999. **144**(2): p. 281-92.

60. Sakamaki, K., et al., *Ex vivo whole-embryo culture of caspase-8-deficient embryos normalize their aberrant phenotypes in the developing neural tube and heart.* Cell Death Differ, 2002. **9**(11): p. 1196-206.

61. Wang, Y., et al., *Chemotherapy drugs induce pyroptosis through caspase-3 cleavage of a Gasdermin.* Nature, 2017.

62. Antonopoulos, C., et al., *Caspase-8 as an Effector and Regulator of NLRP3 Inflammasome Signaling.* J Biol Chem, 2015. **290**(33): p. 20167-84.

Conclusions and Implications for further Research

The influence of human milk oligosaccharides on immune regulation

For the first time we demonstrated that the HMOs FSL and LST-c are capable of inducing a metabolic shift in antigen presenting cells. The human monocytic cell line THP-1 and murine mesenteric lymph node derived dendritic cells react by increasing their lactate secretion when they have been stimulated with FSL or LST-c. Many tumors produce increased amounts of lactate which makes antigen presenting cells such as macrophages secrete more immune dampening cytokines like IL-10 and TGF-β [1]. The immune dampening influence of lactate production by antigen presenting cells may reflect a physiological role of increased lactate production in comparison to the pathophysiological role that is fulfilled by lactate produced by cancer cells.

Gut development in the infant requires a sensitive balance between immune activation and tolerance. The intestine is required for the infant to access the necessary nutrients from its environment and therefore it forms an interface with the outside world which is highly enriched with diverse bacteria. Some of these bacteria are actually beneficial to the infant's health such as *Lactobacillus spp.* or *Bifidobacteria spp.* and should be tolerated however other bacterial species are pathogens such as *Salmonella spp.* or *Campylobacter spp.* and must be eliminated. The human intestine has to learn when to defend and when to attack in this early stage of human life [2]. The glycans in human milk have often been regarded as components in human milk that support the immune systems maturation but also promote the growth of benefactors while inhibiting colonization with pathogens in the human gut [3]. Bacteria in the colon for instance can ferment the HMOs to short-chain fatty acids which make an acidic milieu that is beneficial for the growth of genera such as Bifidobacteria, Lactobacillus or Bacteroides that are associated with the healthy infants gut. Short-chain fatty acids are also able to bind to receptors on regulatory T-cells and support their activation [4], contributing to tolerance in the intestine. The importance of FSL and LST-c mediated lactate production by antigen presenting cells in vivo still remains to be elucidated. One possibility to determine the roles of FSL and LST-c on immunity would be to use rats or mice as they only produce simple trisaccharide milk oligosaccharides such as 3SL and not larger oligosaccharides such as LST-c and FSL [5-7]. It would be possible to then supplement suckling rats or mice with FSL or LST-c to determine alterations in gut immunity and its development. With this type of model system it would be possible to track major changes in gut immunity during challenges such as in the dextran sodium sulphate intestinal bowels disease model [8] or during the development of food allergies like in the peanut allergy model [9].

FSL and LST-c both share certain structural characteristics. As HMOs, they both possess lactose at their reducing end. Furthermore, they both also share an α2-3 linked sialic acid [10, 11]. Possible receptor candidates are galectins [12] and Siglecs [13]. The prior bind to β1-4 linked galactose which occurs in the reducing end lactose, but also in the poly-lactosamine chains, and the latter can bind to sialic acid. LST-d was also able to decrease the acidity of the media but to a lesser extent then LST-c. While LST-d has a terminally linked α2-6 linked sialic acid, LST-c possesses an α2-3 linked sialic acid. As LST-c induced the stronger effect, the receptor on the cell surface must have a stronger affinity to α2-3 linked sialic acid. Therefore possible Siglec receptors are the Siglecs-1, -4, -5 and -8 which have higher affinities for α2-3 linked sialic acid [14]. To determine which Siglec or galectin is involved, the CRISPR-Cas9 technology could be used which enables the placement of site-specific deletory mutations [15].

In the experiments that we conducted, our interest was limited to direct stimulatory roles that HMOs have on antigen presenting cells. However, what is the influence of HMOs on interactions that antigen-presenting cells have with other cells? T-cell activation and the ensuing initiation of specific adaptive immune reactions, requires stimulation by dendritic cells for instance. The binding of α1-2 mannosylated glycans from *Mycobacterium tuberculosis* or N-linked glycans on the glycoprotein gp120 from the human immunodeficiency virus to DC-SIGN on dendritic cells are known to initiate the production of IL-10 for example which leads to tolerating type T-cell responses [16, 17]. As DC-SIGN also can bind to fucosylated glycans it may be possible for fucosylated HMOs to bind to DC-SIGN and initiate similar effects [18]. DC-SIGN normally interacts with ICAM-3 [19] and ICAM-2 [20] on T-cells during activation. That means fucosylated glycans could interfere with or modulate this interaction to alter dendritic cell initiated T-cell responses. Similar mechanisms could also apply for other lectins that interact with receptors on T-cells such as the macrophage Gal/GalNAc-specific C-type lectin that recognizes LeX and LeY containing GalNAc structures and may therefore bind to corresponding HMOs [21].

Antigen-presenting cells such as dendritic cell and macrophages also influence the skewing of T cell responses towards Th1, Th2, Th17 or Treg type immune responses. *Campylobacter jejuni* for instance is a pathogen that possesses lipid bound oligosaccharides (LOS) at its cell surface that have terminal sialic acid residues. Depending on the terminal linkage of the sialic acid on the LOS the profile of cytokines that are produced differs. α2-3-linked sialic acid on LOS will interact with SIGLEC-1 on dendritic cells which will induce a Th2 response by producing IL-4 and TGF-β. On the other hand, terminally linked α2-8-linked sialic acid on the LOS binds to SIGLEC-7 which leads to Th1 polarization

by initiating the secretion of IFN-α or -β and IL-12 [22]. Sialylated HMOs may regulate specific immune reactions in a similar way by binding to the same receptors.

Signaling by C-type lectin receptors also influences the production of cytokines by dendritic cells. The receptors DCIR and MICL have intracellular ITIM-domains which recruit SH2-domain containing phosphatases after ligand binding [23, 24]. This ultimately leads to the inhibition of Toll-like receptor mediated IL-12 and TNF production [25, 26]. Sialylated HMOs can bind to selectins for instance which are a class of C-type lectins that play a role during leukocyte extravasation from the blood into the surrounding tissue [27, 28]. It is likely that HMOs interact with other C-type lectins and initiate signaling or they may block the access of endogenous ligands to their receptor and modulate the secretion of cytokines. Determining the binding specificities of various human milk oligosaccharides to lectins on the surface of dendritic cells would open up the possibility to determine how HMO binding induces signaling or interferes with and therefore modulates signaling by C-type lectin receptors. This may occur in context of T cell priming but also during the direct recognition of pathogen-associated patterns.

In the mammary gland, lactose is synthesized by the lactose synthase complex [29]. In fact, the β1-4 galactosyltransferase that extends glucose with galactose is the same enzyme that is able to extend GlcNAc with β1-4-linked galactose during the synthesis of glycoproteins and -lipids in the Golgi apparatus [29]. Lactose can be extended to HMOs in the Golgi apparatus of the mammary gland and the resulting epitopes are similar to the ones identified on glycoproteins and –lipids produced by other cell types [30]. One possibility is that these HMOs may therefore be responsible for obtaining tolerance towards common oligosaccharide structures. For this it would be necessary to present certain oligosaccharides on MHC-proteins. The zwitterionic polysaccharide A from *Bacteroides fragilis* can be presented on MHC- class II for instance which leads to $CD4^+$ T cell responses [31]. The capsular polysaccharide of *Streptococcus pneumoniae* is also presented on MHC-class II [32]. The presentation of antigens by dendritic cells does not only induce inflammatory immune reactions but is also important to mount regulatory immune responses. Many dendritic cells actually present self-antigens and initiate tolerance reactions via regulatory T cells. Especially dendritic cells that produce retinoic acid by the retinoic acid synthesizing enzyme promote the differentiation of $Foxp3^+$ regulatory T cells [33-36]. In the gut, retinoic acid producing $CD103^+$ dendritic cells are especially common which promotes the development of tolerance towards antigens [33]. One possibility is that HMOs are ingested by $CD103^+$ dendritic cells and presented to naïve T cells that mediate tolerance to common glycan structures.

Discovering novel regulatory roles of multivalent oligosaccharides

With the cyclic-carbamate technology we were able to modify proteins, entire mammalian and bacterial cells with oligosaccharides. We demonstrated that cells could be coated with oligosaccharides to study the binding of glycans on cells to lectins such as E-selectin. Our study was performed solely in vitro but the application of this technology can potentially be expanded to investigating the role of cell-surface glycans in vivo. What could the consequence be of presenting E-selectin ligands on cancer cells? E-selectin is expressed by epithelial cells and is responsible for the extravasation of leukocytes that present the E-selectin ligand sialyl-Lewis X [37]. During tumor cell extravasation, monocytes associate with tumor cells and aid their extravasation from the blood vessels by their binding to E-selectin [38]. The technology we developed enables us to study the consequence of directly modifying cancer cell surfaces such as the colon tumor cell line MC-38 with E-selectin ligands like FSL. Many cancer cells have increased amounts of E-selectin-ligands on their surface [39, 40]. The presentation of additional E-selectin ligands on the cell surface may therefore increase the extent of metastasis.

Increased presentation of sialic acid containing glycans on the cell surface may also increase the tolerance of the immune system towards the cancer cell. Siglecs are receptors that bind to sialic acid which activates the intracellular ITIM-domain, leading to the recruitment of SH2-domain containing phosphatases which counteract immune activation [41, 42]. One possibility is that cell surface sialylation may enable cancer cells to dampen immune responses by NK-cells or antigen presenting cells that express Siglec receptors. The coating of cancer cells with Siglec-ligands would enable us to answer this question. We were able to couple 6SL to 3-sn-phosphatidylethanolamine and incorporate it into the membrane of Jurkat cells that could bind to Siglec-3 as a consequence. Siglec-3 is expressed by the myeloid lineage but its function is not understood. Oligosaccharide-cyclic-carbamate mediated ligation to the cell surface is a suitable method to study the role of Siglec-3 in the myeloid lineage. Another approach involving the presentation of Sia residues as aminooxy glycans condensed to a polymethyl vinyl ketone scaffold by oxime formation, was able to demonstrate the role of Siglec-7 as a negative regulator of NK-cell mediated cancer cell death for example [43].

The cyclic-carbamate technology presented here also enables us to coat bacterial cells with oligosaccharide cyclic-carbamates and study the regulatory roles of glycans on the cell surface. Pathogens such as *Neisseria gonorrhoea* [44] or *Pseudomonas aeruginosa* [45] may present sialic acid at their cell surface. Cell surface sialylation is known to recruit the complement factor H which interferes with the complement reaction by cleaving complement factor 3b [44]. Siglecs on immune

cells such as phagocytes may also recognize bacterial sialic acid. The cyclic-carbamate technology enables us to examine the influence of bacterial surface sialic acid on their interaction with phagocytes and the cytokine environment that they produce. The interaction of bacterial cell surface Sia with Siglecs may enable the bacteria to evade immune surveillance and clearance.

I was also able to modify proteins with the cyclic-carbamate technology. *Staphylococcus aureus* protein A and bovine serum albumin were demonstrated to be suitable acceptors for oligosaccharide cyclic-carbamates in this work. This method opens up the possibility to study the roles of specific oligosaccharide structures that occur on highly glycosylated proteins like mucins. To do this a peptide backbone is required that is rich in lysines that would enable the dense presentation of oligosaccharides by the cyclic-carbamate technology. Furthermore if the N- and C-terminal amino acids were cysteines, this would enable the formation of intramolecular disulfide bonds using glutathione derivatives to synthesize mucin-like gel matrixes [46, 47] (Fig. 1).

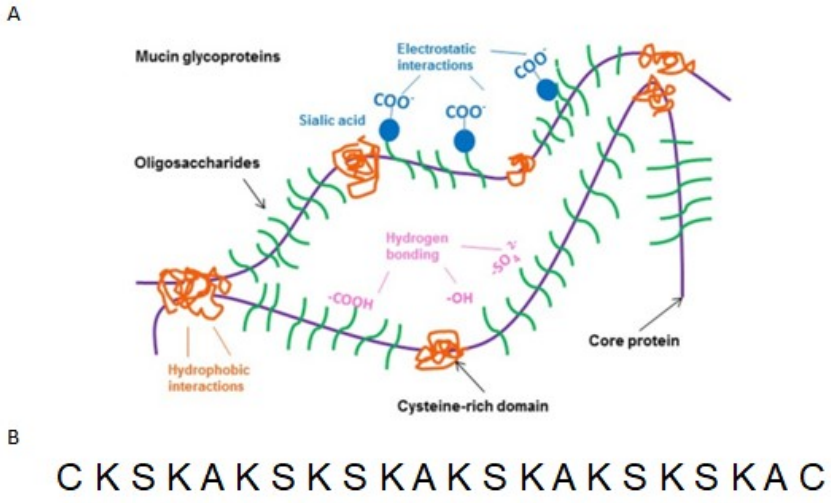

Figure 1: (A) Schematic representation of how mucins form a gel like-barrier by interactions of hydrophobic protein domains, electrostatic interactions, hydrogen bonds and covalent bonds between cysteine-rich domains of different mucin monomers. (B) Possible amino acid sequence of a peptide to form artificial mucin gels. Every second position is a lysine that could be modified with oligosaccharide cyclic-carbamates while the outer flanks are cysteines that can form intermolecular disulfide bonds (modified from [48]).

With this technology the role of the mucin MUC2 could be studied by using the custom-made mucin gel to reconstitute parts of the intestine by caecal injection. The role of the glycans on MUC2 as immune dampeners that stimulate the production of IL-10 but decrease the production of IL-12 by antigen presenting cells in the gut has been previously demonstrated [49]. The technology presented here enables the homogenous presentation of glycans and the identification of specific glycan epitopes that could mediate this change in vivo. It is also possible to modify polylysine stretches with

oligosaccharide-cyclic-carbamates. This opens up the possibility to coat cell culture plates with polylysine and then modify the amine groups with oligosaccharide-cyclic-carbamates. This would enable the creation of high-density oligosaccharide environments in which immune cells could be cultured and the influence of high-density glycans on their activation could be tested. The influence of high-level sialylation may increase the activation of Siglecs and thereby counteract the activation of antigen-presenting cells or even induce regulatory immune responses during the activation of T-cells by dendritic cells for instance.

The glycans on therapeutic proteins such as erythropoietin (EPO) have a key role on the efficacy of the biopharmaceutical. The extent of sialylation increases the serum half-life of EPO for example and therefore highly-sialylated forms of EPO are used as therapeutics [50]. Second generation EPO therapeutics actually have additional N-glycosylation sites to increase the amount of sialylation which leads to more terminal Sia being presented by the protein [51]. The production of protein therapeutics is expensive as they must be synthesized in mammalian cells that can perform glycosylation and sialylation reactions [52]. Furthermore, the production of cell produced biotherapeutics requires extremely stringent production standards to avoid batch variations or even the production of immunogenic biopharmaceuticals [53]. The production of chemically synthesized pharmaceuticals is less expensive and more robust. Non-glycosylated therapeutic proteins such as calcitonin can be synthesized chemically but glycoproteins such as EPO are not synthesized by chemical synthesis yet [54]. A possible chemical strategy to produce glycoproteins such as EPO would be to replace the asparagines at the N-glycosylation sites with lysine residues that can be modified with specific oligosaccharide cyclic-carbamates. Chemical production may lead to a decrease in the production costs for biopharmaceuticals which would alleviate the pressure on health-systems that are confronted with increasing expenses worldwide [55].

Sialyllactose-coating mediated cell death (Sialoptosis)

Coating mammalian cells with 3SL- or 6SL-cyclic-carbamates lead to rapid, caspase-dependent cell death. The precise mechanism and pathway still remain unknown. However, the initial stimulus must be derived from a receptor at the plasma membrane as this is the site of oligosaccharide-cyclic-carbamate ligation. The primary reaction partners of the cyclic-carbamate group are primary amines and thiol groups, whereas secondary amines are less efficient reaction partners [56]. These groups occur on proteins as well as lipids at the cell surface. The incorporation of sialyllactose-modified phosphatidylethanolamine into the plasma membrane did not lead to an increase in cell death and therefore we concluded that specific oligosaccharide-cyclic-carbamate ligation sites at the cell

surface are responsible for the observed cell death. One possibility to determine which sites at the cell surface are modified would be to cleave off surface peptides by digestion with trypsin and then to perform mass spectrometry, to discover which peptides are modified by oligosaccharide-cyclic-carbamate ligation. This technology can be used in combination with the CRISPR-Cas9-screening technology to identify the sites of modification. The initiation of cell death is very rapid and therefore the modified residue must be easily accessible. Interestingly, sialophorin, a candidate resulting from our CRISPR-Cas9 screen, is a membrane inserted mucin that protrudes from the plasma membrane and is therefore easily accessible. Other membrane-bound mucins such as MUC1 or MUC4 also protrude from the plasma membrane (Fig. 2) and would be easily accessible for oligosaccharide-cyclic-carbamate ligation.

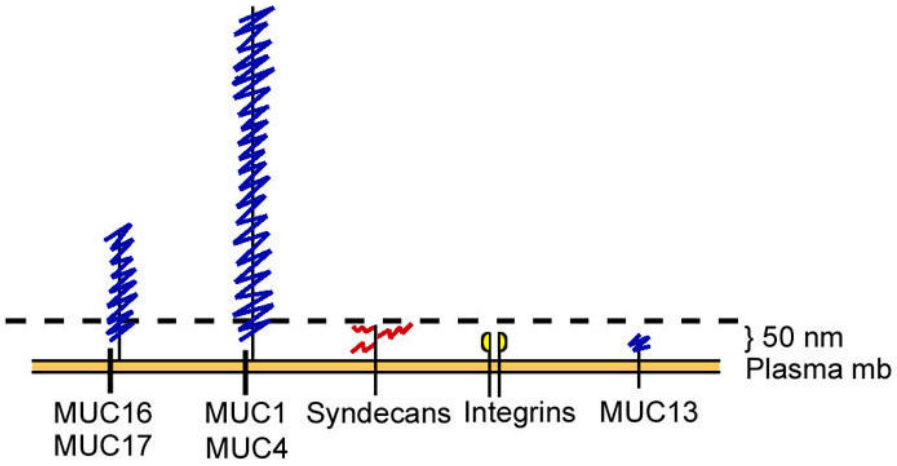

Figure 2: Many membrane incorporated mucins such as MUC1, MUC4, MUC16 and MUC17 depicted here protrude out of the plasma membrane and its surrounding glycocalyx (modified from [57]).

Sialophorin is known to be an important component that can mediate galectin-1 induced cell death by crosslinking cell surface signaling proteins such as CD45 which initiates apoptosis. Probably, other cell surface mucins besides sialophorin are also able to mediate crosslinking of cell surface receptors and regulate cell death in this manner.

Siglecs that bind to sialic-acid containing glycans at the cell surface are also able to induce cell death. Siglec-8 for instance is situated on the plasma membrane of eosinophils and its ligation is known to induce cell death. Siglec-8 stimulation in the presence of IL-5 leads to apoptosis while the presence of IL-5 leads to necrotic cell death. In the presence of IL-5, SIGLEC-8 ligation upregulated ERK1/2 phosphorylation, which ultimately lead to cell death [58]. In neutrophils the ligation and crosslinking of SIGLEC-9 leads to cell death [59]. Galectins are another class of glycan binding proteins that are secreted by cells and bind to glycans containing β1-4-linked galactose at the cell surface. In some

cases, galectin mediated crosslinking of cell surface proteins induces cell death [60]. Due to the bi- or multivalent carbohydrate binding sites that galectins have, they are suitable crosslinkers of glycoprotein containing proteins at the cell surface. Sialylation alters the binding properties of the galectins to the respective glycans. Galectin-2 binding for instance is reduced in the presence of sialic acid. Galectin-1 binding to α2-3-sialylated glycans is not ameliorated but α2-6-sialylation leads to reduced binding. Galectin-3 on the other hand can tolerate both α2-3 and α2-6-linked sialic acid [61]. The binding of the galectins-4 and -9 is also impacted by terminal sialic acid [62, 63], while the binding of galectin-8 is enhanced by sialylation [64, 65].

Cell death initiated by sialyllactose coating is probably mediated by several pathways which makes it difficult to perform genetic screens as the cell can circumvent the blockage of one cell-death pathway by taking an alternate route. Caspase-3 can for instance initiate classical apoptosis but is also able to initiate pyroptosis by activating gasdermin E [66]. Many of the candidates isolated in my research don't completely eliminate cell death due to the likely presence of redundancies. To avoid such compensating mechanisms the generation of mutants in one or several cell death pathways may be necessary. Then, the CRISPR-Cas9 screen can be performed to find more upstream candidates. Caspase-3 is at the center of the apoptotic pathway while caspase-1 and -11 are central pyroptotic initiators and the mixed lineage kinase domain-like protein (MLKL) is the bottleneck of necroptosis. To stop the cell from initiating alternative cell-death pathways during the CRISPR-Cas9 screen, single, double or even triple mutants of the central cell death initiating proteins can be applied.

Finally, what could the meaning of sialylation-mediated cell death be? I stipulate that the sudden sialylation of specific epitopes on the cell surface may serve as signals for the cell to commit suicide. This may be in response to cells becoming malignant but also during infection with intracellular bacteria or with viruses. The presence of extracellular sialyltransferases has been shown but their biological activity on proteins at the membrane remains disputed. In fact, extracellular sialylation by ecto-sialyltransferases has been proposed to occur after exposure to radiation but also lipopolysaccharide stimulation [67] which would support the notion that cell surface sialylation mediated cell death may trigger cell death in response to malignancy or infection. My screen revealed that G-protein coupled receptors and cell-surface bound mucins may play a role during sialic-acid coating mediated cell death but before determining the biological meaning of this phenomenon, a specific pathway and initiator at the cell surface must be identified.

Literature

1. Romero-Garcia, S., et al., *Lactate Contribution to the Tumor Microenvironment: Mechanisms, Effects on Immune Cells and Therapeutic Relevance.* Front Immunol, 2016. **7**: p. 52.
2. Ohland, C.L. and C. Jobin, *Microbial activities and intestinal homeostasis: A delicate balance between health and disease.* Cell Mol Gastroenterol Hepatol, 2015. **1**(1): p. 28-40.
3. Walker, W.A. and R.S. Iyengar, *Breast milk, microbiota, and intestinal immune homeostasis.* Pediatr Res, 2015. **77**(1-2): p. 220-8.
4. Arpaia, N., et al., *Metabolites produced by commensal bacteria promote peripheral regulatory T-cell generation.* Nature, 2013. **504**(7480): p. 451-5.
5. Urashima, T., et al., *Oligosaccharides of milk and colostrum in non-human mammals.* Glycoconj J, 2001. **18**(5): p. 357-71.
6. Prieto, P.A., et al., *Remodeling of mouse milk glycoconjugates by transgenic expression of a human glycosyltransferase.* J Biol Chem, 1995. **270**(49): p. 29515-9.
7. Fuhrer, A., et al., *Milk sialyllactose influences colitis in mice through selective intestinal bacterial colonization.* J Exp Med, 2010. **207**(13): p. 2843-54.
8. Chassaing, B., et al., *Dextran sulfate sodium (DSS)-induced colitis in mice.* Curr Protoc Immunol, 2014. **104**: p. Unit 15 25.
9. Helm, R.M., *Food allergy animal models: an overview.* Ann N Y Acad Sci, 2002. **964**: p. 139-50.
10. Wu, S., et al., *Annotation and structural analysis of sialylated human milk oligosaccharides.* J Proteome Res, 2011. **10**(2): p. 856-68.
11. Bode, L. and E. Jantscher-Krenn, *Structure-function relationships of human milk oligosaccharides.* Adv Nutr, 2012. **3**(3): p. 383S-91S.
12. Barondes, S.H., et al., *Galectins: a family of animal beta-galactoside-binding lectins.* Cell, 1994. **76**(4): p. 597-8.
13. Crocker, P.R., et al., *Siglecs: a family of sialic-acid binding lectins.* Glycobiology, 1998. **8**(2): p. v.
14. Varki, A. and T. Angata, *Siglecs--the major subfamily of I-type lectins.* Glycobiology, 2006. **16**(1): p. 1R-27R.
15. Jinek, M., et al., *RNA-programmed genome editing in human cells.* Elife, 2013. **2**: p. e00471.

16. Geijtenbeek, T.B.H., et al., *Mycobacteria target DC-SIGN to suppress dendritic cell function.* Journal of Experimental Medicine, 2003. **197**(1): p. 7-17.

17. Shan, M., et al., *HIV-1 gp120 mannoses induce immunosuppressive responses from dendritic cells.* PLoS Pathog, 2007. **3**(11): p. e169.

18. van Liempt, E., et al., *Specificity of DC-SIGN for mannose- and fucose-containing glycans.* FEBS Lett, 2006. **580**(26): p. 6123-31.

19. Geijtenbeek, T.B., et al., *Identification of DC-SIGN, a novel dendritic cell-specific ICAM-3 receptor that supports primary immune responses.* Cell, 2000. **100**(5): p. 575-85.

20. Geijtenbeek, T.B., et al., *DC-SIGN-ICAM-2 interaction mediates dendritic cell trafficking.* Nat Immunol, 2000. **1**(4): p. 353-7.

21. van Vliet, S.J., et al., *Carbohydrate profiling reveals a distinctive role for the C-type lectin MGL in the recognition of helminth parasites and tumor antigens by dendritic cells.* Int Immunol, 2005. **17**(5): p. 661-9.

22. Bax, M., et al., *Campylobacter jejuni lipooligosaccharides modulate dendritic cell-mediated T cell polarization in a sialic acid linkage-dependent manner.* Infect Immun, 2011. **79**(7): p. 2681-9.

23. Richard, M., et al., *Granulocyte macrophage-colony stimulating factor reduces the affinity of SHP-2 for the ITIM of CLECSF6 in neutrophils: a new mechanism of action for SHP-2.* Mol Immunol, 2006. **43**(10): p. 1716-21.

24. Marshall, A.S., et al., *Identification and characterization of a novel human myeloid inhibitory C-type lectin-like receptor (MICL) that is predominantly expressed on granulocytes and monocytes.* J Biol Chem, 2004. **279**(15): p. 14792-802.

25. Meyer-Wentrup, F., et al., *DCIR is endocytosed into human dendritic cells and inhibits TLR8-mediated cytokine production.* Journal of Leukocyte Biology, 2009. **85**(3): p. 518-525.

26. Meyer-Wentrup, F., et al., *Targeting DCIR on human plasmacytoid dendritic cells results in antigen presentation and inhibits IFN-alpha production.* Blood, 2008. **111**(8): p. 4245-4253.

27. Bode, L., et al., *Inhibition of monocyte, lymphocyte, and neutrophil adhesion to endothelial cells by human milk oligosaccharides.* Thromb Haemost, 2004. **92**(6): p. 1402-10.

28. Bode, L., et al., *Human milk oligosaccharides reduce platelet-neutrophil complex formation leading to a decrease in neutrophil beta 2 integrin expression.* J Leukoc Biol, 2004. **76**(4): p. 820-6.

29. Ramakrishnan, B., E. Boeggeman, and P.K. Qasba, *beta-1,4-galactosyltransferase and lactose synthase: Molecular mechanical devices.* Biochemical and Biophysical Research Communications, 2002. **291**(5): p. 1113-1118.

30. Kobata, A., *Structures and application of oligosaccharides in human milk.* Proc Jpn Acad Ser B Phys Biol Sci, 2010. **86**(7): p. 731-47.

31. Cobb, B.A., et al., *Polysaccharide processing and presentation by the MHCII pathway.* Cell, 2004. **117**(5): p. 677-87.

32. Stephen, T.L., et al., *Transport of Streptococcus pneumoniae capsular polysaccharide in MHC Class II tubules.* PLoS Pathog, 2007. **3**(3): p. e32.

33. Iwata, M., et al., *Retinoic acid imprints gut-homing specificity on T cells.* Immunity, 2004. **21**(4): p. 527-38.

34. Mora, J.R., et al., *Generation of gut-homing IgA-secreting B cells by intestinal dendritic cells.* Science, 2006. **314**(5802): p. 1157-60.

35. Siddiqui, K.R. and F. Powrie, *CD103+ GALT DCs promote Foxp3+ regulatory T cells.* Mucosal Immunol, 2008. **1 Suppl 1**: p. S34-8.

36. von Boehmer, H., *Oral tolerance: is it all retinoic acid?* J Exp Med, 2007. **204**(8): p. 1737-9.

37. Bevilacqua, M., et al., *Selectins: a family of adhesion receptors.* Cell, 1991. **67**(2): p. 233.

38. Hauselmann, I., et al., *Monocyte Induction of E-Selectin-Mediated Endothelial Activation Releases VE-Cadherin Junctions to Promote Tumor Cell Extravasation in the Metastasis Cascade.* Cancer Res, 2016. **76**(18): p. 5302-12.

39. Glavey, S.V., et al., *The cancer glycome: Carbohydrates as mediators of metastasis.* Blood Reviews, 2015. **29**(4): p. 269-279.

40. Bull, C., M.H. den Brok, and G.J. Adema, *Sweet escape: Sialic acids in tumor immune evasion.* Biochimica Et Biophysica Acta-Reviews on Cancer, 2014. **1846**(1): p. 238-246.

41. Crocker, P.R., S.J. McMillan, and H.E. Richards, *CD33-related Siglecs as potential modulators of inflammatory responses.* Glycobiology of the Immune Response, 2012. **1253**: p. 102-111.

42. O'Reilly, M.K. and J.C. Paulson, *Siglecs as targets for therapy in immune-cell-mediated disease.* Trends in Pharmacological Sciences, 2009. **30**(5): p. 240-248.

43. Hudak, J.E., S.M. Canham, and C.R. Bertozzi, *Glycocalyx engineering reveals a Siglec-based mechanism for NK cell immunoevasion.* Nat Chem Biol, 2014. **10**(1): p. 69-75.

44. Ram, S., et al., *A novel sialic acid binding site on factor H mediates serum resistance of sialylated Neisseria gonorrhoeae.* J Exp Med, 1998. **187**(5): p. 743-52.

45. Khatua, B., et al., *Sialic acids acquired by Pseudomonas aeruginosa are involved in reduced complement deposition and Siglec mediated host-cell recognition.* FEBS Lett, 2010. **584**(3): p. 555-61.

46. Perez-Vilar, J. and R.L. Hill, *The structure and assembly of secreted mucins.* J Biol Chem, 1999. **274**(45): p. 31751-4.

47. Okumura, M., et al., *Acceleration of disulfide-coupled protein folding using glutathione derivatives.* Febs Journal, 2011. **278**(7): p. 1137-1144.

48. Yang, X., et al., *Immobilization of pseudorabies virus in porcine tracheal respiratory mucus revealed by single particle tracking.* PLoS One, 2012. **7**(12): p. e51054.

49. Shan, M., et al., *Mucus enhances gut homeostasis and oral tolerance by delivering immunoregulatory signals.* Science, 2013. **342**(6157): p. 447-53.

50. Byrne, B., G.G. Donohoe, and R. O'Kennedy, *Sialic acids: carbohydrate moieties that influence the biological and physical properties of biopharmaceutical proteins and living cells.* Drug Discovery Today, 2007. **12**(7-8): p. 319-326.

51. Sinclair, A.M., *Erythropoiesis stimulating agents: approaches to modulate activity.* Biologics, 2013. **7**: p. 161-74.

52. Blackstone, E.A. and P.F. Joseph, *The economics of biosimilars.* Am Health Drug Benefits, 2013. **6**(8): p. 469-78.

53. Robinson, C.J. and C. Jones, *Quality control and analytical techniques for biopharmaceuticals.* Bioanalysis, 2011. **3**(1): p. 81-95.

54. Made, V., S. Els-Heindl, and A.G. Beck-Sickinger, *Automated solid-phase peptide synthesis to obtain therapeutic peptides.* Beilstein J Org Chem, 2014. **10**: p. 1197-212.

55. Jakovljevic, M. and T.E. Getzen, *Growth of Global Health Spending Share in Low and Middle Income Countries.* Front Pharmacol, 2016. **7**: p. 21.

56. Ichikawa, Y., Y. Matsukawa, and M. Isobe, *Synthesis of urea-tethered neoglycoconjugates and pseudooligosaccharides in water.* J Am Chem Soc, 2006. **128**(12): p. 3934-8.

57. Brayman, M., A. Thathiah, and D.D. Carson, *MUC1: a multifunctional cell surface component of reproductive tissue epithelia.* Reprod Biol Endocrinol, 2004. **2**: p. 4.

58. Kano, G., et al., *Mechanism of Siglec-8-mediated cell death in IL-5-activated eosinophils: role for reactive oxygen species-enhanced MEK/ERK activation.* J Allergy Clin Immunol, 2013. **132**(2): p. 437-45.

59. von Gunten, S., et al., *Siglec-9 transduces apoptotic and nonapoptotic death signals into neutrophils depending on the proinflammatory cytokine environment.* Blood, 2005. **106**(4): p. 1423-1431.

60. Hernandez, J.D. and L.G. Baum, *Ah, sweet mystery of death! Galectins and control of cell fate.* Glycobiology, 2002. **12**(10): p. 127R-36R.

61. Stowell, S.R., et al., *Galectin-1, -2, and -3 exhibit differential recognition of sialylated glycans and blood group antigens.* J Biol Chem, 2008. **283**(15): p. 10109-23.

62. Bum-Erdene, K., et al., *Structural characterisation of human galectin-4 N-terminal carbohydrate recognition domain in complex with glycerol, lactose, 3'-sulfo-lactose, and 2'-fucosyllactose.* Sci Rep, 2016. **6**: p. 20289.

63. Bi, S., et al., *Structural features of galectin-9 and galectin-1 that determine distinct T cell death pathways.* Journal of Biological Chemistry, 2008. **283**(18): p. 12248-12258.

64. Ideo, H., et al., *Galectin-8-N-domain recognition mechanism for sialylated and sulfated glycans.* J Biol Chem, 2011. **286**(13): p. 11346-55.

65. Ideo, H., et al., *The N-terminal carbohydrate recognition domain of galectin-8 recognizes specific glycosphingolipids with high affinity.* Glycobiology, 2003. **13**(10): p. 713-723.

66. Wang, Y., et al., *Chemotherapy drugs induce pyroptosis through caspase-3 cleavage of a Gasdermin.* Nature, 2017.

67. Manhardt, C.T., et al., *Extrinsic sialylation is dynamically regulated by systemic triggers in vivo.* Journal of Biological Chemistry, 2017. **292**(33): p. 13514-13520.

Acknowledgments

My greatest gratitude goes to Prof. Dr. Thierry Hennet who has supervised me during my PhD. I would like to thank him for creating the great environment in which I have been able to do my work during the past 4 to 5 years. Not only do I value his role as my supervisor but also as my mentor during the past few years. Due to the high standards that he sets I believe I have learnt what it means to be a true professional and this is a very valuable lesson for my further career.

I thank Prof. Dr. Lubor Borsig, Prof. Dr. Dr. Gerhard Rogler and Prof. Dr. Christophe Lacroix for taking time out of their otherwise very busy schedule to supervise my work as part of my PhD committee. I'd also like to especially thank Prof. Dr. Lubor Borsig for his input and expertise that I have benefited from.

I'd like to thank the members of the Hennet and Borsig laboratories for the absolutely smashing time that I have spent here. I will really miss this great working environment. Special thanks go to Dr. Jesus Glaus Garcon, Dr. Andreas Hülsmeier and Dr. Yen-Lin Huang for valuable discussions on science and introducing me to the techniques in the lab. Thank you also Christoph Rutschmann, Luca Plan and Sacha Schneeberger for keeping the lab up and running. Furthermore I'd like to say thank you to Giovanna Roth for her help concerning administrative issues at the University.

I sincerely thank Matthew Adjei for his great support with my work including mice. I'd like to thank Heidi Preisig for her help concerning any administrative issues within the imMed PhD program, and for her great help with the organization of the Vision 2020 event series. I'd also like to thank everybody who has accompanied me within the Vision 2020 committee.

Many thanks also to Prof. Dr. Jack Rohrer, Dr. Célia Baroux and Prof. Dr. Ueli Grossniklaus, three inspiring scientists, who are largely responsible for my enthusiasm towards science.

I'd also like to thank my closest family which includes Barbara Whitehead, Michael Whitehead, and Natasha Whitehead for their support on this path. I'd finally like to thank Catherine Recinos for her support and especially for her patience.

Curriculum Vitae

Name	Marek William James Whitehead
Date of birth	13.10.1987
Citizenship	Switzerland &
	United Kingdom of Great Britain and Northern Ireland

Education

2013-2018	PhD thesis at the Institute of Physiology, University of Zurich, in the group of Prof. Dr. Thierry Hennet
	"Sialylated Glycans as Regulators of Cell Activation and Cell Death"
2012-2013	Master thesis at the Department of Plant and Microbial Biology, University of Zurich, in the group of Prof. Dr. Ueli Grossniklaus
	"The Role of H1 related Chromatin Proteins during Plant Reproduction"
2008-2011	Bachelor Studies in Molecular Life Sciences at the University of Applied Sciences Northwestern Switzerland with major in Molecular Bioanalytics
2004-2008	Fachmaturitätsschule Basel, Fachmatura in health and natural sciences

Publications

1) She W., Grimanelli D., Rutowicz K., Whitehead M. W. J., Puzio M., Kotlinski M., Jerzmanowski A., Baroux C. (2013) Chromatin reprogramming during the somatic-to-reproductive cell fate transition in plants. *Development*. 140: 4008-19.

2) Whitehead M. W. J., Khanzhin N., Borsig L., Hennet T. (2017) Custom glycosylation of cells and proteins using cyclic-carbamate-derivatized oligosaccharides. *Cell Chemical Biology.* 24: 1-11.